



香港城市大學
City University of Hong Kong

專業 創新 胸懷全球
Professional · Creative
For The World

CityU Scholars

Additive manufacturing of structural materials

Liu, Guo; Zhang, Xiaofeng; Chen, Xuliang; He, Yunhu; Cheng, Lizi; Huo, Mengke; Yin, Jianan; Hao, Fengqian; Chen, Siyao; Wang, Peiyu; Yi, Shenghui; Wan, Lei; Mao, Zhengyi; Chen, Zhou; Wang, Xu; Cao, Zhaowenbo; Lu, Jian

Published in:

Materials Science and Engineering R: Reports

Published: 01/07/2021

Document Version:

Final Published version, also known as Publisher's PDF, Publisher's Final version or Version of Record

License:

CC BY-NC-ND

Publication record in CityU Scholars:

[Go to record](#)

Published version (DOI):

[10.1016/j.mser.2020.100596](https://doi.org/10.1016/j.mser.2020.100596)

Publication details:

Liu, G., Zhang, X., Chen, X., He, Y., Cheng, L., Huo, M., Yin, J., Hao, F., Chen, S., Wang, P., Yi, S., Wan, L., Mao, Z., Chen, Z., Wang, X., Cao, Z., & Lu, J. (2021). Additive manufacturing of structural materials. *Materials Science and Engineering R: Reports*, 145, [100596]. <https://doi.org/10.1016/j.mser.2020.100596>

Citing this paper

Please note that where the full-text provided on CityU Scholars is the Post-print version (also known as Accepted Author Manuscript, Peer-reviewed or Author Final version), it may differ from the Final Published version. When citing, ensure that you check and use the publisher's definitive version for pagination and other details.

General rights

Copyright for the publications made accessible via the CityU Scholars portal is retained by the author(s) and/or other copyright owners and it is a condition of accessing these publications that users recognise and abide by the legal requirements associated with these rights. Users may not further distribute the material or use it for any profit-making activity or commercial gain.

Publisher permission

Permission for previously published items are in accordance with publisher's copyright policies sourced from the SHERPA RoMEO database. Links to full text versions (either Published or Post-print) are only available if corresponding publishers allow open access.

Take down policy

Contact lbscholars@cityu.edu.hk if you believe that this document breaches copyright and provide us with details. We will remove access to the work immediately and investigate your claim.



Contents lists available at ScienceDirect

Materials Science & Engineering R

journal homepage: www.elsevier.com/locate/mser

Additive manufacturing of structural materials

Guo Liu^{a,b,1}, Xiaofeng Zhang^{a,1}, Xuliang Chen^{a,1}, Yunhu He^{a,1}, Lizi Cheng^a, Mengke Huo^a, Jianan Yin^a, Fengqian Hao^a, Siyao Chen^a, Peiyu Wang^a, Shenghui Yi^b, Lei Wan^a, Zhengyi Mao^a, Zhou Chen^a, Xu Wang^a, Zhaowenbo Cao^a, Jian Lu^{a,b,c,d,*}

^a Laboratory of Nanomaterials & Nanomechanics, Department of Mechanical Engineering, City University of Hong Kong, Hong Kong, China

^b Centre for Advanced Structural Materials, City University of Hong Kong Shenzhen Research Institute, Greater Bay Joint Division, Shenyang National Laboratory for Materials Science, Shenzhen, China

^c Hong Kong Branch of National Precious Metals Material Engineering Research Center (NPMM), City University of Hong Kong, Hong Kong, China

^d CityU-Shenzhen Futian Research Institute, Shenzhen, China

ARTICLE INFO

Keywords:

Additive manufacturing
Structural materials
3D printing
4D printing

ABSTRACT

Additive manufacturing (AM), also known as three-dimensional (3D) printing, has boomed over the last 30 years, and its use has accelerated during the last 5 years. AM is a materials-oriented manufacturing technology, and printing resolution versus printing scalability/speed trade-off exists among various types of materials, including polymers, metals, ceramics, glasses, and composite materials. Four-dimensional (4D) printing, together with versatile transformation systems, drives researchers to achieve and utilize high dimensional AM. Multiple perspectives of the AM of structural materials have been raised and illustrated in this review, including multi-material AM (MMa-AM), multi-modulus AM (MMo-AM), multi-scale AM (MSc-AM), multi-system AM (MSy-AM), multi-dimensional AM (MD-AM), and multi-function AM (MF-AM). The rapid and tremendous development of AM materials and methods offers great potential for structural applications, such as in the aerospace field, the biomedical field, electronic devices, nuclear industry, flexible and wearable devices, soft sensors, actuators, and robotics, jewelry and art decorations, land transportation, underwater devices, and porous structures.

Abbreviations: 2D, Two-dimensional; 3C, Computer, communication, and consumer electronics; 3D, Three-dimensional; 4D, Four-dimensional; ABS, Acrylonitrile butadiene styrene; AM, Additive manufacturing; APS, Air plasma spray; BJ, Binder jetting; BMG, Bulk metallic glass; CAD, Computer aided design; CNT, Carbon nanotube; CT, Computed tomography; DED, Direct energy deposition; DFT, Density functional theory; DIW, Direct ink writing; DLD, Direct laser deposition; DLP, Digital light processing; DMLS, Direct metal laser sintering; EBM, Electron beam melting; ECG, Electrocardiogram; EDA, Electrodermal activity; EDC, Elastomer-derived ceramic; EEG, Electroencephalogram; EMG, Electromyography; FDM, Fused deposition modeling; FEM, Finite element method; FLDW, Femtosecond laser direct writing; HA, Hydroxyapatite; HARP, High-area rapid printing; HAZ, Heat affected zone; HEA, High entropy alloy; ICs, Integrated circuits; IP, Inkjet printing; LCE, Liquid crystal elastomer; LCST, Lower critical solution temperature; LED, Light emitting diode; LOM, Laminated object manufacturing; LPBF, Laser powder bed fusion; MD-AM, Multi-dimensional additive manufacturing; MEMS, Microelectromechanical system; MF-AM, Multi-function additive manufacturing; MG, Metallica glass; MMa-AM, Multi-material additive manufacturing; MMo-AM, Multi-modulus additive manufacturing; MOF, Metal-organic framework; MPL, Multiphoton lithography; MRI, Magnetic resonance imaging; MSc-AM, Multi-scale additive manufacturing; MSy-AM, Multi-system additive manufacturing; NIR, Near-infrared light; P μ SL, Projection micro-stereolithography; PBP, Powder bed printing; PCB, Printed circuit board; PDC, Polymer-derived ceramic; PDMS, Polydimethylsiloxane; PE, Polyethylene; PEGDA, Poly(ethylene glycol) diacrylate; PET, Polyethylene terephthalate; PETG, Poly(ethylene terephthalate-co-1,4-cyclohexylenedimethylene terephthalate); PGS, Poly glycerol sebacate; PLA, Polylactic acid; PMMA, Polymethylmethacrylate; PNIPAM, Poly(N-isopropyl acrylamide); PPGDMA, Poly(propylene glycol) dimethacrylate; PPNM, Boracic PE/polyethylene wax blends-open-cell nickel foam composites; PU, Polyurethane; PUV, Printed utility vehicle; PVD, Physical vapor deposition; RFID, Radio frequency identification; SEBM, Selective electron beam melting; SEM, Scanning electron microscopy; SLA, Stereolithography; SLM, Selective laser melting; SLS, Selective laser sintering; SMA, Shape memory alloy; SMP, Shape memory polymer; SPPW, Self-propagating photopolymer wave-guide technology; SPS, Suspension plasma spraying; SS, Stainless steel; TBC, Thermal barrier coating; TENG, Triboelectric nanogenerator; TPL, Two-photon lithography; UAV, Unmanned aerial vehicle; UHS, Ultrafast high-temperature sintering; UV, Ultraviolet.

* Corresponding author at: Laboratory of Nanomaterials & Nanomechanics, Department of Mechanical Engineering, City University of Hong Kong, Hong Kong, China.

E-mail address: jianlu@cityu.edu.hk (J. Lu).

¹ These authors contributed equally to this work.

<https://doi.org/10.1016/j.mser.2020.100596>

Received 31 July 2020; Received in revised form 30 October 2020; Accepted 23 November 2020

Available online 1 April 2021

0927-796X/© 2021 The Author(s).

Published by Elsevier B.V. This is an open access article under the CC BY-NC-ND license

(<http://creativecommons.org/licenses/by-nc-nd/4.0/>).

1. Introduction

Use of additive manufacturing (AM) is considered to be a new industrial revolution [1,2], after steam engines, computers, and the internet. Unlike subtractive manufacturing, such as conventional machining, casting, and forging processes, AM constructs a three-dimensional (3D) structure by continuously adding the material

layer by layer with the guidance of a computer-aided design (CAD) model. Various types of promising materials, including polymers, metals, ceramics, glasses, biomaterials, and composite materials, have emerged in various types of AM methods, including stereolithography (SLA), selective laser sintering (SLS), fused deposition modeling (FDM), laminated object manufacturing (LOM), binder jetting (BJ), selective laser melting (SLM). Fig. 1 illustrated the technological roadmap of AM.

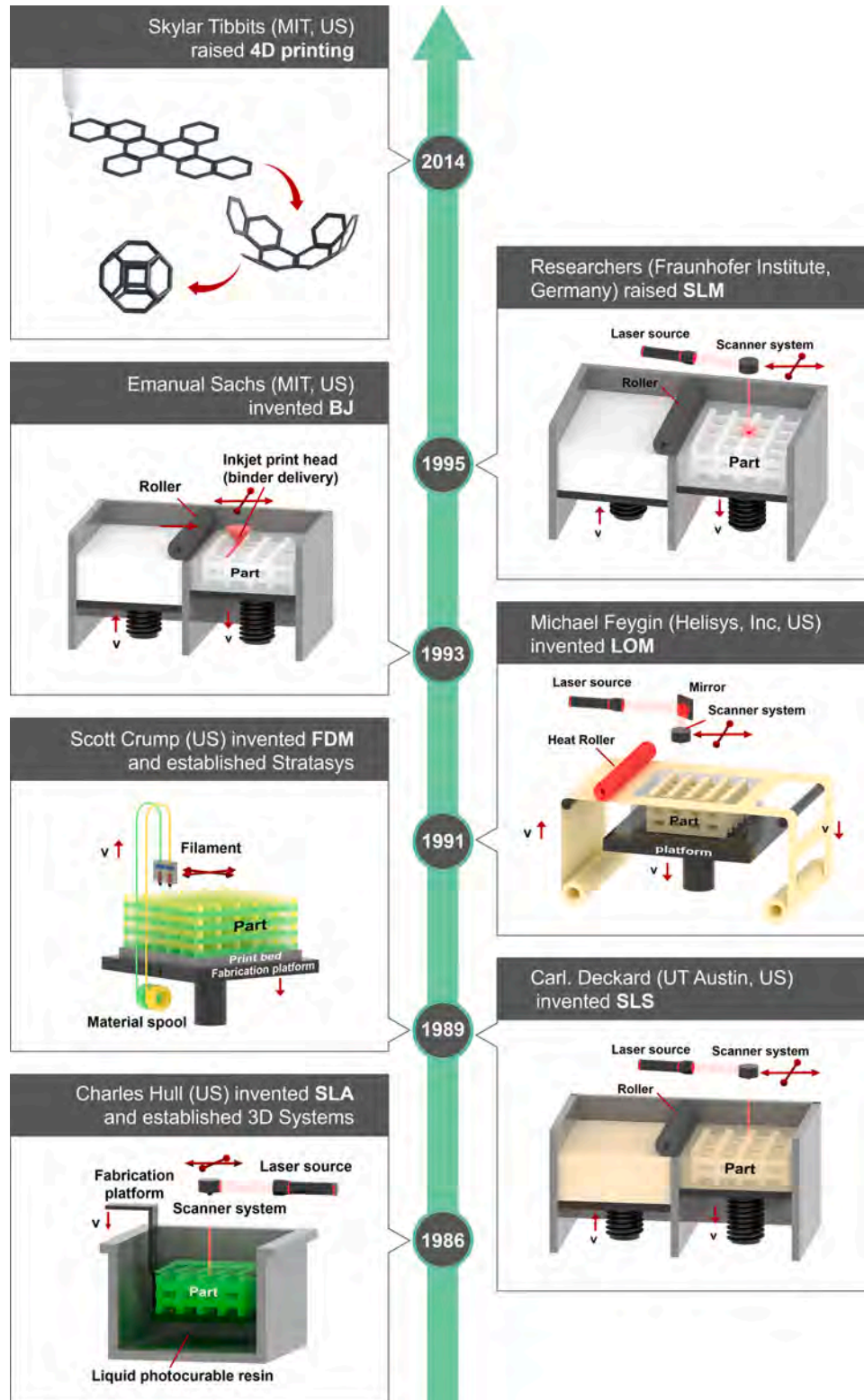


Fig. 1. Technological roadmap of additive manufacturing (AM).

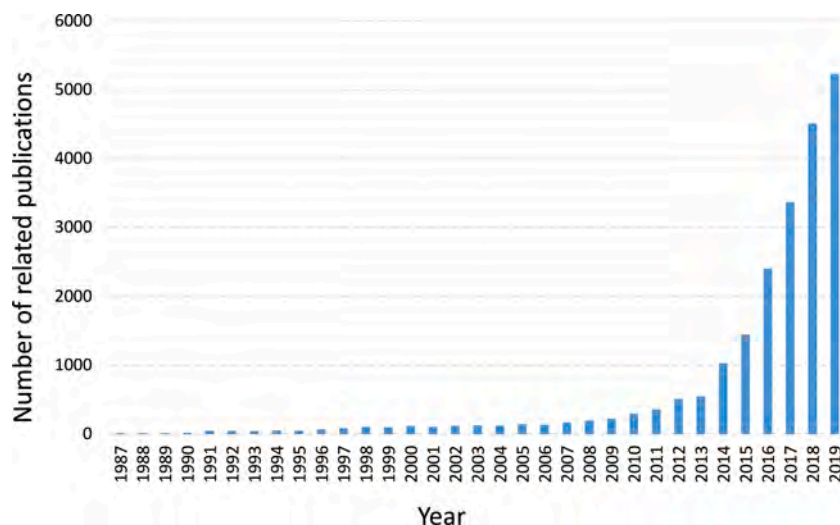


Fig. 2. Statistical data of articles on the topic of “additive manufacturing” published from 1987 to 2019. The data were compiled from the database of Web of Science Core Collection on July 23, 2020.

Four-dimensional (4D) printing has emerged with the involvement of versatile shape-morphing systems. Origami and kirigami, for example, are typical shape-morphing assemblies. Origami is the art of folding thin sheets into 3D objects, with rich geometric algorithms [3]. Kirigami is a variation of origami, in which the material is cut during the folding of the structure. During 4D printing, a 3D-printed material will autonomously and programmably change its configuration or function in response to environmental stimuli, such as exposure to heat, magnetic fields, liquids, electricity, light, gas, prestress, or a combination of the aforementioned stimuli. After the first demonstration of 4D printing with a multi-material strand folded into the letters “MIT” in 2014 [4], various smart materials have been developed for 3D printing and self-shaping assembly.

In recent years, more and more research studies on AM of structural materials have been published in a wide range of journals, as shown in Fig. 2. In the year 2020, a feature article in *Nature* suggested that researchers are developing techniques for faster, bigger, and more innovative printing [5]. In the year 2019, *Science* published several inspiring articles on AM, including three studies on the ultrafast 3D printing of multiscale structures [6–8], and two studies on 3D bioprinting of tissues or organs [9,10]. A broad range of materials developed for AM techniques has been developed, including polymers [11], metals [12], ceramics [12,13], glasses [14], biomaterials [15,16], and multi-material systems [17,18]. Hybrid or multi-process 3D printing also holds potential for improving the functionality of material structures [19]. Interestingly, the printing of soft matter is driving innovation in 4D printing [20]. Meanwhile, the accelerated industrialization of AM techniques, such as Adidas shoes printed by Carbon Inc. and Boeing airplane components printed by GE Aviation, also implies that a broad review on this topic is appropriate to provide sufficient technical suggestions for the ongoing practical applications and technological revolution analysis [21].

In this review article, we present recent progress and advances in 3D/4D AM of various materials, and their potential applications. Critical issues for the AM of structural materials, including the printability, printing resolution/scalability/speed, geometric complexity, mechanical robustness, and cost-efficiency, are discussed, and the current limitations and future directions for designing 3D/4D printable materials, metamaterials, devices, and systems are explained. Furthermore, we believe that the development of AM for structural materials will transition to strategies for multi-material AM (MMa-AM), multi-modulus AM (MMo-AM), multi-scale AM (MSc-AM), multi-system AM (MSy-AM), multi-dimensional AM (MD-AM), and multi-function AM (MF-AM).

2. Structural materials for additive manufacturing

Material candidates for AM have been summarized in Table 1, and analyzed in Fig. 3. In Table 1, the scalability of each AM systems is exhibited by the maximum dimension of resultant structures as reported in the studies, while the corresponding printing speed is exhibited by the reported maximum rate. Printing resolution versus printing scalability/speed trade-off has been observed, and the gray area in Fig. 3 covers the desired region for future studies aiming at overcoming this trade-off.

2.1. Additive manufacturing of polymeric materials

3D printing technology is based on digital model files, and printing materials are used to produce objects through layered printing, which is also referred to as AM [53]. At present, there are many preparation methods of polymer composites, such as deposition molding, selective laser sintering, ink-jet 3D printing, stereolithography, and 3D drawing [54]. Other methods are still in the research and development stage or are only used by a small number of scientists. In the production process of polymer composite products, every technology has its own advantages and disadvantages. The raw material requirements, processing rate and accuracy, cost and final performance requirements of products can affect the manufacturing process. The current polymer 3D printing technologies are shown in Fig. 4.

2.1.1. Thermoplastic polymers

Because the mechanical properties of pure thermoplastic materials are not suitable for some applications, it is necessary to alter the mechanical properties of pure thermoplastic parts prepared by FDM. Ning et al. [22] used the plastic particles (acrylonitrile butadiene styrene (ABS)) and carbon fiber for the FDM process. They found that specimens with 5 wt% carbon fiber had higher bending stresses, bending moduli and bending toughness values than those of pure plastic, with increases of 11.82 %, 16.82 %, and 21.86 %, respectively. The porosities of the samples with 10 % carbon fiber contents were the largest (Fig. 5). Tekinalp et al. [55] studied the processability, microstructure, and mechanical properties of short carbon fibers (0.2–0.4 mm) added to ABS as a 3D printing raw material using FDM technology. The tensile strength and modulus of elasticity of the 3D printed samples increased by about 115 % and 700 %, respectively, compared with the traditionally molded composite. Although the porosities of 3D printed composites is relatively high, they all show large tensile strengths and moduli.

Tian et al. [56] added long carbon fibers as a reinforcement to a

Table 1
Summary of structural materials for additive manufacturing (AM).

Materials	AM technology	Printing resolution (μm)	Printing scalability (mm)	Printing speed (mm s^{-1})	Others (e.g., mechanical properties, and cost-efficiency)	References	
Polymers	ABS+ carbon fiber powders	FDM	50	400	33	Low cost, high strength, multi-material capability, nozzle clogging	[22]
	Polylaurylamide and polyether ketone	SLS	80	300	1500	Good strength, easy removal of support powder, high cost, powdery surface	[23]
	Denture base PMMA	SLA	100	600		High printing resolution, material limitations, cytotoxicity, high cost	[24]
	Epoxy/clay nanocomposites	DIW	200	800	20	High printing resolution, soft material capabilities, low mechanical strength	[25]
Metals	316 L SS	Laser assisted direct metal deposition	40	10	1.33	Stress-strain behavior is comparable to that of commercial stainless steel produced by rolling and forming	[26]
	H13 tool steel	Direct metal deposition	40	60	4.17		[27]
	Ti-Cu alloys	Laser metal deposition		120	13.3	No post heat treatment	[12]
	Al7075, Al6061	SLM	20	80	7900	Post heat treatment is required	[28]
	Ti-6Al-4V	Shaped metal deposition		275	6.67	Tungsten inert gas welding-based AM using metal wire as original materials	[29]
	Ti-6Al-4V	EBM		200		Preheating is required	[30]
	Ti-6Al-4V	EBM	50	47.1	1000		[31]
	Al-Fe alloys	E-beam deposition		100		Vacuum is required	[32]
	Mild steel	Arc additive layer manufacturing		500	8.33		[33]
	Ti-6Al-4 V, aluminum, steel, invar, brass, copper and nickel	Wire + arc AM	500	2500		Deposition rates of 1 kg/h for titanium and aluminum, and 3 kg/h for steel are recommended for cost saving	[34]
	Ni-based superalloys	EBM		4.5		Vacuum is required. Post heat treatment is required	[35]
	Ni-based superalloys	Laser AM			25		[36]
	AlCoCrFeNi HEAs	SLM		10	2000		[37]
	FeCoCrNi HEAs	SLM		60	300		[38]
	CoCrFeNiTi-based HEAs	SEBM		85		Post heat treatment is required. Vacuum is required	[39]
CoCrFeNi HEAs	DIW		10		Reduction sintering is required	[40]	
Zr ₄₄ Ti ₁₁ Cu ₁₀ Ni ₁₀ Be ₂₅ MG	Fused filament fabrication			5		[41]	
Zr _{52.5} Ti ₅ Al ₁₀ Ni _{14.6} Cu _{17.9} MG	Laser foil printing			150		[42]	
Zr ₅₅ Cu ₃₀ Ni ₅ Al ₁₀ MG	SLM		7.2	1200		[43]	
Ni	TPL	0.1	0.05	6		[44]	
Ceramics	SiOC matrix nanocomposites	DIW	200	100	10–20	Specific compressive strength 339 MPa $\text{cm}^3 \text{g}^{-1}$	[45]
	SiOC	SLA/SPPW	50	100		Specific compressive strength 204 MPa $\text{cm}^3 \text{g}^{-1}$	[46]
	SiOC	SLA	25	10		Specific compressive strength 4.7 MPa $\text{cm}^3 \text{g}^{-1}$	[47]
	Al ₂ O ₃	TPL and atomic layer deposition	0.9	0.05	0.05	Specific compressive strength 144 MPa $\text{cm}^3 \text{g}^{-1}$	[48]
	Silica glass	Direct heating method	4500	300	6.3	Optical transmission: almost identical with commercial fused silica	[49]
Glasses	Amorphous silica	SLA	50			Optical transmission: almost identical with commercial fused silica	[14]
	Amorphous silica	DIW	500	10		Locally tunable optical properties can be realized	[50]
	Phase-separating resins	DLP		10		Optical transmission: almost identical with commercial fused silica	[51]
	Tetraethyl orthosilicate	DLP	200	10		Optical transmission: higher than soda lime glass and quartz glass after full densification at 1100 °C and polishing	[52]

polylactic acid (PLA) matrix to make raw silk material for printing, and they used the FDM process to realize sample preparation and molding. By optimizing the process parameters, the maximum bending tensile strengths and elastic moduli of the 3D printed samples with 27 % long carbon fiber contents reached 335 MPa and 30 GPa, respectively. Therefore, due to their superior mechanical properties, the printed samples have potential applications in aerospace. Using FDM, Eutonnat-Diffo et al. [57] studied the relationship between the tensile deformation of non-conductive and conductive PLA filaments deposited

on polyethylene terephthalate (PET) fabrics, the properties of the fabrics, and the printing platform temperature. A theoretical and statistical optimization model was presented. They found that the non-conductive PLA printing guide had better durability after washing or adding conductive filler, but the washing process affected the fracture stress of the woven fabric (after printing).

2.1.2. Thermosetting polymers

Thermosetting plastics can be melted during the first hot processing.

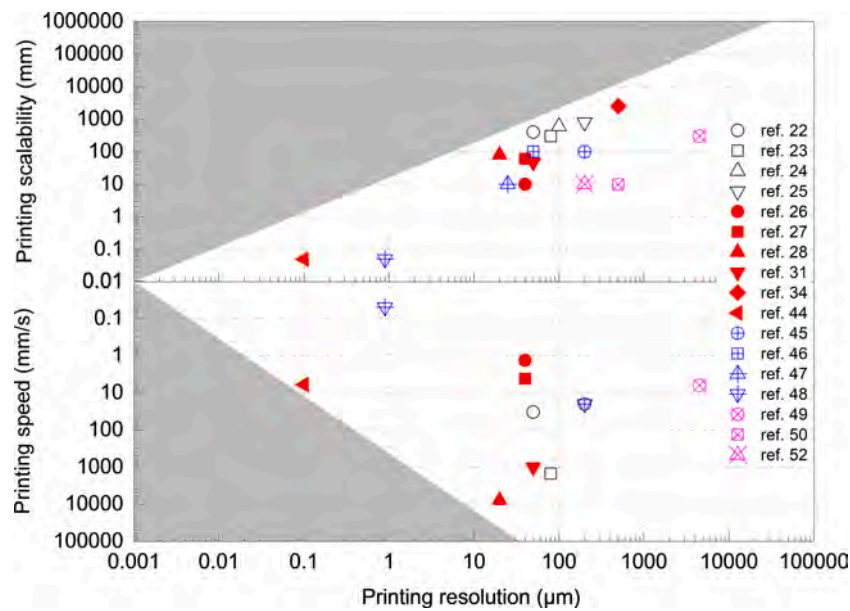


Fig. 3. Printing resolution versus printing scalability/speed trade-off (All the data are from Table 1).

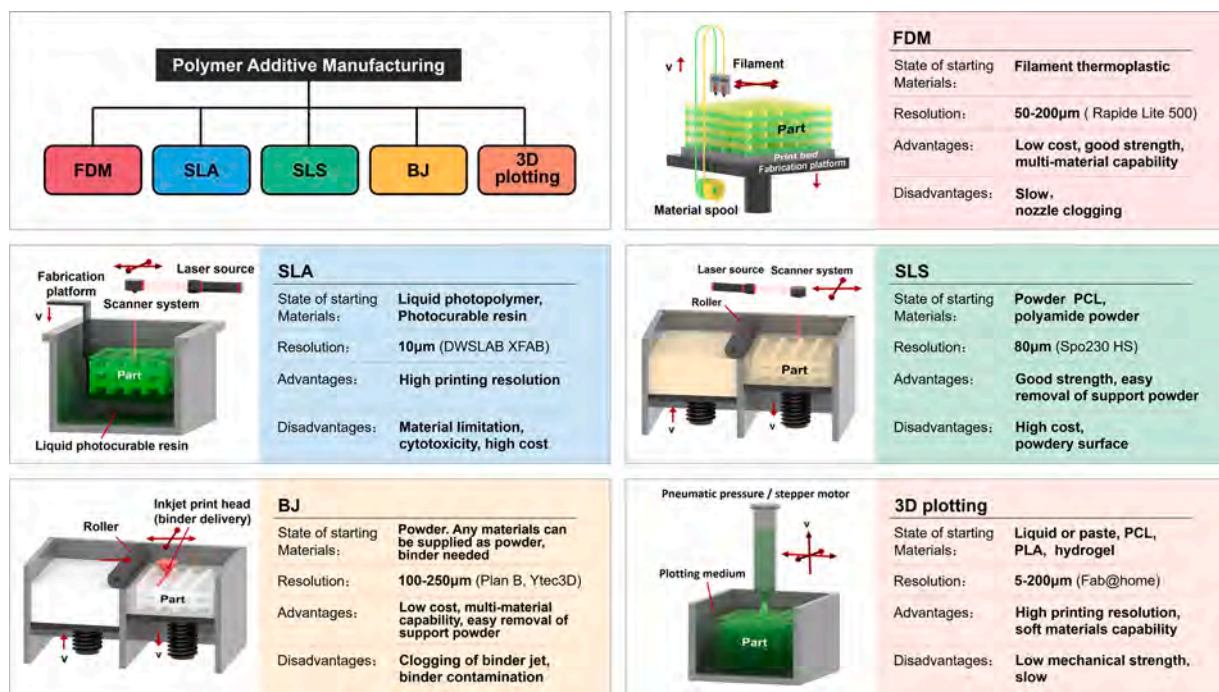


Fig. 4. Polymer 3D printing technologies.

During the formation process, thermosetting plastics will undergo chemical reactions to form cross-linked structures, which will harden after curing and will not melt when reheated. This change is irreversible, and when heated again, the thermosetting plastics can no longer soften. Thermosetting plastics mainly include phenolic plastics, amino plastics, epoxy plastics, unsaturated polyester plastics, organosilicon plastics, and polymethylmethacrylate (PMMA) [58].

Through 3D printing and ceramic conversion, Fu et al. [59] successfully prepared porous carbon-free embedded (larnite/C) scaffolds based on silicon resin loaded with calcium carbonate filler under an inert atmosphere and high temperature treatment. The scaffolds had a good effect on killing bone tumor cells. In addition, compared with the pure scaffold, the scaffolds could promote cell differentiation and had

better bone regeneration abilities. Shim et al. [24] studied the effect of printing samples with PMMA in different printing directions (0° , 45° , and 90°) on the print resolution, bending strength, surface morphology, and microbial reaction of 3D printed denture base resin. They found that the printing direction had a significant effect on the print resolution, bending strength, surface morphology, and reaction of microorganisms. They suggested that the print direction must be carefully selected to produce samples with better performances. Lin et al. [60] prepared ten different photopolymerization resins by using ethoxylated bisphenol A-dimethacrylate, urethane dimethacrylate, and triethylene glycol dimethacrylate. An ultraviolet (UV) 3D printer was used to print the samples. The bending strengths of the printed samples were between 60 and 90 MPa, the bending moduli were between 1.7 and 2.1 GPa, and the








Particle Reinforced Polymer Composites		
a	 Iron/ABS	Improved storage modulus and thermal conductivity, reduced coefficient of thermal expansion
b	 BaTiO₃/ABS	Improved dielectric permittivity and controllable resonance frequency.
c	 Glass bead/Nylon-11	Improved tensile modulus and compressive modulus, whereas reduced elongation at break
Fiber Reinforced Polymer Composites		
d	 Continuous carbon fiber/PLA	Improve tensile strength and comprehensive mechanical properties
e	 Short carbon fiber/ABS	Improved tensile strength and comprehensive mechanical properties
f	 Continuous carbon fiber/nylon	Improved tensile strength and comprehensive mechanical properties
Polymer Nanocomposites		
g	 Graphene oxide/photopolymer	Improved tensile modulus, strength and elongation
h	 Graphene/ABS	Improved electrical conductivity and thermal stability
i	 Silver/PEGDA	Improved electrical conductivity

Fig. 5. Classification and some examples of reinforcement methods of polymer composites: (a) iron/ acrylonitrile butadiene styrene (ABS) [75], (b) BaTiO₃/ABS [79], (c) glass bead/Nylon-11 [80], (d) continuous carbon fiber/polylactic acid (PLA) [56], (e) short carbon fiber/ABS [78], (f) continuous carbon fiber/nylon [81], (g) graphene oxide/photopolymer [82], (h) graphene/ABS [83], and (i) silver/ Poly(ethylene glycol) diacrylate (PEGDA) [84].

surface hardness values were between 14.5 and 24.6 HV. These properties were similar to those of current clinical resin materials. They suggested that these materials were ideal for 3D printing and have potential clinical application value. Hmeidat et al. [25] studied the effect of adding functional nano-clay on the rheological and printing properties of fiber-free reinforced epoxy resin using direct 3D printing technology. The strength range of these samples was 80–143 MPa, which was much higher than any previously reported values of 3D printed thermosetting composites, including short fiber-reinforced materials. Therefore, adding nanomaterials to epoxy resin is promising for direct writing 3D printing.

2.1.3. Elastomers

Polydimethylsiloxane (PDMS) is the dominant polymer in silicone systems [61] because of its mechanical flexibility and stretchability, chemical inertness, biocompatibility, and high thermal stability compared with those of other elastomers. Furthermore, PDMS exhibits high chemical stability at high temperatures and pressures [62].

He et al. [63] printed polydimethylsiloxane (PDMS) ink using a

direct ink writing 3D printer and patterned ordered porous structures with various geometric parameters to make special wetted surfaces. By optimizing the parameters, a sample film with a water contact angle of about 155° was prepared. The superhydrophobic properties of the porous PDMS films printed in this manner also showed excellent thermal aging durabilities. Holländer et al. [64] used a semi-solid extrusion printer and UV-assisted crosslinking technology to prepare a PDMS drug delivery device with a prednisolone structure using UV-light emitting diode (LED) light. They found that using room temperature semi-solid extrusion 3D printing technology combined with UV-LED cross-linking technology was a feasible method to produce PDMS devices containing prednisolone. Because the whole process was performed at room temperature, this production method could be used to produce devices for temperature-sensitive drugs.

Xiang et al. [65] studied the thiol-ene photopolymerization between vinyl and mercapto-functionalized polysiloxane, developed a UV curable silicone elastomer based on the thiol-ene photoreaction, and studied the photo-crosslinking kinetics, biocompatibility, and 3D printing performance. The silicone rubber sample had good cell and

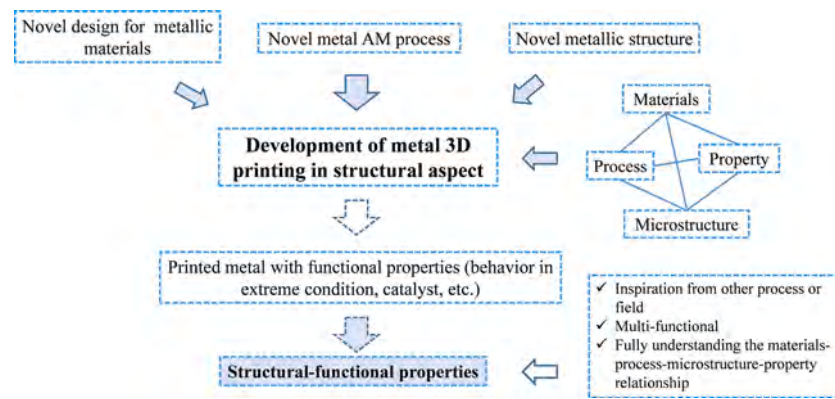


Fig. 6. Outline of metal AM.

tissue compatibility, and it was good for skin wound healing as a wound dressing. In addition, due to the good spatiotemporal controllability of the thiol olefin photoreaction, various soft structures could be prepared by photolithography, as well as three-dimensional elastic structures with smooth surfaces and good performances. Stieghorst et al. [66] developed a mathematical optimization method to calculate the optimal printing parameters of the minimum droplet spread. They used the double Arrhenius equation to link the temperature–time curve of the vulcanization process with the rise and fall of the viscosity due to the vulcanization of liquid silicone rubber. Two kinds of silicone rubber were characterized by a rheometer under different isothermal and anisothermal curing conditions. They found that the actual measured value was close to the calculated value, which made it possible to optimize the rheological properties of the silicone rubber using the curing process parameters.

2.1.4. Polymer composites

Today, 3D printing polymer technology can produce complex workpieces, but the strengths and functions of the workpieces limit their development. The development of composite materials to obtain the required mechanical and functional properties can largely solve this problem. Thus, the use of composite materials has been greatly developed [67–74]. The polymer composites developed today mainly include particle-reinforced polymer composites, fiber-reinforced polymer composites, and nanocomposites (Fig. 5) [54].

Because of the low material costs and the ease of mixing particles with a polymer, particle-reinforced materials are widely used in the polymer matrix to change its properties. Nikzad et al. [75] prepared iron/ABS and copper/ABS composite samples with metal contents up to 40 % by controlled centrifugal mixing, single screw extruder thermal compounding, and compression molding for FDM technology. They found that due to the addition of metal fillers, the thermal and mechanical properties of ABS were largely improved, and the stiffness and tensile properties were improved. The thermal conductivity of 30 %-Cu-filled ABS and 40 %-Cu-filled ABS increased to 3.3 and 1.4 W/m²·C. Isakov et al. [76] mixed perovskite oxide particles with a polymer matrix to prepare the required filaments for printing, which could be used for three-dimensional printing of various media materials with high dielectric anisotropy and spatial variations of the dielectric constant. The structure of the designed sample exhibited metamaterial electromagnetic characteristics and a tunable working frequency, and thus, it has great potential for the manufacture of new electromagnetic devices by fused deposition 3D printing.

Adding fibers to a polymer matrix can significantly improve the properties of a polymer material. FDM and direct writing are two frequently used techniques for manufacturing fiber-reinforced polymer composites. Wang et al. [77] proposed a new method in which thermal expansion microspheres were added to the matrix, and the FDM process was combined with heat treatment. Compared with the untreated

samples, the tensile and compressive strengths of the samples heated at 140 °C for 120 s increased by 25.4 % and 52.2 %, respectively. Compton et al. [78] obtained a 3D printed honeycomb composite composed of oriented-fiber-filled epoxy resin with excellent mechanical properties by direct writing technology. A structure with a good strength and toughness was obtained by adjusting the arrangement of the fibers and whisker reinforcements.

High-performance functional composites can be made by adding nanomaterials to polymer materials. Lin et al. [82] showed that the graphene oxide/photopolymer composite prepared by SLA had good strength and ductility. When only 0.2 % graphene oxide was added, the tensile strength and elongation increased by 62.2 % and 12.8 %, respectively. They speculated that the increase in toughness was due to the increase in the crystallinity of graphene oxide in the polymer composites. Wei et al. [83] found that a graphene-reinforced ABS composite could be used in the FDM process to produce workpieces, and the conductivities of the samples were enhanced. When the content of graphene in the composite was 5.6 wt%, the conductivity of the composite increased by four orders of magnitude.

2.1.5. Perspectives

Due to the variety of available materials, polymer AM can be applied to create light and complex structures in the aerospace industry, structural models for the construction industry, artificial reproductions of artwork, and tissue and organs in the medical field. However, due to the lack of strength and necessary functions of pure polymer products produced by AM, most AM polymer products are still used as concept samples rather than functional components. These disadvantages limit the wide industrial application of polymer AM. To overcome these shortcomings, polymer matrix composites have been prepared by adding particles, fibers, or nanomaterial reinforcements to the polymer. Due to the different reinforcement materials, polymer composites have better mechanical, electrical, and thermal properties.

However, there are some problems in the AM of polymer composites. First, the materials are limited. At present, only thermoplastic polymers, powder forming materials, and a small number of photopolymers with low glass-transition temperatures and appropriate melt viscosities can be used for 3D printing. Consequently, these limited polymer composites cannot meet the diverse industrial requirements. Thus, it is a key problem to develop more suitable polymer composites as printing materials. Second, the performances of these materials are limited. The mechanical strengths of polymer composites made of most additives are still lower than those of polymer composites made using traditional molding methods, and thus, these composites cannot meet the functional requirements. Therefore, the key improvements are to find a suitable enhancement material, better printing parameters, and better printing structures. Finally, the printers for these materials are limited. The key to solving this problem is to shorten the printing time, increase the maximum volume, and improve the printing accuracy. Nonetheless,

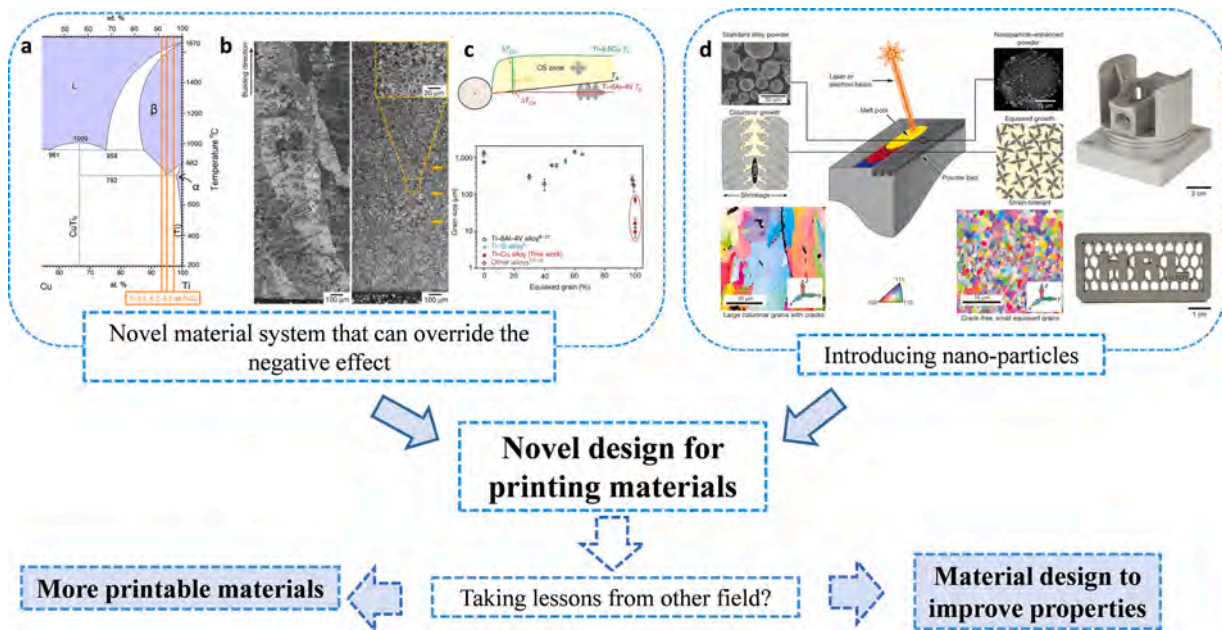


Fig. 7. Development of 3D printed metal designs: (a–c) novel material systems that can overcome the negative effects [12] and (d) the introduction of nano-particles [28].

the AM of polymer composites has good prospects.

2.2. Additive manufacturing of metallic materials

Metals are traditional materials in structural applications and have been widely developed by common manufacturing methods (e.g., casting, forging, and welding). AM can expand the applications of metals by forming complex structures, reducing the number of required structural components and the production costs, and shortening the processing timescale. Thus, AM can change the current lifecycles of metal parts. To fully access the advantages of 3D printing in practical applications, we must explore novel materials, processes, and structures [85]. An outline of metal AM is shown in Fig. 6.

2.2.1. Development of materials, processes, printing structures, and structural–functional properties

2.2.1.1. *Novel design of materials for printing.* The properties of printing materials are highly related to the microstructures and final properties of printed parts. Many novel metallic materials have been designed to form materials with good microstructures and advanced properties, as shown in Fig. 7. Currently, many of these novel metallic materials have been designed to be applicable for AM or improve the structural properties, e.g., high strengths and toughness values.

One limitation of AM is the range of printing alloys, as typical alloys used in industry are not adaptable for AM. It is difficult to obtain parts with desired structures or properties using typical alloys. Therefore, developing novel metallic materials for AM has been a popular topic of recent research, with researchers taking inspiration from other fields, such as casting. Uniform dispersions of nanoparticles in the

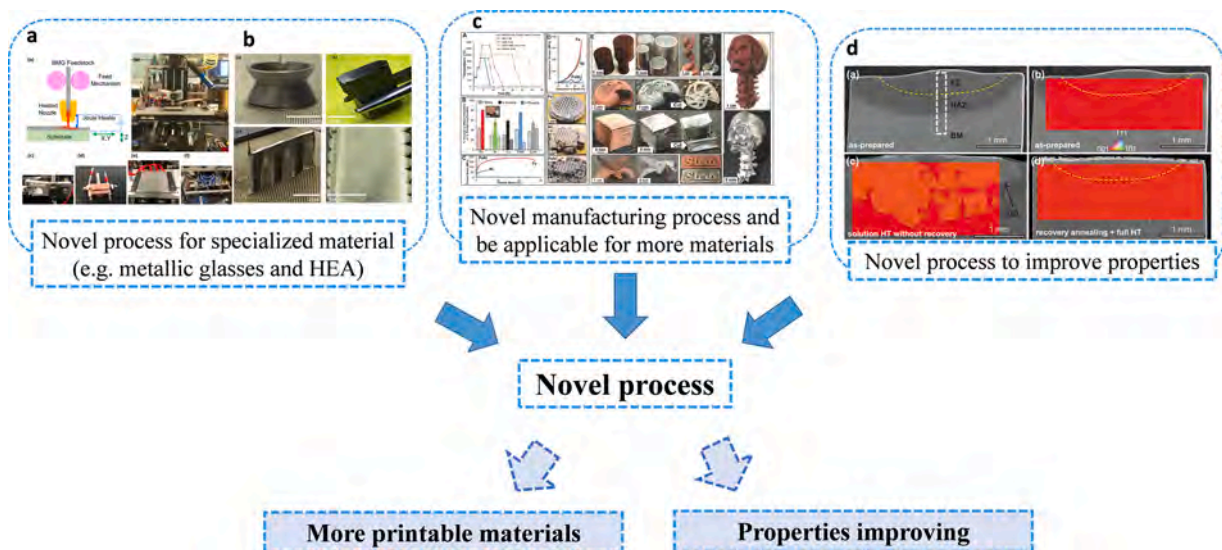


Fig. 8. Novel process for additively manufactured metals: (a, b) novel process for specialized materials [41], (c) novel manufacturing process that is applicable for more materials [91], and (d) novel process to improve the properties of the manufactured component [35].

solidification process during casting can efficiently achieve higher specific yield strengths and specific moduli [86]. Martin et al. [28] developed an approach to expand the metallic material selection to a wide range for application in many AM machines. Like casting, AM involves the process of solidification, which can be similarly controlled by introducing nanoparticles as nucleants. Crack-free, equiaxed, and fine-grained microstructures can be obtained by AM processes with properties comparable to those of wrought material. Similarly, many researchers have utilized nanoparticles to fabricate components with fine microstructures and advanced mechanical properties, for example, Al [87], AlSi10Mg [88], and ferritic stainless steel [89].

Different AM methods have their own characteristics. Most laser- and electron-beam-based AM methods involve high heating and cooling rates, generating high temperature gradients in the printed component. This likely results in columnar grains, and thus, undesired anisotropic mechanical properties [90]. Therefore, some researchers have developed novel materials to overcome the negative effects of the AM method. Zhang et al. [12] reported novel Ti-Cu alloys with high constitutional supercooling capacities, which can obtain ultrafine eutectoid microstructures rather than columnar grains. The ultrafine eutectoid microstructures result from the high cooling rate in the high temperature gradient of a laser process. Novel materials exploit the characteristics of AM process.

2.2.1.2. Novel processes. Despite the development of novel materials for AM, some researchers have made significant efforts to develop novel AM processes for different purposes, as shown in Fig. 8. The term “hard-printing alloy” refers to an alloy that is relatively difficult to fabricate by normal AM processes, for example, amorphous alloys and high-entropy alloys (HEAs). These novel AM processes are modifications of current processes or were developed based on the characteristics of hard-printing alloys. For example, amorphous alloys fabricated by AM, such as SLM, will be partially crystallized due to reheating in the heat affected zone (HAZ). Gibson et al. [41] developed a novel 3D printing system (fused filament fabrication) to fabricate amorphous alloys with complex structures (further details about the 3D printing of amorphous alloys are provided in Section 2.2.2). Kenel et al. [40] and Jakus et al. [91] reported a combined strategy using ink writing printing of metal oxide mixtures following by reduction sintering. This strategy can be used to fabricate complex metallic structures, including Fe, Ni, FeNi, and FeCoNiCr HEAs. Crack and segregation control are necessary in AM processes with high thermal gradients. These researchers utilized ink writing printing to print complex structures and reduction sintering to form alloys from oxides. This novel strategy can expand the range of printable alloys.

Meanwhile, many researchers have focused on improving the mechanical properties of printed alloys. Chen et al. [35] designed a post-3D-printing recovery protocol that utilized a feature of the printing process—the unrelieved residual stress—to prevent single crystals from recrystallizing. This technology modified the whole manufacturing process and showed potential use for additive remanufacturing, including repairing, restoring, and reshaping of superalloy single-crystal products. However, if there are some significant gaps that are hard to overcome, developing completely new AM methods may also be a good choice. Yu et al. [92] proposed a new AM method—additive friction stir deposition—and discussed its benefits and limitations compared to current AM technologies. Wang and co-authors utilized laser-based AM technology to fabricate various materials, including crack-free steel, Ti-based alloys, and superalloys, with relatively large sizes and good mechanical properties [29,36,93–95]. A hybrid deposition and micro-rolling process that combined micro-casting, forging, and milling was proposed to improve the deposition accuracy and microstructure performances [96,97]. Since Wu et al. [98] revealed that dual-phase nanostructures have excellent mechanical properties, achieving such structures in 3D printed alloys has been appealing [99]. Some metallic

glass composites with amorphous and crystal phases with high strengths and fracture toughness values were prepared [100].

Other novel technologies have appeared for AM fabrication, such as combinatorial alloy design for multi-material manufacturing [101], electrochemical-machining-assisted 3D printing [102], and additive remanufacturing [103]. Laser-based deposition, arc melting, and other techniques have been used to repair damaged components, known as additive remanufacturing [29,103]. Industrial components, such as gears, molds, and landing gear, are frequently damaged by daily usage under high-impact, wear, and high-load conditions. These additive remanufacturing methods can clad hard protection coatings with metallurgical bonds to improve the hardness, wear resistance, or other properties, thereby extending the life cycle [104].

Apart from novel experimental methods to improve the properties of additively manufactured components, some researchers have simulated the processes to investigate the formation of defects and optimize the processes. Khairalla et al. [105] revealed spatter-induced defect formation mechanisms using high-fidelity simulations, which could describe the fast multi-transient dynamics even to the nanosecond scale, and then verified the simulations by synchrotron experiments. Other simulations using methods such as the finite element method (FEM), molecular dynamics (MD), and density functional theory (DFT) can simulate processes at different scales, from macroscopic and micro-cosmic scales to the atomic scale. These methods are effective, but they require further multiscale combinations to relate each scale.

Hence, developing novel printing processes combining the features of the materials and AM processes has widened the range of printable materials.

2.2.1.3. Novel structures. Printing structures generally depend on the end applications [106]. Open-cell materials can not only provide structural properties but can also support potential applications related to the internal surfaces, such as catalysis. The structures are easily manufactured by AM methods. However, closed-cell materials are mainly used in structural applications, such as lightweight supporting parts or energy absorbing parts. The outside shape of a component with a closed-cell structure can be formed by AM, but the internal porosity is generally controlled by other factors, such as a foaming agent [106].

Structures with open cells can be used in applications involving direct contact, such as catalysts, where achieving load-bearing capabilities is not the primary goal [107]. Structures with closed pores are more likely to be utilized in applications involving indirect contact, such as energy absorption [108] and electromagnetic shielding [109].

The structure is highly related to the final mechanical properties, as the deformation path is easily influenced by the structure. The designed structure should take the microstructure into consideration. For example, additively manufactured parts sometimes have anisotropic properties. If a part is well designed, the deformation occurs along the anisotropic direction with a higher strength. Thus, a higher strength and lower weight can be achieved.

The printing structures can influence the deformation path and further improve the structural properties. Many efforts have been made to compare the structural properties of different structures using experimental and numerical simulation methods. The compared parameters are mainly related to the density, structural orientation, and lattice structure [108,110–112]. Further breakthroughs are possible by taking inspiration from other fields. Pham et al. [113] designed a lattice structure that was similar to the crystal structure. The results indicated that crystal-like structures could efficiently improve the mechanical properties. Bio-inspired materials have been shown to exhibit improved mechanical properties [114,115]. Though few studies have been performed on metal 3D printing, bio-inspiration can contribute to both structural and functional applications. Some typical strengthening mechanisms for the additively manufactured components, including fine microstructures, secondary phases, special microstructural

Table 2
Typical statistics of strengthening mechanisms, material types, and AM technology.

Strengthening mechanism	Material types	AM technology
Fine microstructures	Al-based alloy [28], Ti-based alloy [12], Inconel 625 [92],	SLM [12,28], additive friction stir deposition [92]
Secondary phases	Al composites [87], SS [89]	SLM [87], laser metal deposition [89]
Special microstructural deformation mechanisms	Zr-based BMG [41], Fe-based BMG [116], CoFeNiCr HEA [40], 316 L SS [108,110], Ni-based superalloy [35]	Fused filament fabrication [41], ink writing printing + reduction sintering [40], SLM [108,110, 116], EBM [35]
Structural factors	Ti-6Al-4 V [111], 316 L SS [113]	EBM [111], SLM [113]

deformation mechanisms, and structural factors, are summarized in Table 2.

2.2.1.4. Printed metals with functional properties. Metals not only have many structural applications but also show potential in functional applications due to their unique physical (e.g., conductive, thermal, and superhydrophobic) and chemical properties (e.g., chemical activity) (Fig. 9). Some functional properties have been developed in addition to structural properties, and the materials exhibit the advantages of metal 3D printing, such as withstanding extreme conditions [35,40], electrochemical properties [117], and superhydrophobic properties [118]. Further functional applications remain to be fully developed.

In addition, functional properties are generally achieved with intrinsic metal properties and further treatment. Ambrosi et al. [117, 119] demonstrated an electrochemical application using stainless steel as electrodes and Pt, IrO₂, and Ni films as functionalized coatings. The functional applications included electrochemical capacitors, an oxygen evolution catalyst, a PH sensor, and a water electrolyzer. Other functional properties, such as superhydrophobicity/superhydrophilicity and electromagnetic properties, have rarely been studied, but these properties have prospects for applications with structural demands. For example, in some cases, electromagnetic shielding, should also provide support. The 3D printed parts should take both the electromagnetic and structural properties into consideration. Other functional fields have

similar requirements, such as oil–water separations.

Unlike normal alloys that must be accompanied by functional films, hard-printing alloys have special functional properties even without further treatment. Metallic glasses (or amorphous alloys) with disordered atomic packing structures have become a research focus in catalyst applications and exhibited advanced catalytic efficiencies [120]. Liang et al. [116] fabricated Fe-based metallic glass (MG) composites with porous structures, which could be reused 45 times in sulfate radical-based reactions. Although the MGs were partially crystallized, MG composites are a suitable material choice if advanced properties can be achieved. There is likely no need to fabricate fully amorphous alloys, and fabricating such alloys is still a problem for AM because crystallization will occur well below the melting point.

2.2.2. Metallic glass and high entropy alloys

MGs (also known as amorphous alloys) and HEAs both show promise for applications in industry due to their unique physical and chemical properties. Crack-free MGs and HEAs are hard-printing materials with typical microstructures, because there are difficulties manufacturing MGs and HEAs using normal fabrication technologies. AM provides new opportunities to expand the applications of MGs and HEAs, which enables them to be fabricated with complicated structures and tailored microstructures.

2.2.2.1. Metallic glasses. MGs have many intrinsic properties due to the randomly packed atoms, including catalytic properties [120,122–127], soft magnetic properties [128,129], corrosion resistances [130], and good mechanical properties [43]. Most AM technologies involve heating and cooling during the fabrication process. However, once the metallic glass is heated to the crystallization temperature, it will begin to crystallize. It is not clear whether MGs and MG composites have better properties [131]. Thus, both MGs and MG composites can be additively manufactured with different properties for various applications.

There are several challenges in the AM of MGs (Fig. 10):

1) Materials of MGs for AM.

Many MGs have been successfully used in AM, including Fe-based [132], Zr-based [42], and Al-based [133] MGs. However, only limited compositions of MGs can be used in AM because AM of MGs can have issues such as cracks [132], non-uniform element concentrations [134], and poor geometries [43].

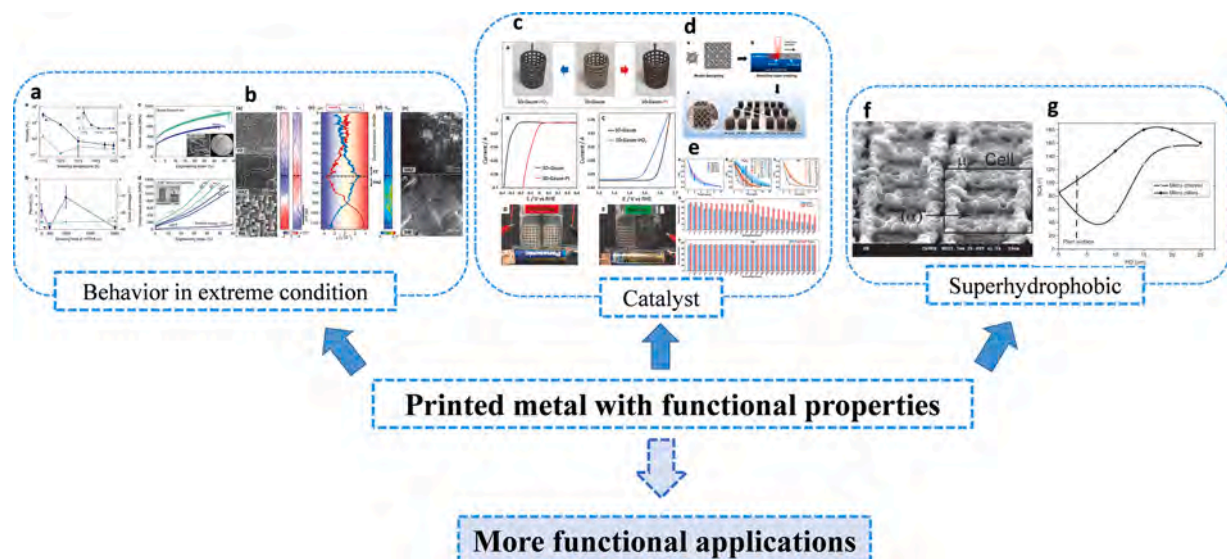


Fig. 9. Development of structural–functional properties: (a, b) behavior in extreme conditions [35,40], (c–e) catalytic materials [116,119], and (f, g) superhydrophobic materials [121].

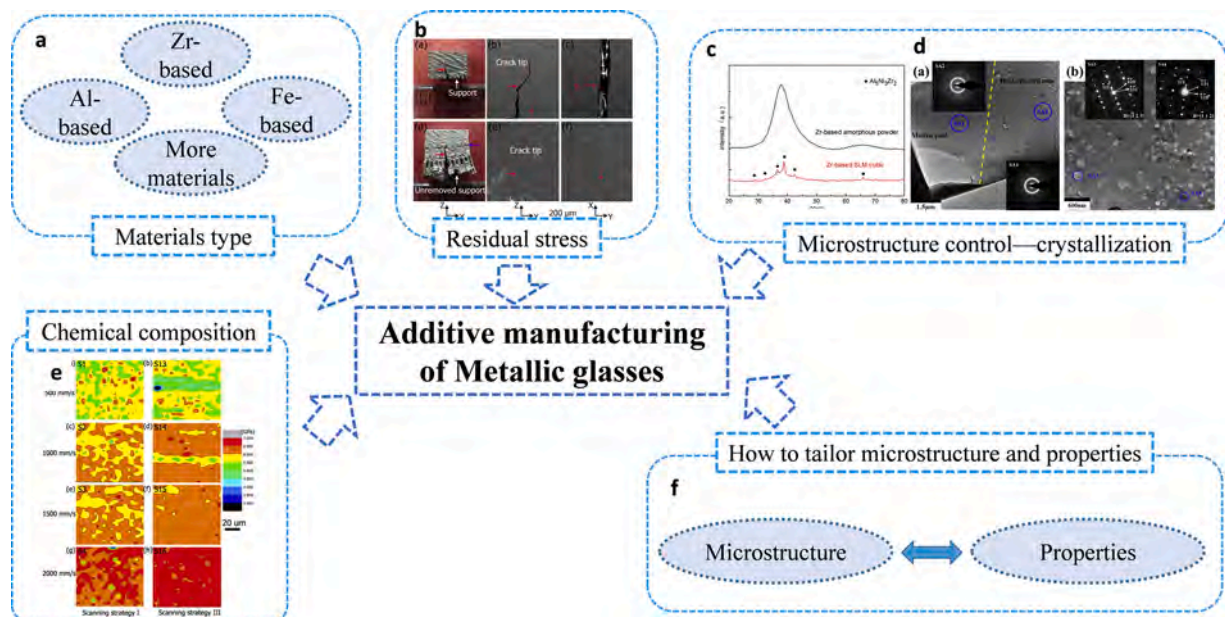


Fig. 10. Challenges of AM of metallic glasses (MGs). (a) materials type, (b) residual stress [133], (c–d) microstructure control during crystallization [43], (e) chemical composition [134], and (f) tailoring of microstructure and properties.

2) Residual stress.

Due to the intrinsic brittleness of metallic glasses, MGs are sensitive to thermally induced residual stresses. The residual stresses induced by phase changes are not discussed for MGs because of their amorphous states. The thermal history from the heat source and thermal gradient cycle will result in thermal stress. Crack-free Zr-based bulk metallic glasses (BMGs) were obtained using current AM technologies [135,136]. However, crack-free Fe-based BMGs have not been fabricated and require further development to override the negative effect of residual stress.

3) Microstructure control during crystallization.

The thermal gradient and thermal cycle will change the heating and cooling rate in the HAZ. Crystallization can be induced, as the critical cooling rates of MGs are generally 10^3 – 10^6 K/s.

4) Chemical composition.

Most AM technologies involve rapid melting and solidification processes. The flow in the molten pool will possibly result in heterogeneity of the chemical elements [134]. This will further change the local composition and the glass-forming abilities of MGs, resulting in crystallization in the MGs.

5) Tailoring microstructures and properties.

Currently, Zr-based MGs are used to achieve desired mechanical properties, while soft magnetic and catalytic properties are achieved using Fe-based MGs. However, few studies have investigated the relationships between the microstructures and various properties. Methods for tailoring the properties and achieving effective fabrication still must be developed.

2.2.2.2. High-entropy alloys. The ability to tune the final properties by selecting the elements from the huge number of combinations of HEA elements is appealing [38]. Two AM technologies, direct laser deposition (DLD) and electron beam melting (EBM), are widely used in the fabrication of HEAs. Unlike BMGs, few studies have focused on the SLM of HEAs [38]. The process parameters are highly related to the quality of the fabricated components. For example, the residual stress can result in cracks [137], but likely increases the tensile and yield strengths [38]. The residual stress, elemental segregation [37], oxygen content [138], and post-treatment [39] are critical for the microstructure and process control. Elemental segregation is induced by chemical heterogeneity, where the element distribution is greatly influenced by thermal

gradients, heating/cooling rates, the melt flow, and the crystallization process [39,139,140].

Current 3D printed metal powders mainly have the same compositions as normal processed HEAs. Not all types of HEAs are suitable for metal AM technology, severely limiting the practical applications and quality of fabricated HEA components [141]. It has been speculated that once the elemental segregation results in a proper elemental ratio, a second-phase-strengthened microstructure can be formed with good properties.

The material properties should be well combined with the process characteristics to develop AM-suitable materials with advanced properties. HEA powders used specifically for AM should be developed to fit the characteristics of AM methods, for example, a material composition that can resist the formation of cracks. Moreover, metal powders of HEAs for AM are generally pre-alloyed or mixed elemental powders. Pre-alloyed powders have been widely investigated in recent studies. However, the mixed elemental powders have a risk of elemental segregation [138]. Kenel et al. [40] utilized oxides as raw materials in ink-based 3D printing followed with reduction sintering, and the fabricated HEAs exhibited a typical HEA microstructure without evident segregation. This may provide a new avenue for the AM of HEAs.

The mechanical properties of additively manufactured HEAs can reach the same values but cannot exceed those of materials fabricated by conventional methods. Joseph et al. [142] reported that DLD-produced $\text{Al}_x\text{CoCrFeNi}$ HEAs had similar yield strengths and ductilities to arc-melted components with similar grain sizes, compositions, and textures. However, the ductilities of these HEAs were much lower than those of the dendritically structured arc-melted samples [142]. Further progress in terms of the mechanical properties should be made to reach or even exceed the properties of materials fabricated by conventional technologies. Additionally, the applications of additively manufactured HEAs should be developed, combining the flexible design capabilities of AM and interesting properties of HEAs.

2.2.3. Precious metals

Au- and Ag-based alloys have almost total reflectivity in the infrared wavelength, unlike the 60%–70% of that of Fe-, Al-, Pd-, Pt-based alloys [143]. Fabricating these materials with AM technologies using laser energy is difficult, as the laser will be reflected, even though Au- and Ag-based precious metals have a low melting temperatures [144]. With

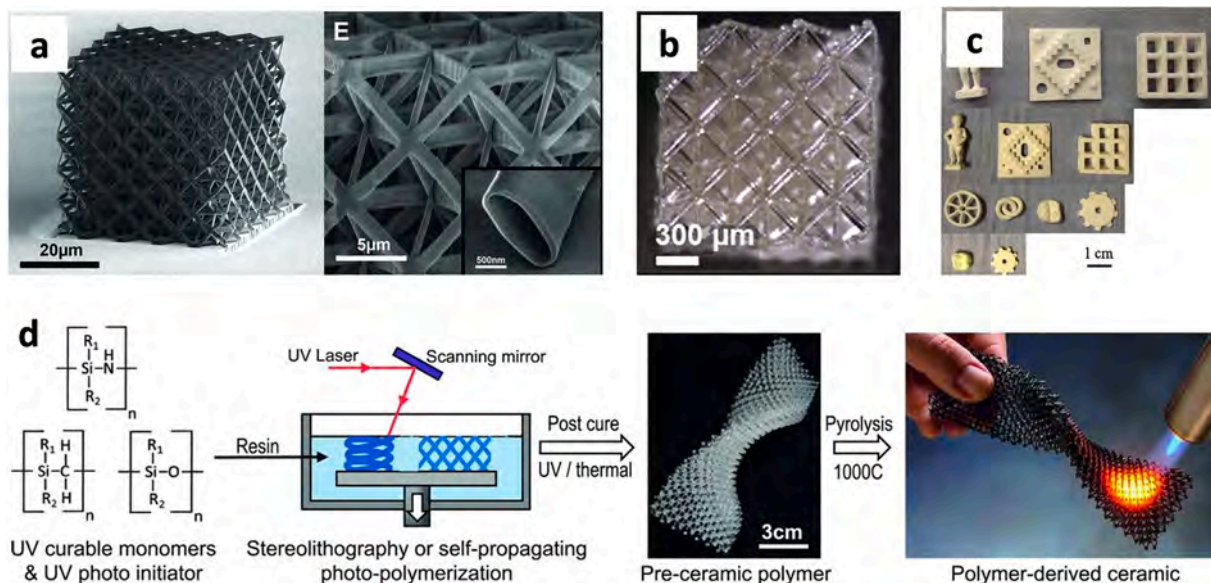


Fig. 11. Examples of some typical ceramic 3D printing techniques. (a and b) 3D printing of small-scale ceramics through coating-film-based ceramic printing feedstocks: (a) hollow-tube Al_2O_3 nanolattice [48]. (b) hollow-tube Al_2O_3 micro-lattice [154]. (c and d) 3D printing of large-scale ceramics: (c) selective laser sintering [151] and (d) stereolithography (SLA)/self-propagating photopolymer wave-guide technology for polymer-derived ceramics [46].

the high reflectivity and the thermal conductivity of Au- and Ag-based alloys, the process window is limited due to the small temperature gradient [144] [145].

Currently, the applications of precious metals are mainly in consumer products, medical applications, and catalysts. There is significant demand for unique or personally designed, commercially produced, high-value-added jewelry and watches composed of Au and Ag. The precious metals can be printed to create jewelry with lower levels of accuracy and control precision compared with those required in the aerospace, automotive, and medical industries [143]. Compared with methods such as casting, which is estimated to be used for 80 % of all jewelry production, AM can produce precious metal components with less material loss and highly complicated structures during fabrication. Fabrication through AM can fulfill the low-volume and rapid response to consumer demand for custom-made, individually designed products [146]. Hence, AM is promising for the jewelry market.

Several methods have been utilized to improve the porosities and strengths of additively manufactured precious metal components, including powder pre-treatment to control the reflectivity [147] and optimizing of the process parameters [145]. Although the mechanical properties of some additively manufactured precious metals are good, gold alloys deposited by laser based powder bed fusion are harder and more brittle than the cast alloys, but the ductility can be increased by 34 % after heat treatment [148]. However, under composition limitations, for example, the Au content should be no less than 75 % to remain attractive to the customer, the porosity and mechanical properties (e.g., strength and wear resistance) of precious metals are relatively low, and this issue remains to be efficiently addressed.

Apart from consumer jewelry products, precious metals are also used in dental restoration. Precious metals have been used for dental restoration for many years because they are easy to manipulate and they exhibit excellent biocompatibilities. The research and application of additively manufactured precious metals have been rarely reported, but the development of this technology for the production of dental copings in porcelain-fused-to-metal crowns is attractive [149].

Precious metals are also used in catalysts, electronics, and electrical contacts due to their special. The studies of precious metals are mainly focused on their catalytic and electrical properties [107]. However, the structural properties of these materials should not be ignored, as these are important for the practical applications of these materials. The

precious metals should have sufficient structural properties to resist complicated environmental conditions.

2.2.4. Perspectives

- 1) Other processes (e.g., casting) and other fields (e.g., machine learning or bionics engineering) can be combined with AM to improve the materials, processes, structures, and properties.
- 2) Multi-functional (but not limited to structural) properties can be developed, and different functional properties can be tailored with advanced structural properties.
- 3) The materials–process–microstructure–property relationship must be understood. High-throughput experimental approaches and multi-scale simulations are important to understand the mechanisms in depth. Machine learning and simulations should be developed in the future, for example, combining the phase-field method for microstructure simulations, FEM for simulating the structural properties, and MD/DFT for simulating the functional properties.
- 4) Further breakthroughs in materials, product size, production efficiency, the full supply chain, and the lifecycle are necessary.
- 5) Applications of MGs, HEAs, and precious metals are promising but require further development in terms of scale and depth, such as basic principles of atom structures, deformation mechanism and industrial applications.

2.3. Additive manufacturing of ceramic materials

2.3.1. Powder/slurry-based ceramic printing feedstocks

Relative to polymers and metals, AM of ceramics is not easy, mainly due to the extremely high melting points of ceramic materials [46] and the challenging preparation of feedstocks [150]. Fig. 11 shows some examples of typical ceramic 3D printing techniques. Ceramic structures are typically made from feedstocks in the form of powders or slurries via various AM methods, including SLS [151], selective laser burn-out [152], SLA [153], projection micro-stereolithography (PμSL) [154], LOM [155], Direct ink writing (DIW) [156], IP [157], FDM [158], and digital light processing (DLP) [159]. Many of these ceramic printing techniques suffer from unavoidable residual porosities and undesirable cracks due to the large thermal gradients, resulting in poor mechanical behaviors of the fabricated ceramic structures. Direct extrusion of

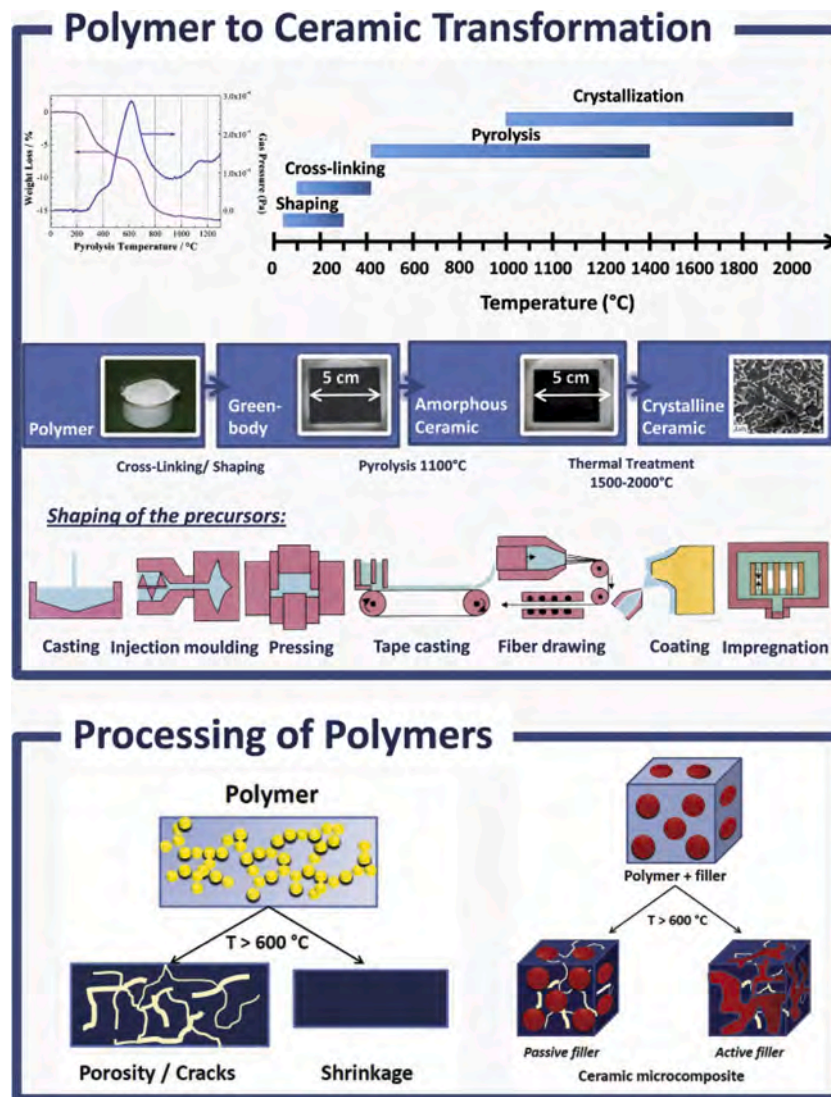


Fig. 12. Polymer-to-ceramic transformation, and effects of fillers in polymer-to-ceramic transformation [169].

melted glass is achieved by processing at over 1000 °C [49], but the huge costs associated with temperature control hinder its applications.

2.3.2. Coating film-based ceramic printing feedstocks

The development of atomic layer deposition enabled the constructions of hollow ceramic nanolattices [48,154,160] or ceramic composite microarchitecture [161] by coating TiN or Al₂O₃ on 3D printed polymer templates. The polymer template can be removed after the coating of ceramic films, resulting in delicate nano-/micro- structures. However, this method is severely limited by slow fabrication rates and microscale dimensions of the fabricated structures.

2.3.3. Polymeric precursor-based ceramic printing feedstocks

AM of preceramic polymers enables tremendous breakthroughs in ceramic processing. Printed polymers can be in-situ converted to ceramics with minor and uniform shrinkage, resulting in complex and precise ceramic architectures. Furthermore, this processing requires considerably less energy than conventional powder or slurry sintering methods because pyrolysis temperatures are relatively lower than sintering temperatures. Some attempts, such as building inverse ceramic structures through infiltration of preceramic precursors into polymer templates [162] or applying a two-photon absorption polymerization process [163] with a preceramic precursor [164,165], pave way for

involving polymer-derived composites in the 3D printing of macroscopic ceramics. Recently, 3D SiOC macroscopic components were obtained via SLA [46,47], self-propagating photo-polymerization technology [46], DIW [166,167], or DLP [168] of siloxane resin systems, with subsequent pyrolysis in an inert atmosphere. AM of ceramic precursors is a novel technology to build complex-shaped ceramic structures.

Polymer-derived ceramics (PDCs), prepared via in-situ thermolysis of preceramic polymers, have enabled tremendous technological breakthroughs in ceramic science for the last five decades [169,170]. PDCs have proven to be promising material candidates for various structural and functional applications [171,172]. Silicon-containing polymers are among the most promising preceramic precursors [173], and these typically include ternary ceramics, such as SiOC [174] and SiCN [175], or multinary ceramics, such as SiCNO [176]. Nanofillers of various types, including ceramics [177,178], metals [179], or polymers, can be added to preceramic polymers before machining, resulting in PDC nanocomposites. These nanofillers can serve as barriers to mass and heat transfer, eliminating the shrinkage upon ceramization [169], and can form jammed network structures in the preceramic polymer matrix to improve the mechanical integrity of the resultant ceramics [180], as shown in Fig. 12. Furthermore, some active fillers can cause reactions during pyrolysis and broadly widen the compositional and functional ranges of PDCs [181]. PDC-nanocomposites exhibit the remarkable

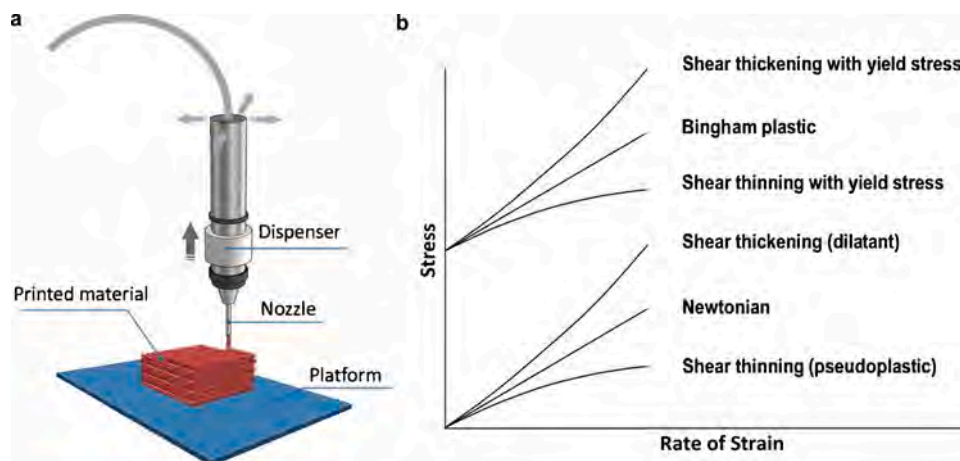


Fig. 13. (a) Schematic diagram of direct ink writing [185]. (b) Classifications of fluids with shear stress as a function of shear rate [188].

properties of conventional ceramics, including high thermal stabilities, chemical resistances to oxidation and corrosion, and mechanical resistances to tribological effects. Moreover, their microstructures and properties are influenced by the chemistries and molecular architectures of the preceramic polymers [175], and the processing methods, and thus, they can be adjusted through tailored polymer systems and heat treatment processes [171].

The effects of NPs on the thermal behaviors of polymers vary with the type and content of reinforcing fillers. These effects are typically referred to as “shielding effects” or “barrier effects.” When inorganic particles are introduced into the polymeric matrix, the particles or clusters can serve as barriers to mass and heat transfer during polymer decomposition [182,183], resulting in enhanced thermal stability of the composites [169]. The polymer-to-ceramic transformation is accompanied by mass loss, linear shrinkage, and the formation of pores/cracks. The introduction of fillers can often lead to better structural retention and mechanical behaviors of the resultant ceramics. Fillers with various types, shapes, and dimensions can be introduced into the polymer matrix. Some fillers are active and react with the products generated during the polymer-to-ceramic transformation. However, some results showed that there was no effect or even an accelerating effect of the NPs on the polymer degradation [184]. Hence the mechanism, which is complicated, remains to be discovered.

DIW is a suitable method for the AM of ceramic precursors that provides freedom to tailor polymer/particle ink systems. The fabrication process of DIW is shown in Fig. 13a, and the most important factor is the printability of the ink. The ink is stored in a temperature-controlled barrel and connected to a nozzle that is fixed on a three-axis platform. The material is extruded from the nozzle and deposited on the substrate through a screw extrusion or pneumatic pressure control system [185]. The printer can build a structure layer by layer by analyzing the model slices and G-code [186]. The printing parameters (pressure and speed) and the printing environment (temperature and ink media) affect the DIW process significantly [187]. Only if the ink is equipped with proper printing parameters and environments can a stable structure be successfully built. The best feature of the DIW technology is that it has a variety of optional materials. Not only can it be used for metals, ceramics, polymers, and hydrogels, it can also print composite materials, biological cells, and food. The ink must be carefully designed for deposition and stable extrusion from the nozzle without clogging. In particular, three aspects must be considered. First, the ink must exhibit a significant shear thinning effect, as shown in Fig. 13b [188]. The pseudoplasticity of the ink can allow the ink to be squeezed out smoothly. Second, the ink should have good viscoelasticity to ensure that the printed structure can maintain a stable shape after extrusion and not collapse layer by layer. Finally, the higher solid content of the ink

can weaken the volume and shape shrinkage that occur during subsequent curing [189].

Liu et al. [45] developed the first ceramic 4D printing system, in which elastic ceramic precursors were printed, deformed, and transformed into rigid ceramic structures, as shown in Fig. 14. A shape-morphing process could be achieved by releasing the elastic energy stored in the pre-strained ceramic precursors, which could be stretched to over a 200 % strain [45]. The above-described work on 4D printing of elastomer-derived ceramics (EDCs) could provide novel methods for soft/rigid hybrid structural materials, which could drive innovation for the application of ceramic precursor/ceramic hybrid systems in versatile fields, including bioimplants and bio-inspired structures [190].

2.3.4. Perspectives

In future studies, PDCs and EDCs will play an increasingly important role in AM of ceramic structures. Ceramic 3D printing will get larger and faster, with the development of novel printing material systems, printing strategies, and post-processing techniques, as demonstrated by two representative recent studies in Fig. 15. Ceramic 4D printing will embrace new material systems, such as shape-memory materials, to get more tunable, precise, and practical. Moreover, the combination of additive, subtractive, and equal material manufacturing, will offer tremendous research and industrial opportunities for the study on ceramic printing technologies.

2.4. Additive manufacturing of glasses

The history of glass manufacturing dates back to the ancient Egyptian period [192]. As glass has excellent optical transparency, mechanical properties, thermal resistance, chemical resistance, chemical tunability, and electrical insulating properties [192–195], it is one of the most important materials, and it exhibits high performance in daily life and industrial manufacturing. The oldest glass fabricating method is kiln glass making [194]. Glass powders or raw materials are shaped in a mold and heated at moderate temperatures. The glass grains then stick together and keep their intrinsic sandy characteristics. Later, the grains melt together, yielding a smooth structure that depends on the heating temperature and duration [193]. The first industrial revolution introduced automation and resulted in an increase in the production efficiency, which changed the blowing and casting processes, improving the quality of glass products [192]. Although mechanization and automation have improved the performance, quality, and production efficiency of glass products compared with traditional manual glass manufacturing process, the geometries of the glass produced by these methods are mainly symmetric and flat. The manufacture of complex-shaped glasses

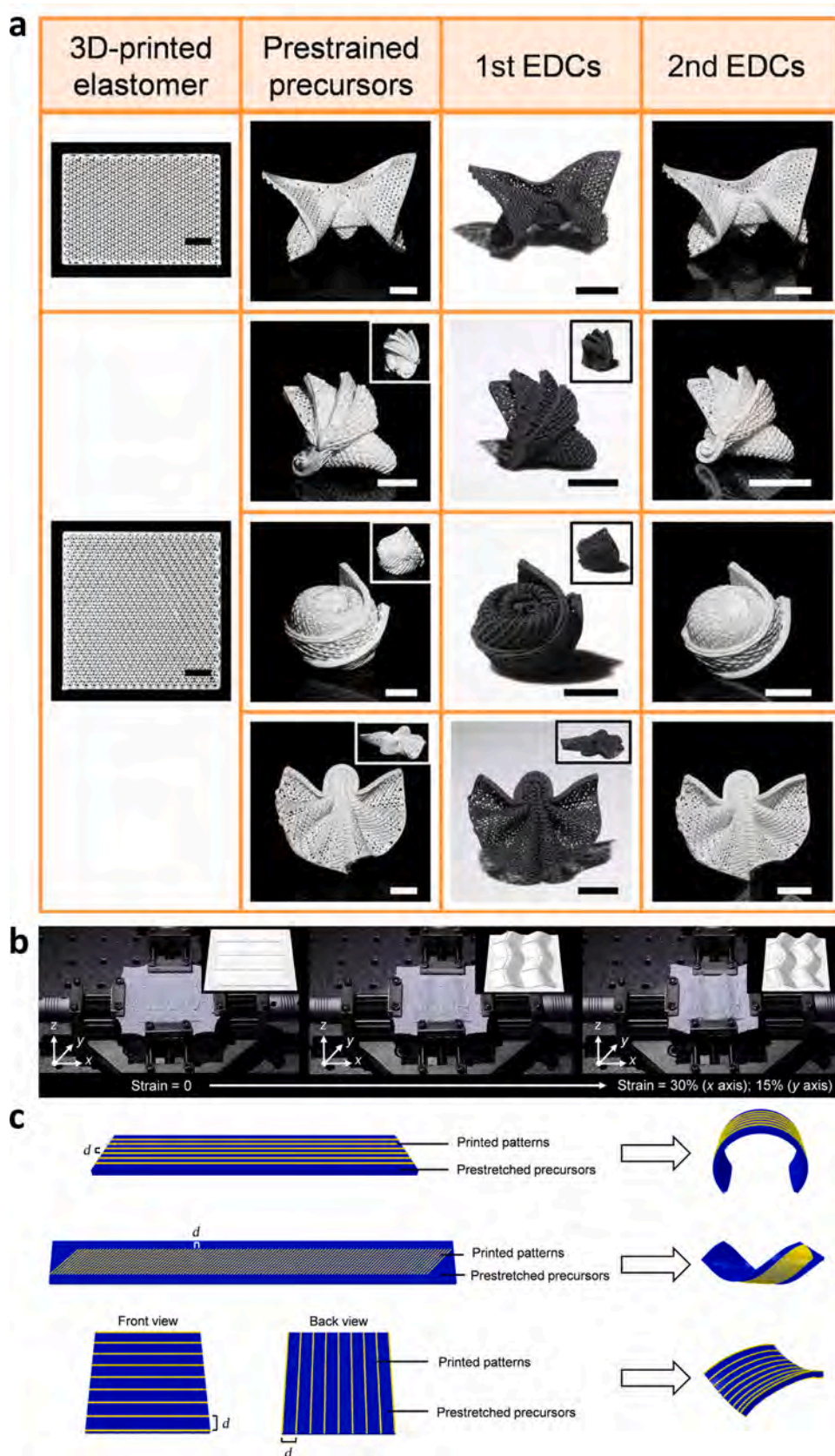


Fig. 14. Origami and 4D printing of elastomer-derived ceramics (EDCs). (a) ceramic origami. (b and c) two representative ceramic 4D printing methods (scalebars: 1 cm) [45].

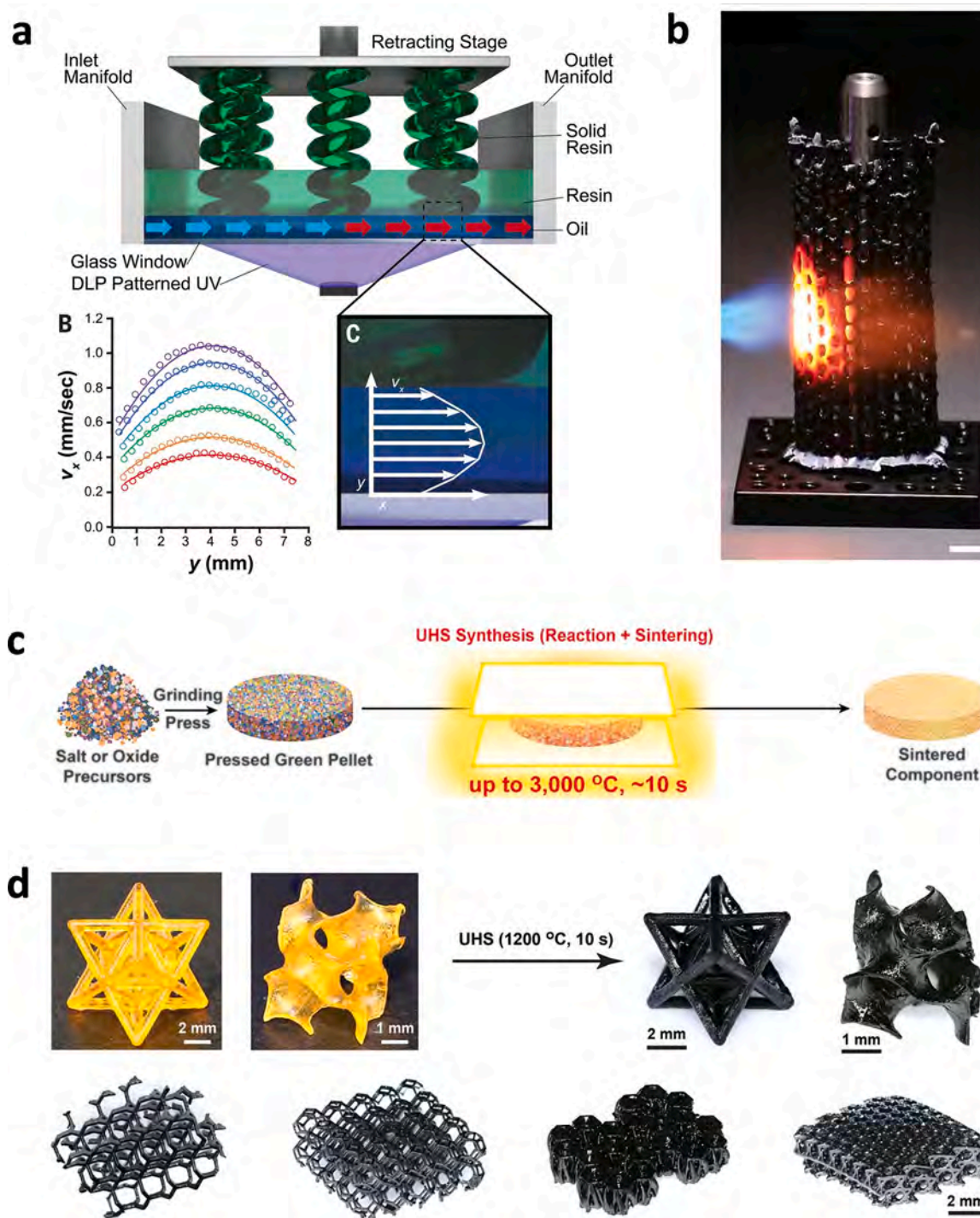


Fig. 15. Trends for 3D printing of polymer-derived ceramics (PDCs). (a and b) Ceramic 3D printing gets larger [6]: (a) schematic of the high-area rapid printing (HARP) process. (b) large-scale polymer-derived SiC structures using HARP method. (c and d) Ceramic 3D printing gets faster [191]: (c) schematic of the ultrafast high-temperature sintering (UHS) synthesis process. (d) SiOC samples derived from polymer precursors and complex-shaped ceramic structures using UHS synthesis process.

is still severely limited.

The advent of 3D printing technologies has opened a new door for the fabrication of complex-shaped products in a fully digital manufacturing process, as shown in Fig. 16. Technically, for glass products, 3D printing can combine the modern industrial automation processes with even higher geometric complexity than those manufactured by manual products. However, glass products, especially high-purity glasses, are usually difficult to fabricate, requiring high temperatures and long melting times and casting processes to obtain a final

product with a microstructure and mechanical properties that meet the requirements [197]. These drawbacks greatly restrict the development of glass manufacturing processes. Thus, researchers are working to solve the above problems to try to manufacture transparent glass by 3D printing methods. Typically, three methods are used, described below.

2.4.1. High-temperature depositing approach

This is a simple and useful method that upgrades the traditional glass manufacturing process to a 3D printing process, usually in two ways.

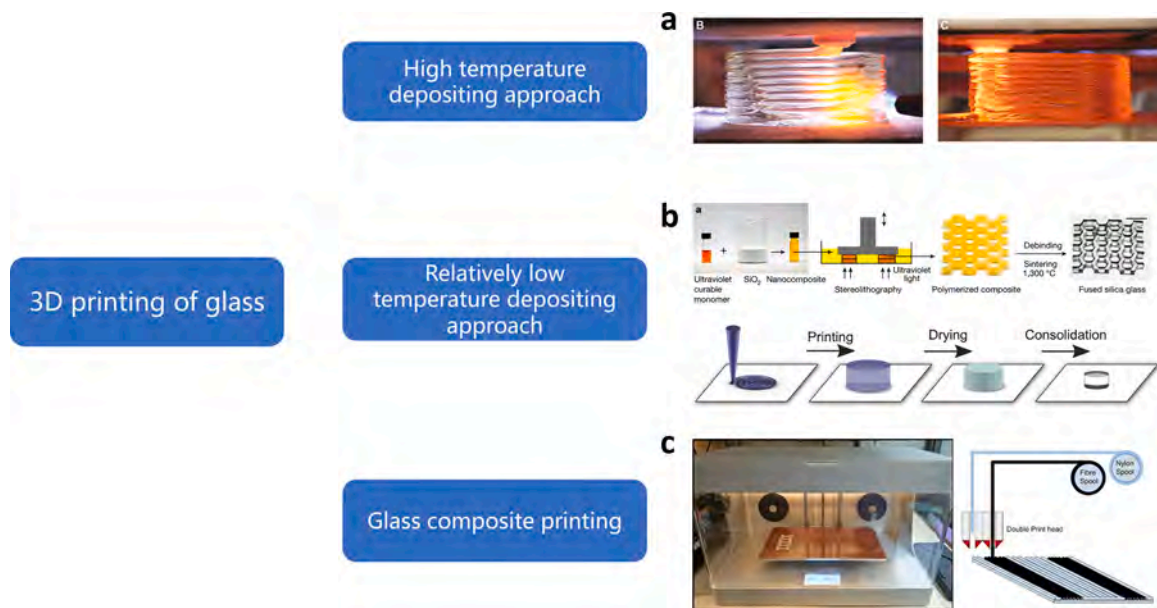


Fig. 16. Approaches of 3D printing glass: (a) direct heating method [49], (b) stereolithography [14] and direct ink writing [50], and (c) fused deposition modeling method [196].

First, heating the glass materials to above its softening point to a flowable state and depositing at the same temperature [49,198]. Second, feeding glass powder into a laser beam equipment or a specific heating equipment for heating and forming [198–202]. For the first route, the key point is to control the viscosity and thermal expansion coefficients of the glass flow, both of which are closely correlated to the heating temperature. Selecting the appropriate heating temperature according to the glass composition can ensure the glass fluid flow stably and avoid bubble formation inside final products. For commercial glass, such as soda-lime glass and silica glass, the softening temperatures are typically within the range of 500–1600 °C, if the heating temperature is relatively high (exceeding 1000 °C), annealing process is also needed to release residual stress and enhance mechanical performance. Furthermore, researchers found that applying BJ approaches could overcome the requirements of the high melting temperatures and high viscosities of the fused glasses [198,200]. For the second route, the heat treatment process is usually more complicated, since the powder feed is heated instantaneously by the high-power laser and then rapidly cooled. Extra binder should be added into the original materials to strengthen and stabilize the printed structure. Since internal defects might be introduced by the binder during heat treatment, a series of segmented heating processes are used to eliminate internal defects and ensure the strength of the printed glass products. After printing, at least one low temperature stage for the de-binding (depending on the type of binder, usually below 500 °C) is needed, and one high temperature stage for formation and homogenization [201]. But for SLM, glass powder can be spread on the powder bed and directly heated by the laser to bond together without adding additional binder. However, glass produced by high-temperature printing approach has significant drawbacks, such as incomplete densification, relatively low transparency, and fragility. Research has shown that the introduction of heated build chambers and nozzle kilns can alleviate these problems [49]. Furthermore, studies have also shown that using a CO₂ laser to melt the glass wire feed through the SLM process [199,202] can produce transparent glass products with higher strength and density. For this kind of 3D printing glass, how to increase printing resolution and its density, and reduce internal defects and surface roughness should be the main focus in the future.

2.4.2. Relatively low temperature printing approach

Another solution for glass 3D printing is printing silica glass at low temperatures (below glass transition temperature) by dispersing silica powders in organic monomer or polymer solvents and then sintering at high temperatures (above glass transition temperature) [14,50–52,203]. At first, methods such as inkjet printing (IP) or direct writing could only be used to manufacture opaque or low-transparency glass products [198, 204]. Later, Rapp and his team first tried printing glass at low temperatures by SLA [14]. They designed a kind of nanocomposite with silica nanoparticles and a monomeric matrix. The slurry was then mixed, and free radical polymerization occurred, resulting in the precursor. Transparent silica glass products were obtained after sintering and de-binding of the precursor at 1300 °C. The resulting glass was dense and fully amorphous. Meanwhile, glass printing by SLA also has the advantages of high precision and the ability to form smooth surfaces. These outstanding performances made the products very suitable for optical and microelectromechanical system (MEMS) applications. Furthermore, researchers have developed some solution-based compositions, for example, a kind of hybrid ceramic precursor [52] or a type of alkoxide inorganic resin [50]. This could avoid the mixing process for silica particles and organic polymers, making them easier to print by commercial DLP printers. This process was conducted within an aqueous medium to avoid the use of some hazardous solvents, and it achieved control of the transparent glass density, allowing the refractive index of the resulting glass to be controlled. Another advantage of DLP is that the exposure can be controlled on the voxel scale by adjusting the greyscale in the target layer, which can only be achieved by the residence time of the laser. The resulting products can be translucent or transparent. Furthermore, this method provides a solution for fabricating complex glass composites from a variety of materials, such as Si-O-Al and Si-O-P [50,52], or functional glass products [205] from simple solutions.

The DIW method is another glass 3D printing fabrication process with a higher printing speed and resolution compared with the fabrication methods for fused silica. A suspension of hydrophilic fumed silica nanoparticles is prepared, in which the fumed silica is used as the silica source for glass formation and also the thixotropic agent for the ink [50]. The key point of successful glass DIW printing is to precisely control the yield stress of the ink to be suitable for glass printing. Preparing a series of germania-silica inks by a sol-gel based method and printing through DIW technology can yield optical glass with a gradient index [203].

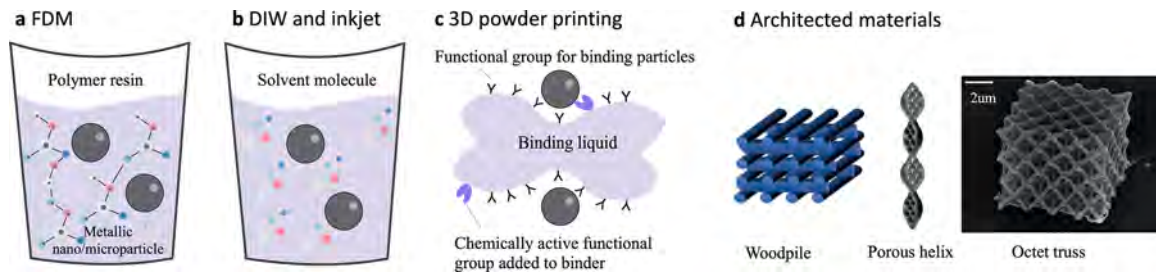


Fig. 17. Overview of metallic nano/microparticles used in various additive manufacturing techniques: (a) polymer–metal filaments in fused deposition modeling, (b) water-based metal inks in direct ink writing and inkjet printing, (c) UV-curable metal resin in stereolithography and 3D powder printing, (d) representative metallic architectures for the catalyst. Right: octet truss of nickel nanolattice after pyrolysis [44,208].

However, for the DIW method, the problem of shrinkage is present. Determining how to prevent the shrinkage of the final DIW glass and further improve the printing accuracy is the main work of future studies.

2.4.3. Glass composite materials

Unlike the methods described above, some scientists have attempted to print glass composites instead of pure silica glass. Related research showed that glass-fiber-reinforced polymers printed by the FDM process [196] and UV-assisted three-dimensional printing process [206] have tensile strengths and elastic moduli, especially glass-fiber-reinforced nylon composites. The printing temperature of FDM is usually under 300 °C, based on the melting point of the main phase material. It should be noted that glass and glass fibers in the process of printing composite materials usually act as reinforcement for the polymers [207]. This provides a concept for the production of new materials that have similar properties to those of glass.

2.4.4. Applications

Compared with traditional craft, 3D printing provides more possibilities in structural design of glass products, especially for ornaments and jewelry. High-quality transparent glass components can be fabricated by 3D printing with precise control over shape, size and structure at low cost [14,204]. 3D printing even allows higher degree of freedom customization, such as gradient density in specific area, determined inner porosity and different colors [49,51,203,205]. In another aspect, 3D printing optical components also evolved. Traditional optical devices are usually manufactured in a fixed mold, which greatly limits the accuracy and complexity of the device. Due to the development of 3D

printing, novel optical devices with new/more functions have emerged without sacrificing transparency and strength, such as gradient-index optics and microfluidic devices [50,52]. In conclusion, due to the precise control of 3D printing, glass products with novel and creative structures can be produced without compromising the quality compared with traditional glass, its advantages on structural design and precise control can provide more creativity, and researchers may pay more attention to optical components at the microscopic scale in future.

2.4.5. Perspectives

The development trends and study emphasis for glass AM mainly focus on the following aspects. (1) The printing speed and accuracy must be improved, which is also the bottleneck of 3D printing technology itself. (2) The smoothness degrees of the surfaces and structures must be improved. Because the application of glass largely depends on its light transmittance, fabricating glass products with more complex shapes and more uniform structures is very important for practical applications, especially in communications and telecommunications, in the future. (3) The manufacturing difficulties and costs must be improved. As described above, glass 3D printing is still in the early stages of investigation. How to use simpler equipment and processes to make glass or glass composites is a key element to greatly increase the value of 3D printed glass technology, not only for artwork displays.

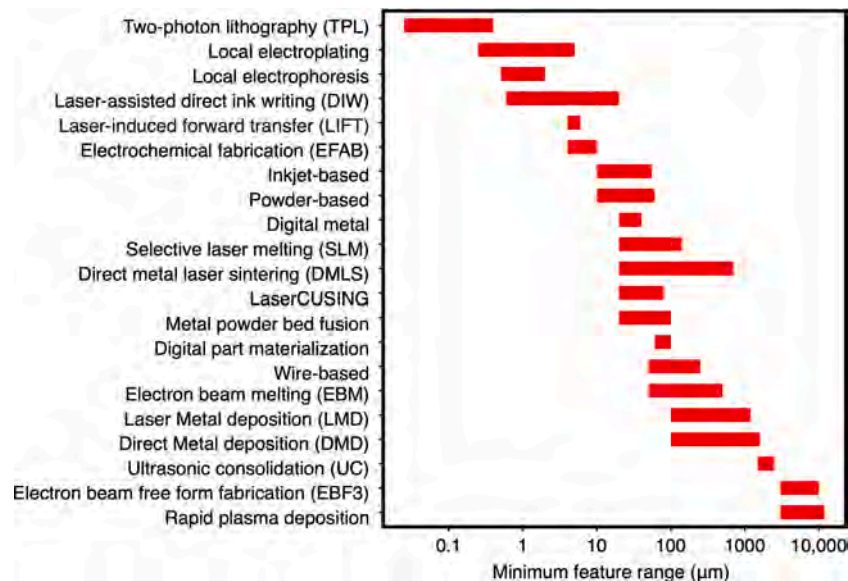


Fig. 18. Comparison of the minimum feature sizes in metal printing via various AM technologies [44,208,213–219].

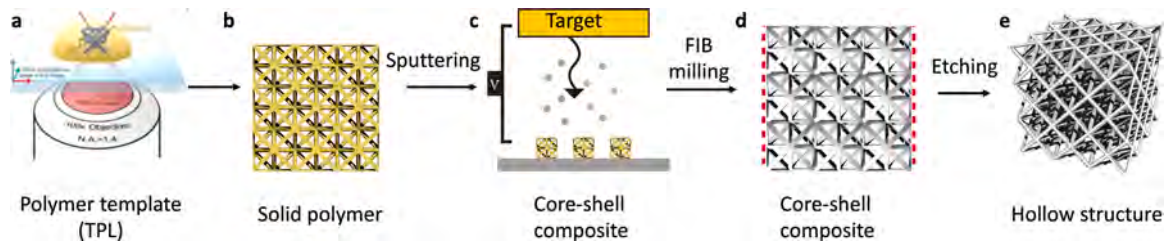


Fig. 19. Schematic of the fabrication process for hierarchical polymer–metal composites: (a–c) surface coating of metals on 3D printed polymers and (d–e) hollow-beam metallic architected material.

2.5. Materials for hybrid printing

2.5.1. Polymer–metal composites

2.5.1.1. 3D printing of polymer–metal composite feedstocks. Polymer–metal feedstocks are metal particles mixed with a liquid polymer resin (an unsaturated polyester) in the form of water-based substances with increased viscosities. Fig. 17 shows different strategies for forming robust architectures of polymer–metal hybrid materials via various 3D printing techniques [208]. Metal filaments and water-based metallic ink can be extruded through the nozzle in specific environments, such as high-temperature environments, and quickly solidified upon cooling or further sintering in a furnace (Fig. 17a and b). The photo-hardening polymers usually contain liquid polymer resin, a crosslinking agent, an initiator, and a photosensitizer so that they can be cured by UV light. The binding liquid can therefore glue the metallic particles together in a powder (Fig. 17c). Such 3D printed objects containing metallic nano-/microparticles have been widely used in the production of catalytic and mechanically robust architected materials (Fig. 17d).

In addition to polymer–metal feedstocks, metal–polymer composites can also be obtained using 3D printed metal as a skeleton and then filled with polymers. This will lead to two significant improvements: increased conductivity in functional applications and enhanced mechanical properties. The synergistic effect of the composite material can effectively disperse energy and lead to a great increase in fracture toughness, especially when traditional 3D printed parts contain imperfections due

to the manufacturing process [209]. The stiffness contrast between the soft and hard phases can be tailored to increase the fracture toughness in the architected materials. The base material for polymers is typically epoxy because of its excellent strength and simple processing. Bapari et al. [210] revealed that the soft phase played an important role in enhancing the rigidity in metal–particulate polymer composites. Li et al. [211] revealed the mechanisms of the interpenetrating phase composites (IPC) in SLM-fabricated metallic micro-lattices. Experiments and simulation models revealed that the uniform deformation of reinforced struts required higher energy than the buckling of freestanding struts.

Printed objects that take advantage of polymers and metals always result in interesting mechanical and functional properties. Though metal–polymer blends cannot be used to rapidly manufacture objects that require high mechanical strengths, considerable work has been performed to explore new classes of materials. Fafenrot and co-workers found polymer–metal feedstocks mostly containing bronze had significantly reduced mechanical properties [212]. Zhu et al. [107] reported hierarchical nanoporous gold with engineered nonrandom macro-architectures via DIW and dealloying techniques. The printed nanoporous metals exhibited markedly improved mass transport properties and reaction rates for liquids and gases. Vyatskikh et al. [44] developed a lithography-based process to achieve complex 3D nano-architected metals with approximately 100-nm resolution, breaking the limitation of approximately 20- to 50- μm resolution of most existing methods for 3D printed metals. Fig. 18 summarizes the most recent minimum feature range in different 3D printing techniques for

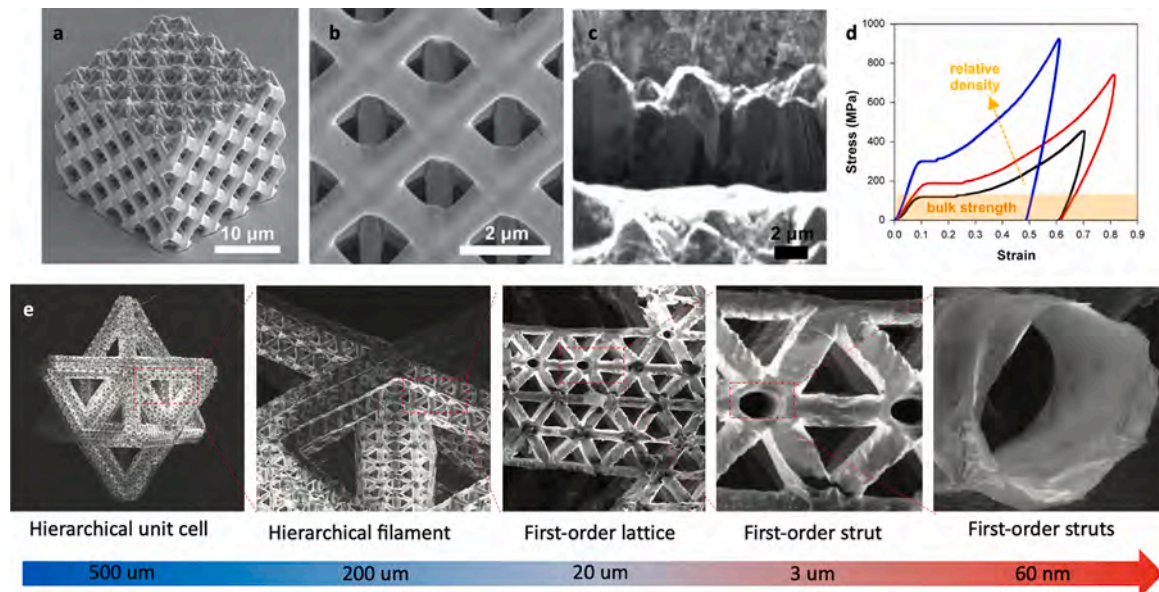


Fig. 20. Hierarchical polymer–metal composites from mesoscale to microscale: (a, b) core-shell Cu meso-lattices, fabricated via two-photon lithography and subsequent electroplating, (c) cross-sectional Cu film milling by focused ion beam, (d) stress–strain curve of core-shell Cu lattice, indicating that the compressive yield strengths of the meso-lattice with octet geometry exceeded its monolithic bulk counterparts [220], and (e) hierarchical metamaterial of Ni micro-lattices that comprised periodic hollow tubes, with the critical feature length scales spanning seven orders of magnitude [223].

metals. The metal objects built from the primary polymer–metal feedstocks usually require sintering to achieve full stability, and they are widely used in medical and aerospace applications.

2.5.1.2. Surface coating of metals on 3D-printed polymers. Nature is particularly adept at developing strong and ductile materials by creating gradient or multi-scale hierarchical materials. Hence, a class of biological layered lattice materials containing several levels of hierarchical structures from the microscale to the nanoscale has been developed. These lightweight mechanical metamaterials exhibit high mechanical strengths by virtue of the “smaller is stronger” size effects from nanoscale components and optimized geometries. Moreover, the special architectures enable unusual mechanical behaviors, for example, twisting or expanding in all directions under uniaxial compression, which cannot be achieved with traditional materials. Many works on architected materials mimic the features of natural structural material to create core–shell composites with plastic but soft polymer cores and a layer of ultra-strong but brittle metallic or MG coatings (Fig. 19a–c). There are many examples of 3D printed trusses, with the feature sizes spanning multiple orders of magnitude, from tens of millimeters to hundreds of nanometers (Fig. 20). Cu octet lattices have achieved a specific strengths of around 400 MPa, and the yield strengths surpassed the bulk counterparts by 80 % (Fig. 20a–d) [220]. We attributed such a high strength of the core–shell metallic lattice to a size effect of the material, which was a single crystalline metal with a submicron size. These results provide insights and an understanding of the mechanical properties by exploiting the hierarchical structure and material design.

The main goal of current studies is to enable the hierarchical polymer–metal composites to achieve astonishing stiffnesses, strengths, and toughness values at very low densities. The challenge is to strike a balance between structure-dominated buckling failure and metal-dominated brittle failure. For example, polymeric octet lattices with strut diameters of 1 μm that were coated with 10-nm NiB metallic film showed delayed buckling.

The elastic buckling allowed for pronounced rotation of the nodes and led to a ductile-like deformation. In contrast, thicker coatings, for example, 100 nm, resulted in brittle failure [221]. The brittle failure also depends on the type of metal and architecture. When substituting HEAs, the film thickness can reach up to 50 nm and overcome the strength – recoverability trade-off ; ; at the same time [222]. Though thicker coatings can better confine the polymer core, the optimal coating thickness was identified to be 14–50 nm to evade catastrophic failure. To harness the “smaller/thinner is more ductile” size effect, it is critical to design novel architectures and explore strong but ductile metallic films. One of the most common methods for architecture design is to etch away the plastic core to obtain a pure, ultra-lightweight metal (Fig. 19d–e). The hollow-beam nickel lattice with a near-constant specific strength exhibited a high tensile elasticity (> 20 %), which could not be achieved for the metallic constituents [223] (Fig. 20e). Future research directions should address both scientific and technological challenges, such as the strength and ductility trade-off [48] and the speed and resolution trade-off [8]. Besides seeking high strengths with very low densities and setting new boundaries in the material-property space, novel designs for innovative materials, such as chiral mechanical metamaterials and materials with tunable mechanical properties and programmable stimulus responses, are just beginning to emerge. To deploy this new class of materials in multi-functional engineering applications, physical models or theories are needed to capture the architectural complexity, and proliferate the superb properties from the nano/microscale to the macroscale.

2.5.2. Polymer–ceramic composites

2.5.2.1. 3D printing of polymer–ceramic composite feedstocks. The feedstock materials for the 3D printing of polymer–ceramic composites

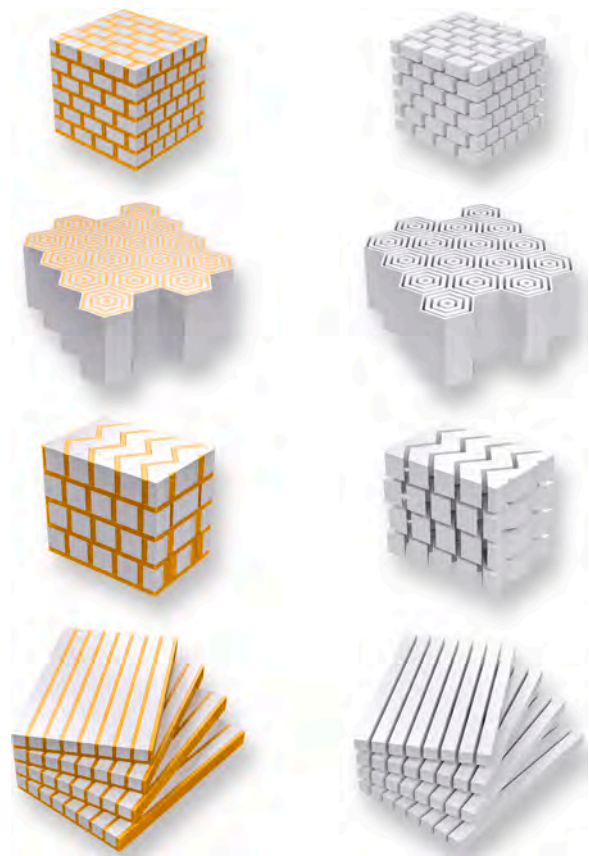


Fig. 21. Mimicking structures of nacre [245], bone osteon [246], dactyl club [247], and conch shell from top to bottom. The left column mimicking structures consist of hard ceramics skeletons (the white) and soft polymer phases (the yellow). The right is the corresponding skeletons of the left.

mainly included ceramics [224], resins [225], and their combinations [226]. Based on the material form, these materials are divided into two types: inks or pastes and fine ceramic particles. Inks/pastes are in a liquid or semi-liquid form. The feedstocks consist of a liquid/paste resin and dispersed fine ceramic particles. Depending on the viscosities of the inks or pastes, the slurry can be 3D printed by methods of photopolymerization, inkjet printing, and extrusion [13]. Fine ceramic particles are bonded by either a powder fusion and melting process by a heat source, such as a laser, or by viscous liquid binders, such as un-hydroxyl resin and liquid paraffin. This kind of feedstock can be 3D printed by either BJ, SLS, or SLM techniques [13].

2.5.2.2. Multi-material printing of polymer–ceramic composite structures. High strength and toughness values are two basic requirements for almost all engineering materials, but they are typically mutually exclusive [227]. For instance, the strength of steel can be improved by cold machining, but this strengthening always results in a loss in toughness. Similarly, engineering ceramics are much harder and stronger than metals. However, their application is limited by their low toughness values [228]. Recently, researchers have reported that natural bio-ceramics, such as bones [229] or shells [230], have unusual combinations of strength and toughness. Inspired by the natural ceramics, many fabrication techniques have emerged to mimic bio-ceramics, such as the ice templating [231], layer-by-layer deposition [232–234], self-assembly [235], and rapid prototyping [236]. These studies demonstrate the toughness–strength tradeoff achieved by preparing architected composites with well-organized microstructures. For example, mimicking the nacre-like structures of shells, ceramic laminations are pressed into interdigitated configurations to improve the

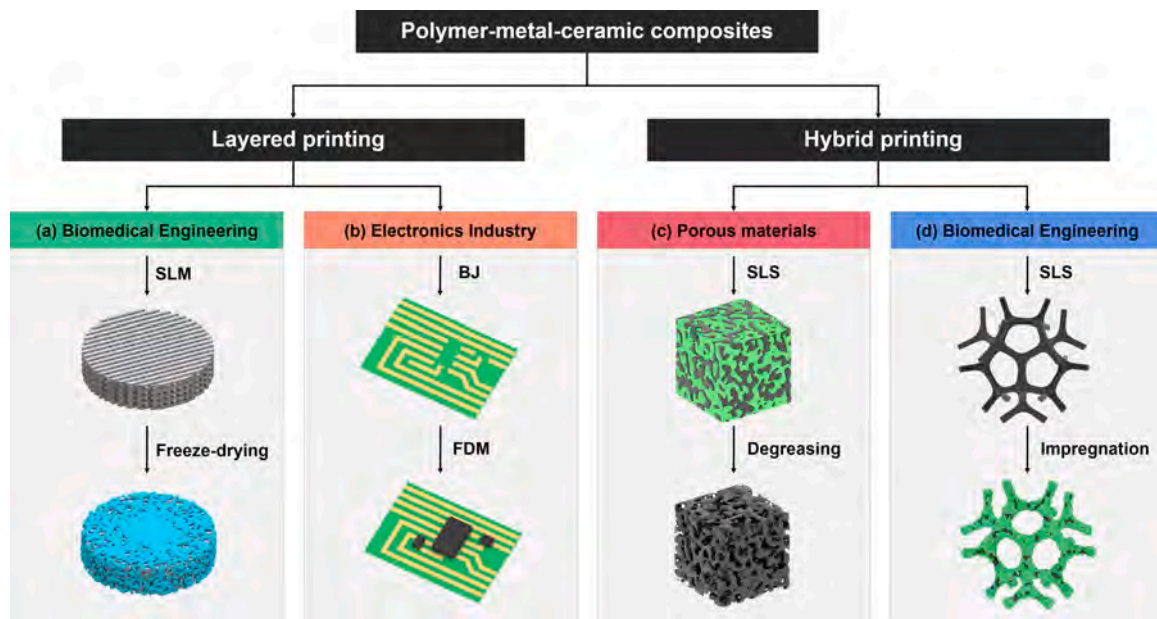


Fig. 22. Application and development prospects of polymer-metal-ceramic composites.

toughness hundreds of times compared with monolithic ceramics [231, 237]. These ceramics fabricated by traditional manufacturing processes, such as pressing and sintering [237] and layer-by-layer deposition [234, 238], generally do not possess the same toughness values observed in natural materials. In fact, natural bio-ceramics have arbitrary geometries and hierarchical structures from the nanoscale to the macroscale [239,240]. Traditional manufacturing processes use top-down approaches, where the desired material is formed from the reduction of the bulk material or by bulk solidification, making it difficult to generate hierarchies across many length scales [241].

Recently, 3D printing has made the fabrication of microstructures with hierarchical or arbitrary geometries possible, and these methods utilize a bottom-up approach analogous to processes that occur in nature. Therefore, the study of bio-ceramics has been largely promoted [28,242–244]. For instance, using a multi-material 3D printer, staggered microstructures mimicking bones [244] were printed. The fracture energy of this material increased more than ten times. In addition, 3D printing methods have been used to mimic the structure of nacre [245], bone osteon [246], dactyl club [247], and conch shell [248], as shown in Fig. 21, to uncover the precise designs in bio-ceramics. A structure mimicking the dactyl club produced a J-shaped R-curve (crack growth resistance curve), while others produced Γ -shaped R-curves. The J-shaped R-curve showed a larger critical energy release rate, which was beneficial for crack arresting. Conversely, the Γ -shaped R-curve exhibited a higher critical failure stress and hindered crack initiation [249]. Furthermore, with the assistance of magnetic fields, the magnetic platelet directions could be guided to form designed shapes [249], such as concentric, layered patterns. Thus, 3D printing methods provide the capabilities to prepare intricate designs to investigate the geometric effects on the mechanical performance, especially the toughness, in bio-ceramics.

Based on the development trends of polymer-ceramic composites, the following are important future research directions. (1) Multi-nozzle printing. Multi-nozzle printing enables the simultaneous printing of polymers and ceramics, which overcomes the compounding of materials with huge differences in melting points. (2) New polymers research and development. New polymers can effectively improve the performances of polymer-ceramic composites. High-temperature-resistant polymers can achieve polymer-ceramic co-sintering.

2.5.3. Metal-ceramic composites

The materials of metal-ceramic composites have high moduli, high strengths, good resistances to high-temperature conditions, and other excellent properties. They have become increasingly important in modern high-tech applications, and they are applied in emerging and traditional industrial fields as a kind of base materials. They are also an indispensable part of the development of modern national defense. Due to the difficulties of the metal-ceramic interface bonding, there are few mature technologies for metal-ceramic 3D printing, and this subject still needs far more research. The most common way is to prepare metal/ceramic ink for 3D printing. This printed ink must be vaporized, plasticized, debonded, and sintered to obtain the desired material. The Fraunhofer Institute for Ceramic Technologies and Systems [250] has developed ceramic and metal powder mixed suspensions for metal-ceramic composite printing. Ceramic/metal powders are mixed in a low-melting thermoplastic binder that melts into a liquid at 80 °C. During the printing process, the melted binder mixed with ceramic/metallic powder material is deposited as droplets. After deposition, the droplets rapidly cool and harden, allowing 3D objects to be printed.

2.5.4. Polymer-metal-ceramic composites

Printing materials are gradually becoming key factors in expanding the application field of 3D printing technology. In recent years, it has become a trend to increase the proportion of composite materials to meet the complex working conditions of the printed products. The composite materials commonly used in 3D printing technology are metal/ceramic, polymer/ceramic, and polymer/metal. However, with the continuous development of “intelligent manufacturing” based on 3D printing, the materials of printing pieces often require the combination of metals, ceramics, and polymers to meet their various performance requirements [251].

At present, although the research on composite 3D printing of metals, ceramics, and polymers is still in its infancy, there are some reports about its application in biomedical, electronics, surface engineering, and other fields. There are two kinds of methods for printing composite materials: layered powder printing and mixed powder printing.

In layered printing, the material is gradually printed into samples. For the repair of bone tissue with a load-bearing function, porous scaffolds are usually printed with metal materials, and the bio-ceramic-polymer coating is constructed on the surface (Fig. 22a) [252]. This

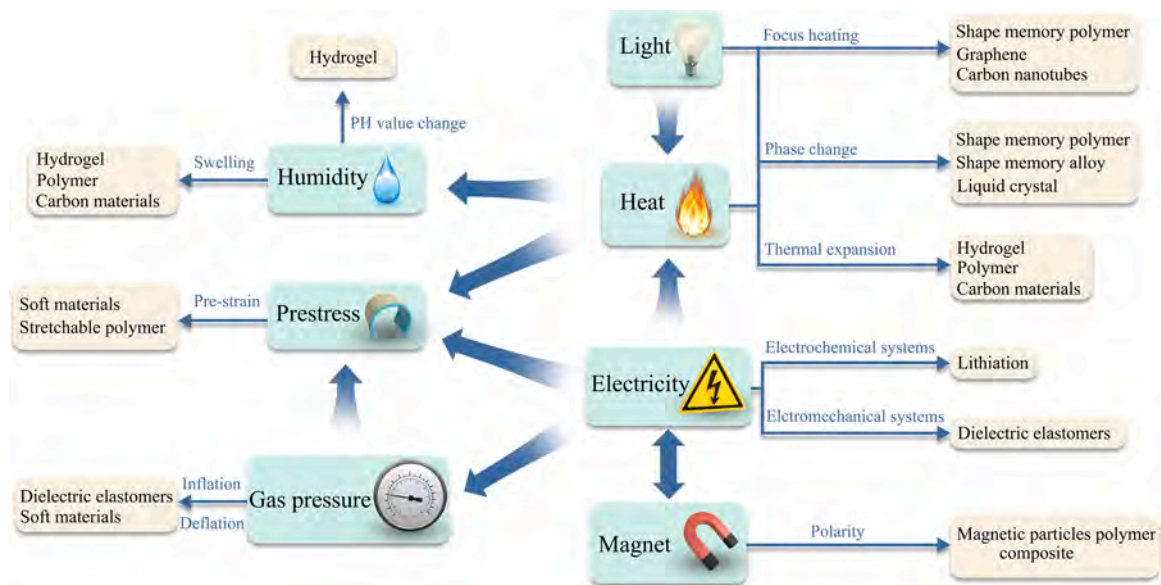


Fig. 23. Relationships between various stimuli.

kind of bone tissue made of metal, ceramic and polymer has the advantages of mechanical matching with natural bone, good corrosion resistance and good biocompatibility. Electronic devices can also be directly manufactured by 3D printing technology and usually must have suitable conductive, insulating, heat dissipating, and other properties [253]. For example, printed circuit boards (PCBs) usually require metal, ceramic, and polymer materials for manufacturing. The PCB is printed with metal material first, and then the capacitor and other parts are printed with ceramics and polymer materials directly on the PCB (Fig. 22b).

In mixed powder printing, most often, metal/ceramic/polymer powders are prepared by mechanical mixing, and then a polymer material is removed during the SLS process to produce a porous material (Fig. 22c). In addition, the initial porous embryos formed by SLS are infiltrated by another material to form a composite material to improve the density and mechanical properties (Fig. 22d). For repairing non-bearing bone tissue, bone tissue is usually printed with calcium phosphate and hydroxyapatite (HA) composite biocompatible polymers [254]. Furthermore, magnesium is evenly compounded into artificial bone during the printing process, which can further enhance the osteoinductive activity and osteoacoustic performance [255].

In electronics, medicine, and other industries, other key parts or products require the combination of the properties of metals, ceramics, and polymers. The traditional process of preparing such parts is usually cumbersome and expensive. However, through 3D printing technology, complex parts can be formed once without multiple processes. This rapid manufacturing method will have an important role due to the lower cost and efficiency. However, the 3D printing technology at this stage cannot support its widespread application in the manufacturing of such multi-material components, and printable materials are also relatively lacking. Thus, this subject requires further research.

3. 4D printing

Although various responsive materials and external stimuli mechanisms exist [291,292], relationships and connections between them can be summarized (Fig. 23). This scheme can provide new inspiration for the design and fabrication of multi-responsive actuators. These advanced smart structures are anticipated to optimize the next generation of soft robotics, and more responsive materials fabricated by AM technology will be exploited in all kinds of applications (Table 3).

3.1. Heat-driven 4D printing

3.1.1. Shape-memory-polymer-based material systems

Heat-actuated polymers can be divided into two main types: soft [256,257,261] and rigid [263,264], depending on their mechanical properties at room temperature. Poly(N-isopropyl acrylamide) (PNIPAM) is a typical soft hydrogel with a lower critical solution temperature (LCST) of about 37 °C, which has been extensively studied as a 3D printing thermal responsive material [258–260]. Gladman et al. [293] reported composite a PNIPAM hydrogel structure that was programmed with anisotropic swelling deformation regulated by the alignment of nano-fibrillated cellulose along the designed printing direction. The printed flower morphologies enabled the transfer from a complex 3D shape to a flat state (Fig. 24a) when the temperature changes. Naficy et al. [294] designed and printed a multi-material actuator with bilayer structures by DIW. The printed 2D structure swelled to a controllable 3D structure and back to a flat state at high temperatures (Fig. 24b). Liquid crystal elastomers (LCEs) have attracted considerable interest in recent years due to its thermal response properties. Ren et al. [295] reported heat-triggered shape-morphing LCE structures fabricated by a DIW technique. Programmable deformation, such as popping-up, self-assembly, oscillations, and snake-like curling, was achieved by regulating the printing speed and path (Fig. 24c).

In addition, some researchers have assembled rigid and soft materials into one structure. Ding et al. [296] created a direct 4D printing technique using the commercial materials TangoBlack + or Tango + as the elastomer and VeroClear as the shape memory polymer (SMP). The compressive strain was introduced during photopolymerization. Upon heating, the residual strain was released, leading to a new permanent shape, which could be reprogrammed into multiple subsequent shapes, as shown in Fig. 24d. Fig. 24e shows the rapid bending and unbending behaviors of a DIW printed thermally responsive epoxy. The epoxy material showed excellent mechanical properties and great printability [263].

Combining heat sensitive polymers with 3D printing, various impressive structures have been developed and show diverse deformation under external stimuli [297–299]. Furthermore, many 3D printable thermal responsive polymers have been created and show fast responses and robust deformation abilities. In the future, heat-stimuli-responsive micro/nanoscale structures with good mechanical properties and response performances will be further explored and will reveal the flexibility and versatility of heat-driven 4D printing.

Table 3
Comparison of 4D printing techniques driven with various stimuli.

Stimuli	Materials	AM technology	Response speed	Advantages	Disadvantages	Applications	References
Heat	PNIPAM	DIW, DLP, SLA	Ms-h	Biocompatibility, high water content, low response temperature	Poor mechanical properties	Biosensors, actuators, soft robotics, bioelectrodes, responsive electronic devices, bio-fabrication	[256,257,258,259,260]
	Agarose/poly (acrylamide)	DIW		Biocompatibility, high modulus	High-temperature printing		[261]
	Polyacrylic acid	DLP/PμSL		Tunable mechanical properties, high precision		Metamaterial	[262]
	Di-glycidyl ether of bisphenol-A	DIW		High mechanical performances		Actuator	[263]
	PLA	FDM	~1 min	Subject to compressive loading		Actuator	[264]
	LCE	IP, DIW	~3 min	High elastic energy density	Slow response	Soft actuator	[265]
	SMP	SLA	~30 s	Low cost	Slow response, sensitive to thermal noise	Soft actuator	[266]
Magnet	SMP, SMA, Hydrogel	DIW, IP, DED, SLM, SEBM	Ms-min	Readily available, low cost	Slow response speed	Aerospace, biomedical implants, soft actuators	[267,268]
	Polymer magnetic composite	DIW, DLP, FDM	Ms	Untethered and wireless control, excellent biocompatibility	Reactive nature concern, frequency control, visualization problem	Soft robotics, minimally invasive surgery	[269,270,271,272,273,274,275,276]
	Chitin	DIW	< 1 min	Robust and fast deformation	2D film structures		[277]
Liquid	PEGDA	DLP	< 1 min	Rapid response	2D film structures		[278]
	Polyacrylic acid	FLDW	< 500 ms	Small scale	Poor mechanical property	Drug delivery	[279]
	Polyacrylic acid/poly (acrylamide) Hydroxyethyl acrylate/hydroxyethyl methacrylate	DIW DLP	< 1 min	High output force Fast fabrication	2D film structures 2D film structures	Actuator	[280] [281]
Electricity	Silicon-lithium alloy	TPL		High controllability, high stability, high reversibility		Tunable phononic crystals, bio-implantable devices	[282,283,284]
	Dielectric elastomers	DIW	~1 s	High elastic energy density, high longevity, fast response	High operating voltage, low power density	Soft actuator	[285]
Light	Graphene, CNTs, LCE, SMP	DIW, FDM, MPL	Ms	Fast response, wireless control, accurate focusing, sustainable	Wavelength limitations, biological toxicity, penetration depth	Soft actuators and robotics, biomedical applications	[286]
Gas pressure	Shore 73A addition cure silicone, thermoplastic polyurethane	FDM	~2 min	Lightweight, rapidly deployable and cost efficient structures	Constrained to only a few key soft mechanic components	Bio-robotic devices, furniture	[287,288,289]
Prestress	PDMS/ceramic nanoparticle composites	DIW		Low cost, high Mechanical performance		3D ceramic structure fabrication	[45]
Multi-drive	SMA, various stimuli materials	DIW, SLA, FDM	Ms-min	Adaptability to various environments	Complex control mechanisms	Soft actuators, medical devices	[290]

3.1.2. Shape-memory-alloy-based material systems

Shape memory alloys (SMAs) are another major category of heat-responsive materials. As shown in Fig. 25, when an SMA is heated, it begins to transform from the martensite phase to the austenite phase [300]. The shape transformation temperature range for SMA materials is very large, ranging from -40 to 900 °C. The biomedical, aerospace, and automotive fields are the three main application fields of SMA materials [300]. Nitinol (nickel-titanium or Ni-Ti) is the most commonly used SMA due to its good superelasticity, low stiffness, excellent shape memory effect, biocompatibility, and corrosion resistance [301,302]. Various AM technologies have been applied in the manufacturing process of Ni-Ti SMAs, including direct energy deposition (DED), SLM [302,303], selective electron beam melting (SEBM), and laser powder bed fusion (LPBF) [304]. The high-temperature NiTi SMA shows tremendous potential in the automotive and aerospace industries due to its morphing

capabilities and heat resistance [267]. SLM was used to manufacture components from NiTiHf powder, and the transformation temperature of this material was above 200 °C [267]. In the biomedical field, SMAs are also applied widely, such as for shape memory stent implants and artificial muscles, due to the excellent biocompatibilities and mechanical properties of Ti and Ni. In addition to NiTi alloys, the AM of Cu-Al-Ni-Mn SMAs by SLM was also studied [268].

3.2. Magnet-driven 4D printing

AM technologies and various stimuli provide tremendous possibilities for the design and fabrication of smart structural materials, such as soft robots [305,306], controlled grippers, and programmable shape change patterns. However, complex mechanisms and control principles hinder the development and application of smart structures, especially

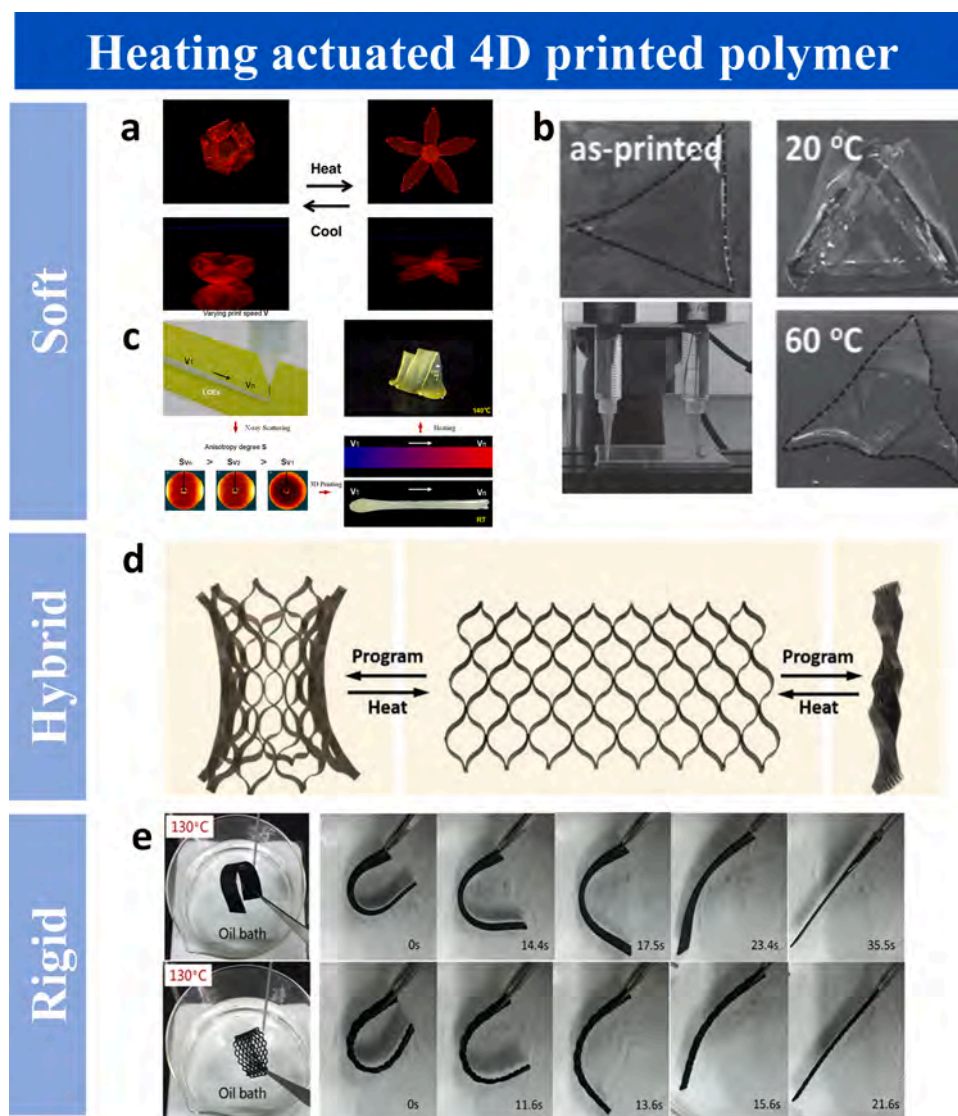


Fig. 24. Shape memory polymer driven by heating: (a) shear-induced alignment of cellulose fibrils during printing can be used to achieve different deformations upon actuation [293], (b) multi-material printed 2D structure deformed into 3D structure at high temperature [294], (c) 4D printed LCE structures [295], (d) lattice structures printed by direct 4D printing technique [296], and (e) 4D printed commercial epoxy [263].

under harsh environmental conditions. Compared with the other stimuli mentioned in this work, magnetic-field-driven smart materials can achieve untethered remote and wireless movement control [307–310], which broadens the applications of these structures in enclosed and narrow environments. Furthermore, delicate control and excellent biocompatibility for living organisms are preconditions for biomedical and therapeutic use. An alternating magnetic field can also be used to induce temperature changes, which can achieve the shape morphing of heat-sensitive materials [310].

3.2.1. Printed magnetically driven smart structures by polymer-derived materials

Various AM technologies and materials have been reported for magnetic-driven smart structures. DIW [269–274], DLP [311,312] and FDM [313] are widely used for the printing of complicated shapes and microstructures. 4D magnetic butterfly structures [269,314] (Fig. 26a) and a 4D flower-like magnetic actuator [271] were printed by doping magnetic particles inside silicon rubber with the DIW method, and simple motions could be achieved and controlled under an external magnetic field. A 3D printed soft filament mesh, as shown in Fig. 26b, could be programmed to achieve isotropic/anisotropic contraction

[270], which could promote the development of soft robots on the water surface and active tissue scaffolds. A magnetically responsive material with tunable mechanical properties [311] and a multi-material magnetic gripper [312] were printed by the DLP method. Zhang et al. [313] printed PLA and PLA/Fe₃O₄ composite filaments by the FDM method, which exhibited a shape memory effect and great potential in the biomedical applications.

3.2.2. Bio-inspired magnetically driven smart structures

Recently, bio-inspired structures and soft robotics have attracted considerable interest not only due to their improved motion and excellent environmental adaptabilities but also because they have better human-interaction capacities and could be safer compared to traditional rigid robotics. Magnetic fields and AM technology allow the design of actuators and soft robotics with biomimetic structures, such as the structures of spirulina cells [308], butterflies [269,314], caterpillars [309,317], starfish (Fig. 26c) [315], and jellyfish [318], and various motions and functionalities have been achieved. Erina et al. [309] reported an inchworm-inspired soft robot that was directly printed by a projection stereolithography technique. Linear locomotion and crawling at a speed of 1.67 mm/s could be achieved under magnetic actuation.

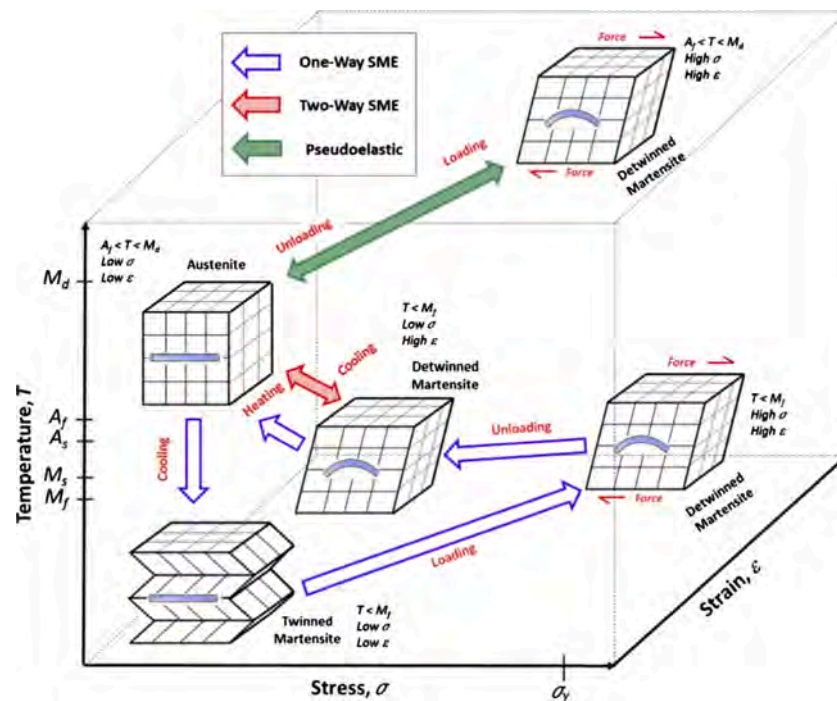


Fig. 25. Shape memory alloy phases and crystal structures [300].

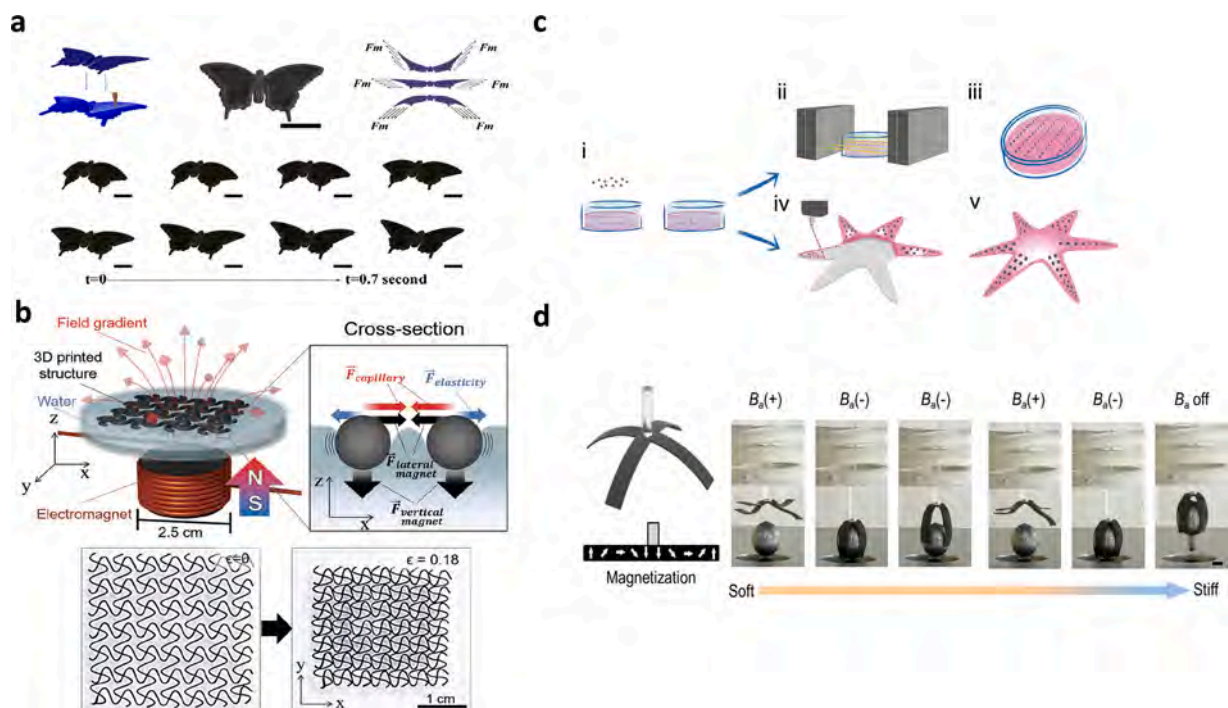


Fig. 26. Magnetically driven smart structures using polymer-derived materials and bio-inspired magnetic designs: (a) 4D magnetic butterfly structure [269], (b) 3D printed soft filament meshes [270], (c) starfish-like hydrogel actuator [315], and (d) magnetic gripper with shape memory effect [316].

Another starfish-like actuator was fabricated by aligning the iron oxide particles inside a gelatin methacryloyl hybrid matrix. Combined with bioprinting technology, magnetic-responsive heterogeneous structures with complex shapes were obtained. Further experiments on aligning the structures showed anisotropic cell guidance effect and the induction of cell differentiation. Thus, this material shows potential applications in novel hydrogel devices [315].

3.2.3. Oriented magnetically driven smart structures

In addition to the homogeneous magnetic structures mentioned above, magnetic assisted printing can align the magnetic polarities of particles inside a matrix to reinforce mechanical architectures [319]. Orientated magnetic polarity patterns have also been studied, which show much more complex and programmable shape transformations. Zhao et al. [273] reported programmed polarity patterns based on the DIW printing of polymer composites containing NdFeB particles. The

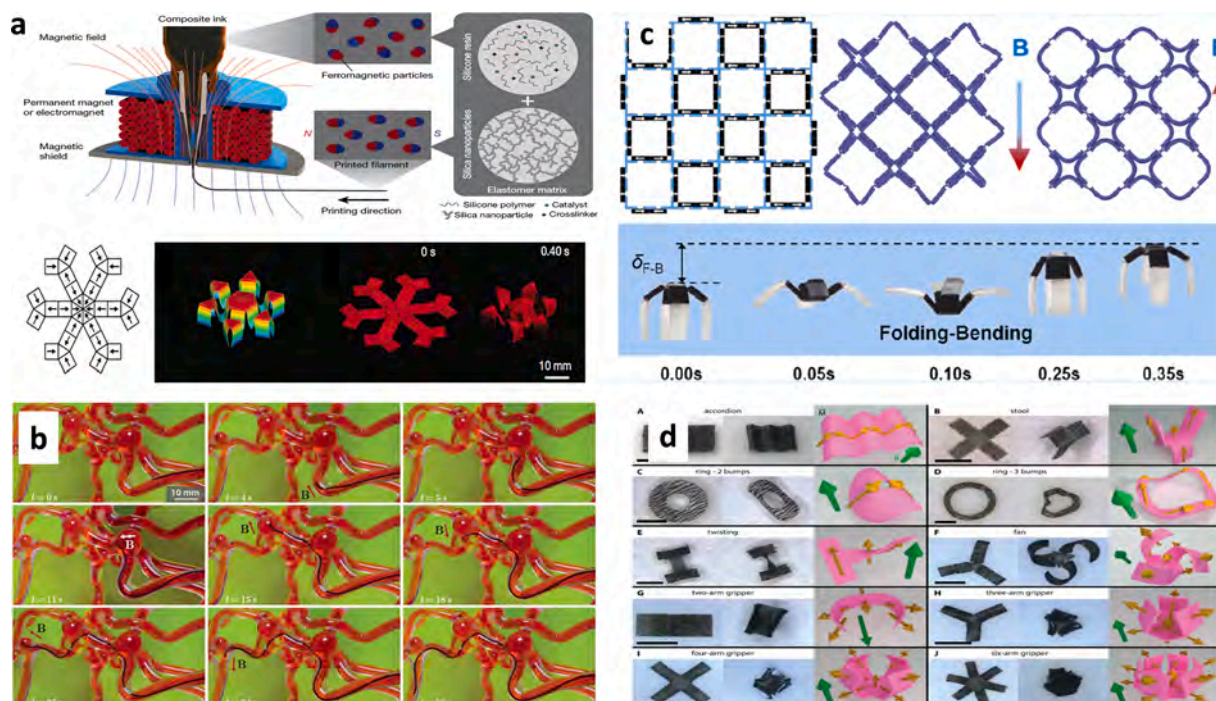


Fig. 27. Oriented magnetically driven smart structures: (a) oriented magnetic polarity patterns based on DIW method [273], (b) oriented continuum soft robot with hydrogel coating [272], (c) symmetry-breaking magnetic actuation mechanism for soft robotics [274], and (d) micrometer-scale magnetic elastic robots [321].

polarities of the particles inside the printing alignment were reoriented by an applied magnetic field around the printing nozzle, as shown in Fig. 27a. A set of pre-designed shape transformations and diverse functionalities, such as soft electronics and mechanical materials with negative Poisson's ratios, were achieved. Furthermore, the same group reported an oriented continuum soft robot with a hydrogel coating, as shown in Fig. 27b [272]. The navigation and active steering abilities of this robot may have applications in minimally invasive surgery. Other than these soft patterns with large sizes, small-size, magnetically oriented patterns from the micrometer to the millimeter scale were also developed. A millimeter-scale soft robot that could perform multiple motions was fabricated by an oriented magnetization process [320], and micrometer-scale magnetic-elastic robots (Fig. 27d) prepared based on a UV lithography method [321] were also reported. At even smaller scales, robots controlled by nanomagnets [275,276] and reconfigured ferromagnetic liquid droplets [322] promote applications of oriented magnetic materials in micro-systems.

Despite these merits of magnetic responsive materials, some drawbacks still exist. Their reactive nature remains a concern, and the frequency of the external magnetic field should be controlled in a safe range to avoid possible harm to living tissue. In addition, the visualization of magnetically responsive actuators in vivo should also be studied. More efforts will be focused on these issues in the near future. Increasing the use of actuators and soft robotics in various fields can yield a higher efficiency and better safety.

3.3. Electrically driven 4D printing

3.3.1. Electrochemically driven 4D printing

The fourth dimension of additive manufacture indicates that the 3D structures can respond to environmental stimuli, resulting in changes in the structure or material properties. The 4D printing structures that have been reported are responsive to external stimuli, such as thermal stimuli and magnetic fields. Smart structures printed using electromechanical materials can be driven by electric fields directly.

Electrochemical lithiation, an unfavorable phenomenon that occurs in lithium-ion batteries, has unique applications in electrically driven 4D

printing. Because of the huge volume changes of materials induced by Li-ion insertion/extraction, silicon electrodes suffer from severe mechanical loads during service. To protect Si materials from failure, honeycombs have been adopted as an optimum structure to improve the storage capacities of electrodes, as shown as Fig. 28a [282]. Bhandakkar et al. [283] investigated the severe morphological changes in honeycomb-like silicon electrodes, as shown in Fig. 28b. They indicated that the buckling of silicon electrodes in honeycomb structures effectively reduces mechanical stresses. Based on buckling analysis of silicon honeycomb electrodes, Greer et al. [284] extended the electrochemical lithiation to the field of 4D printing via two-photon lithography (TPL) technology. As indicated in Fig. 28c, 3D, silicon-coated, tetragonal micro-lattices were developed that converted to sinusoidal patterns via cooperative beam buckling in response to electrochemical lithiation.

3.3.2. Electromechanically driven 4D printing

Dielectric elastomers are soft electromechanical materials that exhibit high efficiencies and fast actuation rates. Many reported dielectric elastomer actuators were fabricated by planar methods. This fabrication method limits the structure-changing modes. Chortos et al. [285] obtained a contractile actuation mode by DIW dielectric elastomer actuators. The printed interdigitated vertical electrodes were printed in a dielectric matrix to form a sandwich structure, as shown as Fig. 29a and b. A representative dielectric elastomer actuator with 16 segments showed an actuation strain up to 9 % and breakdown fields of $25 \text{ V } \mu\text{m}^{-1}$.

3.3.3. Electrothermally driven 4D printing

Heat-sensitive SMPs are polymers that can switch shapes between a temporary state and an initial state in the presence of heat. The heat generated via electrical energy was introduced to 4D printing shape-morphing structures [323]. Zarek et al. [266] fabricated complex shape-memory structures and a custom-made heating resin bath using a SLA printer, as shown as Fig. 30a. The thermally driven switch was proposed by printing a circuit on the shape memory structures. As a demonstration of electrothermally driven 4D printed structures, a shape memory connector closed an electrical circuit when a voltage was

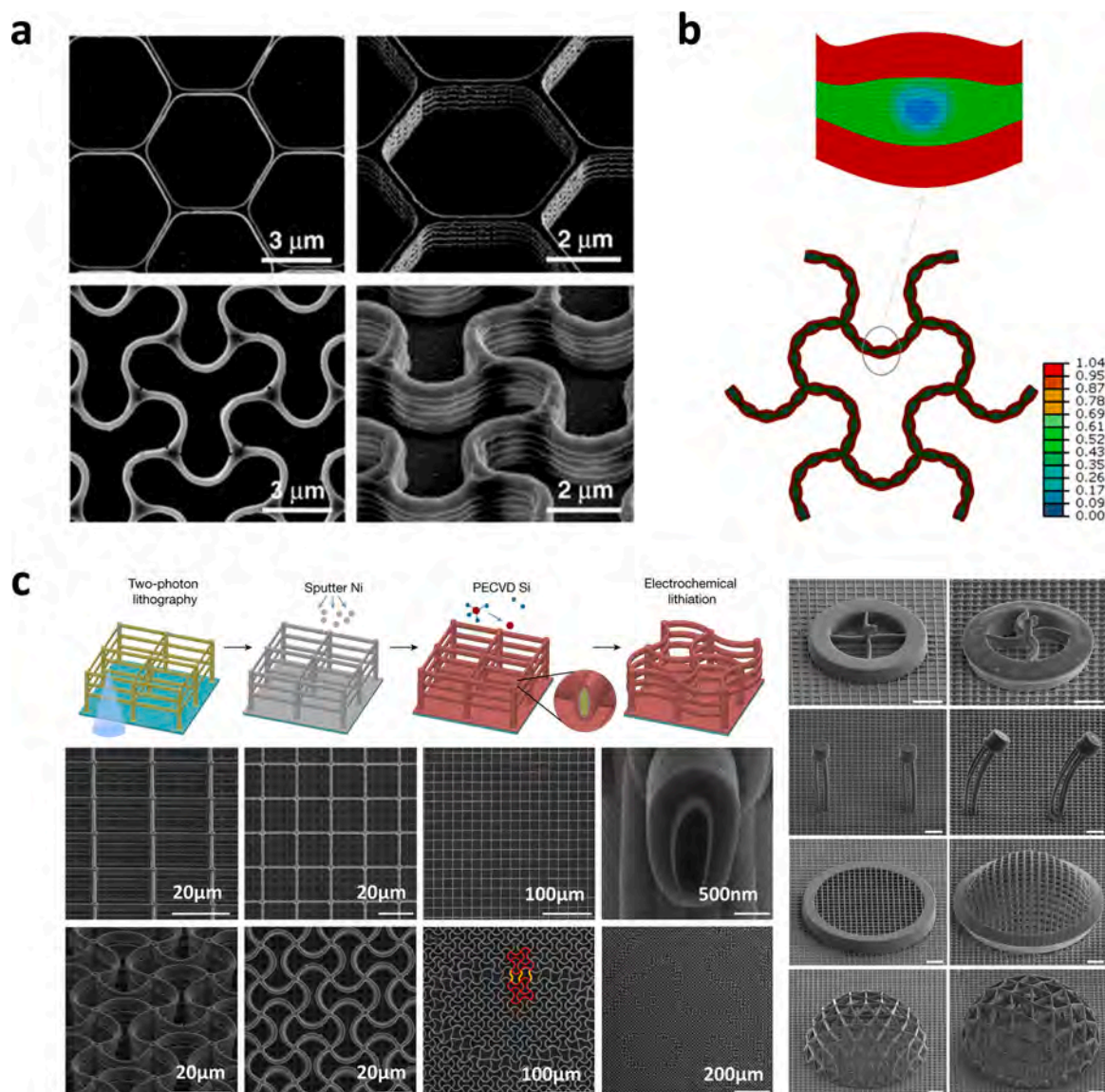


Fig. 28. Electrochemically driven 4D printed structures: (a) as-prepared and morphological changes of silicon honeycombs electrode [282], (b) buckling-like deformation in the electrode unit cell [283], (c) fabrication process and scanning electron microscopy images of electrochemically driven micro-lattices and micro-architectures [284] (scalebars of micro-architectures are 15 μm).

applied.

LCEs activated by heat are regarded as potential materials for electrothermally driven 4D printing. Yuan et al. [265] achieved soft actuators by IP and DIW printing technology. 3D printed single-sided LCE composite structures were activated by Joule heating produced by embedded conductive wires, as shown in Fig. 30b. The thermally driven shape morphing ability originates from the anisotropic–isotropic phase transition behavior. The uniaxial deformation of the LCE ribbon equipped the printed composite with a bending driving force. The composite structure broadened its application in laminated hinges and soft crawlers.

3.4. Liquid-driven 4D printing

Many 4D printed samples are triggered in liquid environments by various stimuli, such as humidity, ethanol, ions, and PH [4,280,324,325]. Tibbits et al. [326] created a series of 4D printed structures composed of rigid plastic bases and expanding materials. By adjusting the ratio and positions of the rigid and expanding materials, precise control of the deformation was realized, including linear expansion and

one-dimensional/2D folding (Fig. 31a).

More recently, Mao et al. [277] demonstrated a hydrophilic/hydrophobic bilayer actuator with rapid and programmable multi-motion. After being immersed in water, the chitin film started to swell, while the PDMS kept its original size, resulting in bending and twisting behaviors. Fig. 31b shows the reversible transition of a printed goldfish structure from a 2D film to a 3D state when switched from a water environment to an ethanol environment. DLP has also been employed to fabricate shape morphing structures, which significantly accelerated the printing speed. Zhao and co-workers used the DLP method to fabricate hydrophilic/hydrophobic composite shape-shifting structures using photopolymers. Poly(ethylene glycol) diacrylate (PEGDA) was used as the active responsive layer to generate the driving force, while poly(propylene glycol) dimethacrylate (PPGDMA) was used as a passive material (Fig. 31c). Various complex patterns were created via this method, demonstrating its feasibility and designability [278]. Hu et al. [279] reported microscale pH-responsive hydrogel actuators based on the femtosecond laser direct writing (FLDW) 4D printing technique. The printed structure was at the microscale, within 100 μm . The torsion, wrinkling, and curling deformation were realized by

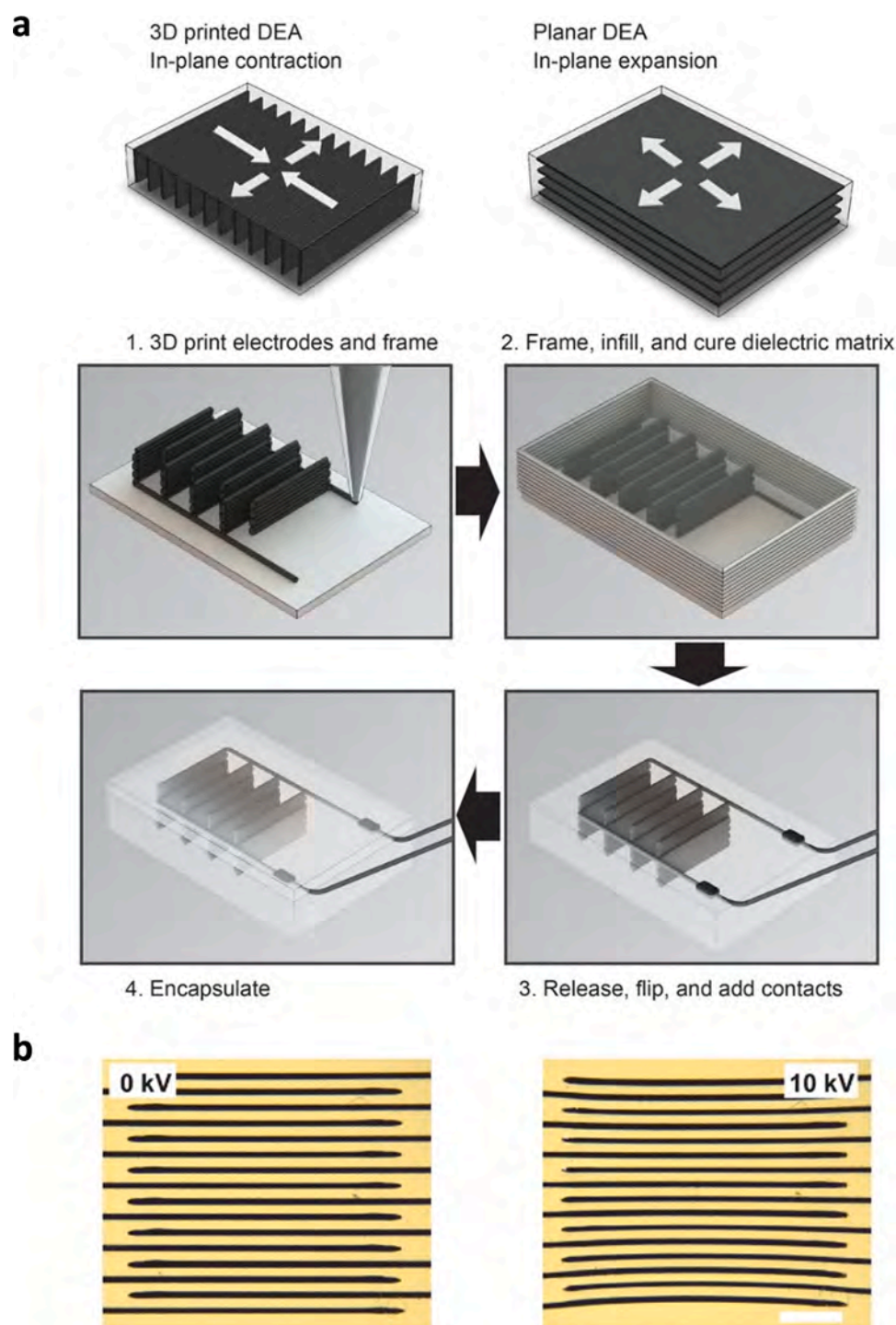


Fig. 29. Electromechanically driven 4D printed structures [285]: (a) schematic diagram of printed dielectric elastomer actuator devices and (b) 3D dielectric elastomer actuator device example with actuation up to 9 % (scalebar is 2 mm).

tailoring the pH of the liquid environment. Fig. 31d shows a fabricated microcage that expanded in an alkaline environment to capture a microparticle and shrank by adjusting the pH to trap and deliver the microparticle. This demonstration of the selective microparticle capturing–delivering–releasing has potential for cell-manipulation, drug delivery, and soft robotics. Different swelling ratios were achieved by spatially variable degrees of monomer conversion and cross-linking density. In the presence of ion stimuli, the cured film was able to transform to the designed 3D shape (Fig. 31e) [281].

Liquids are very common stimuli for triggering the deformation of

4D printed structures, and they have exhibited broad application potential in biomedical applications, commercial products, and soft robotics. However, several challenges must still be overcome, such as low control precision, limited work environments, and poor mechanical performances.

3.5. Light-driven 4D printing

Light-driven actuators or soft robots have attracted considerable attention due to their various merits, such as fast responses, wireless

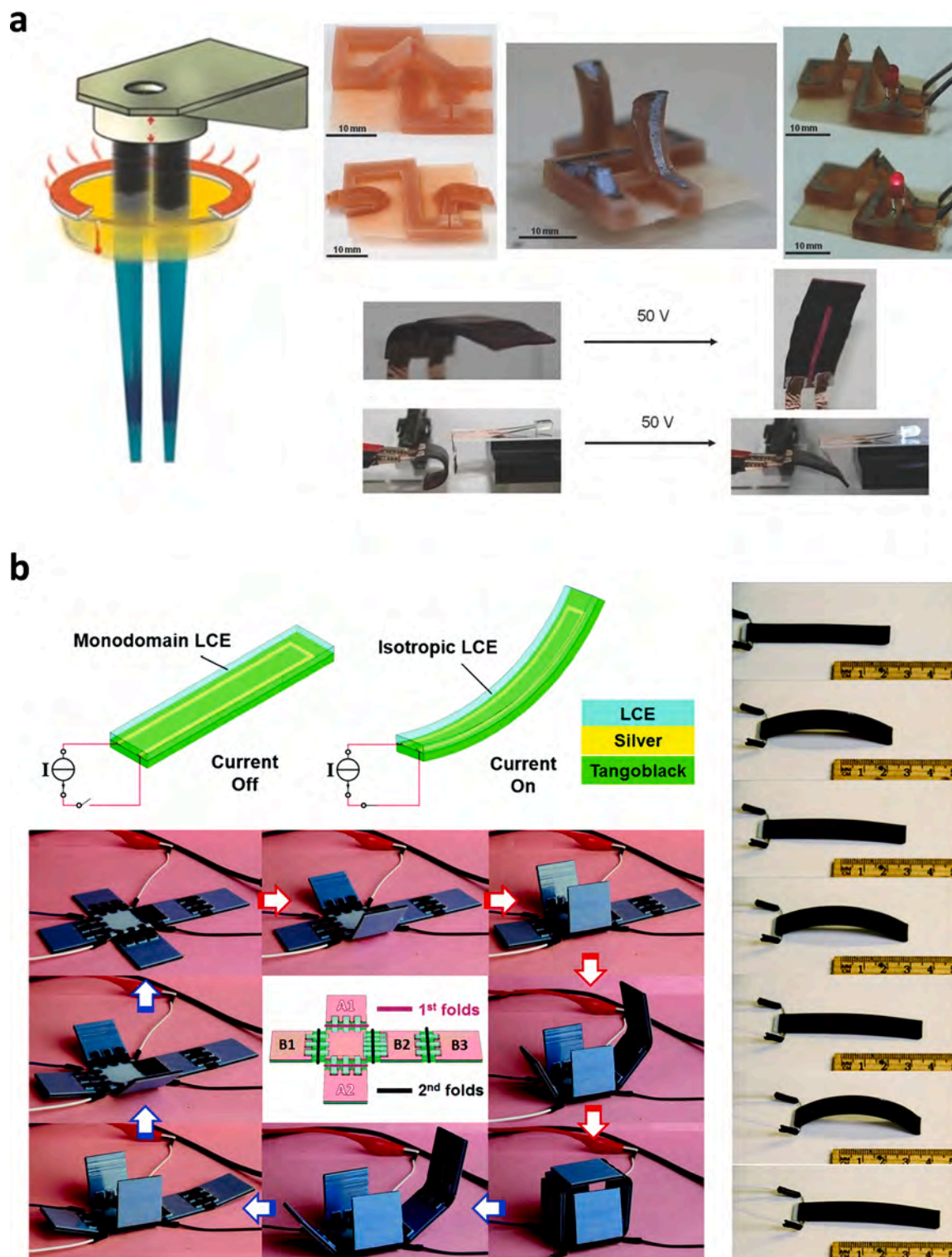


Fig. 30. Electrothermally driven 4D printed structures: (a) SLA printed shape memory structure for electrothermally driven actuator [266] and (b) 3D printed laminated actuator using liquid crystal elastomer [265].

controllability, accurate focusing, and sustainability [327–329]. Various reported materials show light-sensitive properties, for example, graphene- and carbon nanotube (CNT)-based composites [330–332], LCE-based composites [333–335], SMPs [336], hydrogels [337], and other polymers. Among the numerous efforts to fabricate light-triggered smart structures by AM methods, Cui et al. reported a novel near-infrared-light (NIR)-sensitive composite based on graphene and a

thermally responsive SMP, as shown in Fig. 32a [286]. The graphene could absorb photons, and the temperature rose above the glass transition temperature of the SMP, which allowed remote and precise shape transformation control. In this work, dynamic biological structures, and cell behaviors were studied, which is a promising strategy for various biomedical applications. Another approach for printing light-sensitive materials is FDM. A PLA and multi-walled CNT bilayer actuator was

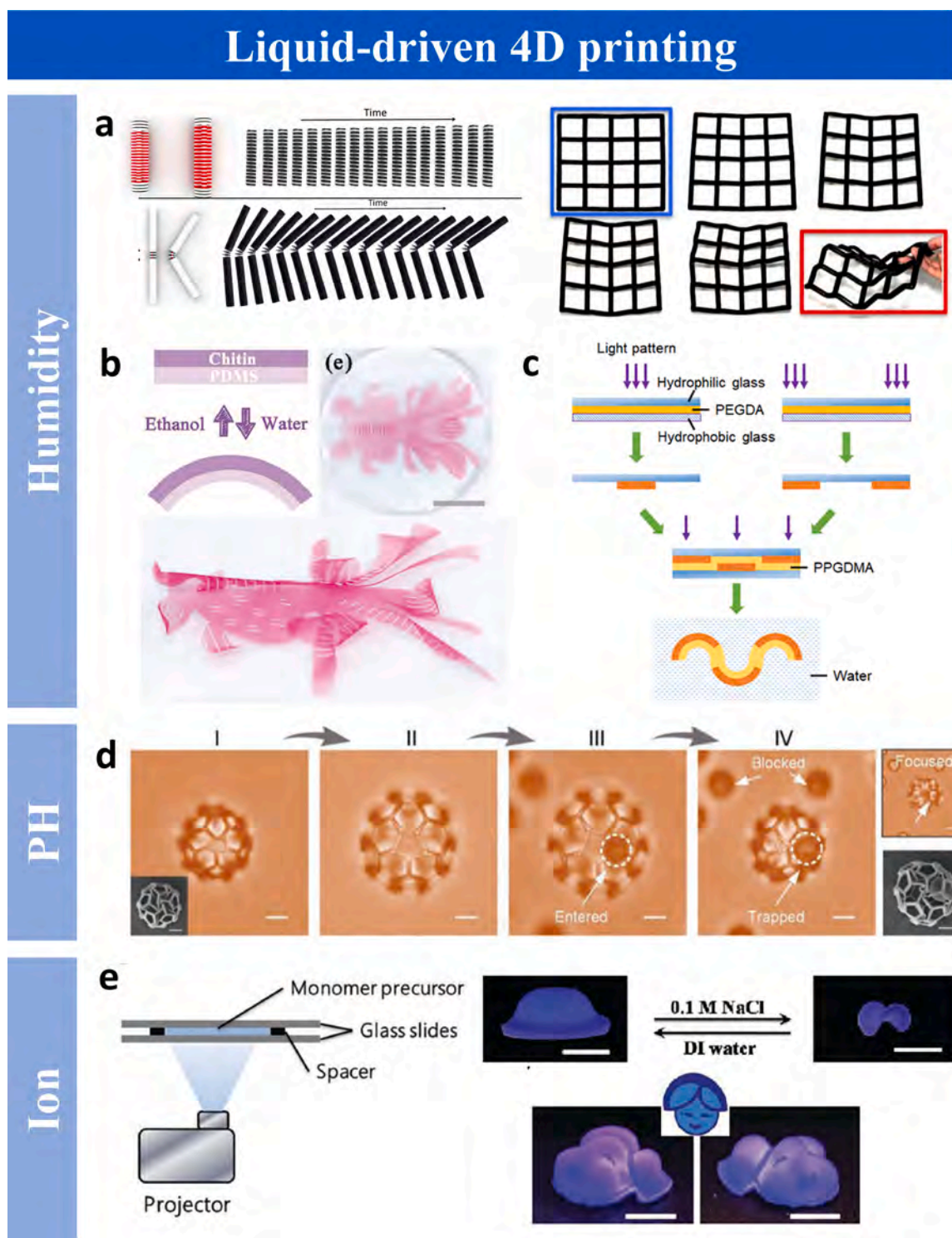


Fig. 31. Liquid-driven 4D printing: (a) 4D printed linear stretching primitive, folding primitive, and grid [326], (b) humidity-actuated shape-morphing structure [277], (c) 4D printing of hydrophilic/hydrophobic composite [278], (d) pH-triggered expanding and shrinking structure [279], (e) DLP fabricated ion-responsive planar patterns [281].

reported by Hua et al. [338], as shown in Fig. 32b. This actuator could change shape under NIR light and recover to the initial shape once the light is turned off. The polyurethane (PU) and carbon black composites shown in Fig. 32c and d were also printed by FDM [339]. External illumination or sunlight can trigger recovery from a temporary shape to the original shape. These light-sensitive printing materials offer tremendous opportunities for the fabrication of smart devices. A light-sensitive micro-swimmer (Fig. 32e) consisting of PNIPAM and gold

nanorods was printed by the multiphoton lithography (MPL) [340] method. The internal micro/nanostructures were well defined due to the high printing resolution.

The use of light as a stimulus opens a new avenue for smart structure fabrication. However, more in-depth studies are needed to overcome the current drawbacks, such as wavelength limitations, the biological toxicity, and the penetration depth of the light for internal applications.

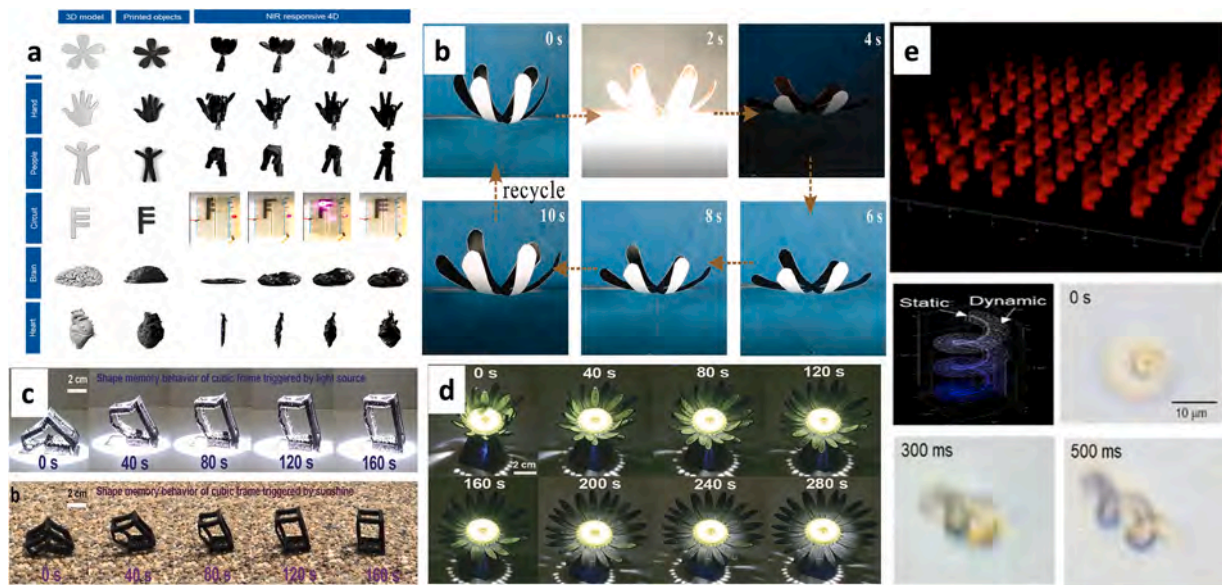


Fig. 32. Light-driven 4D printing: (a) dynamically controlled transformation of 4D printed constructs [286], (b) photo-triggered blooming process of printed flowers [338], (c) recovery from temporary configuration to original configuration under external illumination or sunlight [339], (d) different blooming processes of 3D printed flowers with various illumination time [339], and (e) images of the bilayer and monolayer helices after 300 and 500 ms of laser exposure [340].

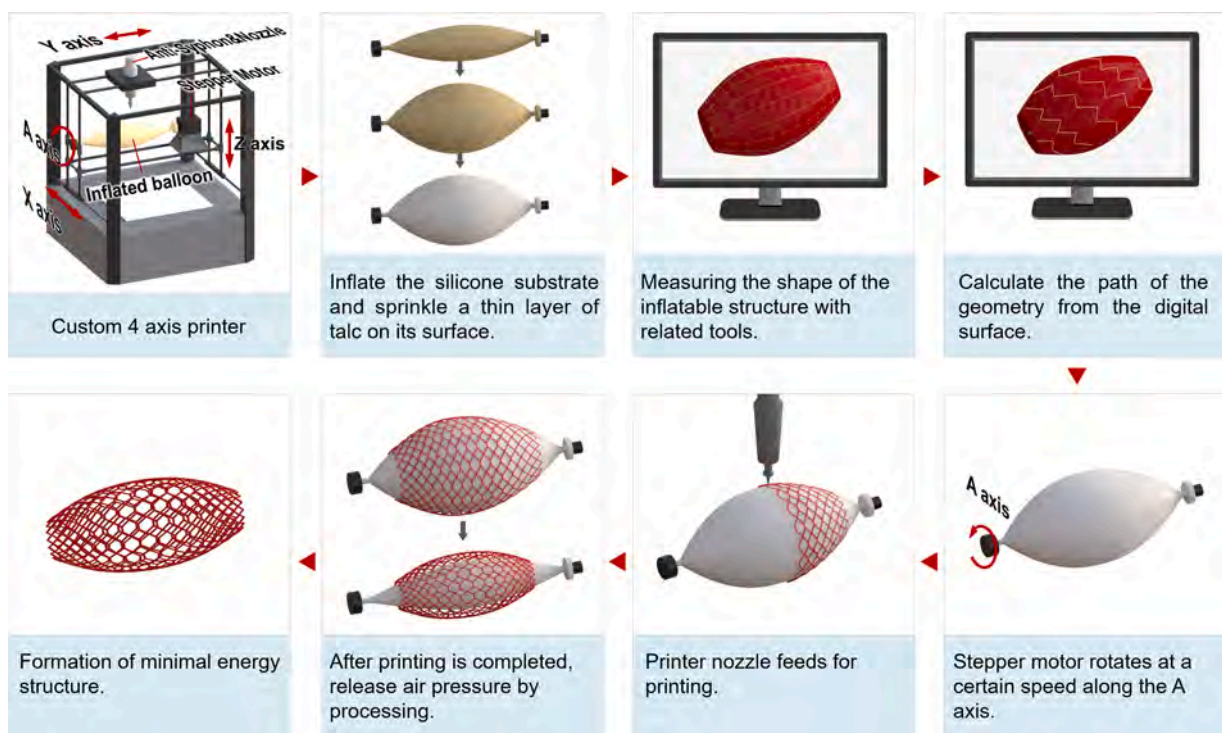


Fig. 33. Pneumatically driven 4D printing principle [289].

3.6. Gas-pressure-driven 4D printing

3.6.1. 3D printing substrate pneumatic deformation

Traditional 4D printing technology is based on the combination of 3D printed and original materials. Under the stimulation of an external environment (e.g., heat [296], light [293,341], and pH [342]), the material deforms over time to achieve the designed structure. However, the traditional 4D printing technology cannot be used in applications with fast rate responses and reversible driving forces [343], and conventional AM technology (either 3D or 4D printing technology) can only

be used to squeeze or deposit materials in a plane, and cannot adapt to the shape printing on the curved surface. Inspired by early architects and engineers, quoting the basic principles of air pressure for lightweight, fast deployment, and low-cost structures [287], a new driven printing technology was developed for this purpose: gas-pressure-driven 4D printing. In recent years, people have combined the developed pneumatic driving technology with 3D printing to realize passive 4D printing with fast responses and reversible driving forces. Coulter et al. [288, 289] used this technology to produce a tubular dielectric elastomer. A four-axis silicone printing system was used to spray a multilayer tubular

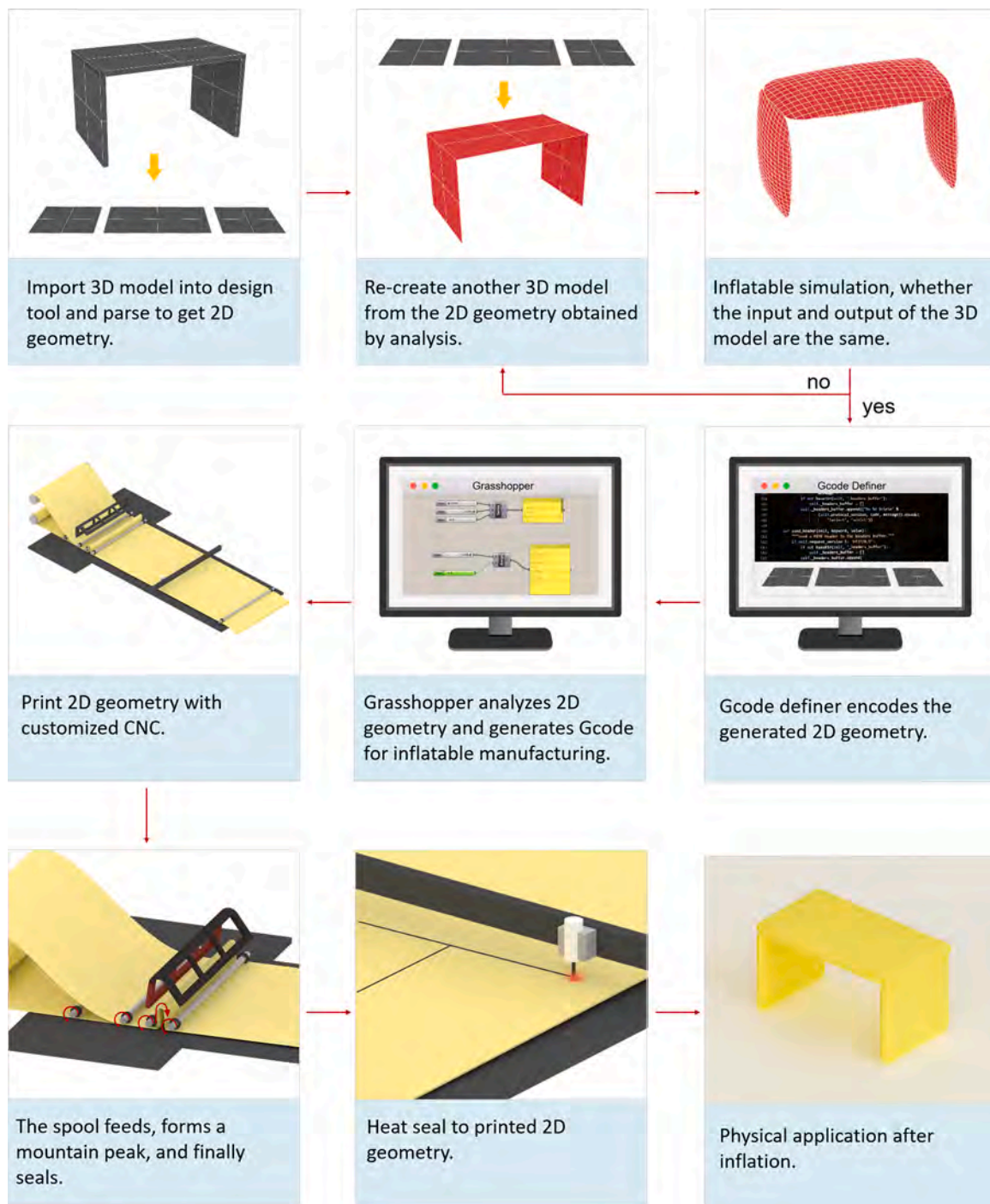


Fig. 34. Inflatable 3D printing process [287].

silicone film onto a ventilating mandrel, which was inflated to cause mechanical strain on the film. Finally, a scanning and hyperbolic extrusion method could be used to print on stretched and inflated balloon-shaped film substrates, using the offset surface function in Grasshopper (parameter design plugin). This could successfully achieve the superimposition of multiple printed layers after the extruded silicone structure was fully cured and the aerodynamic strain release caused the structure to collapse uniformly, resulting in the structure with the smallest energy. The principle of gas-pressure-driven 4D printing is shown in Fig. 33.

3.6.2. 3D printed object pneumatic deformation

The aforementioned automated manufacturing of gas-pressure-driven 4D printing still has limitations. In particular, only a few important soft mechanical components can be printed. On the basis of pressure-driven printing, Salen et al. shifted their focus to aerodynamic structures that require higher strengths and lower flexibilities and developed a pressure-driven printing technology, which was different from that studied by Kurt et al., to transform a 2D plane shape into a 3D structure. First, a new model was generated or an existing solid model was imported in Rhino3D (CAD software), and the imported 3D model was analyzed using Grasshopper to generate a 2D geometry. Finally, the 2D geometry was used to build another 3D model to simulate whether

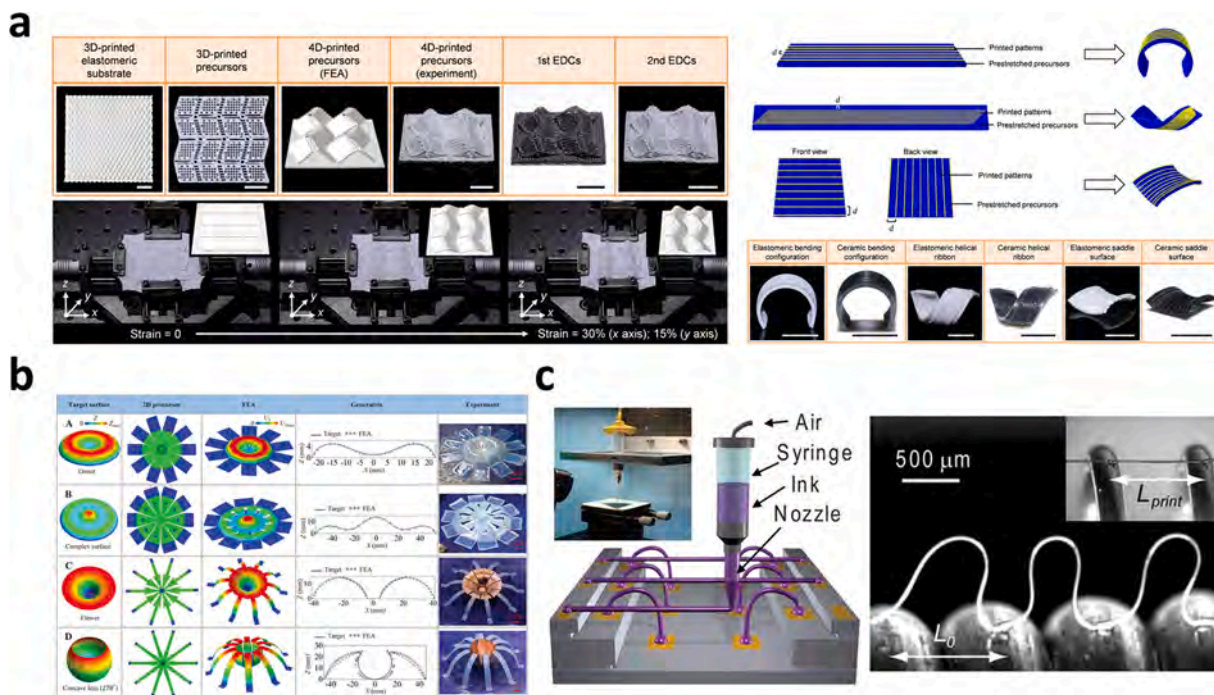


Fig. 35. Mechanically driven 4D printing structures: (a) prestress-driven ceramic structure (scalebars are 1 mm) [45], (b) mechanically driven assembly 3D surfaces [347], and (c) printing of silver microelectrodes, and the buckling arches of spanning silver printed on a spring [348].

the input and output match. Finally, the 2D geometry was processed by a gantry computer numerical control machine tool, and 2D model was expanded to form the expected 3D model [287]. The specific printing flowchart is shown in Fig. 34.

3.6.3. Application of gas-pressure-driven 4D printing

At present, people are committed to manufacturing dielectric elastomer actuators by pneumatically driven 4D printing technology for soft robotic equipment in new fields [285,344]. Due to the high elasticity of dielectric elastomers, flexible pneumatic actuators can maintain high elongation under high air pressures. They can bend and twist, breaking the restrictions of the freedom and movement capacity of traditional rigid robots [345]. As a result, soft robots can safely interact with humans and work in environments that are inaccessible to humans. In addition, the gas-pressure-driven 4D printing technology is also widely used in the medical field, such as for wearable devices printed using this technology to assist rehabilitation treatment. However, the use of these medical treatments has fallen far short of expectations. Researchers are trying to print artificial hearts through 3D and 4D printing technologies. The current problem is that 3D bioprinting has limitations for fabricating stents and materials [346]. Gas pressure may soon be an option to drive 4D printing technology. The myocardium can be printed subject to the limitations of printing materials, and the structure formed by printing is similar to the minimum energy structure described above to eliminate the constraints of the stent to solve the problem of the insufficient supply of organs for transplants.

With current progress and development, 4D printing technology will gradually improve. Traditional 4D printing technology with low efficiency and irreversible driving forces may be eliminated, and it will be replaced by air-pressure-driven 4D printing technology. Although there is not much research on this technology at present, based on previous studies, we can clearly see the superiority of pressure-driven 4D printing technology. This technology can significantly improve the printing speed, with the advantages of conformal printing capabilities on inflatable ultra-thin films (which dramatically increases the printing area), fast responses, and reversible driving forces. At present, this emerging 4D printing technology is being commonly used in the

electronics field. Pressure-driven 4D printing technology will likely be widely used in aviation, manufacturing, construction, smart homes, and other areas.

3.7. Prestress-driven 4D printing

Prestress-driven 3D assembly structures are attracting considerable attention due to their potential applications in flexible electronics, from the buckling of single-crystal silicon ribbons to the 3D assembly of complicated silicon patterns. 3D structures for mechanically driven assemblies require good flexibility of the material. As an efficient driving method, mechanically driven assemblies have also found corresponding applications in the field of 4D printing. Liu et al. [45] developed DIW printable elastomeric poly(dimethylsiloxane) matrix nanocomposites, as shown in Fig. 35a. The elastomeric composite was stretchable and deformable, driven by pre-strain and then transformed into silicon oxycarbide matrix nanocomposites, making mechanically driven complex ceramic structures and 4D-printed ceramic structures possible.

Mechanically driven 3D assembly methods published by Yihui Zhang, Yonggang Huang, and John Rogers have been applied for 3D surfaces [347], as shown in Fig. 35b. Ahn et al. [348] proposed an omnidirectional printing method via concentrated nanoparticle inks. They printed spanning silver lines on a stretchable substrate using a DIW printer, as shown in Fig. 35c, which indicated that concentrated nanoparticle inks and omnidirectional printing methods may find applications in prestress-driven flexible circuits directly.

3.8. Multi-drive 4D printing

Untethered actuators and soft robotics have progressed considerably recently. However, most existing smart structures are only responsive to one stimuli, which limits the interaction capacity with the surroundings and the adaptability under multiple stimuli [349]. Various multi-responsive materials have been studied, including light-thermal dual responsive hydrogels, electrothermal and electrochemical actuation materials [350], magnetic-photo/thermal dual stimuli actuators [310,351–354], a temperature-PH sensitive fluorescence bilayer

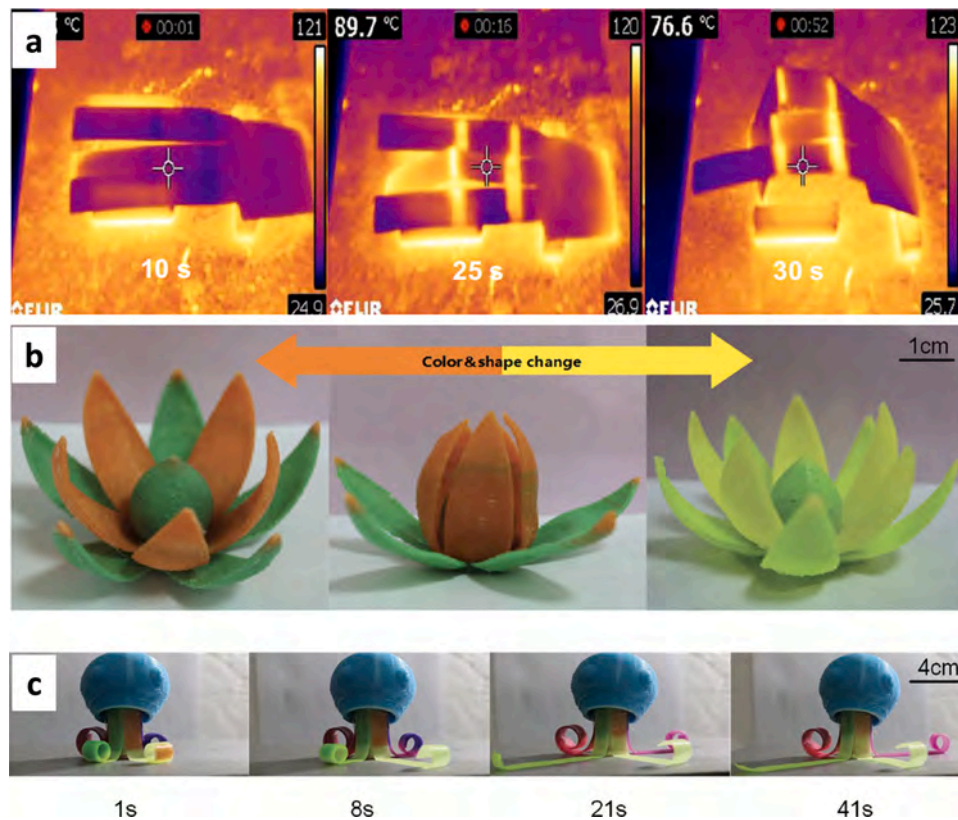


Fig. 36. Multi-drive 4D printing: (a) photo-thermal self-folding origami structure [290], (b) blooming and color-shifting flower printed by a multi-material printer [357], and (c) artificial octopus tentacles [357].

actuator [355], and a humidity-temperature-light triple responsive hydrogel [349].

Application of AM technology in multi-responsive actuators can achieve the efficient fabrication of actuators with complex shapes and delicate structures. A photo-thermal, self-folding origami structure was manufactured using a 3D bio-plotter, as shown in Fig. 36a [290]. The bending angle was related to the external light intensity. Multi-responsive hydrogels are promising materials for this area due to their shear-thinning properties and good printabilities. Karis et al. [356] synthesized and printed a triblock copolymer hydrogel that responded to temperature, pressure, and UV light. In another study, a biomimetic shape-color double-responsive composite based on a shape-memory polymer (PLA) and thermochromic pigments was printed by FDM [357], as shown in Fig. 36b and c. A color-changing flower and a camouflaging octopus were demonstrated. In the medical field, a stereolithography (SLA)-printed hydrogel scaffold showed double responsiveness of its water absorption properties to temperature and PH stimuli [358], showing significant potential for medical device applications.

4. Applications of additive manufactured structural materials

4.1. Aerospace field

The current and potential applications of AM in aerospace field are summarized in Table 4, and explained as follows.

4.1.1. Astronautics

4.1.1.1. Spacecraft engine. The aerospace industry has applied AM to produce parts, because of its benefits for design logistics, high functionality, high production efficiency, and lightweight products. A monolithic thrust chamber was built by SLM® Solutions and CellCore with a design that reduced the number of components, was lightweight,

and exhibited good functionality [359]. EOS introduced a simplified propulsion module build by different types of direct metal laser sintering machines. The all-in-one baseplate and injector head using the conventional injector design contained 248 components. The new design and manufacturing process led to a 50 % lower cost and a shorter production time [379] (Fig. 37a and b).

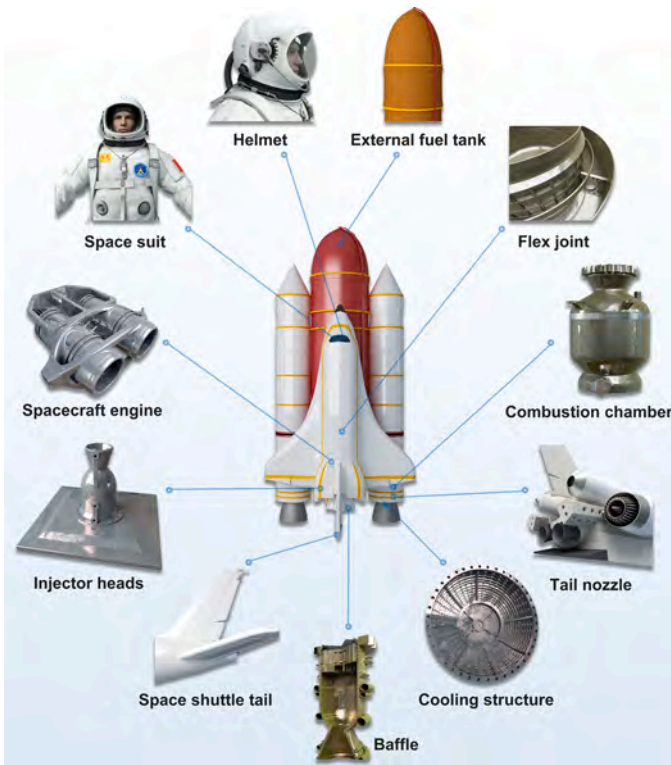
NASA also optimized a rocket engine by AM. A 65 % cost reduction in the production of rocket engine parts was achieved using SLM compared with the cost of conventional methods, because the number of welds and amount of potential rework was reduced. This design also improved the stability and user experience because it reduced the vibrations [380]. A rocket propulsion system involved in AM was tested successfully in 2018. The nickel-alloy jacket in the test was manufactured using an electron beam free form fabrication method, which is shown in Fig. 37c and d.

4.1.1.2. Spacecraft components. 3D printing also has broad prospects for the manufacturing of outer-space antennas and spacecraft components. Initially, official organizations used AM technology to build parts for large military spacecraft, such as fighters and navigational satellites, and gradually expanded to other fields, such as the manufacture of unmanned aerial vehicles (UAVs) and civil near-earth satellites. Before the advent of 3D printing technology, traditional fabrication methods could not further optimize and reduce the weights of spacecraft component materials. AM made it possible, which historically would have been difficult or expensive. AM also can guarantee that the properties will not be diminished with the optimized inner structure. Furthermore, the stress distribution of the components could be more uniform, which could reduce the wear and increase the service life.

NASA has expanded its fabrication strategies to include several states and deposition styles. NASA began research and experiments several decades ago and has advantages over other countries. Its main interests have been on metal materials. Scientists tried to fabricate a turbo pump

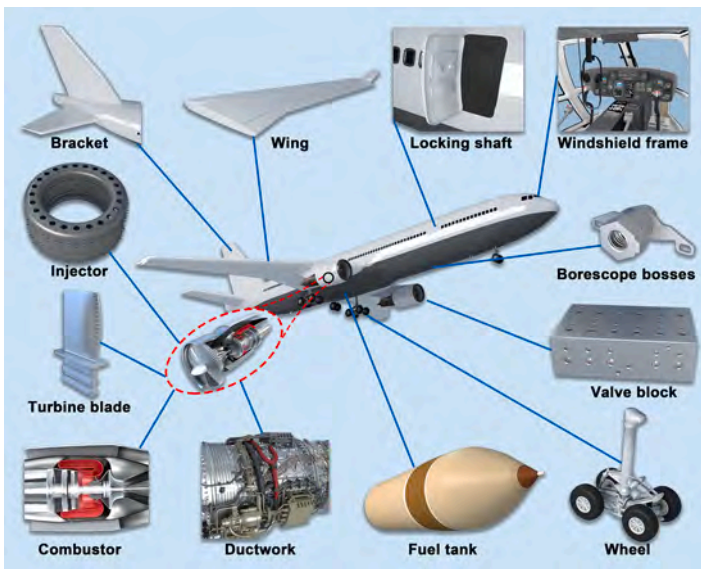
Table 4
Current and potential applications of AM in the aerospace field.

Astronautics



Parts	References	Parts	References
Engines	[359]	Baffles	[360]
Cooling structures	[359]	Combustion chambers	[361]
Baseplates	[359]		

Aeronautics



Parts	References	Parts	References
Engines	[362,363,364,365,366,367,368,369]	Ductwork	[370]
Brackets	[371,372,373]	Tools	[374,375]
Spacer panels	[376]	Injectors	[377]
Valve blocks	[378]	Chambers	[377]

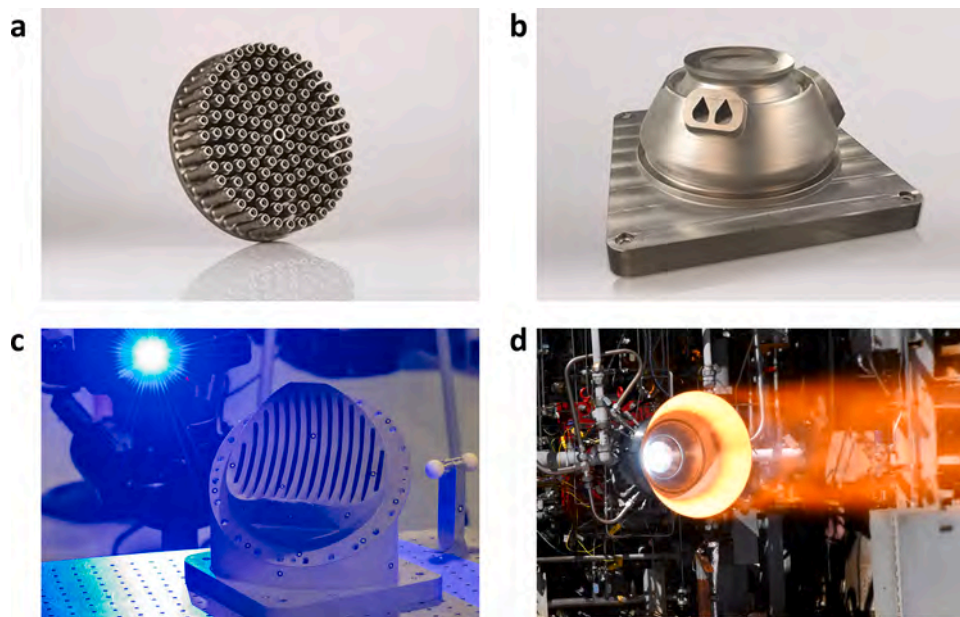


Fig. 37. (a) Baseplate using all-in-one design made by EOS [379], (b) injector head as all-in-one design made by EOS [379], (c) NASA's Pogo Z-baffle for RS-25 engine, which was made by SLM [360], and (d) NASA test on a 3D printed copper combustion chamber liner with an electron beam free form fabrication manufactured nickel-alloy jacket [361].

exhaust port cover of the J-2X rocket engine using the SLM method [381]. The cost of the new part was only 25 % of that of the part fabricated using conventional methods. Another typical case is the flex joint on the RS-25 space shuttle engine [382]. The part successfully passed the hot-fire testing, and using the existing design with robotic casting technology significantly decreased its complexity from 127 to 4 welds. The key components of Super Draco spacecraft's engine were manufactured by 3D printing. With the help of integrated manufacturing advantages of AM, the dozens of different parts required previously were reduced to three. SpaceX's SuperDraco combustion chamber was made from Inconel using the direct metal laser sintering (DMLS) process, which greatly shortened the entire engine design and manufacturing cycle [383]. Furthermore, the two astronauts Bob Behnken and Doug Hurley who traveled by SpaceX's manned dragon spacecraft wore 3D printed helmets for the space mission (Fig. 38). This is another 3D printing application of SpaceX, in addition to the fabrication processes for the Falcon 9 rocket and Dragon V2. Most of the white helmets' parts worn by the two astronauts were manufactured by 3D printing technology [384]. China's "Chang Zheng 5B" carrier rocket was equipped with a 3D printer. This was the first international 3D printing experiment of continuous fiber-reinforced composite materials in space [385]. Fig. 39 shows two samples of continuous fiber-reinforced 3D printing in orbit.

3D printing also has potential applications in antenna manufacturing. For spacecraft and space satellites, E-communication is important part, so the role of antennas is particularly vital. The antenna must meet high surface accuracy requirements and operate normally and stably under the non-gravity conditions of outer space. In addition, there are greater amounts of radiation and cosmic rays in outer space than in the upper earth atmosphere. 3D printing technology is an excellent antenna manufacturing method, especially for the manufacture of frameworks and deployment structures. Researchers from Yasar University developed a product using a conical corrugated horn antenna to feed reflector antennas in satellite communication [386], as shown in Fig. 39. It was designed with the CST Microwave Studio program and could operate normally in the 10.5–18.5 GHz band. In terms of cost and manufacturing time, this antenna was superior to similar antennas made from high conductivity metals.

4.1.2. Aeronautics

4.1.2.1. *Aircraft engine.* The development of AM technology is a technological revolution in the manufacturing industry. AM technology, with manufacturing flexibility and the ability to reduce the quantity of raw materials, has directly caused a revolutionary trend in the processing and manufacturing industry [387]. Therefore, this technology is very suitable for applications in complex, multi-variety, expensive raw material manufacturing industries, especially in the aviation field, and it will inevitably be widely used and promoted. There are four main advantages. (1) It increases productivity. The production cycle of one engine currently is 2–3 weeks, while the huge market demand requires the production capacity of seven engines per week. AM technology can be applied to manufacture complicated engine parts simultaneously [387, 388], avoiding the complicated steps of connecting components, heat treatment, processing, and assembly in the traditional manufacturing process, which can significantly improve the production efficiency and shorten the delivery time. (2) Diverse designs are accessible. Engineering designers are no longer constrained by traditional manufacturing processes and can use AM to produce engine parts that closely resemble products in nature [389]. The AM method also can achieve complex shapes that cannot be completed by conventional manufacturing processes, which is helping to manufacture the most suitable parts for individual projects. (3) Waste and costs are reduced. AM technology allows us to modify almost any point in the design and manufacturing process, reducing the manufacturing time and processing costs. The materials are manufactured where they are needed, and there is no need to process each expensive and technically sophisticated component, reducing the material waste while improving the performance of the product simultaneously [387]. (4) AM is part of the digital industry. While using the AM method, engineers can simply upload the files to a 3D printer and print them immediately. This method significantly reduces the component inventory period and unnecessary shipping time, shortening the delivery cycle [377].

3D printing methods have also been applied to propulsion components in aircraft engines, and there are mainly two kinds of AM methods (EBM and SLM) applied in this field. The method of SLM is actually a layer-by-layer powder-bed approach. During the manufacturing process, the component is sintered and then solidified by a laser. This approach is

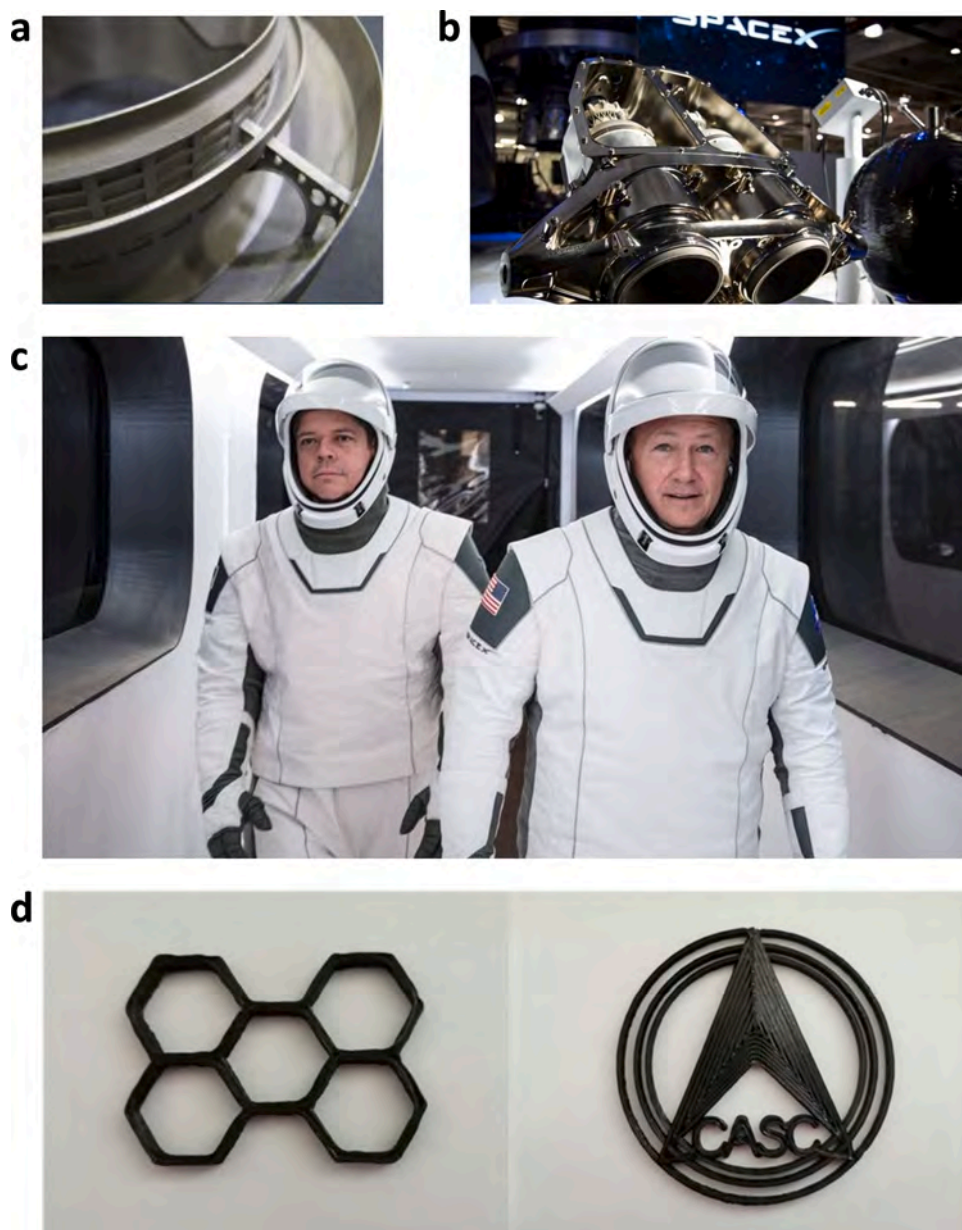


Fig. 38. (a) Flex joint of RS-25 [382], (b) SpaceX's SuperDraco engine [384], (c) astronauts Bob Behnken and Doug Hurley in SpaceX spacesuits [384], and (d) two samples of continuous fiber-reinforced 3D printed components put into orbit by China: honeycomb structure and China Aerospace Science and Technology Group Co., Ltd. Logo [385].

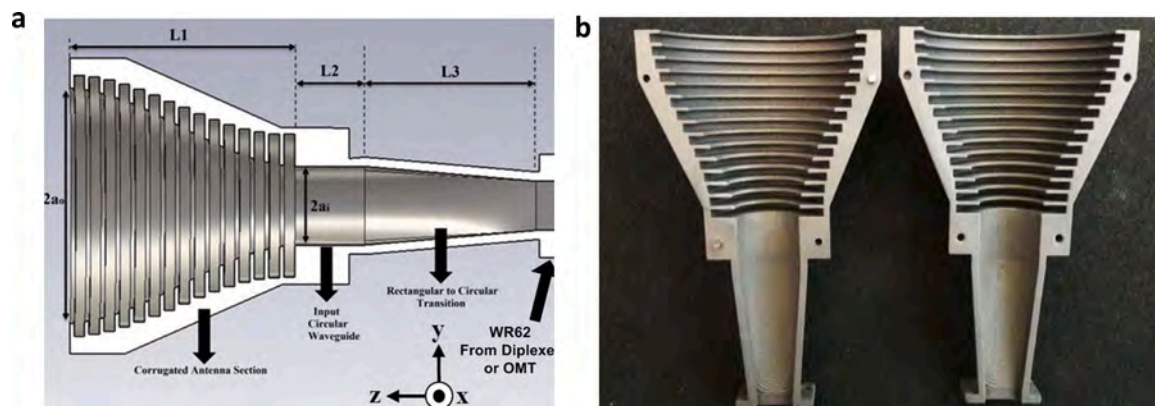


Fig. 39. (a) View of the designed corrugated conical horn antenna and (b) cross-sectional views of the antenna prototype [386].

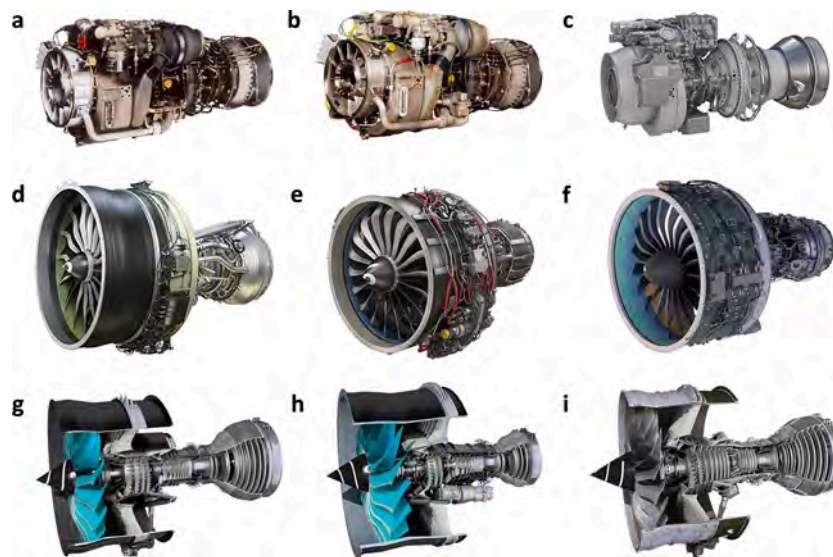


Fig. 40. Civil and military engines involve AM technology: (a) GE CT7-2 engine [365], (b) GE's Catalyst™ advanced turboprop engine [366], (c) GE T901 turboshaft engine [367], (d) GE9X commercial aircraft engine [368], (e) CFM LEAP commercial aircraft engine [369], (f) P&W GTF commercial engine [364], (g) RR Advance3 [362], (h) RR UltraFan® [362], and (i) RR Trent XRB-97 [363].

widely applied in combustion devices, and products with excellent features and high resolution can be manufactured. Furthermore, it also allows internal complex designs for manufacturing. Therefore, the limit of SLM is the scale [377], and thus, it cannot be applied for all components. There is little difference between EBM and SLM. The method of EBM uses an electron beam instead of a laser, and it is performed under a vacuum. Furthermore, it is not commonly applied for combustion devices. The vacuum process allows for reactive materials (Ti, Mg) to be used [377].

Due to the wide application of AM technology in aircraft engines, bimetallic combustion chambers have been developed by NASA [377]. Combustion chambers with copper-alloy liners were fabricated using SLM technology. The SLM method fabricated the liner and directed energy deposition produced structural support parts. A similar manufacturing procedure was also applied by Spark Ignition Systems to form bimetallic systems using wrought material and directed energy deposition. NASA also developed a series of exclusive injectors using the AM method using various materials and element types. The element diameters ranged from 1.125 to 7.5 in. and the injectors were manufactured with a powder-bed process. The use of AM to fabricate the injectors effectively reduced the cost and shortened the schedule. Furthermore, this method is also allowed for individual design [377]. Therefore, the main obstacle of injectors manufactured by AM is the relatively low size resolution, especially in the radial direction. In

addition, the excessive surface roughness remains a challenge to be addressed.

The development of propulsion systems plays a crucial role in the comprehensive performances of aerospace products. With the breakthrough of simulation technology, powder preparation technology, shrinkage deformation control, and other key issues, the databases and standard systems of 3D printing manufacturing processes will be better established, promoting their use in aircraft engines.

AM is widely used in the aviation and aerospace industries, which has accelerated the design and manufacturing of parts. AM has made the production of lighter, more durable, and more efficient designs possible. According to the GE company, AM has benefitted the industry in the following aspects. AM has led to lower costs and simplified supply chains, which allows parts to be consolidated and reduces the supply costs. AM has helped to improve product performances due to the material and geometric flexibilities. AM has reduced the product cycle time and changed the production to distributed manufacturing and on-demand product solutions.

On an aircraft, AM can be used to produce engine components, aerostructures, airframe parts, aircraft parts and systems, interior parts, secondary structures, and avionics parts. As one of the most important applications, AM is used to produce military and civil engines. The world's largest engine manufacturers, including GE, Pratt & Whitney, and Rolls-Royce, have all utilized this technology to improve their

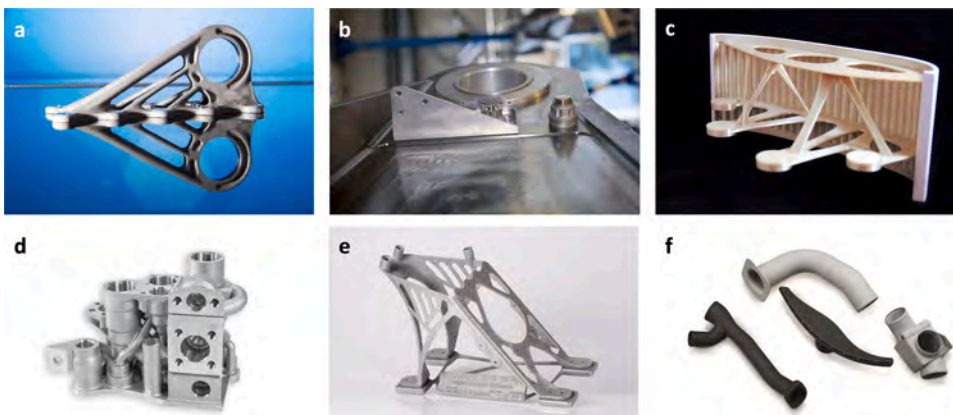


Fig. 41. Parts made by additive manufacturing: (a) 3D printed bracket installed on the Airbus A350 XWB [371], (b) 3D printed titanium bracket installed on the Airbus A350 XWB pylon [372], (c) 3D printed spacer panels installed on the A320 aircraft, which are 15 % lighter than conventional panels [376], (d) 3D printed valve block installed on the A380, which was 35 % lighter and made with ten fewer parts than a conventional valve block [392], (e) 3D printed vertical tail bracket installed on an Airbus A350 XWB, which was 30 % lighter than the conventional tail bracket [373], and (f) 3D printed ductwork installed on helicopters, which required less time and fewer tools to manufacture [370].

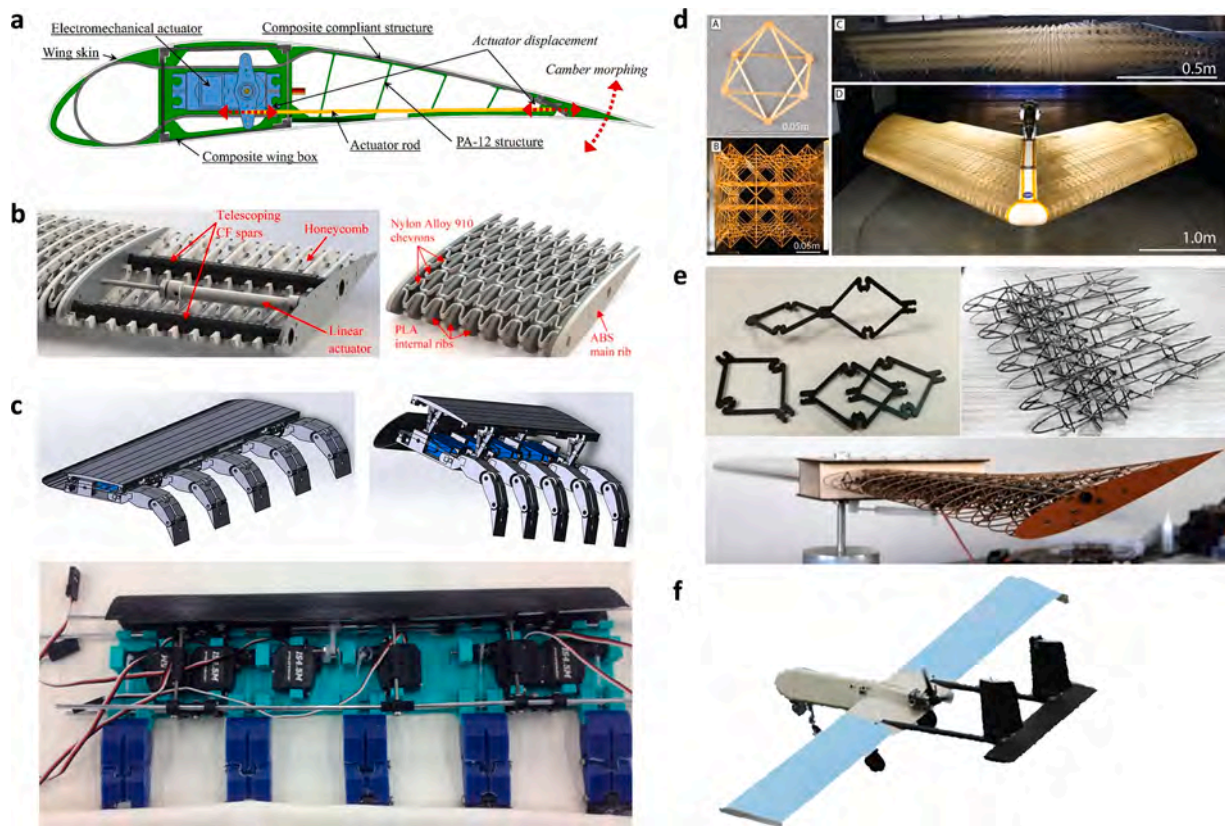


Fig. 42. Applications of AM in morphing wings. (a) 3D printed composite compliant structure (in green color)[399], (b) 3D printed honeycomb chevrons and main ribs [394], (c) adaptive wing segment built by 3D printed components [396], (d) and (e) morphing wing lattice structures built by 3D printed components [401,402], and (f) flight tested UAVs with 3D printed morphing wings [404].

engines (Fig. 40).

4.1.2.2. Aircraft components. The most common AM methods in the aviation and aerospace industries are rapid plasma deposition, direct metal laser melting, SLM, EB, and powder bed fusion. The metal materials used in these industries include titanium, titanium alloys, stainless steel, aluminum, aluminum alloys, nickel-based alloys, and cobalt chrome alloys. Aircraft parts made by 3D printing are being more commonly selected in the aviation industry, as these parts are 30 %–55 % lighter and use 90 % less raw material [390]. The Boeing company indicated that 3D printing technology has great potential in reducing the costs and weights of aircraft structures. In a news report by CNN Business, Grazia Vittadini, the chief technology officer of Airbus, stated that up to a 55 % weight reduction can be achieved [391]. According to the Boeing company, in 2019, over 70,000 parts made by AM were used in commercial and defense-related flights [375]. Fig. 41 shows some other parts made by AM.

Furthermore, AM can also reduce the time and money required to fabricate casts, molds, and tools. In 2018, Boeing fabricated over 7,500 tools by AM and over 14,000 in 2019 [375]. Not only the manufacturers but also the airline have begun to involve AM technology. The KLM Royal Dutch Airline became the first airline to 3D print aircraft repairing and maintenance tools from recycled PET bottles [374].

In addition to industrial applications of AM in engines and frame connection components using metallic and plastic materials, this fast-developing technique has also contributed significantly to the new aircraft design, especially morphing wings. Aircraft wings are key components that provide lift forces for aircraft and the most important components used to adjust aircraft flight states. With the increasing demand for high mobility and fuel efficiency of modern aircraft, morphing wings and adaptive structures are the most commonly

selected techniques to further advance current aircraft with fixed wings, whose adaptive configurations are usually generated by mechanical rotations. Benefitting from the high efficiencies and economic cost of 3D printing, AM is popularly used in conceptual research on morphing wings [393–406], as shown in Fig. 42. Gripper pin structures fabricated using AM were used as the adaptive camber structures [393], which were also built in a compliant structure form using AM of continuous fibre composite materials [399], as shown in Fig. 42a. In Fig. 42b, delicately designed honeycomb chevrons and main ribs made by AM were successfully used for seamless, continuous, and uniform span-morphing wings [394,395], which were stimulated by mechanical actuation and smart materials. The specifically designed mounts, as shown in Fig. 42c, were also made by AM [396]. It is difficult to machine the hollow curved shapes of wings using traditional methods, such as milling or laser cutting, which can be efficiently completed using AM, accelerating research. A morphing wing model for UAVs, which consisted of 40 parts [397], was made from ABS plastic using AM for wind tunnel experiments. Trailing edges, as the most effective part to adjust aerodynamic response, were also built with AM [398]. Some new-concept advanced morphing wing structures [400], such as lattice-based cellular structures [401,402], as shown in Fig. 42d and e, were also constructed using AM to complete the complex element parts. 3D printing is valuable for the preliminary design of morphing wings, whose structures are complex and have multiple degrees of freedoms. AM can also be used to efficiently and economically manufacture components for load bearing frame structures, which can be assembled together with existing parts made by conventional machining. Using AM, the whole frame structure can be fabricated in an entire part without a joint, and the structure is stiffer and exhibits better vibration resistance. Morphing wings and aircraft made via AM are usually tested in wind tunnels to examine their aerodynamic behaviors [395–397,

Table 5
Current applications of AM in the biomedical field.

Biomedical field			
Parts	References	Parts	References
Dental implant and orthopedic prosthesis			
Hip	[407,408,409,410]	Ankle	[411]
Spine	[411,412]	Skull	[413,414,415,416]
Knee	[411,460]	Tooth	[415,417]
Tissue engineering and artificial organs			
Skeleton muscle	[425]	Cardiac patches and hearts	[420]
Vascularization	[10,421]		
Medical diagnosis and treatment			
CT & MRI	[422,423]	Medical Robotics	[272,424]

[401]. Some manufactured UAVs were also flight tested [399,403,404], as shown in Fig. 42f. With the rapid development of 4D AM, this new technique is believed to have wide aerodynamic applications [262,405], especially for morphing wings [406].

As AM technology spreads and matures, custom-made parts and structures will further improve the studies on morphing wings and realize the industrial manufacturing of engineered morphing wings, especially multi-material AM and 4D printing. The achieved morphing structures will not only benefit the civil and military aviation industries but also other aerodynamic application areas, such as morphing cars and wind power generators.

4.2. Biomedical field

The current applications of AM in the biomedical field are summarized in Table 5, and explained as follows.

4.2.1. Dental implant and orthopedic prosthesis

The use of AM for bio-implants has attracted increasing attention. Compared with applications in other fields, medical implants have unique needs, including high complexities, good customization, and small production quantities, and thus, AM is well suited to this field [390]. Orthopedic prosthesis and dental implants are designed to be inserted into a patient body to repair fractured bones or teeth, demanding higher biocompatibility, suitable mechanical properties, and good customization. Fine osteointegration is the key for implant surgery, influenced by three elements of implant design: material selection, surface processing, and structure design. An improper material leads to a mismatch in the mechanics and an uneven stress distribution, followed by osteolysis, which may trigger implant failures, such as loosening of the implant or periprosthetic fracture [425]. Furthermore, the surface between the implant and host tissue also determines the long-term stability. The anchorage points of orthopedic implants depend on the interface between the implant and the host bone [426]. Finally, the optimized structure would also play an important role in the mechanical

conduction and tissue growth, especially for individualized prosthesis design [427,428].

4.2.1.1. Materials. Comparable mechanical properties and good biocompatibility are requirements for the selected material. Three kinds of materials are primarily employed in bone and teeth treatment: metals, ceramics, and polymers. Although traditional Ti-based materials have good bio-compatibilities and corrosion resistance [429] and have been widely used in many studies [430], stress shielding leads to abnormal bone growth around the implant [431]. Alloys, which have good bio-compatibilities and biodegradation behaviors, are becoming popular in implant manufacturing. Control of the degradation rate was studied in dicalcium phosphate dehydrate-coated Mg-Nd-Zn-Zr screws, showing good bio-safety and bio-efficacy [432]. Ceramic materials, due to their similar mechanical properties and compositions to those of bone and teeth, are more suitable in the biomedical industry. Zirconia ceramic implants made using 3D printing, such as teeth and crowns, have comparable mechanical properties to those made using traditional methods [433,434]. In addition to mechanical factors, osteoconductivity is an important indicator when evaluating implants. Diemel et al. [413] presented a mixed material combination of trimethylene carbonate and β -tricalcium phosphate for implant printing, which improved the tensile properties and bio-compatibility. Apart from metals and ceramics, polymers are also popular in prosthetic and dental applications because of their good manufacturability. A polycaprolactone coating was deployed on tricalcium phosphate scaffolds to regulate the release of proteins, leading to a higher compressive strength [435].

4.2.1.2. Surface processing. As mentioned before, modified surfaces lead to better osseointegration between foreign implants and the host bone. Many studies have verified the effect of chemical factors on bone osseointegration. Polycaprolactone scaffolds with embedded bubbles of connective tissue growth factor yielded thicker and denser mineralized tissue on dentin surfaces [436]. Li et al. [437] modified the surface of an SLM printed scaffold with polydopamine, resulting in better

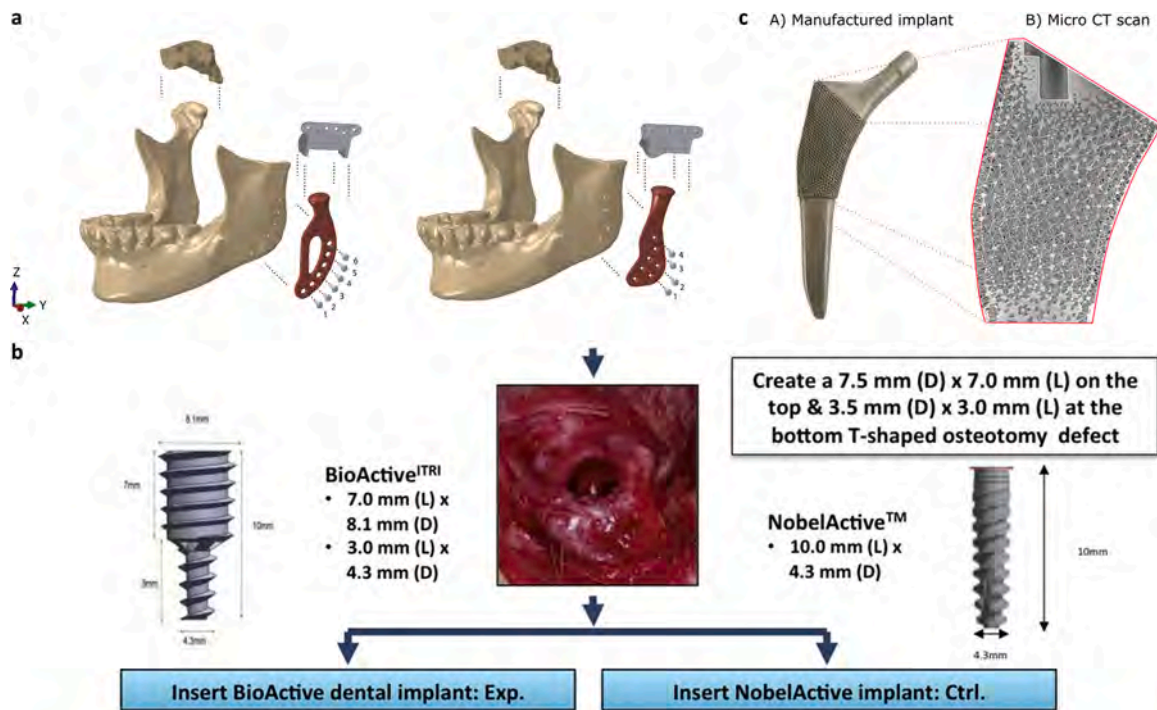


Fig. 43. Structure design is important in dental and prosthetic applications: (a) designed temporomandibular prosthesis provided improved therapy compared with stock [428], (b) more bone formation around the bioactive material compared with the commercial one [434], and (c) reduced stress shielding due to topology-optimization-based design [407].

osseointegration in rabbits. In addition to the chemical factor, the micro-structures of a Ti6-Al4-V implant surface regulated bone cell differentiation [438,439]. For dental implants, Tu et al. [434] proposed a bioactive dental implant and designed a porous-structured Ti6-Al4-V alloy dental implant using a laser AM technique, leading to better bone osseointegration due to its porous surface and individualized structure. Nano-modified 3D printed ceramics with antibacterial properties can be custom designed [440].

4.2.1.3. Structure design. Orthopedic prostheses are medical devices that are used to substitute or form a fixation of a bone or joint. In the past, bone implants or prostheses were confined to fixed models or versions, while the physiologies of orthopedic surgery patients differ in thousands of ways. Implants with the proper structure prompt post-operative recovery. Many studies have sought to determine the optimized structure (Fig. 43). Different pore sizes result in different stress distributions and permeabilities, leading to variations in bone osseointegration [441–443].

These studies provided suggestions for the design of implants. Aside from attempts to generate random structures and structural parameters,

such as random pore sizes, more efficient methods are required to guide the structure design. Topology optimization methods share similar principles with bone adaptation behaviors, which is promising for implant design [444]. The optimization of bone tissue has inspired the design of implants in this way. Based on topology optimization, Wu proposed a local density constraint method to generate a porous microstructure similar to that of trabecular bone that was lightweight and robust and fabricated models through FDM printing to verify its manufacturability [445]. A high-strength, fully porous prosthesis designed through topology optimization was applied in hip replacement, showing that the SLM prosthesis alleviated the stress concentration and bone resorption in a mimicked femur bone [414]. Furthermore, various targets for optimization methods can be used to solve different problems. A cage was designed using topology optimization to maximize its permeability while maintaining connectivity. It was then manufactured using 3D printing and implanted in a dog, which showed no lameness or other complications due to the individualized design [446].

In addition to research, AM has been employed in some commercial products. Zimmer Biomet developed the OsseoTi porous metal technology, which combines human computed tomography data with 3D

Table 6
Common materials for bone and dental implants.

Material	Method	Mechanical properties	Reference
Commercial pure Ti	SLM	Ultimate compressive strength: 1136 ± 15 MPa Ultimate tensile strength: 757 ± 12.5 MPa	[450]
Ti-6Al-4V	SLM	Ultimate tensile strength: 1288.70 ± 6.44 MPa Yield strength: 1063.99 ± 5.32 MPa	[430]
ZrO ₂	3D ink printing	Hardness: 14.4 ± 0.1 GPa Transverse rupture strength: 520 ± 20 MPa	[433,440]
Poly(lactic acid)/ hydroxyapatite	FDM	Compressive strength: 300 MPa Compressive strength: 70–90 MPa Elastic modulus: 1.4–1.8 GPa	[451]
Trimethylene carbonate + β -tricalcium phosphate	SLA	Tensile modulus: 5–353 MPa Yield stress: 0.8–4.0 MPa	[413]
Tricalcium phosphate + polycaprolactone	Sacrificial scaffold	Compressive strength: 0.5–2.5 MPa	[435]

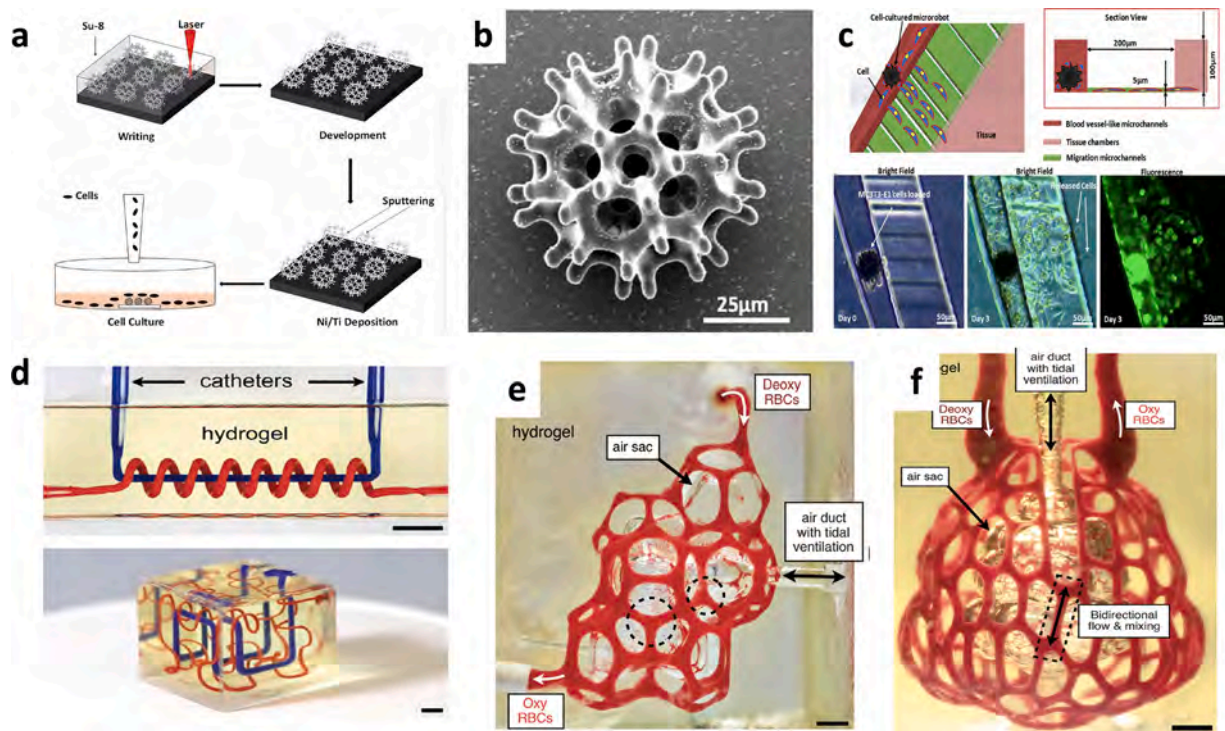


Fig. 44. AM applications in the medical field: (a–c) multi-vascular and intravascular networks printed by hydrogel networks for ventilation process and oxygenation [10] and (d–f) fabrication process and morphology of the burr-like magnetic micro-robot with cell delivery abilities [421].

printing technology. This technology is used to fabricate porous structures that directly mimic human cancellous bone, and it is widely applied for acetabular cups and wedges. The bone-like structure showed a material strength between those cortical and trabecular bone and a proper structure for osseointegration [447]. Stryker used the AM Technology to fabricate cervical cages and knee implants, of which porous structures are designed to mimic cancellous bone [418]. Table 6 shows some examples of marketed 3D printed orthopedic implants.

Clinical case studies have also been reported, including hemi-pelvic prosthesis [410], personalized porous implants [460], designed vertebral body [412], resorbable scaffold for cleft lip, and palate treatment [416]. With the help of customized 3D printed technology, a hemi-pelvic prosthesis was compatible with the patient. Within 12 months of follow-up, no loosening or other problems were detected, and the evaluation index increased [410]. In another case, a personalized porous implant was designed and fabricated by 3D printing to support the graft and subchondral area, which could avoid degeneration and mechanical failure. Limb function was satisfactory, and no further damage was observed [460]. Considering the specific anatomy of a patient with Ewing sarcoma, an individualized 3D printing vertebral body was designed for reconstruction and showed good osseointegration [412]. A bioresorbable scaffold with marrow cells was applied for cleft lip and palate treatment, which took the advantage of patient-specific 3D printing technology [416]. Chimene et al. [448] developed a nano-engineered ionic covalent entanglement bio-ink for 3D printing of bone. A 60-day cell-induced remodeling experiment resulted in the deposition of extracellular matrix proteins, and thus, this shows promise for applications in bone regeneration. Mimicking the complex Haversian structure, a 3D printing scaffold for bone regeneration was fabricated, showing great results in the acceleration of blood vessel growth and the formation of new bone [449].

The application of AM in medical implants is promising as the available materials, intelligent structure designs, and surface modification techniques continue to expand. AM is a bridge connecting patient-specific situations and personalized surgical plans. With the help of scientific optimization and strong manufacturing abilities,

individualized medical treatments will usher in a golden age of the medical field.

4.2.2. Tissue engineering and artificial organs

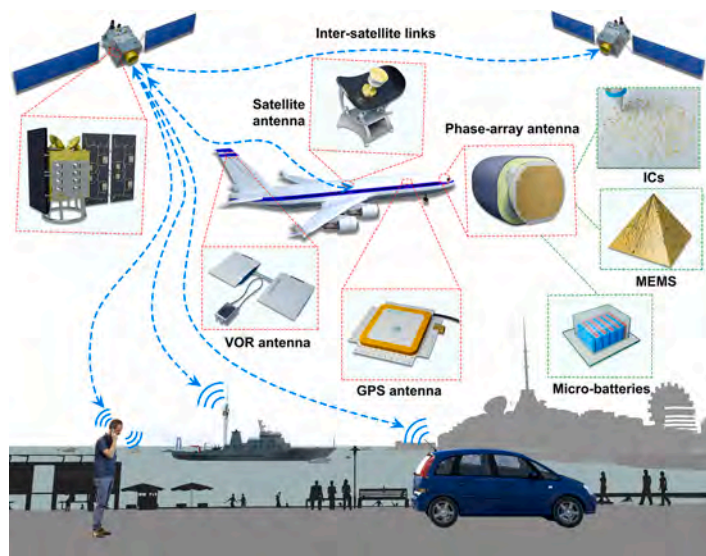
Tissue engineering aims to promote cell proliferation and tissue regeneration by functional construction or scaffolds, and the layer-by-layer principle of AM technologies achieves delicate structural control from the micro-scale to the macro-scale [452]. The ideal scaffolds should provide a biomimetic environment for cell migration, proliferation, and differentiation into various tissues and even organs. A smart 4D printed polymer was reported [453] with a good shape memory ability, adhesion, proliferation, and differentiation of human-bone-marrow-derived mesenchymal stem cells. This work significantly improved the design of bioactive scaffolds with advanced 4D printing technology. Various tissues have been studied using AM technology, including a 3D printed multiscale scaffold that was printed with gelatin methacryloyl (Gel-MA)/chitosan microspheres. This scaffold could promote nerve cell proliferation and differentiation [454]. For the skeletal system, an in-situ printed bio-ink was reported [455] for the treatment of volumetric muscle loss.

During the regeneration process of tissue, vascularization is a vital factor for nutrient transport and gas exchange, and it is still difficult to produce and study the multi-vascular bio-scaffolds. Printed vascular grafts with cells have been reported. These grafts were implanted for three weeks and showed great potential for the treatment of cardiovascular diseases [456].

Recently, a biocompatible photopolymerizable hydrogel based on PEGDA was fabricated into multi-vascular and intravascular networks by an SLA process [10]. The oxygenation process and flow of red blood cells were studied (Fig. 44a–c). In addition, biodegradable carriers based on this material in a chronic liver injury model highlighted the potential translational utility. Many 3D printed cardiac patches and hearts also have been developed [426]. A heart with a natural architecture was printed with a fully personalized bio-ink, which demonstrated the potential of printing patient-specific tissues and organs.

Table 7
Current applications of additive manufacturing in electronic devices.

Electronic devices



Parts	Materials	AM technology	References
Antennas	Polymer resins, alumina, alumina alloys, metal particles, dielectric materials	SLA, DMLS, EBM, SLM, IP	[423,460,461,462,463,464,465,466,467,468,469]
Resonators and filters	Polymer resins, ceramics (zirconia, Ba ₃ ZnTa ₂ O ₉), alloy powders	SLA, SLM	[424,470,471,472,473,474,475,476]
Waveguides	Polymer resins, alloy powders	SLA, SLM, PolyJet technology, FDM	[472,477,478,479]
Lenses	Polymer resins, ceramics (alumina)	SLA, polymer jetting	[480,481,482,483,484]
PCBs/ICs	Dielectric materials, flexible silicone materials	IP/laser printing/FDM	[485,486,487]
MEMS	Silicone-based resins, photoresists, polymers	Electrospray printing/photolithography/IP	[488,489,490,491]
Micro-batteries	Polymer electrolytes, graphite powders, lithium titanate	DIW	[492]

4.2.3. Medical diagnosis and treatment

AM is a strong tool for assisting disease diagnosis and surgery in the medical field. Specific 3D printed models of patients based on private computed tomography (CT) or magnetic resonance imaging (MRI) can assist the planning and simulation of surgery, especially the achievement of minimally invasive surgery [419,457]. Novel smart materials or structures that could be used in medical diagnosis and treatment were reported recently. The previously mentioned submillimeter-scale magnetic continuum soft robot with controllable navigation [272] could access narrow areas, such as distal blood vessels, by further optimizing visualization and magnetic control systems. This robot could open new avenues for minimally invasive surgery and overcome existing challenges. Li et al. [421] designed and fabricated a burr-like porous microrobot using laser lithography, and the robot was coated with Ni and Ti for magnetic actuation and biocompatibility (Fig. 44d and e). Experiments showed that the loading cells on the microrobot could be delivered and released to a desired site. This robot shows great potential in regenerative medicine and cell therapy (Fig. 44f). In addition, a custom-made head support was printed by Jonathan et al. [458], and its advantages included a lower weight, lower cost, and safer properties. AM technology is a powerful tool for the production of delicate and complex components due to its high resolution and high efficiency. Custom-made artificial tissues and organs with specific characteristics will be possible in the near future.

4.2.4. 3D printing and COVID-19

Recently, the severe spread of the novel coronavirus 2019 (COVID-19) throughout the world has had a tremendous impact on the economy and society. Lu design a new and simple projection model for the COVID-19 pandemic [459], which can reliably predict the outbreak and trends

in advance. AM technology shows great potential for the study and manufacture of novel face masks and other medical tools, such as approved respirators and virus test devices.

Various materials are used to print masks and protective glasses, such as poly(ethylene terephthalate-co-1,4-cyclohexylenedimethylene terephthalate (PETG), polyurethane (PU), and ABS. 3D printing technology can be used for the production of masks and protective glasses with complex structures and multiple functionalities. Meanwhile, the material waste can be reduced greatly with higher efficiency and lower cost. Protective glasses are vital for anti-epidemic workers, as traditional glasses have many problems. Researchers at the Zhejiang University invented a platform to design custom-made glasses, which solved the functionality and conformity problem of standard protective glasses.

4.3. Electronic devices

The current applications of AM in electronic devices are summarized in Table 7, and explained as follows.

4.3.1. Microwave devices

Miniaturized, lightweight, high-precision, and low-cost devices operating in the microwave and terahertz bands are increasingly demanded in modern communication systems and electromagnetic application realms. Antennas, filters, and power dividers are essential devices and components of modern microwave communication systems. Conventional manufacturing techniques machine different components and then assemble them into functional devices, which leads to assembly errors and redundant waste. Furthermore, traditional metallic waveguides, antennas, filters, and most other devices are hindering the development of miniaturized and lightweight communication systems.

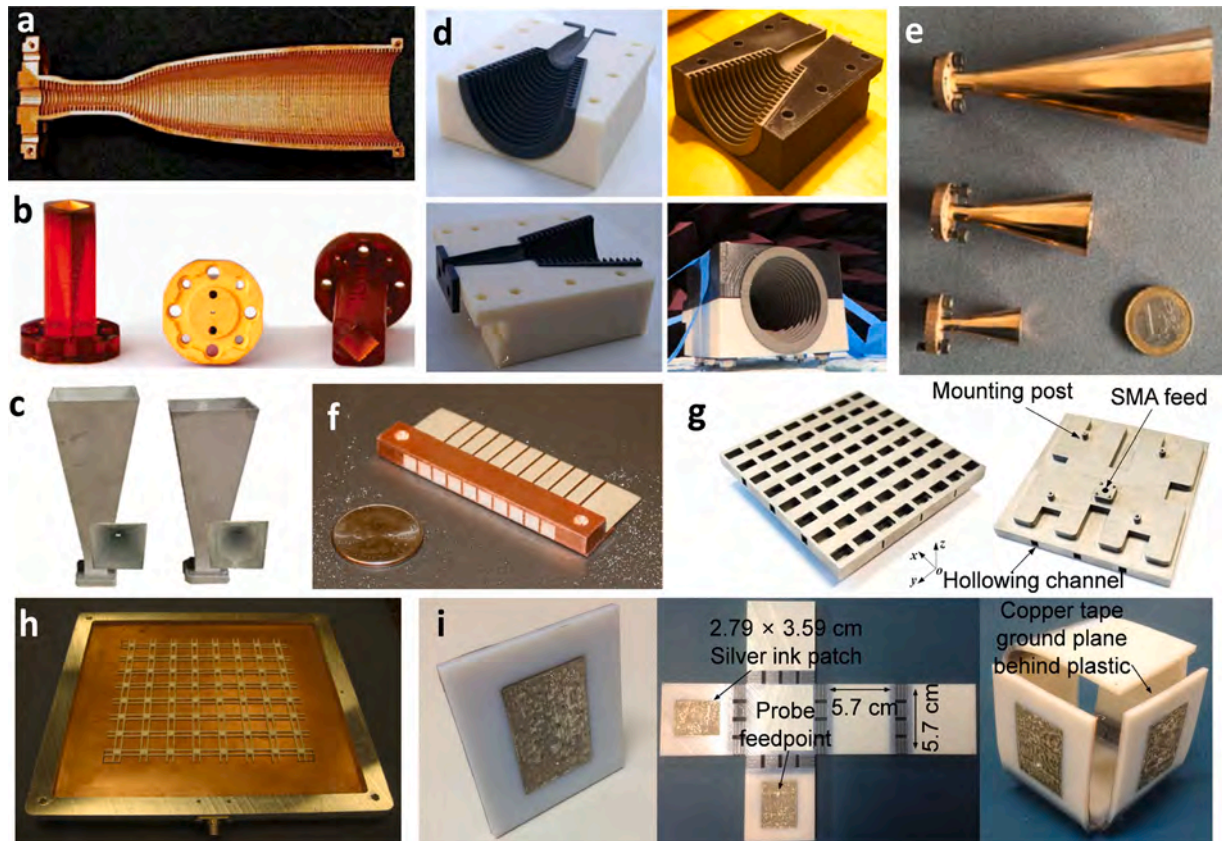


Fig. 45. AM of antennas: (a) corrugated horn antenna (W-band) constructed using stereolithography and plated with copper [460], (b) diagonal horn antenna (WR-3.4) manufactured with stereolithography [423], (c) two-horn antennas (Ku-band) printed using electron beam melting with different surface roughnesses (left: 25.9 μm , right: 39.7 μm) [461], (d) corrugated conical horn antenna (Ku-band) printed using SLA and ABS and coated with conductive aerosol paints [462], (e) SLM Cu-15Sn conical horn antennas (E-, D-, and H-band horns) [463], (f) assembled dielectrically filled horn antenna array fabricated using stereolithography (SLA) [464], (g) waveguide-fed antenna array fabricated with direct metal laser sintering (DMLS) 3D printing technique [465], (h) dielectric resonator antenna array fabricated using ceramic SLA [466], and (i) 3D printed origami packaging with inkjet-printed antennas [467].

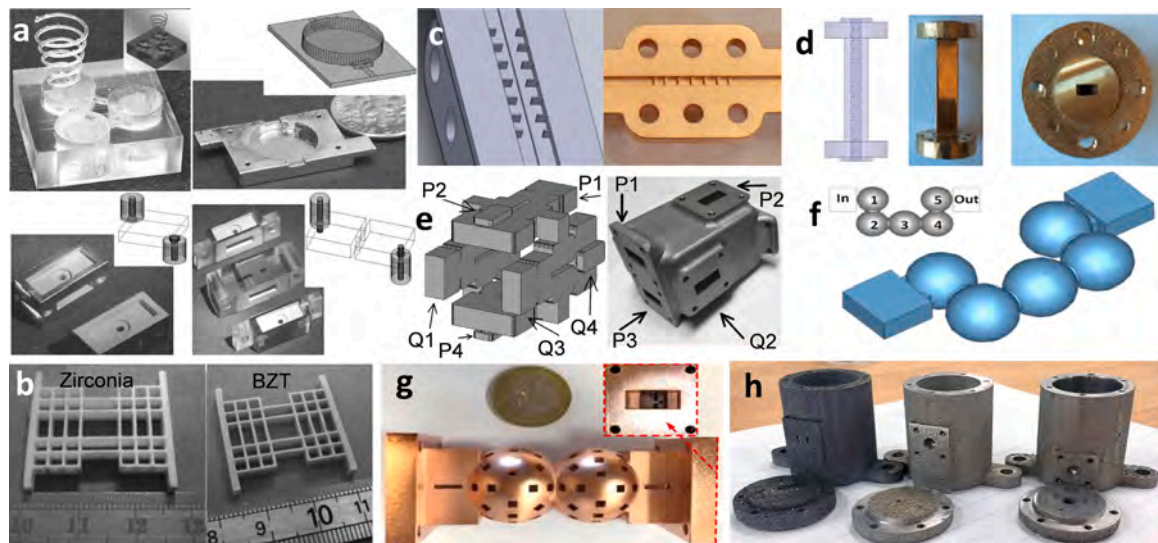


Fig. 46. AM of resonators and filters: (a) a front-end filter module, cavity resonators, and two-pole cavity filter fabricated via layer-by-layer stereolithography (SLA) [470], (b) cavity resonant structures made of zirconia and $\text{Ba}_3\text{ZnTa}_2\text{O}_9$ using ceramic SLA [471], (c) W-band sixth-order inductive iris bandpass filter fabricated using SLA [472], (d) E-band iris bandpass filters fabricated using selective laser melting (SLM) of a CuSn_{15} alloy powder [473], (e) Butler matrix with filtering produced by AM [474], (f) fifth-order X-band waveguide bandpass filter based on spherical resonators fabricated with SLA [475], (g) fourth-order cavity bandpass filter using two spherical dual-mode cavity resonators fabricated with SLA [424], and (h) superconducting aluminum microwave cavity fabricated with Al-12Si alloy using SLM [476].

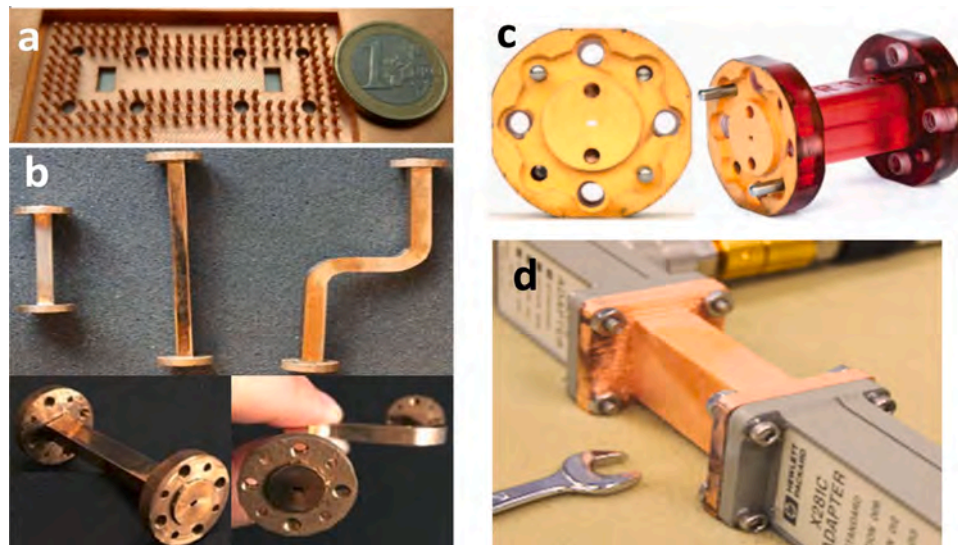


Fig. 47. AM of waveguides: (a) Ka-band groove gap waveguide fabricated using stereolithography (SLA) [477], (b) rectangular waveguides (E-, D-, and H-band) fabricated with Cu-15Sn powder using selective laser melting [478], (c) WR-3.4 band waveguides manufactured using SLA [461], and (d) WR-90 thru-line waveguide manufactured using SLA [472].

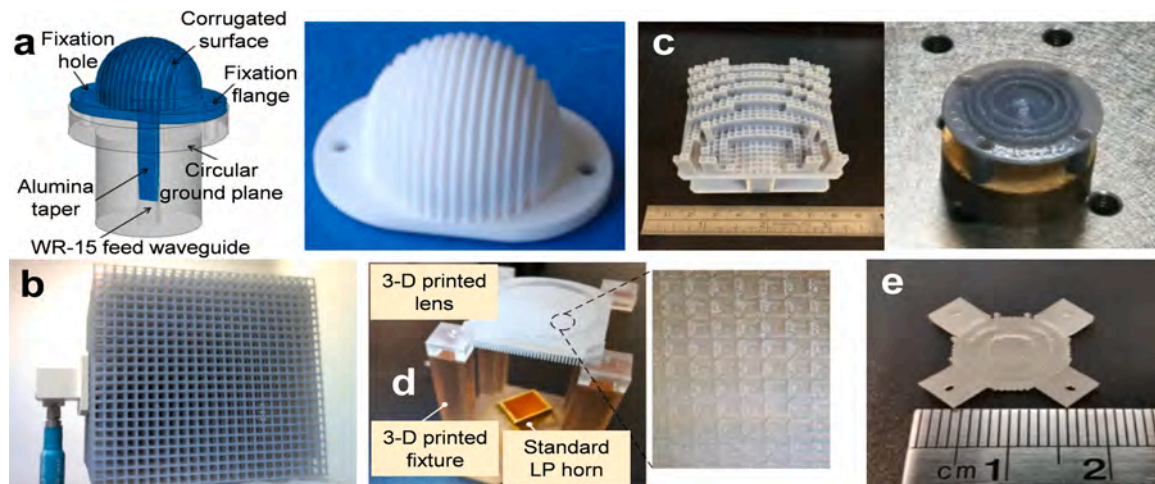


Fig. 48. AM of lenses: (a) alumina lens fabricated by ceramic stereolithography [480], (b) luneburg lens fabricated by polymer jetting rapid prototyping [481], (c) 3D printed beam-scanning lenses in millimeter-wave and terahertz range [482], (d) 3D printed terahertz, high-gain, circularly polarized lens [483], and (e) 3D printed terahertz lens for non-diffraction Bessel beam generation [484].

In recent years, AM techniques have provided an alternative for lightweight and rapid integrated manufacturing.

Several AM methods using different processes, such as metal 3D printing, dielectric 3D printing, and dielectric 3D printing with surface metallization, have been developed and applied to the manufacture of antennas (Fig. 45), resonators and filters (Fig. 46), waveguides (Fig. 47), lenses (Fig. 48), and many other microwave devices.

Despite the rapid development of various AM techniques, several issues must be addressed to further apply them for microwave devices.

1) Improve the process quality of AM techniques.

Molding techniques for metals and ceramics remain to be improved further. Requirements for the accuracy, strength, stiffness, and roughness are much more stringent in microwave devices. Even a tiny deviation may lead to a great variation in the frequency, band, or loss. Therefore, the molding quality of AM must be further improved to meet the development requirement of microwave devices.

2) Research and development of new materials for multi-function demands.

Rapid prototyping materials, which have their own limitations, are still in the development stage. Much attention has been paid to the mechanical properties, while few studies have focused on the electrical properties. To fabricate microwave devices that satisfy both the mechanical and electromagnetic requirements, there should be more investigations of new printable materials.

3) Trends toward higher frequency devices and greater miniaturization.

Fabricating microwave devices in higher frequency bands is challenging due to corresponding requirements for smaller sizes and higher electrical performances. Once the printing precision and surface toughness are improved to meet the high frequency needs, miniaturization and integration will be realized in the AM of microwave devices and systems.

4) Much higher additive manufacturing speed.

For rapid prototyping of large complex structures, it remains a long term goal to improve the additive manufacturing speed to a higher level.

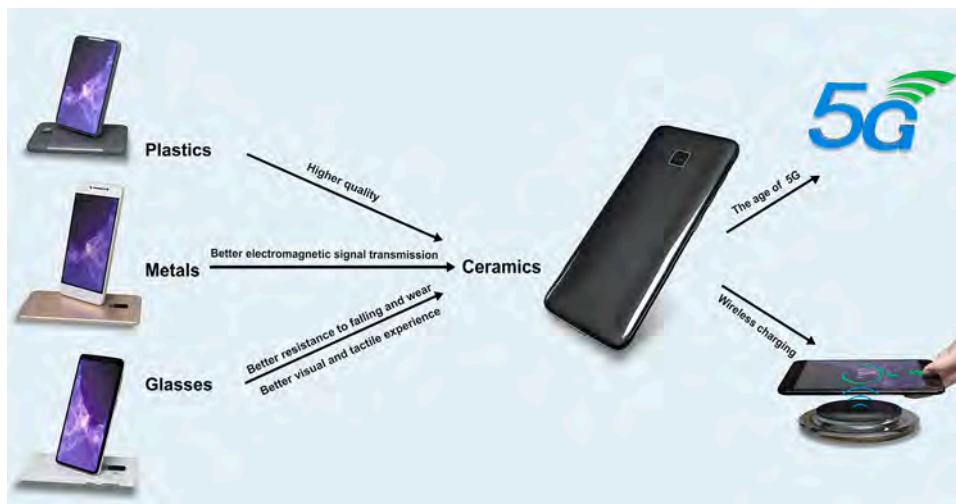


Fig. 49. Advantages of ceramic materials as cellphone back plates over other material candidates.

4.3.2. PCBs, MEMS, micro-batteries, and RFID tags

Silicon-based microelectronics technology has been developed based on largescale integrated circuits, which mainly refers to the fabrication of electronic circuits by the micro-machining of semiconductor materials, and PCBs are the carriers of integrated circuits (ICs). Printed electronics are a new electronic AM technology based on printing principles. The core idea is to use inkjets, aerosol sprays, material extrusion, and other technologies to print conductive, dielectric, or semiconductor materials onto a substrate to manufacture electronic devices and systems. Compared with traditional electronic processing methods, printed electronics have several significant advantages: (1) they can realize mass production and reduce manufacturing costs, (2) the printing process can be simpler than traditional process, energy consumption is low, and no etching is required, and thus, these processes are environmentally friendly, and (3) electronic devices can be fabricated on a variety of substrate materials, including flexible substrates. Researchers are now focused on 3D printed PCBs and ICs by inject printing or laser printing [485,486], which show great potential for achieving high transistor densities, high yields, high uniformity, and long-term stability, which are critical for the realization of organic digital ICs and other intelligent devices.

A MEMS is a system that integrates miniature sensors, actuators, signal processing, control circuits, interface circuits, communication, and power. With the development of communication technology and related fields, the importance of MEMS products is growing. However, the production threshold of MEMS products is very high, and advanced semiconductor manufacturing equipment is needed, which often costs tens of millions of dollars. Such a huge investment requirement has become a major obstacle to the further development of MEMS products. 3D printing technology is expected to change this. Researchers from MIT have developed a method for producing high-quality MEMS devices using a desktop 3D printer [488]. Traditional MEMS manufacturing processes must be performed in high-temperature vacuum environments, while MIT's solutions enabled MEMS production in low-temperature non-vacuum environments. These MEMS can greatly reduce production costs without losing product quality. Thus, 3D printed MEMS systems show great development potential. However, this technology must be further improved to be suitable for commercial applications.

Some achievements have been made in the research of 3D printed batteries [493–496]. As micro-batteries are a kind of battery with low volumes, high specific energies, stable working voltages, good sealing performances, small self-discharge, and high reliability, they are being developed with the miniaturization of electronic components. Researchers from the University of Illinois at Urbana-Champaign

successfully fabricated a sand-sized micro-battery ($<1\text{ mm}^3$) by 3D printing technology with good electrochemical performance [492]. Micro-batteries can provide enough power for micro-devices in the medical and communications fields, including many devices that are still at the laboratory scale and lack small batteries, which is conducive to further tapping into the potential of microelectronic systems.

Radio frequency identification (RFID) is a kind of wireless communication technology that can identify specific targets and read/write related data through radio signals without the need to establish mechanical or optical contact between the identification system and a specific target. RFID technology is widely used, such as in libraries, access control systems, and food safety. When the chip and antenna can be prepared together, the cost of RFID will be greatly reduced, and RFID 3D printing is beginning to move in this direction. Researchers from CAS first proposed the concept and method of “liquid metal suspension-3D printing” [497], which can be used to rapidly manufacture three-dimensional flexible metal deformable bodies with arbitrary complex shapes and structures at room temperature, and they successfully manufactured RFID tags on paper through this technology. If this technology can be widely commercialized in the future, then manufacturers can use this technology to easily print their own customized RFID tags for their products.

4.3.3. 3C back plates

Computer, communication, and consumer electronics (3C) manufacturing is one of the most important industries in the digital age. Highly customized and personalized demands from users continuously stimulate and promote the rapid development of the 3C industry, which has triggered the introduction of 3D printing into the 3C industry. The personalized one-off design of 3D printing caters to the do-it-yourself enthusiasts, and the small-scale production of 3D printing provides such possibilities. 3D printed components or devices are now available in the 3C industry, such as motherboard embellishments, cable covers, fan mounts, cable combs, and finger rests [498].

Compared with many other material candidates (such as plastics, metals, and glasses) in 3C back plates, ceramics have some advantages. For example, ceramic cellphone back plates are of significantly higher quality than plastic ones, as shown in Fig. 49. Currently, most cellphone back plates are made of metals. However, ceramic cellphone back plates deserve further attention, since ceramic materials as cellphone back plates have some advantages over metals.

- 1) The excellent behaviors of ceramics in the transmission of electromagnetic signals can meet the requirements of the 5G age and wireless charging technology.

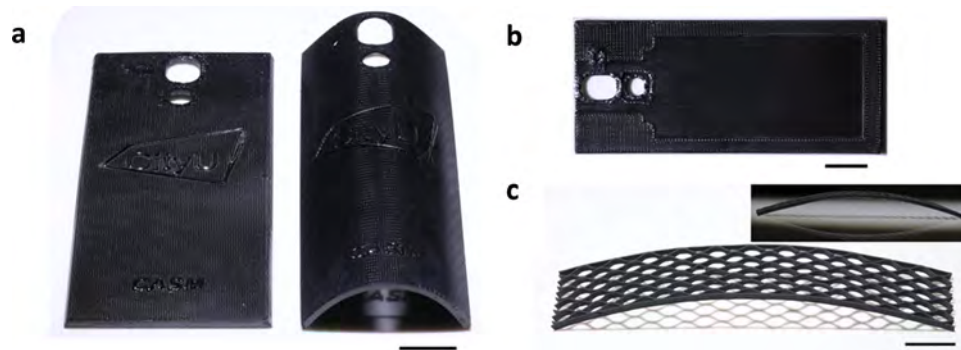
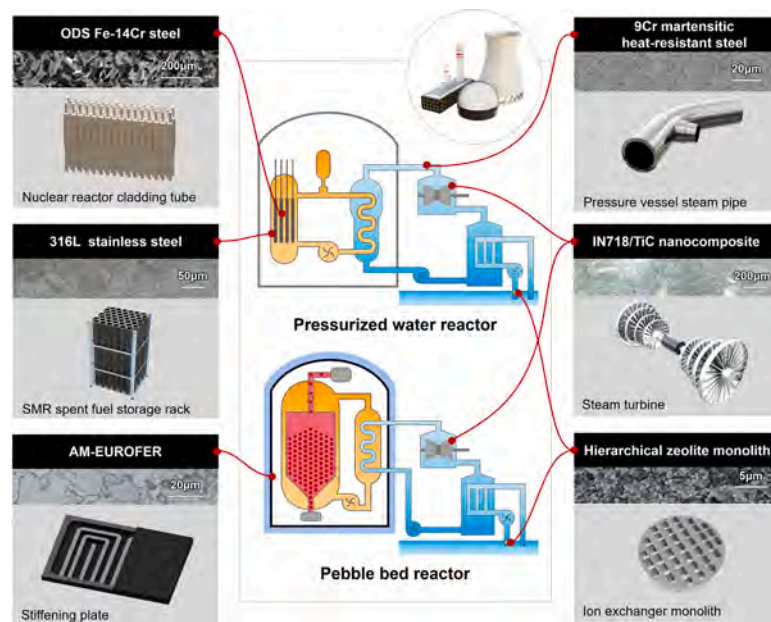


Fig. 50. Demonstration of ceramic cellphone back plates using ceramic 4D printing system: (a) flat (left) and curved (right) cellphone back plate, (b) top view of 3D printed flat cellphone back plate, and (c) curved ceramic honeycomb (scalebars = 1 cm) [45].

Table 8

Current applications of additive manufacturing in the nuclear industry.

Nuclear industry



Parts	References	Parts	References
Oxide dispersion strengthened Fe-14Cr steel	[499]	316 L stainless steel	[500]
AM-EUROFER	[501]	9Cr martensitic heat-resistant steel	[502]
IN718/TiC nanocomposite	[503]	Hierarchical zeolite monolith	[504]

- 2) Ceramics usually provide a better visual and tactile experience due to their glossy appearances and delicate textures.
- 3) Ceramics usually exhibit better resistances to deformation and corrosion, due to their better mechanical, chemical, and thermal properties, such as higher hardness values, strengths, chemical stabilities, and thermal stabilities.
- 4) Ceramics usually have lower densities than metals. Although glass materials also play an important role in 3C industries of the 5 G age, ceramic cellphone back plates exhibit better resistances to falling and wear, and also provide better visual and tactile experience than glass ones.

Ceramics are typically difficult to cast or machine due to their extremely high melting temperatures, hindering the development of ceramic cellphone back plates, especially for curved cellphone back plates. Origami and 4D printing involve conventional 3D printing followed by a shape-morphing step, and these processes have shown

potential in fabricating curved cellphone back plates. The present AM techniques have unique advantages in fabricating ceramic back plates, including programmable and customizable designs, geometrical complexities, cost efficiencies, color versatilities, and excellent mechanical robustness. Liu et al. [45] demonstrated 3D printed flat ceramic cellphone back plates and curved back plates generated by origami of EDCs (Fig. 50).

4.4. Nuclear industry

The current applications of AM in the nuclear industry are summarized in Table 8, and explained as follows.

4.4.1. Radiation shielding

Neutron beams are mainly used in nuclear power plants, imaging technology, neutron capture therapy, and activation analysis, providing huge benefits [505]. However, neutron radiation has destructive effects

on cells. Since the energy of fast neutrons after a nuclear reaction can reach 0–14 MeV and the speed is about 14,000 km/s, they have extremely high penetrating power and can cause great damage to instruments or humans. Prolonged exposure to neutron radiation may cause severe radiobiological effects in living bodies, such as carcinogenesis and DNA damage [506]. The purpose of neutron shielding material is to slow down fast neutrons into thermal neutrons and absorb them. Therefore, the research of neutron shielding materials has been favored by academia and industry.

In fact, composite materials are required to be lightweight in the AM of shielding materials. By reducing the mass and volume of the material, the shielding and thermomechanical performances of the material are improved. In addition, the design of the composite material is targeted, providing convenience for the shielding materials. Because of their excellent thermal stabilities and lightweight structures, carbon-based ceramic composites are widely used in the aerospace industry. Delfini et al. [507] reported the use of a carbon nanocomposite multilayer board (outer layer) combined with a carbon-based ceramic (inner layer) structure to prepare radar absorbing materials space elements. Studies have shown that an outer multilayer board ensures the required microwave absorption, while the inner C/C sheet can protect the interior of the spacecraft by providing appropriate thermal protection. Because of its high boron content and large neutron capture cross section, boron carbide exhibits good shielding performances and is also an important material for preparing shielding materials. DiJulio et al. [508] developed a new type of concrete by adding polyethylene (PE) particles and B_4C into the concrete, which could enhance the neutron capture performance of the concrete. The results showed that the density of the new concrete was lower, and thus, it was lighter and required less material. With the addition of PE particles and B_4C , the neutron shielding performance was significantly improved to under several MeV. After testing, the number of neutrons entering the PE- B_4C -concrete detector decreased by about 40 % compared with that of the reference concrete.

Changing the structures of the materials can also improve their absorption shielding performance. Absorptive honeycombs are common absorbent structures that imitate the regular hexagonal structure of natural beehives [509]. Radiation rays, neutrons, and electromagnetic waves are reflected multiple times on the wall surfaces of honeycombs and then absorbed by the honeycomb, and thus, the honeycomb exhibits better absorption and shielding performances. Stone et al. [510] used SLA technology to directly prepare a boron carbide (B_4C) collimator with a honeycomb structure by infiltrating B_4C with cyanoacrylate adhesive. The results showed that the transmittance of neutron absorption by the boron carbide material was less than 2 %, and the wavelength was about 0.21 Å (neutron energy is about 2 eV). For neutrons with an energy of less than 60 MeV, the collimator reduced the intensity of the beam, causing it to diverge in the scattering direction. Thus, the boron carbide collimator exhibited good absorption of high-energy neutrons. Zhao et al. [509] designed a new graded honeycomb composite absorbing material. Carbonyl iron particles/PETG composites with gradient honeycomb structures were prepared by a 3D printing process. The gradient honeycomb structure was optimized, and the absorption and shielding performances before and after optimization were compared. After optimization, an absorption band with a shielding effectiveness of greater than 20 dB was obtained, an absorption band with a reflection loss of less than -10 dB was 8–12 GHz, and the unoptimized absorption band was only 10–12 GHz. In summary, the material of the honeycomb structure plays the role of absorption and shielding.

Moreover, open-cell foam metals are a new type of structural and functional material. They have porous structures that can connect three-dimensional metal skeletons to each other. Zhang et al. [511] prepared a new type of the boracic PE/polyethylene wax blends-open-cell nickel foam composites (PPNM) by an infiltration method. Compared with PE/polyethylene wax, the energy absorption efficiency of the PPNM increased by 30 %, and the secondary radiation dose rate of PPNM

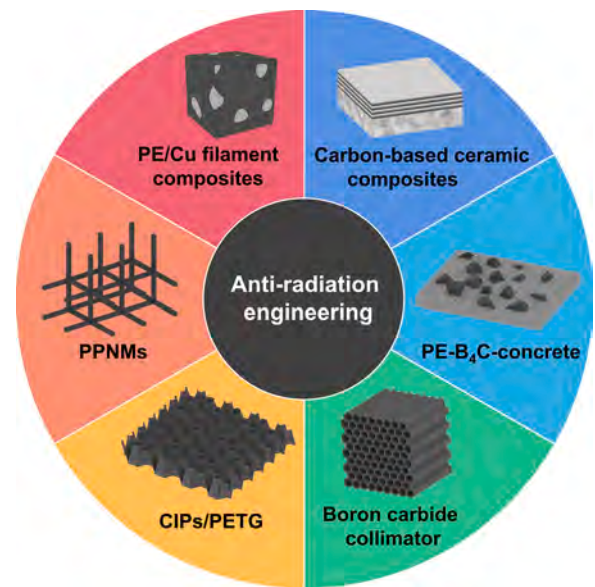


Fig. 51. Application of 3D printing technology in nuclear industry.

containing B_4C was reduced by about 84 %–89 %. The neutron shielding ability of PPNM increased with the increase in the B_4C mass fraction. Thus, the metal foam structure and B_4C could effectively improve the comprehensive radiation shielding ability of composite materials. Nabipour et al. [512] discussed the feasibility of preparing PE composite parts with an FDM 3D printer. In this experiment, they successfully prepared PE/Cu filament composites by FDM technology. This inquiry provided a source of inspiration for the manufacture of new metal/polymer composites through 3D printed FDM technology. Therefore, it is possible to try to prepare PE/boron carbide composite shielding materials by 3D printing FDM technology to prepare components with complicated geometric shapes and structures. Fig. 51 shows the structures prepared in the abovementioned research.

4.4.2. Materials selection

3D printing technology continues to develop and is widely used in the nuclear field. It can not only be used to print components for radiation shielding but also for other applications. The following are some of the studies on preparing parts for other application through 3D printing technology, as summarized in Table 8. To assess the potential use of AM in the nuclear industry, Vasquez et al. [499] used LPBF to prepare oxide dispersion strengthened Fe-14Cr steel and used it to manufacture nuclear reactor cladding tubes. He et al. [500] selected 316 L powder to manufacture small Modular Reactor spent fuel storage rack model by SLM technology and subsequently used it for actual nuclear applications through non-destructive inspection and standard formulations. Neuberger et al. [501] reported the preparation of EUROFER parts with SLS technology, which were connected with EUROFE-97 parts by electron beam welding to form the stiffening plate related to the Helium Cooled Pebble Bed Test Blanket Module. Gao et al. [502] manufactured 9Cr martensitic heat-resistant steel by WAAM technology, which could be applied for pressure vessel steam pipes in nuclear reactors. Yao et al. [503] prepared IN718/TiC nanocomposites by SLM, which have many applications in the nuclear industry, for example, for steam turbines used in pebble layer reactors. Halevi et al. [504] used DLP 3D printing technology to prepare monoliths with porous hierarchical zeolite complex structures with ion exchange performances and placed them in an ion exchange column for nuclear wastewater purification.

However, various single components can only achieve a single function. Therefore, achieving multifunctionality in a single component is a complex issue. The following should be topics of further study: (1) use of CAD and other modeling software to conduct structural design,

Table 9
Current applications of additive manufacturing in flexible and wearable devices.

Flexible and wearable devices			
Parts	References	Parts	References
Sensor	[513,514,515,516,517,518]	Li-ion batteries	[492,519,520,521, 532]
Nanogenerator	[522,523,524,525,526]	Soft electrodes	[527,528,529]
Capacitor	[530,531]		

morphology control, and modification of shielding materials for the preparation of complex and diverse geometric shapes and structures; (2) the addition of additives (such as additives with high neutron cross sections, flame retardants, getters, and adsorbents) to shielding materials to achieve multi-functionalization; (3) adjustment of the preparation parameters and printing process so that the raw materials used for printing can meet the printing requirements. Finally, it is possible to prepare a single component with multiple functions. To sum up, this kind of multifunctional composite material has broad application prospects in nuclear energy applications.

4.5. Flexible and wearable devices

Flexible electronics are attracting growing attention in recent decades. Many published works reported diverse flexible and wearable devices, such as strain sensors, nanogenerators, capacitors, batteries, and flexible electrodes, as shown in Table 9. Due to the high efficiency, material-saving characteristics of AM, 3D printing makes it possible for various functional materials to be applied in the field of flexible electronics. For structural materials, 3D printing can not only ensure the functionality of the material but also improve the robustness of printed materials. Various new printable functional materials pave the way for flexible devices to find applications in wearable electronics. Besides, many efforts on 3D printing structures had been made to broaden the applications in wearable electronics. This section highlights the latest results of 3D printing materials in wearable electronics.

Recently, many published works have focused on the wearable electronics fabricated through AM, including wearable electrodes for electroencephalogram (EEG) signal measurements [528], prosthetic skin integrated with multimodal strain sensors [515], flexible electrodes for electrocardiogram (ECG) signal measurements [529], 3D printed all-fiber Li-ion batteries for wearable electronics [532], wearable electrodes for electromyography (EMG) signal measurements [528], wearable electrodes for electrodermal activity (EDA) signal measurements [528], ultra-flexible 3D-triboelectric nanogenerators (3D-TENGs) that harvest energy from human motions [524], and 3D printed soft electrodes with conducting polymer [527].

4.5.1. Strain sensors

Among 3D printing strategies, DIW has provided possibilities for the fabrication of stretchable devices. Guo et al. [513] prepared a stretchable device using silver nanoparticle conductive inks. A multi-material, multiscale, and multifunctional 3D printing approach was adopted to print tactile sensors. The tactile sensors were assembled using a base layer, a spiral sensor part, two electrodes, an isolating layer, and a

supporting component, as shown in Fig. 52a. The multilayer sensor was demonstrated to be capable of detecting and differentiating human movements, including pulse monitoring and finger motions. Scanning electron microscopy (SEM) results showed that multiscale structures were introduced into the tactile sensor to improve the sensitivity. Wang et al. [514] created hierarchically porous sensing elements by incorporating sodium chloride, shown as Fig. 52b. The salt particles were removed after printing and curing. The sensor developed by this method consisted of micropores (20 – 100 μm) and nanopores (100 – 500 nm). As a result, the sensor was highly sensitive (5.54 kPa^{-1}) with large measurement ranges (from 10 Pa to 800 kPa). The robustness of AM technology provides methods to fabricate a full set of wearable electronics. Valentine et al. [515] developed a hybrid 3D printing method to produce soft electronics. Using this approach, an electronic substrate was directly printed with an insulating and soft matrix, and conductive paths were directly written on the insulating matrix in specific layouts. For functional devices, components were located on target positions using vacuum nozzles, and interconnections were directly written with conductive ink, as shown in Fig. 52c.

4.5.2. Nano-generators

AM, with a high material usage efficiency, can be used to fabricate nano-generators in a short period. Chen et al. [522] firstly reported a 3D ultra-flexible triboelectric nanogenerator (TENG) for wearable electronics. They reported a novel strategy to fabricate ultra-flexible 3D-TENG hybrids, as shown in Fig. 53a. Unlike previous TENG fabrication methods, the ultra-flexible 3D-TENG was composed of a composite resin component and ionic hydrogel. The nano-generator could harvest biomechanical energy, such as the energy of human motions. Chen et al. [523] fabricated a single integrated TENG nano-generator. As indicated in Fig. 53b, the electrification component of TENG was made of poly(glycerol sebacate) (PGS) and CNTs as the two electrification components. The conductive CNTs acted as electrodes and a flexible matrix. The hierarchical porous structure contributed to the higher efficiency than that of a traditional TENG fabricated by molding.

4.5.3. Flexible electrodes

Electrodes are used to measure the physiological indicators widely. The flexible ones can constantly monitor these indicators in a non-invasive way. 3D printing technology provides a new method to fabricate flexible electrodes by introducing unique multilevel structures. Ho et al. [528] reported a new fabrication process for 3D microlevel interconnected network-like conductive materials. This method was used to prepare a porous sugar scaffold through 3D powder bed printing (PBP), as shown in Fig. 54a. This scaffold was filled with conductive silicone

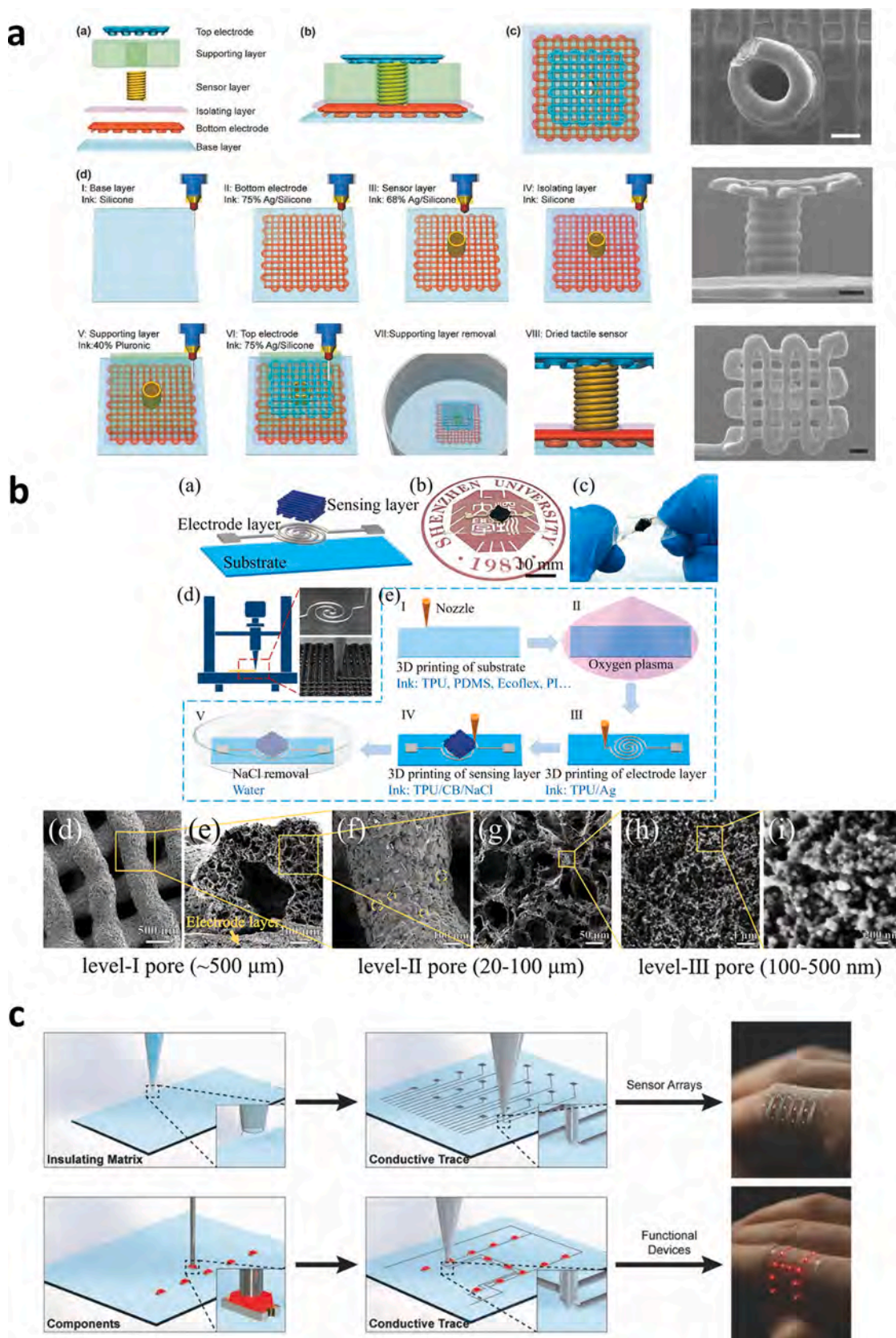


Fig. 52. 3D printing strain sensors: (a) schematic illustration of the fabrication procedure of tactile sensors and SEM images of a tactile sensor (scalebars: 200 μm) [513], (b) design principle and printing procedure of stretchable piezo-resistive sensor and SEM images of multiscale porous structure introduced to 3D printed sensing layer [514], (c) hybrid 3D printing method for soft electronics: sensor and functional device [515].

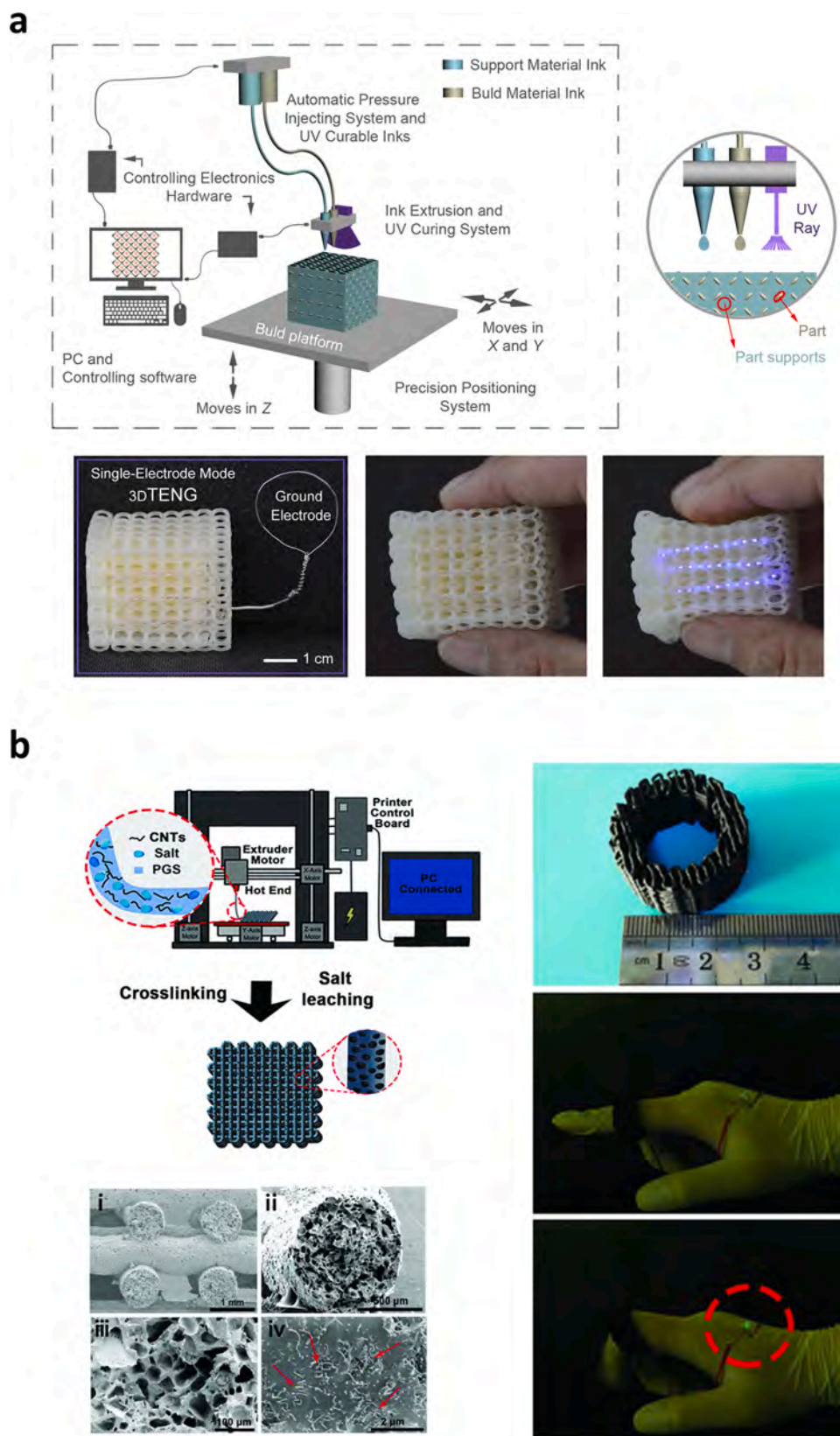


Fig. 53. 3D printed nano-generator: (a) fabrication process of ultra-flexible 3D-TENG and ultra-flexible self-powered light emitting diode (LED) devices that could flash “SOS” (sizes of 3.5 cm \times 3.5 cm \times 3.5 cm) [522], (b) fabrication and properties of the 3D printed TENGs and a ring-shaped 3D printed TENG lighting an LED [523].

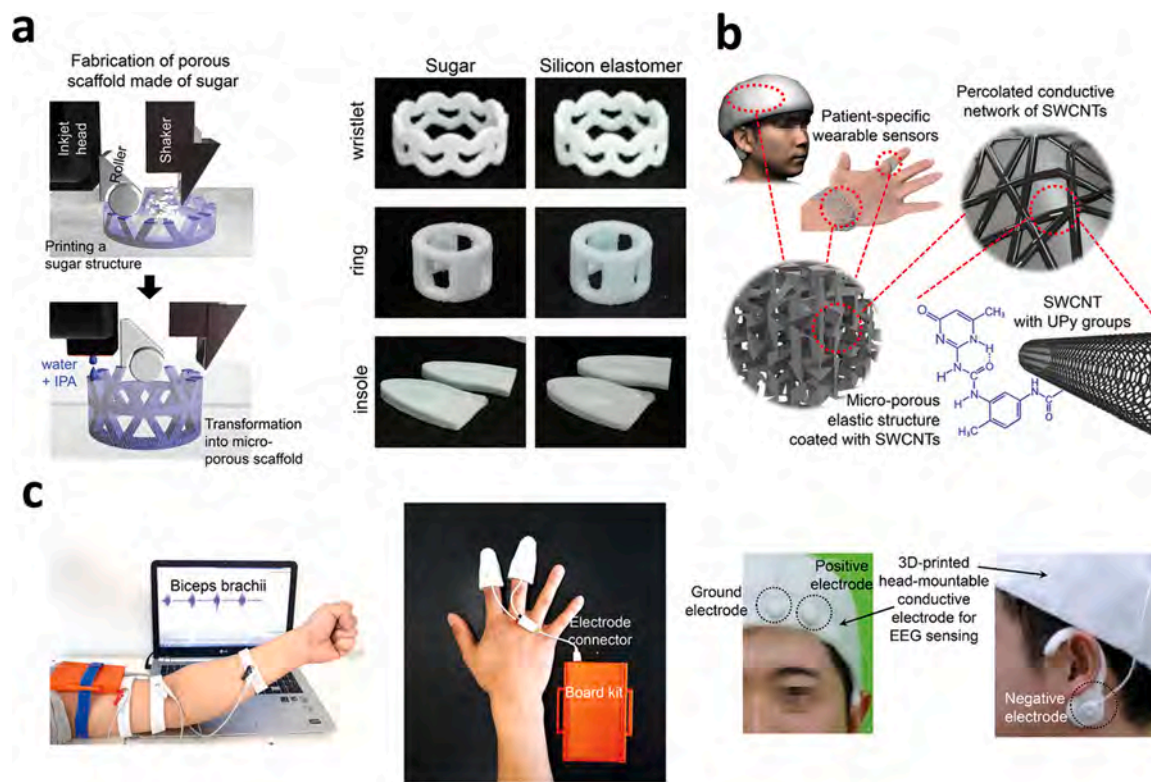
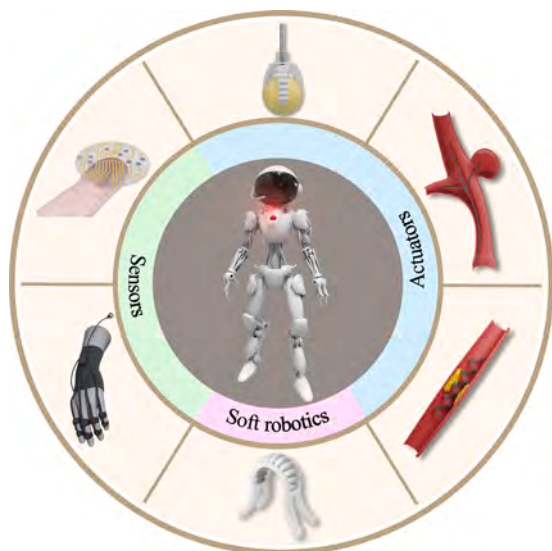


Fig. 54. 3D printed flexible electrodes [528]: (a) fabrication process of 3D flexible and conductive porous structure via 3D powder bed printing (PBP), (b) multilevel structure of 3D printed porous and conductive single-wall CNTs, (c) applications of conductive porous structure in flexible electrodes for EMG, EEG, and EDA signal measurements.

Table 10

Current applications of additive manufacturing in soft sensors, actuators, and robotics.

Soft sensors, actuators, and robotics



Parts	Materials	AM technology	Others	References
Sensors	Poly(3,4-ethylenedioxythiophene) polystyrene sulfonate	DIW		[527,533,534,535,536]
	Carbon conductive grease	DIW		[517]
Actuators	Ecoflex	DIW	Grasper	[537]
	PLA/Fe ₃ O ₄	DIW	Intravascular stent	[68,316,536]
	PDMS/NdFeB	DIW	Magnetic response	[272,273]
Soft robotics	LCEs	DIW	Heating response	[538]
	PDMS	DIW/soft lithography technique	Autonomously operated	[539]

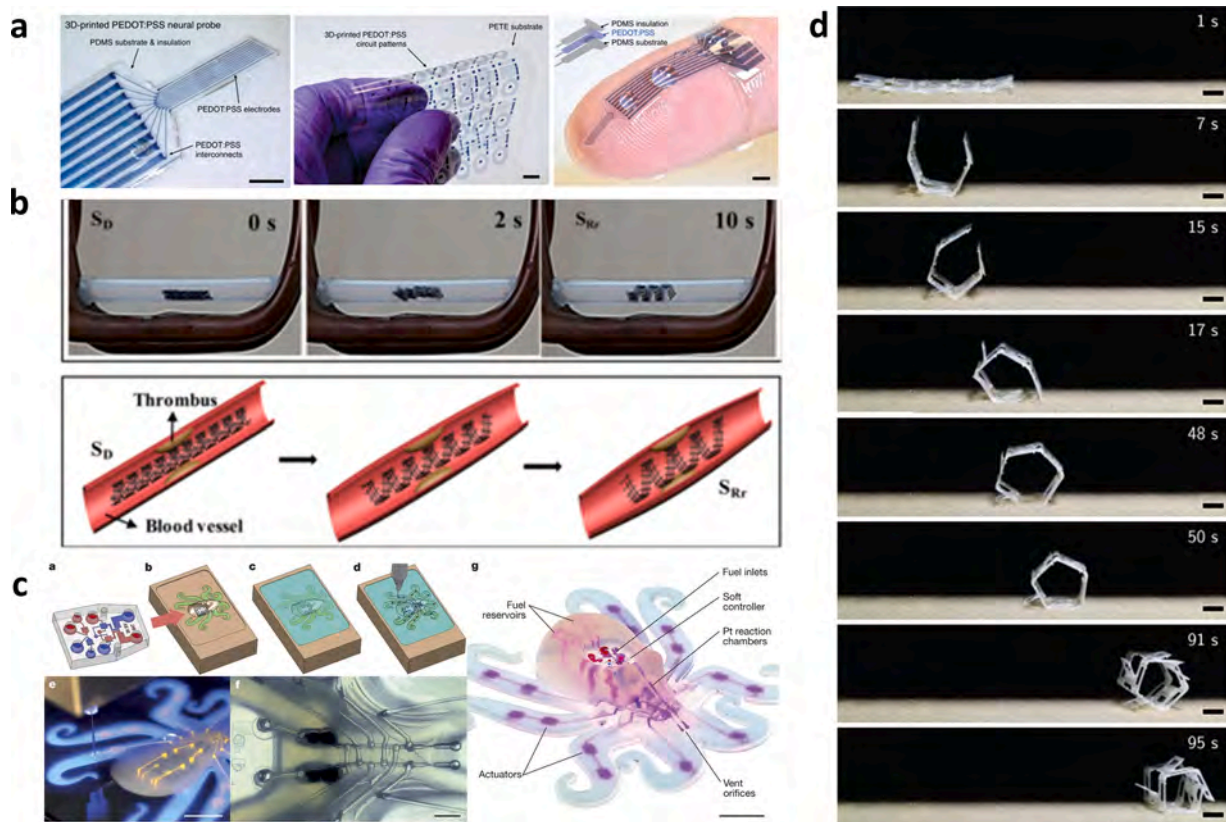


Fig. 55. (a) 3D printing of neural probe [527], (b) demonstration of potential application of the 4D printed scaffold as an intravascular stent [68], (c) fully soft, autonomous robot assembly [539], (d) printed self-propelling structure [538].

elastomers, and the removal of the scaffold yielded a porous flexible electrode. The high-resolution 3D scanned data of the body outlines applied in the 3D printing process made the flexible electrode sensitive, precise, and close-fitting. These fabricated electrodes measure the body's physiological signals successfully, for example, EMG, EDA, and EEG signals, as shown in Fig. 54c.

Compared to conventional fabrication technology, 3D printing structures have significant advantages, including precise control, material saving, and multilevel fabrication capabilities. Recently reported works show the robustness of 3D printed structure materials in wearable electronics. Printable elastomers with special structures are more sensitive to faint deformation, which is good for many kinds of sensors. The porous-structure materials with reversible deformation properties contribute to the high-efficiencies of nanogenerators. The precise control of the 3D structure via state-of-art technology, a 3D scanning technique, plays an important role in improving the sensitivity and precision of flexible electrodes. Attributable to the electrical properties of printing ink, the performances of 3D printed materials applied in wearable electronics are not as good as those of conventional devices. Therefore, further efforts should aim at not only improving the electrical performances but also at optimizing the printable properties.

Considerable research and progress have moved 3D printing wearable electronics to the forefront, despite the current challenges. With the recent material innovations and technological progress, the soft and functional structures will be designed and introduced to the field of wearable electronics.

4.6. Soft sensors, actuators, and robotics

AM also shows great potential for sensors, actuators, and robotics [533,534]. The current applications of AM in soft sensors, actuators, and robotics are summarized in Table 10. By definition, a sensor can detect

and respond to environmental stimuli [535,536]. 3D printed sensors can be divided into two main types: (i) 3D printed sensors that detect and respond to external stimuli directly, which are fabricated from materials that generate signals in response to stimuli, and (ii) 3D printed sensors as the matrix to support the responsive substances (e.g. nanoparticles, biomolecules, and living cells) [536]. Recently, Zhao's group created a soft neural probe by 3D printing to record the in-vivo bioelectronic signal. A conductive polymer was used as the electronic circuit, and PDMS was employed as the insulation and substrate to fabricate a neural probe (Fig. 55a) [68,527]. However, actuators can convert other forms of energy into mechanical energy. Various 3D printed actuators have been created and applied in the biomedical field. Wei and co-workers designed remotely actuated shape-changing structures by 4D printing. The fabricated scaffold shows great potential as an intravascular stent. Upon exposure to a stimulus, the scaffold will deform by a large amount and expand a blood vessel narrowed by a thrombus to keep blood flowing normally (Fig. 55b) [68]. Ze et al. [316] created novel SMP composites that exhibited adjustable mechanical properties under the actuation of magnetic fields. The fabricated grippers were demonstrated to be effective actuators, showing great potential for widespread applications. In addition, 3D/4D printed soft robotics have attracted increasing attention, due to their flexibility and diversity [272,273,540]. Wehner et al. [539] designed an entirely soft autonomous robot using an integrated design and fabrication strategy. 3D printing and soft lithography were employed to fabricate different parts of the robot. Fig. 55c shows the fabricated autonomous octobots, demonstrating its integrated capability. Kotikian and co-workers printed a liquid crystal elastomer soft robot, which exhibited the ability to repeatedly shape-morph and self-propel in response to external stimuli. The printed self-propelling "rollbot" completed a full roll on a hot surface without manual intervention (Fig. 55d) [538].

4D printing has great potential applications in sensors, actuators, and

Table 11
Current applications of additive manufacturing in jewelry and art decorations.

Jewelry and art decorations			
Parts	References	Parts	References
Ceramic pendant	[541]	Indirect fabrication of metal ring	[542]
Resin bracelet and earring	[543,544]	Metal necklace	[146]
Metal ring	[545,546]		

soft robotics (Table 10). In recent years, an increasing number of applications have been developed by researchers and used to solve the challenges that cannot be settled by conventional fabrication methods. However, there is still a long way to go before realizing the practical application of 4D printing in industry.

4.7. Jewelry and art decorations

3D printing is an emerging powerful tool for the production of jewelry and art decorations because it has the characteristics of rapid manufacturing, personalized customization, flexible design, and zero waste generation [547,548]. The traditional jewelry and decoration manufacturing process must go through various processes, including manual carving, investment casting, polishing, and other fine surface processing, which is time-consuming and requires considerable effort, especially the manual carving process [549]. As 3D technology is used to manufacture jewelry and art decorations, many cumbersome and time-consuming manual processes are avoided. As a result, a growing amount of 3D printed jewelry and decorations are being sold by jewelers. The main current applications of 3D printed jewelry and art decorations are shown in the Table 11, and the 3D printed versions can basically replace traditional jewelry.

The most direct and significant impact of 3D printing on the jewelry and art decoration industry is to shorten the production cycle of products, because CAD software facilitates the design and automatic rapid printing [550]. At present, the production of 3D printed jewelry and art decorations are mainly divided into two categories based on the raw materials: non-metal products and metal products (Fig. 56). Resin is one of the most commonly used non-metallic materials for 3D printing, because it is easily processed, inexpensive, and decorative. Thus, resin is widely made into jewelry and art decorations, and it is generally processed by light-cured 3D printing technology, such as SLA and DLP [543, 544]. The working principle is to produce free radicals by irradiating a photo-initiator to initiate the polymerization and crosslinking of the monomers and pre-polymer or to produce strong protonic acids by irradiating a cationic photo-initiator to catalyze and accelerate polymerization and solidify the resin. The jewelry and art decorations made

by light-cured 3D printing technology have exquisite detail and high surface finishes. However, printed resin products are usually considered to be low-end products of the jewelry industry or used as investment molds to make expensive metal jewelry due to the cheapness and low melting points of the raw materials [551,552]. In contrast, resin products are fashionable in the decoration industry. They are made into small decorations, such as tabletop ornaments and lighting, and they are widely sold on e-commerce platforms. In addition, plastic is similar to resin as a non-metallic 3D printing material, but it has better mechanical properties. It can not only make pure decorative ornaments but can also be processed into load-bearing members, such as art furniture parts. Seat backs and bases with complex grid structures are the representatives of 3D plastic art furniture parts at present. Moreover, FDM is the main production technology of plastic ornaments because its equipment is simple and inexpensive.

As one of the earliest art forms, ceramics have important artistic and cultural value and are popular for 3D printed jewelry and decorations at present. The 3D printing of ceramics is mainly through sintering to form, in which a BJ and SLS are the main ceramic printing technologies. BJ can not only perform fast automatic printing but can also further achieve color ceramic printing through three primary color binders, and they are usually used to print large-scale ceramic art decorations [553]. In addition, ceramic materials can also be made into rings, pendants, and other ceramic jewelry, usually processed by SLS technology, and the raw material is usually ceramic powder with a polymer as the sintering binder [541]. However, 3D printed ceramic jewelry is still a new product in the jewelry market, which requires further testing and development to become popularized.

Metal jewelry occupies a large proportion of the jewelry market, but because of the high price of raw materials and the characteristics of traditional processing technology, a large number of precious metals are wasted every year. In recent years, metal 3D printing technology not only has flexible design capabilities but also can be used for direct integrated forming, which has been widely of interest to jewelers. Among the many 3D printing technologies, lasers have gradually become the main heat source of metal 3D printing because of their easy operation. 3D printing methods with a laser as heat source are mainly divided into laser sintering forming and laser melting forming. The representative 3D printing technologies are SLS and SLM [545]. In the jewelry industry, SLS technology usually directly sinters a multi-component metal powder as the raw material to make jewelry and decorations [146]. However, due to the low quality of the surface of the sintered forming jewelry, the further application of SLS technology in the jewelry industry is limited. In addition, in precious metal jewelry, such as gold and silver, the addition of low melting point metal components has a negative impact on the purity of the jewelry. Conversely, SLM does not require an additional sintering binder and has a high printing quality. Thus, it has become the main preparation method of directly formed metal jewelry [146,545,554]. However, gold and silver powders are difficult to melt using a laser due to their high reflectivities and thermal conductivities [546]. Therefore, the heating process of gold and silver powder must be optimized in SLM 3D printing. The surface treatment and micro-alloying of the raw material powder are currently the main optimization measures to reduce the reflectivity and thermal conductivity of the alloy to improve the printing quality [145]. The powder surface treatment can increase the surface oxidation degree of gold and silver alloys to reduce the reflection of the laser. As for micro-alloying, trace elements such as iron and germanium are usually added to reduce the thermal conductivity, improve the surface oxidation performance, and depress the melting point of the gold and silver alloy powders.

Although, SLM technology can build metal jewelry and decorations with complex structure, the whole forming surface must be covered with metal powder. When printing precious metals, the cost will be very high. Therefore, SLM manufacturing is less commonly used for the fabrication of precious metal jewelry. Indirect manufacturing of metal jewelry and decorations by 3D printing is still a popular concept. Generally, wax or

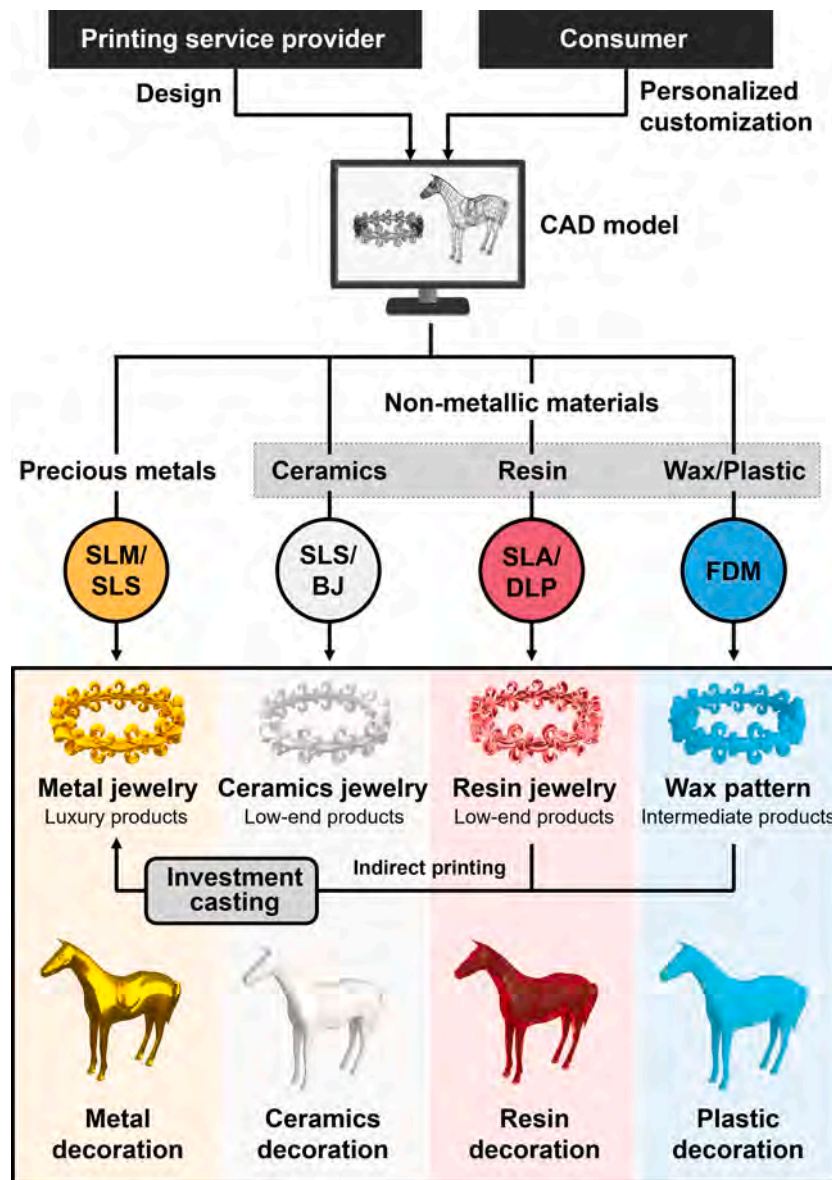


Fig. 56. Common printing materials and corresponding 3D printing technologies for jewelry and art decorations.

resin intermediates are manufactured by FDM and light curing 3D printing technology for investment casting of precious metal jewelry [542]. This method of 3D printing technology in jewelry manufacturing greatly shortens the jewelry production cycle and reduces the production cost.

In general, because 3D printing technology has flexible design capabilities, zero waste, automated manufacturing capabilities, and other characteristics, a growing amount of 3D printing jewelry and decorations with novel appearances are being designed, and these designs have become popular to the public. In addition, because of the convenience of CAD modeling, jewelry and art decoration consumers can propose their own designs and create print models. In recent years, with the increase in the proportion of online sales of jewelry and decorations, this personalized customized sales model is becoming more and more popular [555]. At present, Orori, American Pearl, and other jewelry companies have successively launched online customized jewelry services. Personalized art decorations have also become common on e-commerce platforms.

At present, 3D printing technology is being actively used to manufacture jewelry and art decorations, but the products on the market are

mainly low-end and cheap products, while the printing of precious metal jewelry and high-quality ceramics still requires further exploration. With the development of 3D printing technology and printing materials, 3D printing will become an indispensable and powerful tool in the jewelry and art decoration industry due to its automatic, rapid production, personalized customization, and zero waste. The 3D printed products will also play an important role in luxury high-end jewelry and fine decoration.

4.8. Land transportation

Recent progress in AM, such as 3D printing, has rapidly accelerated its application in the manufacturing industry. Among the many manufacturing applications, there is tremendous potential for the use of AM for road vehicles, for example, automobiles, bicycles, and rolling stocks, due to the ever-growing needs for newer, lighter, stronger, safer, time-saving, and energy-saving designs [556]. As automobiles represent the largest market share of all types of road vehicles, AM has tremendous application potential. According to a recent report on AM for automotive part production from 2019 to 2029 issued by SmarTech Analysis, the

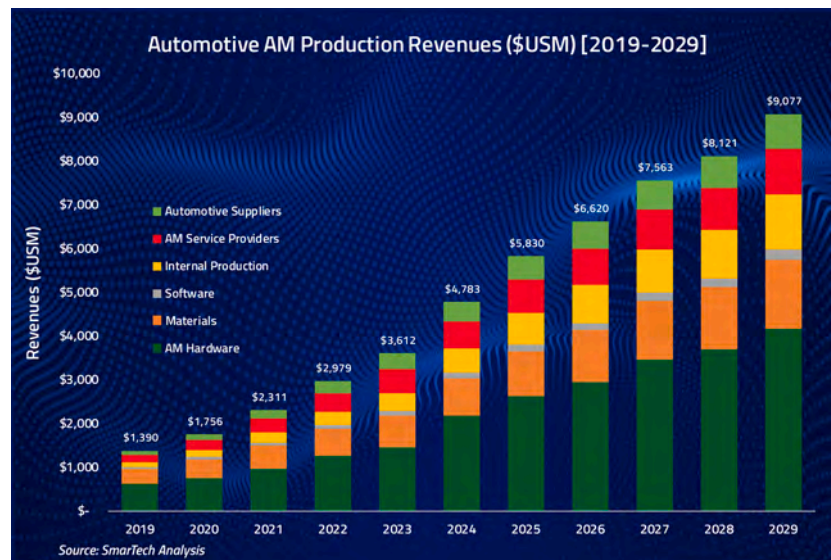


Fig. 57. Automotive AM production revenue 2019–2029 [557].

revenue of automotive AM production has an opportunity to reach over \$9 billion by 2029 [557], as shown in Fig. 57. AM techniques have not only influenced the development of the original equipment manufacturers and suppliers but they have also stimulated the emergence of innovative designs and manufacturing methods, such as direct and integral manufacturing [558].

Vehicle manufacturers are pioneers for the application of AM techniques to their products. From the early used rapid prototyping to the currently popular 3D printing, AM technology has been applied in the automobile field for more than 20 years. AM, for the moment, is mainly used for communication of design intension, prototype performance validation, pre-production for low-cost, rapid tooling, small-lot production of small and medium-sized products for multiple design iterations, tooling production, end part production, and spare part production to meet demand [559]. Many automobile manufactures have already adopted AM to fabricate car components and develop personalized services. For example, the supercar manufacturer Bugatti utilized the metal 3D printing technology to manufacture brake caliper [560]. Porsche started to offer a rare part printing service for classic car owners using the SLM process in 2018 [561]. Similarly, Ford also adopted the 3D printing technology for the fabrication of spare parts, such as the heating/venting/air-conditioning parts for the 2006 Ford Focus, and manufacturing tools [562]. BMW has utilized AM for prototyping and development since 1990 and has printed more than one million components in series production. Volkswagen has also applied metal and desktop 3D printers, for mass end-use part production and tooling design. It also provides 3D printed customized car parts (for example, individualized gear knobs [563]), and parts for motorsports (for example, the Motorsport's I.D. R Pikes Peak racing car) [564]. Furthermore, other traditional automotive original equipment manufacturer, such as Daimler, Audi, GM, Toyota, and Chrysler, all have invested in 3D printing technology [565]. In addition to the production of small or medium-sized parts, AM technology is also used for the production of large-sized parts or even full-scale vehicles. The first car with a 3D printed body, URBEE, was fabricated in 2003 by KOR [566]. In 2014, the first 3D printed electric car in the world, Strati, was manufactured by ORNL and Cincinnati Inc. using a large-scale 3D printer during the International Manufacturing Technology Show [567]. Furthermore, ORNL also created a 3D printed utility vehicle (PUV), which could be powered by a solar 3D printed home, and in return, could also power a house [568].

In conclusion, AM technology has had a positive influence in automotive manufacturing. It provides more possibilities for smart designs

with complex structures and novel combinations of materials, for example, lattice structures and combinations of different alloys for lightweight designs. AM has a high efficiency in terms of time and cost savings because no additional tooling is required and the supply chain is simplified. Moreover, compared with traditional manufacturing methods, AM methods only use certain materials they need, thereby reducing material wastage [569]. Although AM technology has a bright future in automotive manufacturing, it still faces several challenges [570]. First, the current production speed of AM is low and cannot keep pace with the enormous automobile production. Second, the development of low-cost, large-sized AM methods is necessary for future applications in automotive manufacturing. Third, more professional technical AM staff are needed for long-term development. Fourth, the intellectual property of AM products should be examined.

In addition to automobiles, bicycles and rolling stocks are the other two common road vehicles that have been influenced by AM technology. Unlike traditional bicycle manufacturing methods, 3D printing has proven to be a better method for lightweight bicycle production due to its superiority in manufacturing parts from titanium and carbon fiber. 3D printing also can help to achieve design flexibility, affordable customization, and faster times to market for bicycle production [571–573]. However, so far, 3D printing has not been used for mass production in the bicycle industry and only shines in one-off projects, such as customized, high-end bicycles. For railway sectors, a train or subway can be used for several decades. Therefore, a common problem is that it is difficult to find replacements in a short time when components are damaged. To solve this problem, the railway sector, such as the Deutsche Bahn, has begun to apply 3D printing to manufacture rare parts [574]. In summary, AM in the rail industry can be used for time- and cost-saving replacement part production, cutting-edge and high-performance material exploration, customized design fabrication, and service life extension of vehicles due to fast part replacement [575].

For the moment, although AM technology has been adopted by many vehicle manufacturers for their product manufacturing processes, traditional manufacturing technologies still play a dominant role in the land transportation manufacturing industry. However, there is no denying that AM now is penetrating this industry at a high speed and will accelerate the formation of new trends. It will not only influence the evolution of the product but may also affect the business model. The future development prospects of AM technology in the land transportation manufacturing industry will largely depend on the development trends of this technology in the future.

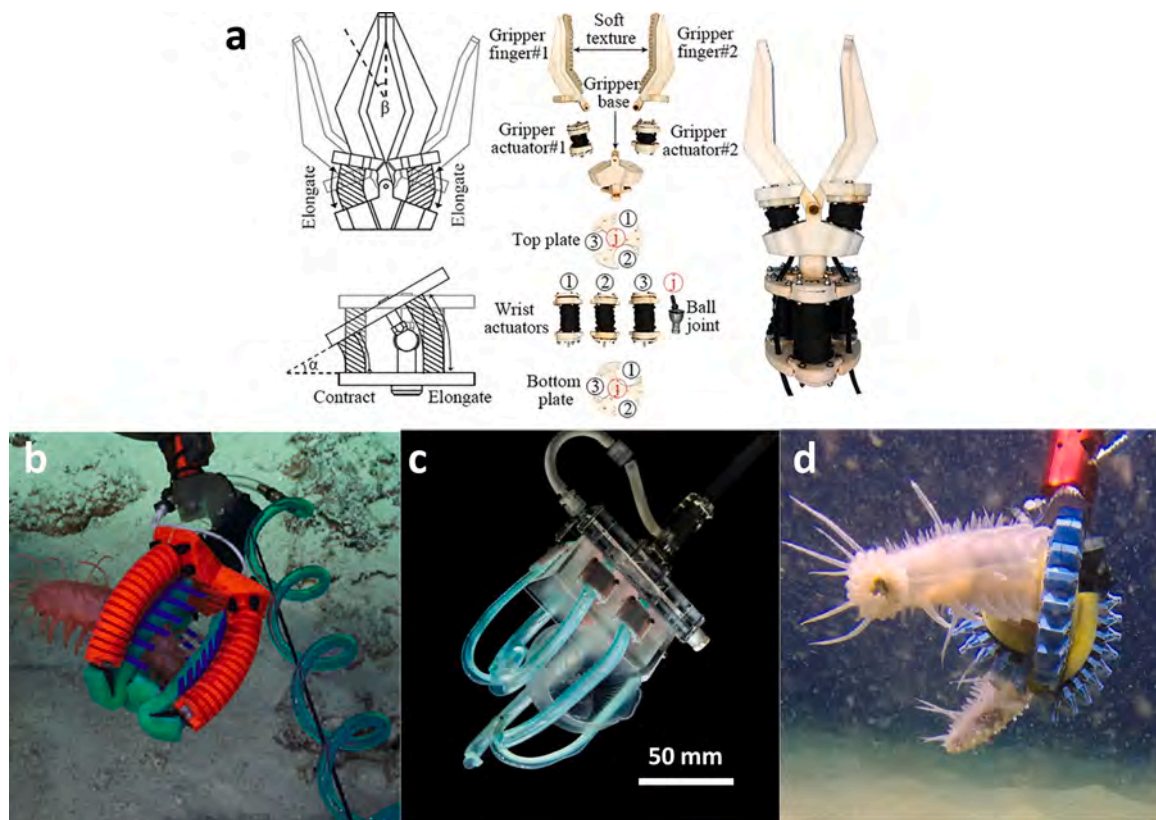


Fig. 58. Additively manufactured grippers for trapping deep sea specimens: (a) [582], (b) [576], (c) [581], (d) [584].

4.9. Underwater devices

AM is also promising for underwater applications, especially deep sea applications, which are far from land with limited resources and face the most severe environment. The fast custom-design and manufacturing abilities enable AM adopted in the underwater studies to be a real-time solution for engineering problems that arise in unpredictable scenarios. Currently, the soft robotic manipulators made by 3D printing, whose typical structures are shown in Fig. 58a, have been well applied to catch delicate and aged deep-sea organisms 2224 m underwater in the Phoenix Islands Protected Area [576], which were used on the remotely operated vehicle shown in Fig. 58b. With the fast development and maturity of AM, various materials can be printed for custom designed structures [577], including dielectric elastomer actuators, hydrogels, electroactive polymers, SMAs, SMPs, and fluidic elastomers. 3D printed parts for operating in the deep sea under a high static pressure should be printed without void spaces to prevent collapse of the air trapped inside the structures [576]. To reduce mechanical damage to the deep sea specimens, specific soft grippers [578–584] were made by AM and tested in the sea. Compared with conventional rigid grippers made from traditional machining, 3D printed soft grippers can have larger shape transition abilities and better contact with soft materials, which also have better performances for trapping deep sea specimens, as shown in Fig. 58c and d. To better support engineering development and the shipboard maintenance of seagoing vessels, SLA printing on onboard passive stabilization platforms was investigated [585] in order to lower down undesired influences from the dynamic environment on the sea surface.

The extreme environment in deep sea studies prevents many mature devices from being applied for simple functions, such as grabbing objects. With limited resources and space on seagoing vessels, which are far away from the mainland, AM is a promising solution for manufacturing soft robots or manipulating parts. However, AM is also a



Fig. 59. Potential application scenarios of additive manufacturing in sea, land, and air transportation.

valuable solution to support engineering development and maintenance during voyages, especially metal AM. With the further development and maturity of AM, AM machines will be standard equipment for seagoing vessels. Furthermore, with its rapid development, AM is valuable for the advancement of commercial amphibious cars and aircraft, which may open a new commercial market as amphibian vehicles and aircraft are primarily used for military purposes currently. As shown in Fig. 59, component structures made via AM are promising, and they are becoming popular in transportation vehicles in the air, on the land, and in the sea, including on the surface and underwater. It is believed that the AM technique will contribute much more to transportation vehicles in the future, especially to the development of new structures for the vehicles.

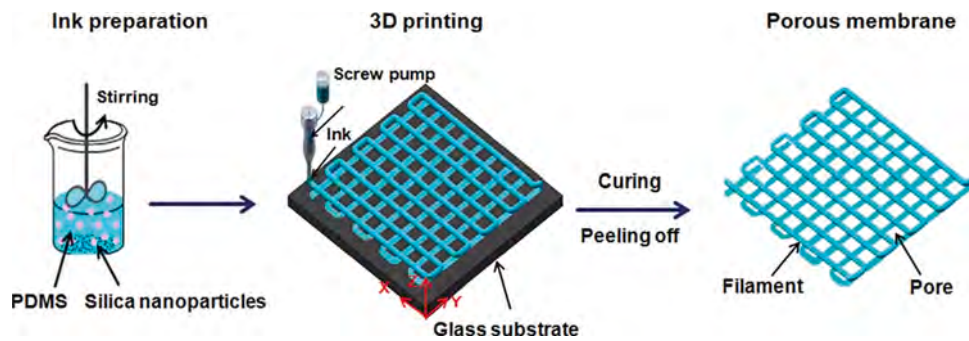


Fig. 60. Schematic of the 3D printing of a porous membrane [593].

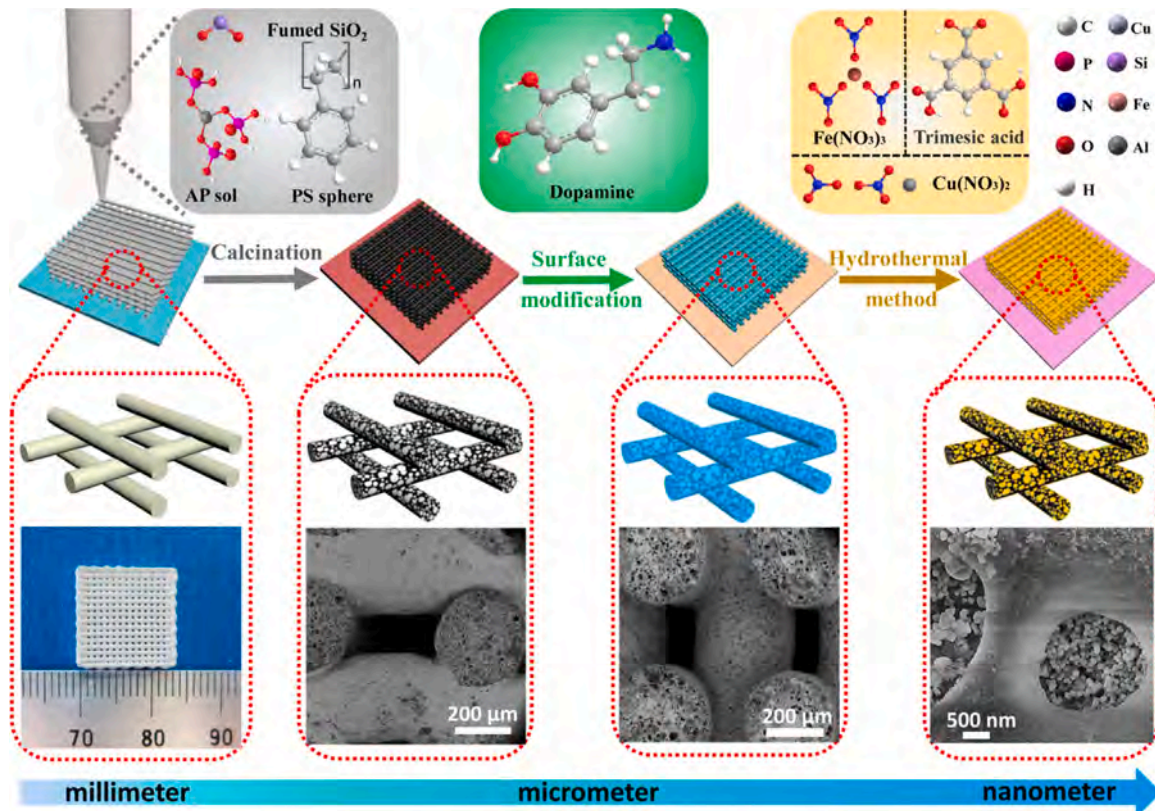


Fig. 61. Multilayer porous ceramics prepared by DIW [595].

4.10. Porous structures

Different microstructures as porous structures [123,586–588] are becoming increasingly important owing to the booming development of all kinds of AM technologies. There are many potential applications for porous structures by using AM technology, especially in the medical field, such as the fabrication of bone scaffolds. Components with different size distributions and morphologies can be fabricated using different 3D printing technologies [589]. With the aid of CAD, porous scaffolds with designed shapes could regulate chemistry and have interconnected pores. Due to individual patient differences, traditional implants cannot fully satisfy the needs of all patients, which results in implant limitations, poor biomechanical effects, and short service lives. Nevertheless, different porous bone scaffolds fabricated by 3D printing can be customized based on different bone features, and thus, personalized implants fabricated through AM methods can eliminate these problems. However, 3D printing technology can print porous bone trabecular prostheses to create prosthesis-bone interfaces that can

effectively reduce the occurrence of stress shielding and prolong the life of the implant [590,591].

Porous scaffolds are a crucial part of bone tissue engineering. Porous scaffolds act as templates for the attachment of cells as well as stimulating bone tissue growth [591,592]. The pore size and volume are integral factors that affect the porous scaffold's performance. A minimum pore size between 100 and 150 μm is required for bone formation. However, the pore sizes of the scaffolds that enhance bone formation and vascularization are greater than 300 μm [593]. Bone scaffolds with porous structures could be fabricated in various ways, such as gas foaming, drying through freezing, and separation induced by a thermal phase.

Besides, 3D printed porous structures have enormous potential in filtration applications, particularly for the oil–water separation or water purification. Fig. 60 schematically shows the porous membranes fabricated by the AM approach, particularly the DIW method. Indeed, porous membranes are manufactured through a programmed mesh structure by using PDMS ink, which is a superhydrophobic material [594]. The

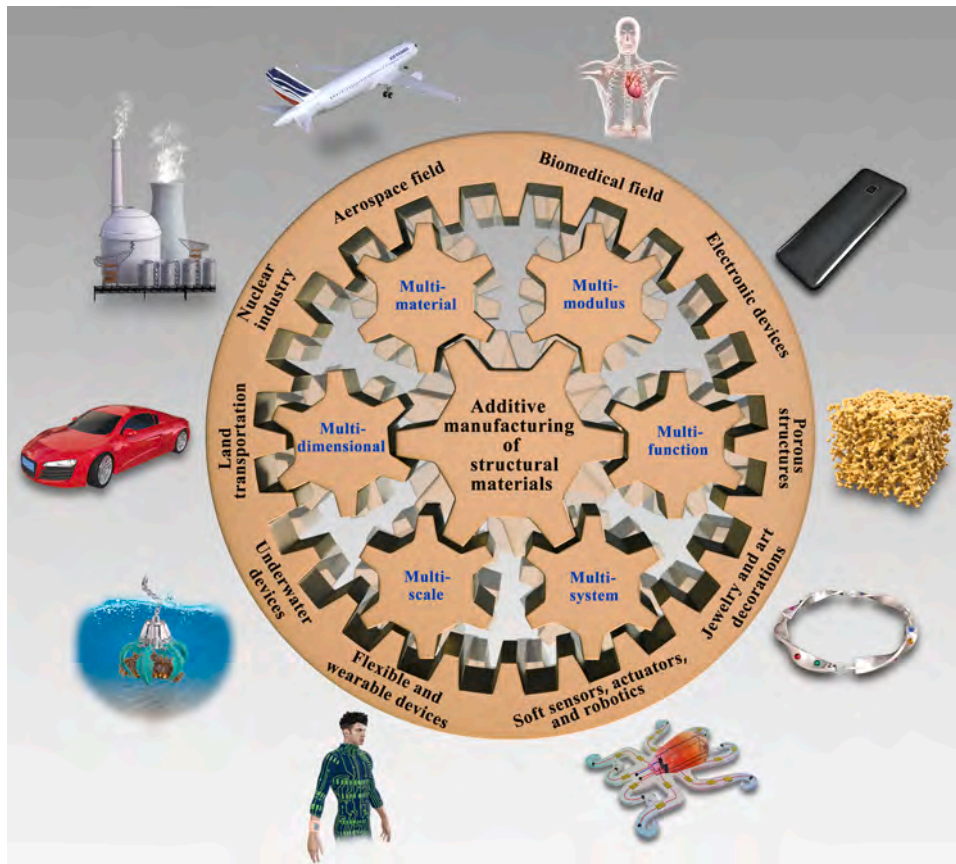


Fig. 62. Multiple perspectives of the AM of structural materials.

structures of the porous membranes can be programmed with the aid of a computer to obtain the desired properties, integrating the superhydrophobic surface within a porous lattice to avoid the weak interface adhesion problem and achieve mechanical stability. Thus, such membranes exhibit high efficiency in oil–water separations with low costs and no secondary pollution. Research on porous ceramic catalytic materials and devices modified by 3D printing metal–organic frameworks (MOFs) [595] (Fig. 61) was carried out by using DIW 3D printing technology to prepare multilayer porous catalysts with structural tenability, high catalytic capabilities, and long-term stabilities. The results show that MOF-modified 3D printed multilayer porous catalysts exhibited excellent catalytic performances for organic pollutants in water.

With the rapid improvement of technology, 3D printing of porous structures will be widely applied in bone tissue engineering and catalysis. The breakthrough taking in artificial intelligence algorithms based on biological inspiring will benefit complicated porous structure design and laser processing parameter optimization, and it will promote the development of 3D printing in porous structures.

5. Perspectives

This review has covered a broad range of topics, including structural materials for AM (polymers, metals, ceramics, glasses, and composite materials), 4D printing, and promising applications. Furthermore, new perspectives on the strategies of AM for structural materials are proposed (as shown in Fig. 62), including MMA-AM, MMo-AM, MSc-AM, MSy-AM, MD-AM, and MF-AM. MMA-AM will include material combinations among printing host materials, supporting materials, and medium materials. Soft/rigid hybrid systems and hierarchical structures with excellent behaviors will be achieved using MMo-AM and MSc-AM, respectively. MSy-AM involves material–structure–process–property integration and concurrent manufacturing. MD-AM has two meanings: (1) the printing dimension increasing from 2D/3D/4D AM to even higher dimensional AM and (2) the printing efficiency increasing from dot-by-dot/line-by-line/sheet-by-sheet/volume-by-volume printing to block-by-block printing (Fig. 63). MF-AM, or AM+, includes pre-programming, real-time treatment, or post-processing of the printed structural materials to generate functional materials for various applications. Moreover, 3D printers may print everything with self-printing capabilities, as shown in Fig. 64.

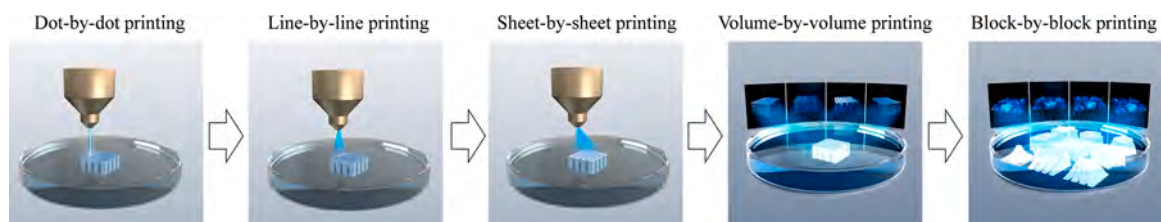


Fig. 63. Multi-dimensional additive manufacturing: higher dimensions and higher printing efficiencies.



Fig. 64. 3D printers may print everything with self-printing capabilities.

Declaration of Competing Interest

The authors declare that they have no known competing financial interests or personal relationships that could have appeared to influence the work reported in this paper.

Acknowledgements

This work was supported by the Guangdong Provincial Department of Science and Technology (Key-Area Research and Development Program of Guangdong Province) under the grant 2020B090923002; Shenzhen-Hong Kong Science and Technology Innovation Cooperation Zone Shenzhen Park Project: HZQB-KCZYB-2020030; the Major Program of National Natural Science Foundation of China (NSFC) (Grant No. 51590892); the National Key R&D Program of China (Project No. 2017YFA0204403); the JLFS - RGC-joint Laboratory Funding Scheme (Reference No.: JLFS/E-103/18).

Appendix A. Supplementary data

Supplementary material related to this article can be found, in the online version, at doi:<https://doi.org/10.1016/j.msar.2020.100596>.

References

- [1] H. Lipson, 3D Print. *Addit. Manuf.* 1 (2014), 61–61.
- [2] T. Economist, A Third Industrial Revolution, 2012. <https://www.economist.com/schumpeter/2012/04/19/a-third-industrial-revolution>.
- [3] J.A. Faber, A.F. Arrieta, A.R. Studart, *Science* 359 (2018) 1386.
- [4] S. Tibbits, *Archit. Des.* 84 (2014) 116–121.
- [5] M. Zastrow, *Nature* 578 (2020) 20.
- [6] D.A. Walker, J.L. Hedrick, C.A. Mirkin, *Science* 366 (2019) 360.
- [7] B.E. Kelly, I. Bhattacharya, H. Heidari, M. Shusteff, C.M. Spadaccini, H.K. Taylor, *Science* 363 (2019) 1075.
- [8] S.K. Saha, D. Wang, V.H. Nguyen, Y. Chang, J.S. Oakdale, S.-C. Chen, *Science* 366 (2019) 105.
- [9] A. Lee, A.R. Hudson, D.J. Shiwarski, J.W. Tashman, T.J. Hinton, S. Yerneni, J. M. Bliley, P.G. Campbell, A.W. Feinberg, *Science* 365 (2019) 482.
- [10] B. Grigoryan, S.J. Paulsen, D.C. Corbett, D.W. Sazer, C.L. Fortin, A.J. Zaita, P. T. Greenfield, N.J. Calafat, J.P. Gounley, A.H. Ta, F. Johansson, A. Randles, J. E. Rosenkrantz, J.D. Louis-Rosenberg, P.A. Galie, K.R. Stevens, J.S. Miller, *Science* 364 (2019) 458.
- [11] J.R. Tumbleston, D. Shrivanyants, N. Ermoshkin, R. Januszewicz, A.R. Johnson, D. Kelly, K. Chen, R. Pinschmidt, J.P. Rolland, A. Ermoshkin, E.T. Samulski, J. M. DeSimone, *Science* 347 (2015) 1349.
- [12] D. Zhang, D. Qiu, M.A. Gibson, Y. Zheng, H.L. Fraser, D.H. StJohn, M.A. Easton, *Nature* 576 (2019) 91–95.
- [13] Z. Chen, Z. Li, J. Li, C. Liu, C. Lao, Y. Fu, C. Liu, Y. Li, P. Wang, Y. He, *J. Eur. Ceram. Soc.* 39 (2019) 661–687.
- [14] F. Kotz, K. Arnold, W. Bauer, D. Schild, N. Keller, K. Sachsenheimer, T. M. Nargang, C. Richter, D. Helmer, B.E. Rapp, *Nature* 544 (2017) 337–339.
- [15] A. Kumar, S. Mandal, S. Barui, R. Vasireddi, U. Gbureck, M. Gelinsky, B. Basu, *Mater. Sci. Eng. R Rep.* 103 (2016) 1–39.
- [16] W. Sun, B. Starly, A.C. Daly, J.A. Burdick, J. Groll, G. Skeldon, W. Shu, Y. Sakai, M. Shinohara, M. Nishikawa, J. Jang, D.-W. Cho, M. Nie, S. Takeuchi, S. Ostrovidov, A. Khademhosseini, R.D. Kamm, V. Mironov, L. Moroni, I. T. Ozbolat, *Biofabrication* 12 (2020), 022002.
- [17] M.A. Skylar-Scott, J. Mueller, C.W. Visser, J.A. Lewis, *Nature* 575 (2019) 330–335.
- [18] A. Bandyopadhyay, B. Heer, *Mater. Sci. Eng. R Rep.* 129 (2018) 1–16.
- [19] E. MacDonald, R. Wicker, *Science* 353 (2016), aaf2093.
- [20] R.L. Truby, J.A. Lewis, *Nature* 540 (2016) 371–378.
- [21] C. Perez, *Technological Revolutions and Financial Capital*, Edward Elgar, Cheltenham, UK, 2003.
- [22] F. Ning, W. Cong, J. Qiu, J. Wei, S. Wang, *Compos. Part B Eng.* 80 (2015) 369–378.
- [23] P. Peyre, Y. Rouchausse, D. Defauchy, G. Régnier, *J. Mater. Process. Technol.* 225 (2015) 326–336.
- [24] J.S. Shim, J.-E. Kim, S.H. Jeong, Y.J. Choi, J.J. Ryu, *J. Prosthet. Dent.* 124 (2019) 468–475.
- [25] N. Hmeidat, J. Kemp, B. Compton, *Compos. Sci. Technol.* 160 (2018) 9–20.
- [26] S.H. Riza, S.H. Masood, C. Wen, D. Ruan, S. Xu, *Mater. Des.* 64 (2014) 650–659.
- [27] M.K. Imran, S.H. Masood, M. Brandt, S. Bhattacharya, J. Mazumder, *Mater. Sci. Eng. A* 528 (2011) 3342–3349.
- [28] J.H. Martin, B.D. Yahata, J.M. Hundley, J.A. Mayer, T.A. Schaedler, T.M. Pollock, *Nature* 549 (2017) 365–369.
- [29] B. Baufeld, O.Vd. Biest, R. Gault, *Mater. Des.* 31 (2010) S106–S111.
- [30] H. Galarraga, D.A. Lados, R.R. Dehoff, M.M. Kirka, P. Nandwana, *Addit. Manuf.* 10 (2016) 47–57.
- [31] Z.C. Cordero, R.B. Dinwiddie, D. Immel, R.R. Dehoff, *J. Mater. Sci.* 52 (2017) 3429–3435.
- [32] T. Mukai, S. Suresh, K. Kita, H. Sasaki, N. Kobayashi, K. Higashi, A. Inoue, *Acta Mater.* 51 (2003) 4197–4208.
- [33] J. Ding, P. Colegrove, J. Mehnen, S. Ganguly, P.M. Sequeira Almeida, F. Wang, S. Williams, *Comput. Mater. Sci.* 50 (2011) 3315–3322.
- [34] S.W. Williams, F. Martina, A.C. Addison, J. Ding, G. Pardal, P. Colegrove, *Mater. Sci. Technol.* 32 (2016) 641–647.
- [35] K. Chen, R. Huang, Y. Li, S. Lin, W. Zhu, N. Tamura, J. Li, Z.-W. Shan, E. Ma, *Adv. Mater.* 32 (2020), 1907164.
- [36] Y.-J. Liang, J. Li, A. Li, X. Cheng, S. Wang, H.-M. Wang, *J. Alloys Compd.* 697 (2017) 174–181.
- [37] D. Karlsson, A. Marshal, F. Johansson, M. Schuisky, M. Sahlberg, J.M. Schneider, U. Jansson, *J. Alloys Compd.* 784 (2019) 195–203.
- [38] Y. Brif, M. Thomas, I. Todd, *Scr. Mater.* 99 (2015) 93–96.
- [39] T. Fujieda, H. Shiratori, K. Kuwabara, M. Hirota, T. Kato, K. Yamanaka, Y. Koizumi, A. Chiba, S. Watanabe, *Mater. Lett.* 189 (2017) 148–151.
- [40] C. Kenel, N.P.M. Casati, D.C. Dunand, *Nat. Commun.* 10 (2019) 904.
- [41] M.A. Gibson, N.M. Mykulowycz, J. Shim, R. Fontana, P. Schmitt, A. Roberts, J. Ketkaew, L. Shao, W. Chen, P. Bordeenithakasem, J.S. Myerberg, R. Fulop, M. D. Verminski, E.M. Sachs, Y.-M. Chiang, C.A. Schuh, A. John Hart, J. Schroers, *Mater. Today* 21 (2018) 697–702.
- [42] Y. Shen, Y. Li, C. Chen, H.-L. Tsai, *Mater. Des.* 117 (2017) 213–222.
- [43] D. Ouyang, N. Li, W. Xing, J. Zhang, L. Liu, *Intermetallics* 90 (2017) 128–134.
- [44] A. Vyatskikh, S. Delalande, A. Kudo, X. Zhang, C. Portela, J. Greer, *Nat. Commun.* 9 (2018) 593.
- [45] G. Liu, Y. Zhao, G. Wu, J. Lu, *Sci. Adv.* 4 (2018), eaat0641.
- [46] Z.C. Eckel, C. Zhou, J.H. Martin, A.J. Jacobsen, W.B. Carter, T.A. Schaedler, *Science* 351 (2016) 58–62.
- [47] E. Zanchetta, M. Cattaldo, G. Franchin, M. Schwentenwein, J. Homa, G. Brusatin, P. Colombo, *Adv. Mater.* 28 (2016) 370–376.
- [48] L.R. Meza, S. Das, J.R. Greer, *Science* 345 (2014) 1322–1326.
- [49] J. Klein, M. Stern, G. Franchin, M. Kayser, C. Inamura, S. Dave, J.C. Weaver, P. Houk, P. Colombo, M. Yang, N. Oxman, *3D Print. Addit. Manuf.* 2 (2015) 92–105.
- [50] D.T. Nguyen, C. Meyers, T.D. Yee, N.A. Dudukovic, J.F. Destino, C. Zhu, E. B. Duoss, T.F. Baumann, T. Suratwala, J.E. Smay, R. Dylla-Spears, *Adv. Mater.* 29 (2017), 1701181.
- [51] D.G. Moore, L. Barbera, K. Masania, A.R. Studart, *Nat. Mater.* 19 (2020) 212–217.

- [52] I. Cooperstein, E. Shukrun, O. Press, A. Kamyshny, S. Magdassi, *ACS Appl. Mater. Interfaces* 10 (2018) 18879–18885.
- [53] S.C. Ligon, R. Liska, J. Stampfl, M. Gurr, R. Mülhaupt, *Chem. Rev.* 117 (2017) 10212–10290.
- [54] X. Wang, M. Jiang, Z. Zhou, J. Gou, D. Hui, *Compos. Part B Eng.* 110 (2017) 442–458.
- [55] H.L. Tekinalp, V. Kunc, G.M. Velez-Garcia, C.E. Duty, L.J. Love, A.K. Naskar, C. A. Blue, S. Ozcan, *Compos. Sci. Technol.* 105 (2014) 144–150.
- [56] X. Tian, T. Liu, C. Yang, Q. Wang, D. Li, *Compos. Part A Appl. Sci. Manuf.* 88 (2016) 198–205.
- [57] P.A. Eutougnat-Diffo, Y. Chen, J. Guan, A. Cayla, C. Campagne, X. Zeng, V. Nierstrasz, *Sci. Rep.* 9 (2019) 14333.
- [58] A. Bircă, O. Gherasim, V. Grumezescu, A.M. Grumezescu, in: V. Grumezescu, A. M. Grumezescu (Eds.), *Materials for Biomedical Engineering*, Elsevier, 2019, pp. 1–28.
- [59] S. Fu, H. Hu, J. Chen, Y. Zhu, S. Zhao, *Chem. Eng. J.* 382 (2020), 122928.
- [60] C.-H. Lin, Y.-M. Lin, Y.-L. Lai, S.-Y. Lee, *J. Prosthet. Dent.* 123 (2019).
- [61] M.L. Hammock, A. Chortos, B.C.K. Tee, J.B.H. Tok, Z. Bao, *Adv. Mater.* 25 (2013) 5997–6038.
- [62] K. Chenoweth, S. Cheung, A.C.T. van Duin, W.A. Goddard, E.M. Kober, *J. Am. Chem. Soc.* 127 (2005) 7192–7202.
- [63] Z. He, Y. Chen, J. Yang, C. Tang, J. Lv, Y. Liu, J. Mei, W.-m. Lau, D. Hui, *Compos. Part B Eng.* 129 (2017).
- [64] J. Holländer, R. Hakala, J. Suominen, N. Moritz, J. Yliruusi, N. Sandler, *Int. J. Pharm.* 544 (2017).
- [65] H. Xiang, X. Wang, Z. Ou, G. Lin, J. Yin, Z. Liu, L. Zhang, X. Liu, *Prog. Org. Coat.* 137 (2019), 105372.
- [66] J. Stieghorst, T. Doll, *Addit. Manuf.* 24 (2018) 217–223.
- [67] H. Wei, X. Cauchy, I.O. Navas, Y. Abderrafai, K. Chizari, U. Sundararaj, Y. Liu, J. Leng, D. Theriault, *ACS Appl. Mater. Interfaces* 11 (2019) 24523–24532.
- [68] H. Wei, Q. Zhang, Y. Yao, L. Liu, Y. Liu, J. Leng, *ACS Appl. Mater. Interfaces* 9 (2017) 876–883.
- [69] W. Zhao, F. Zhang, J. Leng, Y. Liu, *Compos. Sci. Technol.* 184 (2019), 107866.
- [70] Y. Liu, W. Zhang, F. Zhang, J. Leng, S. Pei, L. Wang, X. Jia, C. Cotton, B. Sun, T.-W. Chou, *Compos. Sci. Technol.* 181 (2019), 107692.
- [71] Q. Zhao, D. Yang, C. Zhang, X.-H. Liu, X. Fan, A.K. Whittaker, X.S. Zhao, *ACS Appl. Mater. Interfaces* 10 (2018) 43730–43739.
- [72] V. Viswanathan, T. Laha, K. Balani, A. Agarwal, S. Seal, *Mater. Sci. Eng. R Rep.* 54 (2006) 121–285.
- [73] J. Li, C. Wu, P.K. Chu, M. Gelinsky, *Mater. Sci. Eng. R Rep.* 140 (2020), 100543.
- [74] S. Yuan, F. Shen, C.K. Chua, K. Zhou, *Prog. Polym. Sci.* 91 (2019) 141–168.
- [75] M. Nikzad, S. Masood, I. Sbarski, *Mater. Des.* 32 (2011) 3448–3456.
- [76] D.V. Isakov, Q. Lei, F. Castles, C.J. Stevens, C.R.M. Grovenor, P.S. Grant, *Mater. Des.* 93 (2016) 423–430.
- [77] J. Wang, H. Xie, Z. Weng, T. Senthil, L. Wu, *Mater. Des.* 105 (2016) 152–159.
- [78] B.G. Compton, J.A. Lewis, *Adv. Mater.* 26 (2014) 5930–5935.
- [79] F. Castles, D. Isakov, A. Lui, Q. Lei, C.E.J. Dancer, Y. Wang, J.M. Janurudin, S. C. Speller, C.R.M. Grovenor, *P.S. Grant, Sci. Rep.* 6 (2016) 22714.
- [80] H. Chung, S. Das, *Mater. Sci. Eng. A* 437 (2006) 226–234.
- [81] F.V.D. Klift, Y. Koga, A. Todoroki, M. Ueda, Y. Hirano, R. Matsuzaki, *Open J. Composite Mater.* 06 (No. 01) (2016) 10.
- [82] D. Lin, S. Jin, F. Zhang, C. Wang, Y. Wang, C. Zhou, G.J. Cheng, *Nanotechnology* 26 (2015), 434003.
- [83] X. Wei, D. Li, W. Jiang, Z. Gu, X. Wang, Z. Zhang, Z. Sun, *Sci. Rep.* 5 (2015) 11181.
- [84] E. Fantino, A. Chiappone, F. Calignano, M. Fontana, F. Pirri, I. Roppolo, *Materials* 9 (2016) 589.
- [85] C. Panwisawas, Y.T. Tang, R.C. Reed, *Nat. Commun.* 11 (2020) 2327.
- [86] L.-Y. Chen, J.-Q. Xu, H. Choi, M. Pozuelo, X. Ma, S. Bhowmick, J.-M. Yang, S. Mathaudhu, X.-C. Li, *Nature* 528 (2015) 539–543.
- [87] T.-C. Lin, C. Cao, M. Sokoluk, L. Jiang, X. Wang, J.M. Schoenung, E.J. Lavernia, X. Li, *Nat. Commun.* 10 (2019) 4124.
- [88] Q. Tan, J. Zhang, N. Mo, Z. Fan, Y. Yin, M. Birmingham, Y. Liu, H. Huang, M.-X. Zhang, *Addit. Manuf.* (2020), 101034.
- [89] C. Donate-Buendía, F. Frömel, M.B. Wilms, R. Streubel, J. Tenkamp, T. Hupfeld, M. Nachev, E. Gökce, A. Weisheit, S. Barcikowski, *Mater. Des.* 154 (2018) 360–369.
- [90] K.N. Amato, S.M. Gaytan, L.E. Murr, E. Martinez, P.W. Shindo, J. Hernandez, S. Collins, F. Medina, *Acta Mater.* 60 (2012) 2229–2239.
- [91] A.E. Jakus, S.L. Taylor, N.R. Geisendorfer, D.C. Dunand, R.N. Shah, *Adv. Funct. Mater.* 25 (2015) 6985–6995.
- [92] H.Z. Yu, M.E. Jones, G.W. Brady, R.J. Griffiths, D. Garcia, H.A. Rauch, C.D. Cox, N. Hardwick, *Scr. Mater.* 153 (2018) 122–130.
- [93] Y.F. Li, X. Cheng, D. Liu, H.M. Wang, *Mater. Sci. Eng. A Struct. Mater. Properties Microstruct. Process.* 713 (2018) 75–80.
- [94] J. Liu, J. Li, X. Cheng, H. Wang, *Surf. Coat. Technol.* 325 (2017) 352–359.
- [95] Y. Wang, H. Tang, Y. Fang, H. Wang, *Chinese J. Aeronaut.* 26 (2013) 481–486.
- [96] G.W. Haiyu Zhang, *Huayu Zhang, Combined Additive Manufacturing Method Applicable to Parts and Molds*, 2019.
- [97] Y. Fu, H. Zhang, G. Wang, H. Wang, *J. Mater. Process. Technol.* 250 (2017) 220–227.
- [98] G. Wu, K.-C. Chan, L. Zhu, L. Sun, J. Lu, *Nature* 545 (2017) 80–83.
- [99] N.G. Sun, G. Wu, Q. Wang, *J. Lu, Mater. Today* (2020).
- [100] N. Li, J.J. Zhang, W. Xing, D. Ouyang, L. Liu, *Mater. Des.* 143 (2018) 285–296.
- [101] H. Knoll, S. Ocylok, A. Weisheit, H. Springer, E. Jagle, D. Raabe, *Steel Res. Int.* 88 (2017) 11.
- [102] T. Sathish, *J. Mater. Res. Technol.* 8 (2019) 4354–4363.
- [103] X.H. Chen, J. Li, X. Cheng, H.M. Wang, Z. Huang, *Mater. Sci. Eng. A Struct. Mater. Properties Microstruct. Process.* 715 (2018) 307–314.
- [104] H. Liu, Z. Hu, X. Qin, Y. Wang, J. Zhang, S. Huang, *Int. J. Adv. Manuf. Technol.* 91 (2017) 3967–3975.
- [105] S.A. Khairallah, A.A. Martin, J.R.I. Lee, G. Guss, N.P. Calta, J.A. Hammons, M. H. Nielsen, K. Chaput, E. Schwalbach, M.N. Shah, M.G. Chapman, T.M. Willey, A. M. Rubenchik, A.T. Anderson, Y.M. Wang, M.J. Matthews, W.E. King, *Science* 368 (2020) 660–665.
- [106] L.P. Lefebvre, J. Banhart, D.C. Dunand, *Adv. Eng. Mater.* 10 (2008) 775–787.
- [107] C. Zhu, Z. Qi, V.A. Beck, M. Luneau, J. Lattimer, W. Chen, M.A. Worsley, J. Ye, E. B. Duoss, C.M. Spadaccini, C.M. Friend, J. Biener, *Sci. Adv.* 4 (2018), eaas9459.
- [108] T. Tancogne-Dejean, A.B. Spierings, D. Mohr, *Acta Mater.* 116 (2016) 14–28.
- [109] S. Hwang, E.I. Reyes, K.-s. Moon, R.C. Rumpf, N.S. Kim, *J. Electron. Mater.* 44 (2015) 771–777.
- [110] C. Yan, L. Hao, A. Hussein, P. Young, D. Raymont, *Mater. Des.* 55 (2014) 533–541.
- [111] E. Hernández-Nava, C.J. Smith, F. Derguti, S. Tamas-Williams, F. Léonard, P. J. Withers, I. Todd, R. Goodall, *Acta Mater.* 85 (2015) 387–395.
- [112] L. Dong, V. Deshpande, H. Wadley, *Int. J. Solids Struct.* 60–61 (2015) 107–124.
- [113] M.-S. Pham, C. Liu, I. Todd, J. Lertthanasarn, *Nature* 565 (2019) 305–311.
- [114] R. Martini, Y. Balit, F. Barthelat, *Acta Biomater.* 55 (2017) 360–372.
- [115] M.M. Porter, N. Ravikumar, F. Barthelat, R. Martini, *J. Mech. Behav. Biomed. Mater.* 73 (2017) 114–126.
- [116] S.-X. Liang, X. Wang, W. Zhang, Y.-J. Liu, W. Wang, L.-C. Zhang, *Appl. Mater. Today* 19 (2020), 100543.
- [117] A. Ambrosi, J.G.S. Moo, M. Pumera, *Adv. Funct. Mater.* 26 (2016) 698–703.
- [118] L.O. Jose, R. Jagdheesh, J.J. García-Ballesteros, *Adv. Opt. Technol.* 5 (2016) 87–93.
- [119] A. Ambrosi, M. Pumera, *Adv. Funct. Mater.* 28 (2018), 1700655.
- [120] S.-X. Liang, Z. Jia, Y.-J. Liu, W. Zhang, W. Wang, J. Lu, L.-C. Zhang, *Adv. Mater.* 30 (2018), 1802764.
- [121] J.L. Ocaña, R. Jagdheesh, J.J. García-Ballesteros, *Adv. Opt. Technol.* 5 (2016).
- [122] C. Yang, C. Zhang, W. Xing, L. Liu, *Intermetallics* 94 (2018) 22–28.
- [123] L.-C. Zhang, Z. Jia, F. Lyu, S.-X. Liang, J. Lu, *Prog. Mater. Sci.* 105 (2019), 100576.
- [124] Z. Jia, X. Duan, P. Qin, W. Zhang, W. Wang, C. Yang, H. Sun, S. Wang, L.-C. Zhang, *Adv. Funct. Mater.* 27 (2017) 1702258.
- [125] Z. Jia, Q. Wang, L. Sun, Q. Wang, L.-C. Zhang, G. Wu, J.-H. Luan, Z.-B. Jiao, A. Wang, S.-X. Liang, M. Gu, J. Lu, *Adv. Funct. Mater.* 29 (2019), 1807857.
- [126] Z. Jia, W.C. Zhang, W.M. Wang, D. Habibi, L.C. Zhang, *Appl. Catal. B Environ.* 192 (2016) 46–56.
- [127] Z. Jia, J. Kang, W.C. Zhang, W.M. Wang, C. Yang, H. Sun, D. Habibi, L.C. Zhang, *Appl. Catal. B Environ.* 204 (2017) 537–547.
- [128] S. Nakahara, E.A. Périgo, Y. Pittini-Yamada, Y. de Hazan, T. Graule, *Acta Mater.* 58 (2010) 5695–5703.
- [129] D. Liu, C. Wu, M. Yan, J. Wang, *Acta Mater.* 146 (2018) 294–303.
- [130] J. Farmer, J.-S. Choi, C. Saw, J. Haslam, D. Day, P. Hailey, T. Lian, R. Rebak, J. Perepezko, J. Payer, D. Branagan, B. Beardsley, A. D'amato, L. Aprigliano, *Metall. Mater. Trans. A* 40 (2009) 1289–1305.
- [131] H.X. Li, Z.C. Lu, S.L. Wang, Y. Wu, Z.P. Lu, *Prog. Mater. Sci.* 103 (2019) 235–318.
- [132] S. Pauly, L. Löber, R. Petters, M. Stoica, S. Scudino, U. Kühn, J. Eckert, *Mater. Today* 16 (2013) 37–41.
- [133] X.P. Li, C.W. Kang, H. Huang, T.B. Sercombe, *Mater. Des.* 63 (2014) 407–411.
- [134] X.P. Li, M.P. Roberts, S. O'Keefe, T.B. Sercombe, *Mater. Des.* 112 (2016) 217–226.
- [135] G. Yang, X. Lin, F. Liu, Q. Hu, L. Ma, J. Li, W. Huang, *Intermetallics* 22 (2012) 110–115.
- [136] S. Pauly, C. Schrickler, S. Scudino, L. Deng, U. Kühn, *Mater. Des.* 135 (2017) 133–141.
- [137] D. Zhang, S. Sun, D. Qiu, M.A. Gibson, M.S. Dargusch, M. Brandt, M. Qian, M. Easton, *Adv. Eng. Mater.* 20 (2018), 1700952.
- [138] H. Dobbela, M. Thiele, E.L. Gurevich, E.P. George, A. Ostendorf, *Procedia* 83 (2016) 624–633.
- [139] T. Fujieda, H. Shiratori, K. Kuwabara, T. Kato, K. Yamanaka, Y. Koizumi, A. Chiba, *Mater. Lett.* 159 (2015) 12–15.
- [140] H. Shiratori, T. Fujieda, K. Yamanaka, Y. Koizumi, K. Kuwabara, T. Kato, A. Chiba, *Mater. Sci. Eng. A* 656 (2016) 39–46.
- [141] X. Li, *Adv. Eng. Mater.* 20 (2018), 1700874.
- [142] J. Joseph, T. Jarvis, X. Wu, N. Stanford, P. Hodgson, D.M. Fabijanic, *Mater. Sci. Eng. A* 633 (2015) 184–193.
- [143] J.O. Milewski, *Addit. Manuf. Metals* (2017).
- [144] D.Ta.F.H.Ulrich E. Klotz, *Additive Manufacturing of 18-karat Yellow-gold Alloys, Jewelry Technology Forum* 2017, 2016.
- [145] U.E. Klotz, D. Tiberto, F. Held, *Gold Bull.* 50 (2017) 111–121.
- [146] F. Cooper, *Johnson Matthey Technol. Rev.* 59 (2015) 233–242.
- [147] P.D. Mushtaq Khan, *Rapid Prototyp. J.* 18 (2012) 81–94.
- [148] A.C. Damiano Zito, Alessandro Loggi, D.M. Patrizio Sbornicchia, P. S.p.A, *Progrod S.p.A* 39 (2015) 1–26.
- [149] A.L.M. Hancox, A. Jeffrey, *Int. J. Powder Metall.* 45 (2009) 43–52.
- [150] A. Zocca, P. Colombo, C.M. Gomes, J. Günster, D.J. Green, *J. Am. Ceram. Soc.* 98 (2015) 1983–2001.
- [151] K. Shahzad, J. Deckers, Z. Zhang, J.-P. Kruth, J. Vleugels, *J. Eur. Ceram. Soc.* 34 (2014) 81–89.
- [152] H.-H. Tang, H.-C. Yen, *J. Eur. Ceram. Soc.* 35 (2015) 981–987.

- [153] T. Chartier, C. Duterte, N. Delhote, D. Baillargeat, S. Verdeyme, C. Delage, C. Chapat, *J. Am. Ceram. Soc.* 91 (2008) 2469–2474.
- [154] X. Zheng, H. Lee, T.H. Weisgraber, M. Shusteff, J. DeOtte, E.B. Duoss, J.D. Kuntz, M.M. Biener, Q. Ge, J.A. Jackson, *Science* 344 (2014) 1373–1377.
- [155] H. Windsheimer, N. Travitzky, A. Hofenauer, P. Greil, *Adv. Mater.* 19 (2007) 4515–4519.
- [156] Q. Fu, E. Saiz, A.P. Tomsia, *Adv. Funct. Mater.* 21 (2011) 1058–1063.
- [157] E. Özkol, A.M. Wätjen, R. Bermejo, M. Deluca, J. Ebert, R. Danzer, R. Telle, *J. Eur. Ceram. Soc.* 30 (2010) 3145–3152.
- [158] M. Jafari, W. Han, F. Mohammadi, A. Safari, S. Danforth, N. Langrana, *Rapid Prototyp. J.* 6 (2000) 161–175.
- [159] Y. Liu, Z. Chen, J. Li, B. Gong, L. Wang, C. Lao, P. Wang, C. Liu, Y. Feng, X. Wang, *Addit. Manuf.* 35 (2020), 101348.
- [160] D. Jang, L.R. Meza, F. Greer, J.R. Greer, *Nat. Mater.* 12 (2013) 893–898.
- [161] J. Bauer, S. Hengsbach, I. Tesari, R. Schwaiger, O. Kraft, *Proc. Natl. Acad. Sci.* 111 (2014) 2453.
- [162] Y. Xu, M. Guron, X. Zhu, L.G. Sneddon, S. Yang, *Chem. Mater.* 22 (2010) 5957–5963.
- [163] W. Denk, J.H. Strickler, W.W. Webb, *Science* 248 (1990) 73.
- [164] T.A. Pham, D.P. Kim, T.W. Lim, S.H. Park, D.Y. Yang, K.S. Lee, *Adv. Funct. Mater.* 16 (2006) 1235–1241.
- [165] S. Park, D.-H. Lee, H.-I. Ryoo, T.-W. Lim, D.-Y. Yang, D.-P. Kim, *Chem. Commun.* (2009) 4880–4882.
- [166] G. Pierin, C. Grotta, P. Colombo, C. Mattevi, *J. Eur. Ceram. Soc.* 36 (2016) 1589–1594.
- [167] K. Huang, H. Elsayed, G. Franchin, P. Colombo, *Addit. Manuf.* 33 (2020), 101144.
- [168] Z. Li, Z. Chen, J. Liu, Y. Fu, C. Liu, P. Wang, M. Jiang, C. Lao, *Virtual Phys. Prototyp.* (2020) 1–15.
- [169] P. Colombo, G. Mera, R. Riedel, G.D. Sorarù, *J. Am. Ceram. Soc.* 93 (2010) 1805–1837.
- [170] C. Vakifahmetoglu, D. Zeydanli, P. Colombo, *Mater. Sci. Eng. R Rep.* 106 (2016) 1–30.
- [171] E. Ionescu, H.-J. Kleebe, R. Riedel, *Chem. Soc. Rev.* 41 (2012) 5032–5052.
- [172] C. Minas, D. Carnelli, E. Tervoort, A.R. Studart, *Adv. Mater.* 28 (2016) 9993–9999.
- [173] G. Mera, A. Navrotsky, S. Sen, H.-J. Kleebe, R. Riedel, *J. Mater. Chem. A* 1 (2013) 3826–3836.
- [174] K. Lu, J. Li, *J. Eur. Ceram. Soc.* 36 (2016) 411–422.
- [175] B. Papendorf, K. Nonnenmacher, E. Ionescu, H.-J. Kleebe, R. Riedel, *Small* 7 (2011) 970–978.
- [176] Y. Yu, Y. Liu, J. Fang, L. An, *J. Am. Ceram. Soc.* 98 (2015) 2894–2901.
- [177] E. Ionescu, C. Linck, C. Fasel, M. Müller, H.J. Kleebe, R. Riedel, *J. Am. Ceram. Soc.* 93 (2010) 241–250.
- [178] J. Li, K. Lu, T. Lin, F. Shen, *J. Am. Ceram. Soc.* 98 (2015) 1753–1761.
- [179] J. Kaspar, C. Terzioglu, E. Ionescu, M. Graczyk-Zajac, S. Hapis, H.-J. Kleebe, R. Riedel, *Adv. Funct. Mater.* 24 (2014) 4097–4104.
- [180] T. Kashiwagi, F. Du, J.F. Douglas, K.I. Winey, R.H. Harris, J.R. Shields, *Nat. Mater.* 4 (2005) 928–933.
- [181] P. Colombo, E. Bernardo, G. Parcianello, *J. Eur. Ceram. Soc.* 33 (2013) 453–469.
- [182] F.Y. Hsieh, *Fire Mater.* 22 (1998) 69–76.
- [183] D. Yang, W. Zhang, B. Jiang, Y. Guo, *Compos. Part A Appl. Sci. Manuf.* 44 (2013) 70–77.
- [184] D. Bikiaris, *Thermochim. Acta* 523 (2011) 25–45.
- [185] A. Ambrosi, M. Pumera, *Chem. Soc. Rev.* 45 (2016) 2740–2755.
- [186] J.A. Lewis, *J. Am. Ceram. Soc.* 83 (2000) 2341–2359.
- [187] G.M. Gratson, M. Xu, J.A. Lewis, *Nature* 428 (2004), 386–386.
- [188] T. Sochi, *Polymer* 51 (2010) 5007–5023.
- [189] J.A. Lewis, *Adv. Funct. Mater.* 16 (2006) 2193–2204.
- [190] A.R. Studart, *Chem. Soc. Rev.* 45 (2016) 359–376.
- [191] C. Wang, W. Ping, Q. Bai, H. Cui, R. Hensleigh, R. Wang, A.H. Brozema, Z. Xu, J. Dai, Y. Pei, C. Zheng, G. Pastel, J. Gao, X. Wang, H. Wang, J.-C. Zhao, B. Yang, X. Zheng, J. Luo, Y. Mo, B. Dunn, L. Hu, *Science* 368 (2020) 521.
- [192] L.L. Hench, D.E. Day, W. Höland, V.M. Rheinberger, *Int. J. Appl. Glass Sci.* 1 (2010) 104–117.
- [193] A.J. Ikushima, T. Fujiwara, K. Saito, *J. Appl. Phys.* 88 (2000) 1201–1213.
- [194] N.P. Bansal, R.H. Doremus, in: N.P. Bansal, R.H. Doremus (Eds.), *Handbook of Glass Properties*, Academic Press, San Diego, 1986, pp. 207–219.
- [195] N.P. Bansal, R.H. Doremus, in: N.P. Bansal, R.H. Doremus (Eds.), *Handbook of Glass Properties*, Academic Press, San Diego, 1986, pp. 381–449.
- [196] A. Dickson, J. Barry, K. McDonnell, D. Dowling, *Addit. Manuf.* 16 (2017).
- [197] D. Hülsenberg, A. Harnisch, A. Bismarck, *Microstruct. Glasses* (2008).
- [198] G. Marchelli, R. Prabhakar, D. Storti, M. Ganter, *Rapid Prototyp. J.* 17 (2011) 187–194.
- [199] J. Luo, H. Pan, E.C. Kinzel, *J. Manuf. Sci. Eng.* 136 (2014).
- [200] S. Klein, S. Simske, C. Parraman, P. Walters, D. Huson, S. Hoskins, HP Laboratories Technical Report, 2012.
- [201] M. Fateri, M. Khosravi, *LPI Contributions*, 2012, p. 4368.
- [202] P. von Witzendorf, L. Pohl, O. Suttmann, P. Heinrich, A. Heinrich, J. Zander, H. Bragard, S. Kaierle, *Procedia CIRP* 74 (2018) 272–275.
- [203] K. Sasan, A. Lange, T.D. Yee, N. Dudukovic, D.T. Nguyen, M.A. Johnson, O. D. Herrera, J.H. Yoo, A.M. Sawvel, M.E. Ellis, C.M. Mah, R. Ryerson, L.L. Wong, T. Suratwala, J.F. Destino, R. Dylla-Spears, *ACS Appl. Mater. Interfaces* 12 (2020) 6736–6741.
- [204] M. Fateri, A. Gebhardt, *Int. J. Appl. Ceram. Technol.* 12 (2015) 53–61.
- [205] C. Liu, B. Qian, R. Ni, X. Liu, J. Qiu, *RSC Adv.* 8 (2018) 31564–31567.
- [206] M. Invernizzi, G. Natale, M. Levi, S. Turri, G. Griffini, *Materials* (Basel, Switzerland) 9 (2016) 583.
- [207] M.B. McKinnon, G.E. Martin, S.I. Stolarov, *J. Appl. Polym. Sci.* 137 (2020) 47697.
- [208] M.R. Hartings, Z. Ahmed, *Nat. Rev. Chem.* 3 (2019) 305–314.
- [209] T. Li, Y. Chen, L. Wang, *Compos. Sci. Technol.* 167 (2018) 251–259.
- [210] S. Bapari, A.H. Chokshi, *Compos. Part A Appl. Sci. Manuf.* 123 (2019) 114–122.
- [211] X. Li, Y.H. Tan, P. Wang, X. Su, H.J. Willy, T.S. Herng, J. Ding, *Compos. Part A Appl. Sci. Manuf.* 135 (2020), 105934.
- [212] S. Fafenrot, N. Grimmelsmann, M. Wortmann, A. Ehrmann, *Materials* 10 (2017) 1199.
- [213] S.K. Seol, D. Kim, S. Lee, J.H. Kim, W.S. Chang, J.T. Kim, *Small* 11 (2015) 3896–3902.
- [214] L. Hirt, S. Ihle, Z. Pan, L. Dorwling-Carter, A. Reiser, J.M. Wheeler, R. Spolenak, J. Vörös, T. Zambelli, *Adv. Mater.* 28 (2016) 2311–2315.
- [215] T. Tanaka, A. Ishikawa, S. Kawata, *Appl. Phys. Lett.* 88 (2006), 081107.
- [216] S. Shukla, E.P. Furlani, X. Vidal, M.T. Swihart, P.N. Prasad, *Adv. Mater.* 22 (2010) 3695–3699.
- [217] A. Cohen, R. Chen, U. Frodis, M.T. Wu, C. Folk, *Rapid Prototyp. J.* 16 (2010) 209–215.
- [218] M.S. Onses, E. Sutanto, P.M. Ferreira, A.G. Alleyne, J.A. Rogers, *Small* 11 (2015) 4237–4266.
- [219] P. Heinel, L. Müller, C. Körner, R.F. Singer, F.A. Müller, *Acta Biomater.* 4 (2008) 1536–1544.
- [220] X. Wendy Gu, J.R. Greer, *Extreme Mech. Lett.* 2 (2015) 7–14.
- [221] M. Mieszala, M. Hasegawa, G. Guillonnet, J. Bauer, R. Raghavan, C. Frantz, O. Kraft, S. Mischler, J. Michler, L. Philippe, *Small* 13 (2017), 1602514.
- [222] X. Zhang, J. Yao, B. Liu, J. Yan, L. Lu, Y. Li, H. Gao, X. Li, *Nano Lett.* 18 (2018) 4247–4256.
- [223] X. Zheng, W. Smith, J. Jackson, B. Moran, H. Cui, D. Chen, J. Ye, N. Fang, N. Rodriguez, T. Weisgraber, C.M. Spadaccini, *Nat. Mater.* 15 (2016) 1100–1106.
- [224] E. Sachs, M. Cima, P. Williams, D. Brancazio, J. Cornie, *J. Eng. Ind.* 114 (1992) 481–488.
- [225] B.M. Wu, S.W. Borland, R.A. Giordano, L.G. Cima, E.M. Sachs, M.J. Cima, *J. Control. Release* 40 (1996) 77–87.
- [226] R. Singh, *Adv. Mat. Res.* 83 (2010) 342–349. *Trans Tech Publ.*
- [227] R.O. Ritchie, *Nat. Mater.* 10 (2011) 817–822.
- [228] M. Mirkhalaq, A.K. Dastjerdi, F. Barthelat, *Nat. Commun.* 5 (2014) 3166.
- [229] M. Yahyazadehfar, D. Bajaj, D.D. Arola, *Acta Biomater.* 9 (2013) 4806–4814.
- [230] J.D. Currey, J.D. Taylor, *J. Zool.* 173 (1974) 395–406.
- [231] E. Munch, M.E. Launey, D.H. Alsem, E. Saiz, A.P. Tomsia, R.O. Ritchie, *Science* 322 (2008) 1516.
- [232] Z. Tang, N.A. Kotov, S. Magonov, B. Ozturk, *Nat. Mater.* 2 (2003) 413–418.
- [233] L.J. Bonderer, A.R. Studart, L.J. Gauckler, *Science* 319 (2008) 1069.
- [234] P. Podsiadlo, A.K. Kaushik, E.M. Arruda, A.M. Waas, B.S. Shim, J. Xu, H. Nandivada, B.G. Pumphlin, J. Lahann, A. Ramamoorthy, N.A. Kotov, *Science* 318 (2007) 80.
- [235] P. Walley, Y. Zhang, J.R.G. Evans, *Bioinspir. Biomim.* 7 (2012), 046004.
- [236] H.D. Espinosa, A.L. Juster, F.J. Latourte, O.Y. Loh, D. Gregoire, P.D. Zavattieri, *Nat. Commun.* 2 (2011) 173.
- [237] W.J. Clegg, K. Kendall, N.M. Alford, T.W. Button, J.D. Birchall, *Nature* 347 (1990) 455–457.
- [238] X. Wu, M. Yang, F. Yuan, G. Wu, Y. Wei, X. Huang, Y. Zhu, *Proc. Natl. Acad. Sci.* 112 (2015) 14501.
- [239] Y.A. Shin, S. Yin, X. Li, S. Lee, S. Moon, J. Jeong, M. Kwon, S.J. Yoo, Y.-M. Kim, T. Zhang, H. Gao, S.H. Oh, *Nat. Commun.* 7 (2016) 10772.
- [240] M.A. Meyers, P.-Y. Chen, A.Y.-M. Lin, Y. Seki, *Prog. Mater. Sci.* 53 (2008) 1–206.
- [241] A. Velasco-Hogan, J. Xu, M.A. Meyers, *Adv. Mater.* 30 (2018), 1800940.
- [242] L.R. Meza, A.J. Zelhofer, N. Clarke, A.J. Mateos, D.M. Kochmann, J.R. Greer, *Proc. Natl. Acad. Sci.* 112 (2015) 11502.
- [243] L. Wang, J. Lau, E.L. Thomas, M.C. Boyce, *Adv. Mater.* 23 (2011) 1524–1529.
- [244] L.S. Dimas, G.H. Bratzel, I. Eylon, M.J. Buehler, *Adv. Funct. Mater.* 23 (2013) 4629–4638.
- [245] F. Barthelat, H. Tang, P. Zavattieri, C.M. Li, H. Espinosa, *J. Mech. Phys. Solids* 55 (2007) 306–337.
- [246] U.G.K. Wegst, H. Bai, E. Saiz, A.P. Tomsia, R.O. Ritchie, *Nat. Mater.* 14 (2015) 23–36.
- [247] L.K. Grunenfelder, N. Suksangpanya, C. Salinas, G. Milliron, N. Yaraghi, S. Herrera, K. Evans-Lutterodt, S.R. Nutt, P. Zavattieri, D. Kisailus, *Acta Biomater.* 10 (2014) 3997–4008.
- [248] H. Li, J. Shen, Q. Wei, X. Li, *Mater. Sci. Eng. C* 103 (2019), 109820.
- [249] Z. Jia, L. Wang, *Acta Mater.* 173 (2019) 61–73.
- [250] U. Scheithauer, E. Schwarzer, A. Haertel, H. Richter, T. Moritz, A. Michaelis, *Addit. Manuf. Strat. Technol. Adv. Ceramics* 258 (2016) 19.
- [251] J. Saroia, Y. Wang, Q. Wei, M. Lei, X. Li, Y. Guo, K. Zhang, *Int. J. Adv. Manuf. Technol.* 106 (2020) 1695–1721.
- [252] X.-Y. Ma, Y.-F. Feng, Z.-S. Ma, X. Li, J. Wang, L. Wang, W. Lei, *Biomaterials* 35 (2014) 7259–7270.
- [253] S.J. Leigh, R.J. Bradley, C.P. Purcell, D.R. Billson, D.A. Hutchins, *PLoS One* 7 (2012).
- [254] E.H. Backes, L.D.N. Pires, C.A.G. Beatrice, L.C. Costa, F.R. Passador, L.A. Pessan, *Polym. Eng. Sci.* 60 (2020) 636–644.
- [255] C. Li, Y. Lai, L. Li, H. Cao, J. Long, X. Wang, L. Qin, *J. Orthop. Translat.* 7 (2016) 78.
- [256] H. Arslan, A. Nojoomi, J. Jeon, K. Yum, *Adv. Sci.* 6 (2019), 1800703.

- [257] M.D.N.I. Shiblee, K. Ahmed, M. Kawakami, H. Furukawa, *Adv. Mater. Technol.* 4 (2019), 1900071.
- [258] T. Chen, H. Bakhshi, L. Liu, J. Ji, S. Agarwal, *Adv. Funct. Mater.* 28 (2018), 1800514.
- [259] J. Wang, T. Lu, M. Yang, D. Sun, Y. Xia, T. Wang, *Sci. Adv.* 5 (2019) eaau8769-
eaau8769.
- [260] J. Liu, O. Erol, A. Pantula, W. Liu, Z. Jiang, K. Kobayashi, D. Chatterjee, N. Hibino, L.H. Romer, S.H. Kang, T.D. Nguyen, D.H. Gracias, *ACS Appl. Mater. Interfaces* 11 (2019) 8492–8498.
- [261] J. Guo, R. Zhang, L. Zhang, X. Cao, *ACS Macro Lett.* 7 (2018) 442–446.
- [262] C. Yang, M. Boorugu, A. Dopp, J. Ren, R. Martin, D. Han, W. Choi, H. Lee, *Mater. Horiz.* 6 (2019) 1244–1250.
- [263] Y. Guo, Y. Liu, J. Liu, J. Zhao, H. Zhang, Z. Zhang, *Compos. Part A Appl. Sci. Manuf.* (2020), 105903.
- [264] Y. Liu, W. Zhang, F. Zhang, X. Lan, J. Leng, S. Liu, X. Jia, C. Cotton, B. Sun, B. Gu, T.-W. Chou, *Compos. Part B Eng.* 153 (2018) 233–242.
- [265] C. Yuan, D.J. Roach, C.K. Dunn, Q. Mu, X. Kuang, C.M. Yakacki, T. Wang, K. Yu, H.J. Qi, *Soft Matter* 13 (2017) 5558–5568.
- [266] M. Zarek, M. Layani, I. Cooperstein, E. Sachyani, D. Cohn, S. Magdassi, *Adv. Mater.* 28 (2016) 4449–4454.
- [267] M. Elahinia, N. Shayesteh Moghaddam, A. Amerinatanzi, S. Saedi, G.P. Toker, H. Karaca, G.S. Bigelow, O. Benafan, *Scr. Mater.* 145 (2018) 90–94.
- [268] T. Gustmann, A. Neves, U. Kühn, P. Gargarella, C.S. Kiminami, C. Bolfarini, J. Eckert, S. Pauly, *Addit. Manuf.* 11 (2016) 23–31.
- [269] P. Zhu, W. Yang, R. Wang, S. Gao, B. Li, *ACS Appl. Mater. Interfaces* 10 (2018) 36435–36442.
- [270] S. Roh, L.B. Okello, N. Golbasi, J.P. Hankwitz, J.A.C. Liu, J.B. Tracy, O.D. Velev, *Adv. Mater. Technol.* 4 (2019), 1800528.
- [271] W. Gao, L. Wang, X. Wang, H. Liu, *ACS Appl. Mater. Interfaces* 8 (2016) 14182–14189.
- [272] Y. Kim, G.A. Parada, S. Liu, X. Zhao, *Sci. Robot.* 4 (2019), eaax7329.
- [273] Y. Kim, H. Yuk, R. Zhao, S.A. Chester, X. Zhao, *Nature* 558 (2018) 274–279.
- [274] S. Wu, Q. Ze, R. Zhang, N. Hu, Y. Cheng, F. Yang, R. Zhao, *ACS Appl. Mater. Interfaces* 11 (2019) 41649–41658.
- [275] J. Cui, T.-Y. Huang, Z. Luo, P. Testa, H. Gu, X.-Z. Chen, B.J. Nelson, L. J. Heyderman, *Nature* 575 (2019) 164–168.
- [276] X. Zhao, Y. Kim, *Soft Microbots Programmed by Nanomagnets*, Nature Publishing Group, 2019.
- [277] Z. Mao, K. Zhu, L. Pan, G. Liu, T. Tang, Y. He, J. Huang, J. Hu, K.W.Y. Chan, J. Lu, *Adv. Mater. Technol.* 5 (2020), 1900974.
- [278] Z. Zhao, X. Kuang, C. Yuan, H.J. Qi, D. Fang, *ACS Appl. Mater. Interfaces* 10 (2018) 19932–19939.
- [279] Y. Hu, Z. Wang, D. Jin, C. Zhang, R. Sun, Z. Li, K. Hu, J. Ni, Z. Cai, D. Pan, X. Wang, W. Zhu, J. Li, D. Wu, L. Zhang, J. Chu, *Adv. Funct. Mater.* 30 (2020), 1907377.
- [280] S.Y. Zheng, Y. Shen, F. Zhu, J. Yin, J. Qian, J. Fu, Z.L. Wu, Q. Zheng, *Adv. Funct. Mater.* 28 (2018), 1803366.
- [281] L. Huang, R. Jiang, J. Wu, J. Song, H. Bai, B. Li, Q. Zhao, T. Xie, *Adv. Mater.* 29 (2017), 1605390.
- [282] L. Baggetto, D. Danilov, P.H.L. Notten, *Adv. Mater.* 23 (2011) 1563–1566.
- [283] T.K. Bhandakkar, H.T. Johnson, *J. Mech. Phys. Solids* 60 (2012) 1103–1121.
- [284] X. Xia, A. Afshar, H. Yang, C.M. Portela, D.M. Kochmann, C.V. Di Leo, J.R. Greer, *Nature* 573 (2019) 205–213.
- [285] A. Chortos, E. Hajiesmaili, J. Morales, D.R. Clarke, J.A. Lewis, *Adv. Funct. Mater.* 30 (2020), 1907375.
- [286] H. Cui, S. Miao, T. Esworthy, S.-j. Lee, X. Zhou, S.Y. Hann, T.J. Webster, B. T. Harris, L.G. Zhang, *Nano Res.* 12 (2019) 1381–1388.
- [287] H. Sareen, U. Umaphathi, P. Shin, Y. Kakehi, J. Ou, H. Ishii, P. Maes, *Printflatable: Printing Human-Scale, Functional and Dynamic Inflatable Objects*, in: Proceedings of the 2017 CHI Conference on Human Factors in Computing Systems, Association for Computing Machinery, Denver, Colorado, USA, 2017, pp. 3669–3680.
- [288] F.B. Coulter, A. Ianakiev, *3D Print. Addit. Manuf.* 2 (2015) 140–144.
- [289] F.B. Coulter, B.S. Coulter, E. Papastavrou, A. Ianakiev, *3D Print. Addit. Manuf.* 5 (2018) 17–28.
- [290] A. Zolfagharian, A. Kouzani, B. Nasri-Nasrabadi, S. Adams, S.Y. Khoo, M. Norton, I. Gibson, A. Kaynak, *3D Printing of a Photo-thermal Self-folding Actuator*, DesTech 2016, Proceedings of the International Conference on Design and Technology, Knowledge E (2017) 15–22.
- [291] F. Momeni, S.M. Mehdi, N. Hassani, X. Liu, J. Ni, *Mater. Des.* 122 (2017) 42–79.
- [292] J. Choi, O.C. Kwon, W. Jo, H.J. Lee, M.-W. Moon, *3D Print. Addit. Manuf.* 2 (2015) 159–167.
- [293] A. Sydney Gladman, E.A. Matsumoto, R.G. Nuzzo, L. Mahadevan, J.A. Lewis, *Nat. Mater.* 15 (2016) 413–418.
- [294] S. Naficy, R. Gatley, R. Gorkin Iii, H. Xin, G.M. Spinks, *Macromol. Mater. Eng.* 302 (2017), 1600212.
- [295] L. Ren, B. Li, Y. He, Z. Song, X. Zhou, Q. Liu, L. Ren, *ACS Appl. Mater. Interfaces* 12 (2020) 15562–15572.
- [296] Z. Ding, C. Yuan, X. Peng, T. Wang, H.J. Qi, M.L. Dunn, *Sci. Adv.* 3 (2017), e1602890.
- [297] T. Liu, L. Liu, C. Zeng, Y. Liu, J. Leng, *Compos. Sci. Technol.* 186 (2020), 107935.
- [298] C. Zeng, L. Liu, W. Bian, Y. Liu, J. Leng, *Compos. Part B Eng.* 194 (2020), 108034.
- [299] C. Lin, J. Lv, Y. Li, F. Zhang, J. Li, Y. Liu, L. Liu, *J. Leng, Adv. Funct. Mater.* 29 (2019), 1906569.
- [300] J. Mohd Jani, M. Leary, A. Subic, M.A. Gibson, *Mater. Des.* (1980-2015) 56 (2014) 1078–1113.
- [301] C. Wang, X.P. Tan, Z. Du, S. Chandra, Z. Sun, C.W.J. Lim, S.B. Tor, C.S. Lim, C. H. Wong, *J. Mater. Process. Technol.* 271 (2019) 152–161.
- [302] C.J. Chekottu, R. Groarke, K. O'Toole, D. Brabazon, *Materials* 12 (2019).
- [303] H.Z. Lu, C. Yang, X. Luo, H.W. Ma, B. Song, Y.Y. Li, L.C. Zhang, *Mater. Sci. Eng. A* 763 (2019), 138166.
- [304] V. Laitinen, A. Sozinov, A. Saren, A. Salminen, K. Ullakko, *Addit. Manuf.* 30 (2019), 100891.
- [305] M. Schaffner, J.A. Faber, L. Pianegonda, P.A. Ruhs, F. Coulter, A.R. Studart, *Nat. Commun.* 9 (2018) 878.
- [306] S. Mao, E. Dong, L. Zhou, H. Jin, Y. Tan, G. Liu, M. Xu, K.H. Low, Design and gait analysis of a tortoise-like robot with soft limbs, ASSISTIVE ROBOTICS: Proceedings of the 18th International Conference on CLAWAR 2015 (2016) 215–223.
- [307] V. Du, N. Luciani, S. Richard, G. Mary, C. Gay, F. Mazuel, M. Reffay, P. Menasche, O. Agbulut, C. Wilhelm, *Nat. Commun.* 8 (2017) 400.
- [308] D. Gong, J. Cai, N. Celi, L. Feng, Y. Jiang, D. Zhang, *J. Magn. Magn. Mater.* 468 (2018) 148–154.
- [309] E.B. Joyee, Y. Pan, *Soft Robot.* 6 (2019) 333–345.
- [310] J. Tang, Q. Yin, Y. Qiao, T. Wang, *ACS Appl. Mater. Interfaces* 11 (2019) 21194–21200.
- [311] S. Lantean, G. Barrera, C.F. Pirri, P. Tiberto, M. Sangermano, I. Roppolo, G. Rizza, *Adv. Mater. Technol.* 4 (2019), 1900505.
- [312] Z. Ji, C. Yan, B. Yu, X. Wang, F. Zhou, *Adv. Mater. Interfaces* 4 (2017), 1700629.
- [313] F. Zhang, L. Wang, Z. Zheng, Y. Liu, J. Leng, *Compos. Part A Appl. Sci. Manuf.* 125 (2019), 105571.
- [314] Y. Zhang, L. Wang, W. Gao, T. Gu, Z. Li, X. Li, R. Li, G. Ye, W. Jiang, Y. Zhu, H. Liu, *Smart Mater. Struct.* 28 (2019), 075014.
- [315] R. Tognato, A.R. Armiento, V. Bonfrate, R. Levato, J. Malda, M. Alini, D. Eglin, G. Giancane, T. Serra, *Adv. Funct. Mater.* 29 (2019), 1804647.
- [316] Q. Ze, X. Kuang, S. Wu, J. Wong, S.M. Montgomery, R. Zhang, J.M. Kovitz, F. Yang, H.J. Qi, R. Zhao, *Adv. Mater.* 32 (2020), 1906657.
- [317] H. Lu, M. Zhang, Y. Yang, Q. Huang, T. Fukuda, Z. Wang, Y. Shen, *Nat. Commun.* 9 (2018) 3944.
- [318] Z. Ren, W. Hu, X. Dong, M. Sitti, *Nat. Commun.* 10 (2019) 2703.
- [319] J.J. Martin, B.E. Fiore, R.M. Erb, *Nat. Commun.* 6 (2015) 8641.
- [320] W. Hu, G.Z. Lum, M. Mastrangeli, M. Sitti, *Nature* 554 (2018) 81–85.
- [321] T. Xu, J. Zhang, M. Salehizadeh, O. Onaizah, E. Diller, *Sci. Robot.* 4 (2019), eaav4494.
- [322] X. Liu, N. Kent, A. Ceballos, R. Streubel, Y. Jiang, Y. Chai, P.Y. Kim, J. Forth, F. Hellman, S. Shi, D. Wang, B.A. Helms, P.D. Ashby, P. Fischer, T.P. Russell, *Science* 365 (2019) 264.
- [323] X. Wan, F. Zhang, Y. Liu, J. Leng, *Carbon* 155 (2019) 77–87.
- [324] Z. Song, L. Ren, C. Zhao, H. Liu, Z. Yu, Q. Liu, L. Ren, *ACS Appl. Mater. Interfaces* 12 (2020) 6351–6361.
- [325] W. Choi, T.-Y. Kim, Y.-G. Lee, *Macromol. Mater. Eng.* 303 (2018), 1700675.
- [326] D. Raviv, W. Zhao, C. McKnelly, A. Papadopoulou, A. Kadambi, B. Shi, S. Hirsch, D. Dikovskiy, M. Zyracki, C. Olguin, R. Raskar, S. Tibbits, *Sci. Rep.* 4 (2014) 7422.
- [327] Y. Zhao, C. Xuan, X. Qian, Y. Alsaid, M. Hua, L. Jin, X. He, *Sci. Robot.* 4 (2019), eaax7112.
- [328] K.W. Kwan, S.J. Li, N.Y. Hau, W.-D. Li, S.P. Feng, A.H.W. Ngan, *Sci. Robot.* 3 (2018), eaat4051.
- [329] O.M. Wani, H. Zeng, A. Priimagi, *Nat. Commun.* 8 (2017) 15546.
- [330] L. Chen, M. Weng, P. Zhou, F. Huang, C. Liu, S. Fan, W. Zhang, *Adv. Funct. Mater.* 29 (2019), 1806057.
- [331] J. Liang, Y. Xu, Y. Huang, L. Zhang, Y. Wang, Y. Ma, F. Li, T. Guo, Y. Chen, *J. Phys. Chem. C* 113 (2009) 9921–9927.
- [332] E. Wang, M.S. Desai, S.-W. Lee, *Nano Lett.* 13 (2013) 2826–2830.
- [333] H. Jiang, C. Li, X. Huang, *Nanoscale* 5 (2013) 5225–5240.
- [334] L. Dong, Y. Zhao, *Mater. Chem. Front.* 2 (2018) 1932–1943.
- [335] A.H. Gelebart, D.J. Mulder, G. Vantomme, A.P.H.J. Schenning, D.J. Broer, *Angew. Chemie Int. Ed.* 56 (2017) 13436–13439.
- [336] D. Iqbal, M.H. Samiullah, *Materials* 6 (2013) 116–142.
- [337] L. Li, J.M. Scheiger, P.A. Levkin, *Adv. Mater.* 31 (2019), 1807333.
- [338] D. Hua, X. Zhang, Z. Ji, C. Yan, B. Yu, Y. Li, X. Wang, F. Zhou, *J. Mater. Chem. C* 6 (2018) 2123–2131.
- [339] H. Yang, W.R. Leow, T. Wang, J. Wang, J. Yu, K. He, D. Qi, C. Wan, X. Chen, *Adv. Mater.* 29 (2017), 1701627.
- [340] A. Nishiguchi, H. Zhang, S. Schweizerhof, M.F. Schulte, A. Mourran, M. Möller, *ACS Appl. Mater. Interfaces* 12 (2020) 12176–12185.
- [341] J.J. Schwartz, A.J. Boydston, *Nat. Commun.* 10 (2019) 791.
- [342] M. Nadgorny, Z. Xiao, C. Chen, L.A. Connal, *ACS Appl. Mater. Interfaces* 8 (2016) 28946–28954.
- [343] H. Hingorani, Y.-F. Zhang, B. Zhang, A. Serjouei, Q. Ge, *Int. J. Smart Nano Mater.* 10 (2019) 225–236.
- [344] A. Hamidi, Y. Tadesse, *Mater. Des.* 187 (2020), 108324.
- [345] L. Ge, L. Dong, D. Wang, Q. Ge, G. Gu, *Sens. Actuators A Phys.* 273 (2018) 285–292.
- [346] C.S. Ong, L. Nam, K. Ong, A. Krishnan, C.Y. Huang, T. Fukunishi, N. Hibino, *Biomed Res. Int.* 2018 (2018).
- [347] Z. Fan, Y. Yang, F. Zhang, Z. Xu, H. Zhao, T. Wang, H. Song, Y. Huang, J. A. Rogers, Y. Zhang, *Adv. Mater.* 32 (2020), 1908424.
- [348] B.Y. Ahn, E.B. Duoss, M.J. Motala, X. Guo, S.-I. Park, Y. Xiong, J. Yoon, R. G. Nuzzo, J.A. Rogers, J.A. Lewis, *Science* 323 (2009) 1590.
- [349] Y. Dong, J. Wang, X. Guo, S. Yang, M.O. Ozen, P. Chen, X. Liu, W. Du, F. Xiao, U. Demirci, B.-F. Liu, *Nat. Commun.* 10 (2019) 4087.
- [350] Y. Ji, Y. Xing, X. Li, L.-H. Shao, *Nanomaterials* 9 (2019).

- [351] Y. Wang, Q. Guo, G. Su, J. Cao, J. Liu, X. Zhang, *Adv. Funct. Mater.* 29 (2019), 1906198.
- [352] J.A.C. Liu, J.H. Gillen, S.R. Mishra, B.A. Evans, J.B. Tracy, *Sci. Adv.* 5 (2019), eaaw2897.
- [353] M. Li, Y. Wang, A. Chen, A. Naidu, B.S. Napier, W. Li, C.L. Rodriguez, S. A. Crooker, F.G. Omenetto, *Proc. Natl. Acad. Sci.* 115 (2018) 8119.
- [354] M. Pilz da Cunha, Y. Foelen, R.J.H. van Raak, J.N. Murphy, T.A.P. Engels, M. G. Debijs, A.P.H.J. Schenning, *Adv. Opt. Mater.* 7 (2019), 1801643.
- [355] C. Ma, W. Lu, X. Yang, J. He, X. Le, L. Wang, J. Zhang, M.J. Serpe, Y. Huang, T. Chen, *Adv. Funct. Mater.* 28 (2018), 1704568.
- [356] D.G. Karis, R.J. Ono, M. Zhang, A. Vora, D. Storti, M.A. Ganter, A. Nelson, *Polym. Chem.* 8 (2017) 4199–4206.
- [357] J. Wang, Z. Wang, Z. Song, L. Ren, Q. Liu, L. Ren, *Adv. Mater. Technol.* 4 (2019), 1900293.
- [358] S. Dutta, D. Cohn, *J. Mater. Chem. B* 5 (2017) 9514–9521.
- [359] SLM Solutions, Case Report Monolithic Thrust Chamber, <https://exhibitorsearch.messefrankfurt.com/images/original/userdata/bata/212474/5d3fd794ac6fe.pdf>.
- [360] NASA/MSFC, Pogo Z-Baffle for RS-25 Engine, 2013. <https://www.nasa.gov/explore/systems/sls/j2x/turbocover2.html>.
- [361] S. Ridinger, NASA Advances Additive Manufacturing for Rocket Propulsion, May, 9, 2018, <https://www.nasa.gov/centers/marshall/news/nasa-advances-additive-manufacturing-for-rocket-propulsion.html>.
- [362] RollsRoyce, Advance and UltraFan, 2016. <https://www.rolls-royce.com/media/our-stories/innovation/2016/advance-and-ultrafan.aspx#overview>.
- [363] RollsRoyce, Trent XWB, 2021. [https://www.rolls-royce.com/products-and-services/civil-aerospace/airlines/trent-xwb.aspx#/#/](https://www.rolls-royce.com/products-and-services/civil-aerospace/airlines/trent-xwb.aspx#/).
- [364] Pratt & Whitney, Pratt & Whitney GTF Engine, 2021. <https://prattwhitney.com/products-and-services/products/commercial-engines/pratt-and-whitney-gtf>.
- [365] GE, The CT7 Engine, 2021. <https://www.geaviation.com/commercial-engines/ct7-engine>.
- [366] GE, Introducing GE's Catalyst™ Advanced Turboprop Engine, 2021. <https://www.geaviation.com/bga/engines/ge-catalyst>.
- [367] GE, The T901 Is Here, 2021. <https://www.geaviation.com/military-engines/t901-turboshaft-engine>.
- [368] GE, GE9X Commercial Aircraft Engine, 2021. <https://www.geaviation.com/commercial-engines/ge9x-commercial-aircraft-engine>.
- [369] CFM, <https://www.cfmaeroengines.com/engines/leap/>.
- [370] EOS, Bell Helicopter and Harvest Technologies Utilize Design-Driven Manufacturing With EOS Technology, 2021. <https://www.eos.info/en/3d-printing-g-examples-applications/innovation-stories/bell-helicopter-flight-certified-hardware-using-industrial-3d-printing-for-aviation>.
- [371] Printing the Future: Airbus Expands Its Applications of the Revolutionary Additive Layer Manufacturing Process, 2014, March, 14, <https://www.airbus.com/newsroom/news/en/2014/03/printing-the-future-airbus-expands-its-applications-of-the-revolutionary-additive-layer-manufacturing-process.html>.
- [372] First Titanium 3D-printed Part Installed into Serial Production Aircraft, 2017, September, 13, <https://www.airbus.com/newsroom/press-releases/en/2017/09/first-titanium-3d-printed-part-installed-into-serial-production.html>.
- [373] Aerospace, Sogeti - Additive Manufacturing for the New A350 XWB, 2021. https://www.eos.info/press/case_studies/sogeti-additive-manufacturing-for-the-new-a350-xwb.
- [374] Amstelveen, From Drink to Ink — KLM Makes Tools from PET Bottles, October, 22, 2019, <https://news.klm.com/from-drink-to-ink-klm-makes-tools-from-pet-bottles/>.
- [375] A. Broda, Additive Manufacturing Insight 3D Printing Matures for Tooling, 2019. https://www.boeing.com/features/innovation-quarterly/2019_q4/btj-additive-manufacturing-page.
- [376] Bridging the Gap With 3D Printing, 2018, April, 9, <https://www.airbus.com/newsroom/news/en/2018/04/bridging-the-gap-with-3d-printing.html>.
- [377] M.O. Gradl Paul, Andrews Nathan, 2018.
- [378] Aerospace, Liebherr - First Metal 3D Printed Primary Flight Control Hydraulic Component Flies on an Airbus A380, 2021. https://www.eos.info/press/case_studies/first-3d-printed-hydraulic-component-flies-on-airbus-a380.
- [379] EOS, Aerospace: ArianeGroup - Future Ariane Propulsion Module Simplified by Additive Manufacturing, 2021. https://www.eos.info/press/case_studies/future-ariane-propulsion-module-simplified-with-3d-printing.
- [380] B. Hubscher, The Future of Exploration Starts With 3-D Printing, 2013. https://www.nasa.gov/exploration/systems/sls/j2x/3d_print.html.
- [381] D. Thomas, AIAA Technical Committee on Management Center Overview and Additive Manufacturing at MSFC, 2014.
- [382] T. Prater, Study of Material Consolidation at Higher Throughput Parameters in Selective Laser Melting of Inconel 718, in: *The Materials Society (TMS) Annual Meeting and Exhibition*, Nashville, Tennessee, USA, 2016.
- [383] J.M. Waller, B.H. Parker, K.L. Hodges, E.R. Burke, J.L. Walker, E.R. Generazio, Nondestructive evaluation of additive manufacturing. National Aeronautics and Space Administration, 2014.
- [384] S. X, SpaceX Astronaut Wearing a 3D Printed Helmet, 2020. <https://www.spacex.com/human-spaceflight/>.
- [385] CCTV, (2020). <http://news.cctv.com/2020/05/07/ARTItd3hfFa9I0TnzWAgDINA200507.shtml>.
- [386] M.E. Carkaci, M. Secmen, *Adv. Electromagn.* 8 (2019) 39–47.
- [387] T.D. Ngo, A. Kashani, G. Imbalzano, K.T.Q. Nguyen, D. Hui, *Compos. Part B Eng.* 143 (2018) 172–196.
- [388] M. Molitch-Hou, Boeing Talks 3D Printing for Aerospace, 2017. <https://www.eneering.com/3DPrinting/3DPrintingArticles/ArticleID/15475/Boeing-Talks-3D-Printing-for-Aerospace.aspx.%202013/10/2017>.
- [389] J.E.G.A.K. Misra, R. Carter, Additive Manufacturing of Aerospace Propulsion Components, Additive Manufacturing for Small Manufacturers, Pittsburgh, PA; United States, 2015.
- [390] M.H. Wong, Singapore Airshow: 5 Ways Aviation Will Change, 2016. <https://editon.cnn.com/travel/article/aviation-emerging-tech-singapore-airshow/index.html>.
- [391] I. Kottasová, How 3D Printers Are Transforming Flying, 2018. <https://edition.cnn.com/2018/12/14/tech/3d-printer-plane-airbus/index.html>.
- [392] EOS, Cost-Efficient 3D Printing-Based Manufacturing for Aviation Reduce Fuel Consumption and Material Costs, Lower CO2 Emissions, 2021. https://www.eos.info/press/case_studies/first-3d-printed-hydraulic-component-flies-on-airbus-a380.
- [393] H. You, S. Kim, W.Y. Joe, G.J. Yun, *AIAA J.* 57 (2019) 1786–1792.
- [394] L.P. Bishay, E. Burg, A. Akinwunmi, R. Phan, K. Sepulveda, *Designs* 3 (2019).
- [395] J. Kimaru, A. Bouferrouk, Design, manufacture and test of a camber morphing wing using MFC actuated mart rib, 2017 8th International Conference on Mechanical and Aerospace Engineering (ICMAE) (2017) 791–796.
- [396] A. Menshchikov, A. Somov, *Phys. Fluids* 31 (2019), 037105.
- [397] D. Keidel, G. Molinari, P. Ermanni, *J. Intell. Mater. Syst. Struct.* 30 (2019) 908–923.
- [398] F. Svoboda, M. Hromčík, Construction of the smooth morphing trailing edge demonstrator, 2019 22nd International Conference on Process Control (PC19) (2019) 136–139.
- [399] U. Fasel, D. Keidel, L. Baumann, G. Cavolina, M. Eichenhofer, P. Ermanni, *Manuf. Lett.* 23 (2020) 85–88.
- [400] M. Eichenhofer, J.C.H. Wong, P. Ermanni, *Addit. Manuf.* 18 (2017) 48–57.
- [401] N.B. Cramer, D.W. Cellucci, O.B. Formoso, C.E. Gregg, B.E. Jenett, J.H. Kim, M. Lendraitis, S.S. Swee, G.T. Trinh, K.V. Trinh, K.C. Cheung, *Smart Mater. Struct.* 28 (2019), 055006.
- [402] B. Jenett, S. Calisch, D. Cellucci, N. Cramer, N. Gershenfeld, S. Swee, K.C. Cheung, *Soft Robot.* 4 (2016) 33–48.
- [403] C. Abdessemed, Y. Yao, A. Bouferrouk, P. Narayan, Analysis of a 3D Unsteady Morphing Wing with Seamless Side-edge Transition, 2018 Applied Aerodynamics Conference, American Institute of Aeronautics and Astronautics (2018).
- [404] Q. Chanzy, A.J. Keane, *Aeronaut. J.* 122 (2017) 390–408.
- [405] T.A. Campbell, S. Tibbits, B. Garrett, Washington, DC: The Atlantic Council, 2014, pp. 1–15.
- [406] K. Ntounoglou, P. Stavropoulos, D. Mourtzis, *Procedia Manuf.* 18 (2018) 120–129.
- [407] S. Arabnejad, B. Johnston, M. Tanzer, D. Pasini, *J. Orthop. Res.* 35 (2017) 1774–1783.
- [408] G. Gupta, OsseoTi Porous Metal for Enhanced Bone Integration an Animal Study, 2012. <https://www.zimmerbiomet.com/medical-professionals/common/our-science/osseoti-porous-metal.html>.
- [409] A. Medical, 3D Printed Products, 2019. http://www.ak-medical.net/en/product/list_43.html.
- [410] Q. Han, K. Zhang, Y. Zhang, C. Wang, K. Yang, Y. Zou, B. Chen, J. Wang, *Medicine* 98 (2019) e16658-e16658.
- [411] Stryker, One Step Ahead, 2021. <https://www.stryker.com/us/en/portfolios/ortho-paedics.html>.
- [412] N. Xu, F. Wei, X. Liu, L. Jiang, H. Cai, Z. Li, M. Yu, F. Wu, Z. Liu, *Spine* 41 (2016) E50–E54.
- [413] K.E.G. Diemel, B. van Bochove, J.V. Seppälä, *Biomacromolecules* 21 (2020) 366–375.
- [414] J. Johnson, TRUMATCH® Titanium 3D-Printed Implants Launch in the U.S., 2017. <https://www.jnjmedicaldevices.com/en-US/news-events/trumatch-titanium-3d-printed-implants-launch-us>.
- [415] LITHOZ, Additive Manufacturing Systems for Dental and Medicinal Purposes, 2021. <https://www.lithoz.com/en/3D-printing/medical-dental>.
- [416] G. Ahn, J.-S. Lee, W.-S. Yun, J.-H. Shim, U.-L. Lee, *J. Craniofac. Surg.* 29 (2018) 1880–1883.
- [417] M. Lu, J. Wang, F. Tang, L. Min, Y. Zhou, W. Zhang, C. Tu, *BMC Surg.* 19 (2019) 29.
- [418] EOS, Additive Manufacturing for the Dental Industry - Final Dental Products on the Basis of Industrial 3D Printing, 2021. <https://www.eos.info/dental>.
- [419] A.A. Giannopoulos, D. Mitsouras, S.-J. Yoo, P.P. Liu, Y.S. Chatzizisis, F.J. Rybicki, *Nat. Rev. Cardiol.* 13 (2016) 701–718.
- [420] N. Noor, A. Shapira, R. Edri, I. Gal, L. Wertheim, T. Dvir, *Adv. Sci.* 6 (2019), 1900344.
- [421] J. Li, X. Li, T. Luo, R. Wang, C. Liu, S. Chen, D. Li, J. Yue, S.-h. Cheng, D. Sun, *Sci. Robot.* 3 (2018), eaat8829.
- [422] E. Mods, 3D Printing Hits Case Modding, 2014. <https://reprapsquad.wordpress.com/2014/12/20/3d-printing-hits-case-modding/?wref=tp>.
- [423] Av. Bieren, Ed. Rijk, J. Ansermet, A. Macor, Monolithic metal-coated plastic components for mm-wave applications, 2014 39th International Conference on Infrared, Millimeter, and Terahertz Waves (IRMMW-THz) (2014) 1–2.
- [424] C. Guo, X. Shang, J. Li, F. Zhang, M.J. Lancaster, J. Xu, *IEEE Microw. Wirel. Compon. Lett.* 26 (2016) 568–570.
- [425] M. Vasso, P. Beaufils, S. Cerciello, A. Schiavone Panni, *Arch. Orthop. Trauma Surg.* 134 (2014) 543–553.

- [426] Z. Li, R. Müller, D. Ruffoni, J. Orthop. Res. 36 (2018) 584–593.
- [427] X. Wang, S. Xu, S. Zhou, W. Xu, M. Leary, P. Choong, M. Qian, M. Brandt, Y. M. Xie, *Biomaterials* 83 (2016) 127–141.
- [428] D.C. Ackland, D. Robinson, M. Redhead, P.V.S. Lee, A. Moskaljuk, G. Dimitroulis, *J. Mech. Behav. Biomed. Mater.* 69 (2017) 404–411.
- [429] S. Bose, D. Ke, H. Sahasrabudhe, A. Bandyopadhyay, *Prog. Mater. Sci.* 93 (2018) 45–111.
- [430] D. Wang, Y. Wang, S. Wu, H. Lin, Y. Yang, S. Fan, C. Gu, J. Wang, C. Song, *Materials* 10 (2017) 35.
- [431] C. Oldani, A. Dominguez, *Recent Adv. Arthroplasty* 218 (2012) 149–162.
- [432] X. Kong, L. Wang, G. Li, X. Qu, J. Niu, T. Tang, K. Dai, G. Yuan, Y. Hao, *Mater. Sci. Eng. C* 86 (2018) 42–47.
- [433] Y. Shi, W. Wang, *Mater. Lett.* 261 (2020), 127131.
- [434] C. Chang Tu, P.-I. Tsai, S.-Y. Chen, M.Y.-P. Kuo, J.-S. Sun, J.Z.-C. Chang, *J. Formos. Med. Assoc.* 119 (2020) 420–429.
- [435] W. Xue, A. Bandyopadhyay, S. Bose, *J. Biomed. Mater. Res. Part B Appl. Biomater.* 91 (2009) 831–838.
- [436] H. Cho, S. Tarafder, M. Fogge, K. Kao, C.H. Lee, *Connect. Tissue Res.* 57 (2016) 488–495.
- [437] L. Li, Y. Li, L. Yang, F. Yu, K. Zhang, J. Jin, J. Shi, L. Zhu, H. Liang, X. Wang, Q. Jiang, *Ann. Transl. Med.* 7 (2019) 11.
- [438] G. Bouet, F. Cabanettes, G. Bidron, A. Guignandon, S. Peyroche, P. Bertrand, L. Vico, V. Dumas, *ACS Biomater. Sci. Eng.* 5 (2019) 4376–4385.
- [439] H. Liang, Y. Yang, D. Xie, L. Li, N. Mao, C. Wang, Z. Tian, Q. Jiang, L. Shen, *J. Mater. Sci. Technol.* 35 (2019) 1284–1297.
- [440] Y. Zhu, K. Liu, J. Deng, J. Ye, F. Ai, H. Ouyang, T. Wu, J. Jia, X. Cheng, X. Wang, *Int. J. Nanomed.* 14 (2019) 5977–5987.
- [441] A. Entezari, I. Roohani, G. Li, C.R. Dunstan, P. Rognon, Q. Li, X. Jiang, H. Zreiqat, *Adv. Healthc. Mater.* 8 (2019), 1801353.
- [442] V.S. Cheong, P. Fromme, M.J. Coathup, A. Mumith, G.W. Blunn, *Ann. Biomed. Eng.* 48 (2020) 502–514.
- [443] J.-p. Zheng, L.-j. Chen, D.-y. Chen, C.-s. Shao, M.-f. Yi, B. Zhang, *Trans. Nonferrous Met. Soc. China* 29 (2019) 2534–2545.
- [444] A.A. Zadpoor, *Int. J. Mol. Sci.* 18 (2017) 1607.
- [445] J. Wu, N. Aage, R. Westermann, O. Sigmund, *IEEE Trans. Vis. Comput. Graph.* 24 (2018) 1127–1140.
- [446] M. Castilho, M. Dias, E. Vorndran, U. Gbureck, P. Fernandes, I. Pires, B. Gouveia, H. Armés, E. Pires, J. Rodrigues, *Biofabrication* 6 (2014) 025005.
- [447] Z. Biomet, OsseoTi® Porous Metal Technology, 2021. <https://www.zimmerbiomet.com/medical-professionals/common/our-science/osseoti-porous-metal.html>.
- [448] D. Chimene, L. Miller, L.M. Cross, M.K. Jaiswal, I. Singh, A.K. Gaharwar, *ACS Appl. Mater. Interfaces* 12 (2020) 15976–15988.
- [449] M. Zhang, R. Lin, X. Wang, J. Xue, C. Deng, C. Feng, H. Zhuang, J. Ma, C. Qin, L. Wan, J. Chang, *C. Wu, Sci. Adv.* 6 (2020), eaaz6725.
- [450] H. Attar, M. Calin, L.C. Zhang, S. Scudino, J. Eckert, *Mater. Sci. Eng. A* 593 (2014) 170–177.
- [451] D. Wu, A. Spanou, A. Diez-Escudero, C. Persson, *J. Mech. Behav. Biomed. Mater.* 103 (2020), 103608.
- [452] D.J. Richards, Y. Tan, J. Jia, H. Yao, Y. Mei, *Isr. J. Chem.* 53 (2013) 805–814.
- [453] S. Miao, W. Zhu, N.J. Castro, J. Leng, L.G. Zhang, *Tissue Eng. Part C Methods* 22 (2016) 952–963.
- [454] J. Chen, D. Huang, L. Wang, J. Hou, H. Zhang, Y. Li, S. Zhong, Y. Wang, Y. Wu, W. Huang, *J. Colloid Interface Sci.* (2020).
- [455] C.S. Russell, A. Mostafavi, J.P. Quint, A.C. Panayi, K. Baldino, T.J. Williams, J. G. Daubendiek, V. Hugo Sánchez, Z. Bonick, M. Trujillo-Miranda, *ACS Appl. Bio Mater.* 3 (2020) 1568–1579.
- [456] G. Gao, H. Kim, B.S. Kim, J.S. Kong, J.Y. Lee, B.W. Park, S. Chae, J. Kim, K. Ban, J. Jang, *Appl. Phys. Rev.* 6 (2019), 041402.
- [457] F. Rengier, A. Mehndiratta, H. von Tengg-Kobligh, C.M. Zechmann, R. Unterhinninghofen, H.U. Kauczor, F.L. Giesel, *Int. J. Comput. Assist. Radiol. Surg.* 5 (2010) 335–341.
- [458] J.D. Howard, D. Eggbeer, P. Dorrington, F. Korkees, L.H. Tasker, *Proc. Inst. Mech. Eng. Part H: J. Eng. Med.* (2020), 0954411919899844.
- [459] J. Lu, A new, simple projection model for COVID-19 pandemic, medRxiv (2020).
- [460] P.T. Timbie, J. Grade, Dvd. Weide, B. Maffei, G. Pisano, *Stereolithographed MM-wave corrugated horn antennas*, 2011 International Conference on Infrared, Millimeter, and Terahertz Waves (2011) 1–3.
- [461] C.R. Garcia, R.C. Rumpf, H.H. Tsang, J.H. Barton, *Electron. Lett.* 49 (2013) 734–736.
- [462] J.S. Chieh, B. Dick, S. Loui, J.D. Rockway, *IEEE Antennas Wirel. Propag. Lett.* 13 (2014) 201–204.
- [463] B. Zhang, Z. Zhan, Y. Cao, H. Gulan, P. Linnér, J. Sun, T. Zwick, H. Zirath, *IEEE Trans. Terahertz Sci. Technol.* 6 (2016) 592–600.
- [464] L. Schulwitz, A. Mortazawi, A compact millimeter-wave horn antenna array fabricated through layer-by-layer stereolithography, 2008 IEEE Antennas and Propagation Society International Symposium (2008) 1–4.
- [465] G.-L. Huang, S.-G. Zhou, T.-H. Chio, T.-S. Yeo, 3-D metal-direct-printed wideband and high-efficiency waveguide-fed antenna array, 2015 IEEE MTT-S International Microwave Symposium (2015) 1–4.
- [466] A. Buerkle, K.F. Brakora, K. Sarabandi, *IEEE Antennas Wirel. Propag. Lett.* 5 (2006) 479–482.
- [467] J. Kimionis, M. Isakov, B.S. Koh, A. Georgiadis, M.M. Tentzeris, *IEEE Trans. Microw. Theory Tech.* 63 (2015) 4521–4532.
- [468] S. Alkaraki, Y. Gao, arXiv preprint arXiv:2001.03925, 2020.
- [469] E. Miralles, B. Schoenlinner, B. Á, H. Esteban, V. Ziegler, *Radio Sci.* 54 (2019) 158–165.
- [470] L. Bosui, G. Xun, W.J. Chappell, Layer-by-layer polymer stereolithography fabrication for three-dimensional RF components, in: 2004 IEEE MTT-S International Microwave Symposium Digest (IEEE Cat. No.04CH37535), vol. 2, 2004, pp. 481–484. Vol.482.
- [471] N. Delhote, D. Baillargeat, S. Verdeyme, C. Delage, C. Chaput, *IEEE Trans. Microw. Theory Tech.* 55 (2007) 548–554.
- [472] M. D'Auria, W.J. Otter, J. Hazell, B.T.W. Gillatt, C. Long-Collins, N.M. Ridler, S. Lucyszyn, *IEEE Trans. Comp. Packaging Manuf. Technol.* 5 (2015) 1339–1349.
- [473] B. Zhang, H. Zirath, *Electron. Lett.* 51 (2015) 1791–1793.
- [474] V.Td. Crestvolant, P.M. Iglesias, M.J. Lancaster, *IEEE Trans. Microw. Theory Tech.* 63 (2015) 3433–3444.
- [475] C. Guo, X. Shang, M.J. Lancaster, J. Xu, *IEEE Microw. Wirel. Comp. Lett.* 25 (2015) 442–444.
- [476] D.L. Creedon, M. Goryachev, N. Kostylev, T.B. Sercombe, M.E. Tobar, *Appl. Phys. Lett.* 109 (2016), 032601.
- [477] A. Tamayo-Domínguez, J. Fernández-González, M. Sierra-Pérez, *IEEE Trans. Microw. Theory Tech.* 65 (2017) 4138–4147.
- [478] B. Zhang, H. Zirath, *IEEE Trans. Comp. Packaging Manuf. Technol.* 6 (2016) 796–804.
- [479] S. Pandey, B. Gupta, A. Nahata, *Opt. Express* 21 (2013) 24422–24430.
- [480] N.T. Nguyen, N. Delhote, M. Etorre, D. Baillargeat, L.L. Coq, R. Sauleau, *IEEE Trans. Antennas Propag.* 58 (2010) 2757–2762.
- [481] M. Liang, W. Ng, K. Chang, K. Gbele, M.E. Gehm, H. Xin, *IEEE Trans. Antennas Propag.* 62 (2014) 1799–1807.
- [482] H. Yi, S. Qu, K. Ng, C.H. Chan, X. Bai, *IEEE Trans. Antennas Propag.* 64 (2016) 442–449.
- [483] G.B. Wu, Y. Zeng, K.F. Chan, S. Qu, C.H. Chan, *IEEE Antennas Wirel. Propag. Lett.* 18 (2019) 921–925.
- [484] G. Wu, K.F. Chan, W.C. Mok, C.H. Chan, 3-D Printed Terahertz Lens for Bessel Beam Generation, 2019 IEEE Asia-Pacific Microwave Conference (APMC) (2019) 637–639.
- [485] J. Kwon, Y. Takeda, K. Fukuda, K. Cho, S. Tokito, S. Jung, *ACS Nano* 10 (2016) 10324–10330.
- [486] G.-W. Huang, Q.-P. Feng, H.-M. Xiao, N. Li, S.-Y. Fu, *ACS Nano* 10 (2016) 8895–8903.
- [487] T. Ching, Y. Li, R. Karyappa, A. Ohno, Y.-C. Toh, M. Hashimoto, *Sens. Actuators B Chem.* 297 (2019), 126609.
- [488] A.P. Taylor, L.F. Velásquez-García, *Nanotechnology* 26 (2015), 505301.
- [489] T. Blachowicz, A. Ehrmann, *Micromachines* 11 (2020).
- [490] E. Saleh, F. Zhang, Y. He, J. Vaithilingam, J.L. Fernandez, R. Wildman, I. Ashcroft, R. Hague, P. Dickens, C. Tuck, *Adv. Mater. Technol.* 2 (2017), 1700134.
- [491] R. Hensleigh, H. Cui, Z. Xu, J. Massman, D. Yao, J. Berrigan, X. Zheng, *Nat. Electron.* 3 (2020) 216–224.
- [492] K. Sun, T.-S. Wei, B.Y. Ahn, J.Y. Seo, S.J. Dillon, J.A. Lewis, *Adv. Mater.* 25 (2013) 4539–4543.
- [493] K. Fu, Y. Wang, C. Yan, Y. Yao, Y. Chen, J. Dai, S. Lacey, Y. Wang, J. Wan, T. Li, Z. Wang, Y. Xu, L. Hu, *Adv. Mater.* 28 (2016) 2587–2594.
- [494] A. Maurel, S. Grugeon, B. Fleutot, M. Courty, K. Prashantha, H. Tortajada, M. Armand, S. Panier, L. Dupont, *Sci. Rep.* 9 (2019) 18031.
- [495] X. Gao, Q. Sun, X. Yang, J. Liang, A. Koo, W. Li, J. Liang, J. Wang, R. Li, F. B. Holness, A.D. Price, S. Yang, T.-K. Sham, X. Sun, *Nano Energy* 56 (2019) 595–603.
- [496] H. Ragonés, A. Vinegrad, G. Ardel, M. Goor, Y. Kamir, M.M. Dorfman, A. Gladkikh, D. Golodnitsky, *J. Electrochem. Soc.* 167 (2019), 070503.
- [497] J. Zhang, Y. Yao, L. Sheng, J. Liu, *Adv. Mater.* 27 (2015) 2648–2655.
- [498] R. Gill, *Introducing 3D-printable Parts for ASUS Motherboards, Graphics Cards, and Peripherals*, 2016. <https://edgeup.asus.com/2016/introducing-asus-3d-printable-parts-motherboards-gpus-peripherals/>.
- [499] E. Vasquez, P.-F. Giroux, F. Lomello, M. Nussbaum, H. Maskrot, F. Schuster, P. Castany, *Powder Technol.* 360 (2020) 998–1005.
- [500] X. He, Z. Zhu, C. Shao, R. Huang, Additive Manufacturing of Spent Fuel Storage Rack Model by Selective Laser Melting, International Conference on Nuclear Engineering, Vol 51548, American Society of Mechanical Engineers (2018) p. V001T002A001.
- [501] H. Neuberger, J. Rey, M. Hees, E. Materna-Morris, D. Bolich, J. Aktaa, A. Meier, S. Fischer, C. Schorle, U. Fuhrmann, *Fusion Sci. Technol.* 72 (2017) 667–672.
- [502] C. Gao, X. Chen, C. Su, A.R. Singh, S. Jayalakshmi, *Mater. Express* 9 (2019) 179–184.
- [503] X. Yao, S.K. Moon, B.Y. Lee, G. Bi, *Int. J. Precis. Eng. Manuf.* 18 (2017) 1693–1701.
- [504] O. Halevi, T.-Y. Chen, P.S. Lee, S. Magdassi, J.A. Hriljac, *RSC Adv.* 10 (2020) 5766–5776.
- [505] M.A. Kiani, S.J. Ahmadi, M. Outokesh, R. Adeli, A. Mohammadi, *Radiat. Phys. Chem.* 141 (2017) 223–228.
- [506] X. Zhang, X. Zhang, S. Guo, *Polym. Eng. Sci.* 59 (2019) E348–E355.
- [507] A. Delfini, M. Albano, A. Vricella, F. Santoni, G. Rubini, R. Pastore, M. Marchetti, *Materials (Basel, Switzerland)* 11 (2018) 1730.
- [508] D.D. DiJulio, C.P. Cooper-Jensen, H. Perrey, K. Fissum, E. Rofors, J. Scherzinger, P.M. Bentley, *Nucl. Instrum. Methods Phys. Res. Sect. A Accelerators Spectrometers Detectors Assoc. Equip.* 859 (2017) 41–46.
- [509] Z. Pei, Y. Xu, F. Wei, T. Liu, D. Su, *J. Magn. Magn. Mater.* 493 (2020), 165742.
- [510] M.B. Stone, D.H. Siddell, A.M. Elliott, D. Anderson, D.L. Abernathy, *Rev. Sci. Instrum.* 88 (2017), 123102.

- [511] Y. Zhang, F. Chen, X. Tang, H. Huang, T. Chen, X. Sun, J. Reinf. Plast. Compos. 37 (2017) 181–190.
- [512] M. Nabipour, B. Akhond, A. Bagheri Saed, J. Appl. Polym. Sci. 137 (2020) 48717.
- [513] S.-Z. Guo, K. Qiu, F. Meng, S.H. Park, M.C. McAlpine, Adv. Mater. 29 (2017), 1701218.
- [514] Z. Wang, X. Guan, H. Huang, H. Wang, W. Lin, Z. Peng, Adv. Funct. Mater. 29 (2019), 1807569.
- [515] A.D. Valentine, T.A. Busbee, J.W. Boley, J.R. Raney, A. Chortos, A. Kotikian, J. D. Berrigan, M.F. Durstock, J.A. Lewis, Adv. Mater. 29 (2017), 1703817.
- [516] Z. Lei, Q. Wang, P. Wu, Mater. Horiz. 4 (2017) 694–700.
- [517] J.T. Muth, D.M. Vogt, R.L. Truby, Y. Mengüç, D.B. Kolesky, R.J. Wood, J.A. Lewis, Adv. Mater. 26 (2014) 6307–6312.
- [518] A. Frutiger, J.T. Muth, D.M. Vogt, Y. Mengüç, A. Campo, A.D. Valentine, C. J. Walsh, J.A. Lewis, Adv. Mater. 27 (2015) 2440–2446.
- [519] A.J. Blake, R.R. Kohlmeier, J.O. Hardin, E.A. Carmona, B. Maruyama, J. D. Berrigan, H. Huang, M.F. Durstock, Adv. Energy Mater. 7 (2017), 1602920.
- [520] T.-S. Wei, B.Y. Ahn, J. Grotto, J.A. Lewis, Adv. Mater. 30 (2018), 1703027.
- [521] R.R. Kohlmeier, A.J. Blake, J.O. Hardin, E.A. Carmona, J. Carpena-Núñez, B. Maruyama, J.D. Berrigan, H. Huang, M.F. Durstock, J. Mater. Chem. A 4 (2016) 16856–16864.
- [522] B. Chen, W. Tang, T. Jiang, L. Zhu, X. Chen, C. He, L. Xu, H. Guo, P. Lin, D. Li, J. Shao, Z.L. Wang, Nano Energy 45 (2018) 380–389.
- [523] S. Chen, T. Huang, H. Zuo, S. Qian, Y. Guo, L. Sun, D. Lei, Q. Wu, B. Zhu, C. He, X. Mo, E. Jeffries, H. Yu, Z. You, Adv. Funct. Mater. 28 (2018), 1805108.
- [524] H. Li, R. Li, X. Fang, H. Jiang, X. Ding, B. Tang, G. Zhou, R. Zhou, Y. Tang, Nano Energy 58 (2019) 447–454.
- [525] S. He, Z. Yu, H. Zhou, Z. Huang, Y. Zhang, Y. Li, J. Li, Y. Wang, D. Li, Nano Energy 52 (2018) 134–141.
- [526] C. Qian, L. Li, M. Gao, H. Yang, Z. Cai, B. Chen, Z. Xiang, Z. Zhang, Y. Song, Nano Energy 63 (2019), 103885.
- [527] H. Yuk, B. Lu, S. Lin, K. Qu, J. Xu, J. Luo, X. Zhao, Nat. Commun. 11 (2020) 1604.
- [528] D.H. Ho, P. Hong, J.T. Han, S.-Y. Kim, S.J. Kwon, J.H. Cho, Adv. Sci. 7 (2020), 1902521.
- [529] Y.Y. Choi, D.H. Ho, J.H. Cho, ACS Appl. Mater. Interfaces 12 (2020) 9824–9832.
- [530] B. Chen, Y. Jiang, X. Tang, Y. Pan, S. Hu, ACS Appl. Mater. Interfaces 9 (2017) 28433–28440.
- [531] G. Sun, J. An, C.K. Chua, H. Pang, J. Zhang, P. Chen, Electrochem. Commun. 51 (2015) 33–36.
- [532] Y. Wang, C. Chen, H. Xie, T. Gao, Y. Yao, G. Pastel, X. Han, Y. Li, J. Zhao, K. Fu, L. Hu, Adv. Funct. Mater. 27 (2017), 1703140.
- [533] Y. Ni, R. Ji, K. Long, T. Bu, K. Chen, S. Zhuang, Appl. Spectrosc. Rev. 52 (2017) 623–652.
- [534] C.L. Manzanera Palenzuela, M. Pumera, TrAC Trends Anal. Chem. 103 (2018) 110–118.
- [535] D. Buenger, F. Topuz, J. Groll, Prog. Polym. Sci. 37 (2012) 1678–1719.
- [536] X. Liu, J. Liu, S. Lin, X. Zhao, Mater. Today (2020).
- [537] R.L. Truby, M. Wehner, A.K. Grosskopf, D.M. Vogt, S.G.M. Uzel, R.J. Wood, J. A. Lewis, Adv. Mater. 30 (2018), 1706383.
- [538] A. Kotikian, C. McMahan, E.C. Davidson, J.M. Muhammad, R.D. Weeks, C. Daraio, J.A. Lewis, Sci. Robot. 4 (2019), eaax7044.
- [539] M. Wehner, R.L. Truby, D.J. Fitzgerald, B. Mosadegh, G.M. Whitesides, J.A. Lewis, R.J. Wood, Nature 536 (2016) 451–455.
- [540] M. López-Valdeolivas, D. Liu, D.J. Broer, C. Sánchez-Somolinos, Macromol. Rapid Commun. 39 (2018), 1700710.
- [541] T. Chartier, C. Dupas, M. Lasgorceix, J. Brie, N. Delhote, C. Chaput, J. Ceram. Sci. Technol. 6 (2014) 95–104.
- [542] W. Chang, Y. Jun-ping, J. Gems Gemmol. 3 (2007).
- [543] Z.W. Zou, X.C. Ye, Appl. Mech. Mater. 697 (2015) 340–343.
- [544] D. Wu, Z. Zhao, Q. Zhang, H.J. Qi, D. Fang, Soft Matter 15 (2019) 6151–6159.
- [545] L.T. Dean, K. Niedderer, Craft Res. 7 (2016) 51–77.
- [546] M. Khan, P. Dickens, Gold Bull. 43 (2010) 114–121.
- [547] Y. Zhai, D.A. Lados, J.L. LaGoy, JOM 66 (2014) 808–816.
- [548] A. Pasricha, R. Greeninger, Fash. Text. 5 (2018) 30.
- [549] W. Chang, Y. Jun-ping, J. Gems Gemmol. 3 (2007).
- [550] L.T. Dean, E. Pei, Experimental 3D digital techniques in design practice, DS 73-2 Proceedings of the 2nd International Conference on Design Creativity Volume 2 (2012) 220–226.
- [551] E. Bassoli, A. Gatto, L. Iuliano, M. Grazia Violante, Rapid Prototyp. J. 13 (2007) 148–155.
- [552] S. Pattnaik, D.B. Karunakar, P.K. Jha, J. Mater. Process. Technol. 212 (2012) 2332–2348.
- [553] D.p.a.D.p. news, Studio Under Develops a Large & Fast Ceramic 3D Printer, 2014. <https://www.3ders.org/articles/20140403-studio-under-develops-a-large-fast-ceramic-3d-printer.html>.
- [554] C.Y. Yap, C.K. Chua, Z.L. Dong, Z.H. Liu, D.Q. Zhang, L.E. Loh, S.L. Sing, Appl. Phys. Rev. 2 (2015), 041101.
- [555] D.S. Vlley, What Kind of Internet Can Meet the Demand Trend of Light Luxury and Customized Jewelry?, 2016. www.3dsciencevalley.com/?p=6777.
- [556] B. Artley, Automotive 3D Printing Applications, 2021. <https://www.3dhubs.com/knowledge-base/automotive-3d-printing-applications/#industry>.
- [557] S.M. Publishing, SmarTech Analysis Issues New Report on Automotive Additive Manufacturing Market, Sees a \$9 Billion (\$USD) Opportunity on the Horizon, 2019. <https://www.globenewswire.com/news-release/2019/08/01/1895642/>
- [558] C.A. Giffi, B. Gangula, P. Illinda, Additive Manufacturing Hits the Road, Deloitte University Press, 2014. https://dupress.deloitte.com/content/dam/dup-us-en/articles/additive-manufacturing-3d-opportunity-in-automotive/DUP_707-3D-Opportunity-Auto-Industry_MASTER.pdf.
- [559] S.G. Sarvankar, S.N. Yewale, Int. J. Res. Aeronaut. Mech. Eng. 7 (2019) 1–10.
- [560] BUGATTI, World Premiere: Brake Caliper From 3-D Printer, 2018. <https://www.bugatti.com/media/news/2018/world-premiere-brake-caliper-from-3-d-printer/>.
- [561] A.m. news, Get to Know How Additive Manufacturing Is Contributing to Classic Car Revival, 2021. <https://additivenews.com/get-know-how-additive-manufacturing-contributing-classic-car-revival/>.
- [562] P. Malnati, Plast. Eng. 75 (2019) 48–55.
- [563] Volkswagen, Ready for Mass Production: Volkswagen Uses the Latest 3D Printing Process for Production, 2018. https://www.volkswagenag.com/en/news/2018/09/volkswagen_3d_printing.html.
- [564] Volkswagen, Brake Calipers and Wheels? Now From a 3D Printer, 2018. <https://www.volkswagenag.com/en/news/stories/2018/12/brake-calipers-and-wheels-now-from-a-3d-printer.html#>.
- [565] S. Goehrke, Additive Manufacturing is Driving the Future of the Automotive Industry, 2018. <https://www.forbes.com/sites/sarahgoehrke/2018/12/05/additive-manufacturing-is-driving-the-future-of-the-automotive-industry/#3821707a75cc>.
- [566] K.E. Inc, URBEE, 2014. <https://korecologic.com/media/pictures/>.
- [567] M. Chinthavali, 3D printing technology for automotive applications, 2016 International Symposium on 3D Power Electronics Integration and Manufacturing (3D-PEIM) (2016) 1–13.
- [568] Autoblog, We Drive a 3D-printed Utility Vehicle That Can Power a Home | Translogic 203, 2016. <https://www.autoblog.com/2016/06/30/3d-printed-utility-vehicle-wireless-home-translogic-203/>.
- [569] R. Manghni, Int. J. Curr. Eng. Technol. 5 (2015) 3407–3410.
- [570] C.W.J. Lim, K.Q. Le, Q. Lu, C.H. Wong, IEEE Potentials 35 (2016) 18–22.
- [571] N. Tanikella, J. Gershenson, B. Savonen, J.M. Pearce, (2017).
- [572] AMFG, Application Spotlight: 3D Printing for Bike Manufacturing, 2019. <https://amfg.ai/2019/08/01/3d-printing-for-bike-manufacturing-application-spotlight/>.
- [573] L. Nickels, Met. Powder Rep. 69 (2014) 38–40.
- [574] P. Kingsland, 3D Printing in the Railway Sector with Deutsche Bahn, 2019. <https://www.railway-technology.com/features/3d-printing-in-the-railway-sector/>.
- [575] RAILENGINEER, Bringing 3D Printing to the UK Rail Industry, 2020. <https://www.railengineer.co.uk/2020/02/06/bringing-3d-printing-to-the-uk-rail-industry/>.
- [576] D.M. Vogt, K.P. Becker, B.T. Phillips, M.A. Graule, R.D. Rotjan, T.M. Shank, E. E. Cordes, R.J. Wood, D.F. Gruber, PLoS One 13 (2018), e0200386.
- [577] J.Z. Gul, M. Sajid, M.M. Rehman, G.U. Siddiqui, I. Shah, K.-H. Kim, J.-W. Lee, K. H. Choi, Sci. Technol. Adv. Mater. 19 (2018) 243–262.
- [578] M. Tessler, M.R. Brugler, J.A. Burns, N.R. Sinatra, D.M. Vogt, A. Varma, M. Xiao, R.J. Wood, D.F. Gruber, Curr. Biol. 30 (2020) R157–R158.
- [579] B. Liao, H. Zang, Y. Liu, Y. Wang, X. Lang, J. Jin, N. Zhu, Q. Yin, Programmable Design of Soft Actuators and Robots*, 2019 WRC Symposium on Advanced Robotics and Automation (WRC SARA) (2019) 222–227.
- [580] C.B. Teeple, T.N. Koutros, M.A. Graule, R.J. Wood, Int. J. Rob. Res. (2020), 0278364920910465.
- [581] N.R. Sinatra, C.B. Teeple, D.M. Vogt, K.K. Parker, D.F. Gruber, R.J. Wood, Sci. Robot. 4 (2019), eaax5425.
- [582] Z. Shen, H. Zhong, E. Xu, R. Zhang, K.C. Yip, L.L. Chan, L.L. Chan, J. Pan, W. Wang, Z. Wang, Soft Robot. (2020).
- [583] N. Jackson, P. Chastain, M. Crowther, M. Shin, Int. J. Precis. Eng. Manuf. 20 (2019) 2183–2192.
- [584] B.T. Phillips, K.P. Becker, S. Kurumaya, K.C. Galloway, G. Whittredge, D.M. Vogt, C.B. Teeple, M.H. Rosen, V.A. Pieribone, D.F. Gruber, R.J. Wood, Sci. Rep. 8 (2018) 14779.
- [585] B.T. Phillips, J. Allder, G. Bolan, R.S. Nagle, A. Redington, T. Hellebrekers, J. Borden, N. Pawlenko, S. Licht, Addit. Manuf. 31 (2020), 100969.
- [586] Z. Jia, T. Yang, L. Sun, Y. Zhao, W. Li, J. Luan, F. Lyu, L.-C. Zhang, J.J. Krucic, J.-J. Kai, J.C. Huang, J. Lu, C.T. Liu, Adv. Mater. 32 (2020), 2000385.
- [587] Q. Zhao, X. Wang, J. Liu, H. Wang, Y. Zhang, J. Gao, J. Liu, Q. Lu, J. Electrochem. Soc. 162 (2015) A845–A851.
- [588] Q. Zhao, D. Yang, A.K. Whittaker, X.S. Zhao, J. Power Sources 396 (2018) 12–18.
- [589] L.C. Hwa, S. Rajoo, A.M. Noor, N. Ahmad, M.B. Uday, Curr. Opin. Solid State Mater. Sci. 21 (2017) 323–347.
- [590] S. Bose, S. Vahabzadeh, A. Bandyopadhyay, Mater. Today 16 (2013) 496–504.
- [591] H. Seitz, W. Rieder, S. Irsen, B. Leukers, C. Tille, J. Biomed. Mater. Res. Part B Appl. Biomater. 74B (2005) 782–788.
- [592] S.C. Cox, J.A. Thornby, G.J. Gibbons, M.A. Williams, K.K. Mallick, Mater. Sci. Eng. C 47 (2015) 237–247.
- [593] V. Karageorgiou, D. Kaplan, Biomaterials 26 (2005) 5474–5491.
- [594] J. Lv, Z. Gong, Z. He, J. Yang, Y. Chen, C. Tang, Y. Liu, M. Fan, W.-M. Lau, J. Mater. Chem. A 5 (2017) 12435–12444.
- [595] D. Liu, P. Jiang, X. Li, J. Liu, L. Zhou, X. Wang, F. Zhou, Chem. Eng. J. 397 (2020), 125392.



Dr. Guo LIU received the B.E. in Mechanical Engineering and Automation from the University of Science and Technology of China in 2013 and the Ph.D. in Mechanical and Biomedical Engineering from City University of Hong Kong in 2018 under the supervision of Prof. Jian LU. He currently works as Postdoc at City University of Hong Kong with his research interests focused on 3D/4D printing, polymer-derived ceramics, and nano-materials.



Dr. Xiaofeng ZHANG is a senior engineer at National Engineering Laboratory of Modern Materials Surface Engineering Technology, Guangdong Institute of New Materials, China. He received his Ph.D. degree in Materials Processing Engineering from South China University of Technology in 2016. Now, he works in City University of Hong Kong as senior research associate. His research interests focus on thermal/environmental barrier coatings. So far, he published 113 papers and received 11 patents.



Xuliang CHEN received his bachelor's degree of Engineering in Material Forming and Control Engineering from Huazhong University of Science and Technology in 2015. He did research on surface cladding for 3 years in Wuhan University of Technology. Currently he is a PhD student in City University of Hong Kong supervised by Prof. Jian LU. His research interests focus on additive manufacturing of metallic materials, especially microstructural control and mechanical/functional performance of crystal and amorphous alloy. He is also interested in numerical simulation of additive manufacturing process and residual stress estimation using thermomechanical coupled finite element method.



Yunhu HE is a PhD research student from Department of Mechanical Engineering at City University of Hong Kong. He received his bachelor's degree (2017) from Sichuan University and master's degree (2018) from The Chinese University of Hong Kong. His research interests include 3D printing of soft materials, manufacturing of smart materials and their applications.



Prof. Jian LU received the Dip. Ing., Master (DEA) degree and Doctoral degree from University of Technology of Compiègne France. He is Chair Professor of Mechanical Engineering in the Department of Mechanical Engineering, Department of Material Science and Engineering, Department of Biomedical Science. He is an academician of the National Academy of Technologies of France. He is a Fellow of Hong Kong Academy of Engineering Science and a Fellow of the Society for Experimental Mechanics (SEM).